OPTIMIZATION OF THAI TEA FERMENTATION TO PRODUCE BACTERIAL CELLULOSE FOR APPLICATION IN JELLY CANDY

WAWAN AGUSTINA

A Thesis Submitted in Partial Fulfillment of the Requirements for the
Degree of Doctor of Philosophy in Biotechnology
Suranaree University of Technology
Academic Year 2024

การปรับปรุงกระบวนการหมักชาไทยเพื่อผลิตแบคทีเรียลเซลลูโลส สำหรับใช้ในลูกกวาดเยลลี่

นายวาวาน อกุสติน่า

วิทยานิพนธ์นี้เป็นส่วนหนึ่งของการศึกษาตามหลักสูตรปริญญาปรัชญาดุษฎีบัณฑิต
สาขาวิชาเทคโนโลยีชีวภาพ
มหาวิทยาลัยเทคโนโลยีสุรนารี
ปีการศึกษา 2567

OPTIMIZATION OF THAI TEA FERMENTATION TO PRODUCE BACTERIAL CELLULOSE FOR APPLICATION IN JELLY CANDY

Suranaree University of Technology has approved this thesis submitted in partial fulfillment of the requirements for the Degree of Doctor of Philosophy.

Thesis Examining Committee

.....

(Assoc. Prof. Dr. Prakit Sukyai)
Chairperson

.....

(Assoc. Prof. Dr. Apichat Boontawan)
Member (Thesis Advisor)

.....

(Dr. Chaiwut Gamonpilas)
Member (Thesis Co-advisor)

.....

(Prof. Dr. Montarop Yamabhai)
Member

.....

(Assoc. Prof. Dr. Kaemwich Jantama)
Member

.....

(Assoc. Prof. Dr. Sunanta Tongta)
Member

.....

(Assoc. Prof. Dr. Yupaporn Ruksakulpiwat)
Vice Rector for Academic Affairs
and Quality Assurance

.....

(Prof. Dr. Neung Teaumroong)
Dean of Institute of Agricultural
Technology

วาวาน อกุสติน่า: การปรับปรุงกระบวนการหมักชาไทยเพื่อผลิตแบคทีเรียลเซลลูโลสสำหรับใช้ในลูกกวาดเยลลี่ (OPTIMIZATION OF THAI TEA FERMENTATION TO PRODUCE BACTERIAL CELLULOSE FOR APPLICATION IN JELLY CANDY) อาจารย์ที่ปรึกษา: รองศาสตราจารย์ ดร.อภิชาติ บุญทาวัน, 328 หน้า

คำสำคัญ: เส้นใยนาโนเซลลูโลสจากแบคทีเรีย (BCNF)/การหมักคอมบูชา/ชาแดงไทย/ การเพิ่มประสิทธิภาพด้วยวิธี CCD-RSM/ผลิตภัณฑ์เสริมอาหาร/เยลลี่แคนดี้/ โปรไฟล์สารออกฤทธิ์ทางชีวภาพ/การจำลองการย่อยในทางเดินอาหาร

เซลลูโลสเป็นพอลิเมอร์ที่หมุนเวียนได้และย่อยสลายทางชีวภาพ มีการใช้งานอย่างกว้างขวางในอุตสาหกรรมอาหารและยา เซลลูโลสจากแบคทีเรีย (BC) ซึ่งผลิตจากกระบวนการหมัก เช่น *Komagataeibacter xylinum* มีคุณสมบัติเด่นด้านความบริสุทธิ์ ความยืดหยุ่น และสมบัติเชิงกล ในระบบอาหาร สาร BC ทำหน้าที่เป็นสารเพิ่มความข้นเหนียวที่ให้พลังงานต่ำ สารเพิ่มความคงตัว สารทดแทนไขมัน และตัวพารส ช่วยสนับสนุนการพัฒนาผลิตภัณฑ์ฟังก์ชันและเพื่อสุขภาพได้ อย่างไรก็ตาม การผลิตเซลลูโลสจากแบคทีเรียยังถูกจำกัดด้วยต้นทุนที่สูง จึงมีความต้องการวัตถุดิบทางเลือกที่มีต้นทุนต่ำ เช่น ชา มาใช้ในกระบวนการผลิตดังกล่าว ด้วยเหตุนี้ งานวิจัยนี้มุ่งศึกษาการผลิต BC จากคอมบูชาชาไทย โดยเน้นการพัฒนาให้ได้ผลผลิตและ คุณสมบัติของ BC ที่ดี และการผลิตเส้นใยนาโนผ่านกระบวนการไมโครฟลูอิไดเซชันแรงดันสูง เพื่อให้ได้เส้นใยนาโนเซลลูโลสจากแบคทีเรีย (BCNF) และการประยุกต์ใช้ BCNF ในผลิตภัณฑ์เยลลี่แคนดี้เพื่อสุขภาพ โดยงานวิจัยนี้แบ่งการศึกษาออกเป็น 4 ส่วน ดังรายละเอียดต่อไปนี้

การศึกษาส่วนที่ 1 ศึกษาการใช้คอมบูชาชาไทย ซึ่งเป็นวัตถุดิบต้นทุนต่ำ สำหรับการผลิตเซลลูโลสจากแบคทีเรีย (BC) ภายใต้สภาวะการเพาะเลี้ยงแบบนิ่ง ที่อุณหภูมิ 30 °C เป็นเวลา 15 วัน โดยใช้ SCOBY เชิงพาณิชย์ และตัวอย่างชา 4 ชนิด ได้แก่ ชาจีนดำ ชาอัสสัมดำ ชาเขียว และชาแดงไทย พบว่าชาแดงไทย (RTC) ให้ผลผลิต BC แบบเปียกสูงสุด (168.00 ± 2.93 กรัม/ลิตร) จึงถูกเลือกมาศึกษาต่อ เพื่อวิเคราะห์แนวทางการเพิ่มประสิทธิภาพการผลิตต่อไป การศึกษาการเติมสารเสริมบางชนิดส่งผลให้ปริมาณผลผลิต BC เพิ่มขึ้นอย่างมีนัยสำคัญ เช่น การเติมเอทานอล (RTC-EtOH) หรือ ส่วนผสมซูโครส-กลูโคส (RTC-SGlu) ให้ผลผลิต BC แบบเปียก เท่ากับ 218.36 ± 12.85 และ 259.54 ± 8.92 กรัม/ลิตร ตามลำดับ นอกจากนี้ การเพิ่มประสิทธิภาพการผลิต BC สามารถทำได้จากการปรับค่า pH ความเข้มข้นของชา ความถี่ในการเก็บเกี่ยว และวิธีการเพาะเลี้ยง ซึ่งพบว่าสภาวะที่ให้ผลผลิตดีที่สุดคือ pH ~5.20, ความเข้มข้นชา 2% การเก็บเกี่ยวทุก 2 สัปดาห์ และการเพาะเลี้ยงแบบนิ่ง การวิเคราะห์สมบัติทางเคมีกายภาพและสมบัติเชิงกล (SEM, FTIR, XRD, TGA, nanoindentation) ยืนยันว่า BC ที่ได้มีคุณสมบัติโดยรวมที่ดี แสดงให้เห็นว่าคอมบูชาชาแดงไทยเป็น วัตถุดิบที่มีศักยภาพสำหรับการผลิต BC

การศึกษาส่วนที่ 2 ได้นำระเบียบวิธีพื้นผิวตอบสนอง (RSM) ร่วมกับการออกแบบการทดลองแบบ Central Composite Design (CCD) มาใช้เพื่อเพิ่มประสิทธิภาพการผลิตเซลลูโลสจากแบคทีเรีย (BC) โดยใช้คอมบูชาชาแดงไทย มีการทดลองทั้งหมด 34 ครั้ง เพื่อศึกษาอิทธิพล

ของอัตราส่วนซูโครส-กลูโคส ความเข้มข้นของชา และปริมาณเอทานอล ต่อผลผลิต และสมบัติจอง BC โดยโมเดลดังกล่าวได้ทำนายสูตรที่ให้ประสิทธิภาพการผลิตที่สูงขึ้นทั้งหมด 53 สูตร ซึ่งมี 3 สูตรที่ได้รับการยืนยันผล ทั้งนี้ สูตรแนะนำ (RTC-V1) ให้ผลผลิต BC แบบเปียกสูงถึง 621.71 ± 24.06 กรัม/ลิตร ซึ่งเพิ่มขึ้น 238% เมื่อเทียบกับสูตร RTC-SGlu นอกจากนี้ การวิเคราะห์สมบัติต่างๆ ของตัวอย่าง BC ที่ได้ ยืนยันว่า BC มีค่าการตกผลึกสูง (83.23–85.97%) ความเสถียรทางความร้อน และสมบัติทางกลที่ดี แสดงให้เห็นว่าการใช้ RSM-CCD เป็นวิธีที่มีประสิทธิภาพในการเพิ่มผลผลิตจากการผลิต BC โดยใช้คอมบูชาชาแดงไทย

การศึกษาส่วนที่ 3 ศึกษาอิทธิพลของกระบวนการไมโครฟลูอิไดเซชันแรงดันสูง (10,000 psi, 10, 15 และ 20 รอบ) ต่อสมบัติต่างๆ ของ BC พบว่าขนาดเส้นใยลดลง (~25 nm) ความสามารถในการอุ้มน้ำลดลง (จาก 96.6 เหลือ ~31.0 g/g) ขนาดอนุภาคเล็กลงและมีความสม่ำเสมอเพิ่มขึ้น การวิเคราะห์ด้วย SEM, XRD และ TGA แสดงให้เห็นถึงการเปลี่ยนแปลงเชิงโครงสร้างและสมบัติทางความร้อน ดังนั้น กระบวนการนี้สามารถปรับปรุงคุณสมบัติของ BC เพื่อการใช้งานที่กว้างขึ้นได้

การศึกษาส่วนที่ 4 ได้นำ BCNF จากการศึกษาก่อนหน้านี้มาใช้ในผลิตภัณฑ์เยลลี่ลูกอม ร่วมกับส่วนผสมที่มีฤทธิ์ทางชีวภาพ (วิตามินซี วิตามิน อี อัญชัน และ สารสกัดจากมะเขือเทศ) โดย BCNF มีผลต่อเนื้อสัมผัสของเยลลี่ลูกอม โดยการเติมวิตามินอีให้เนื้อสัมผัสที่แน่นที่สุด ในขณะที่สารสกัดจากมะเขือเทศและวิตามินซีทำให้เนื้อสัมผัสนิ่มลง ในการจำลองการย่อย พบว่าตัวอย่างที่เติม BCNF เพิ่มการคงอยู่ของสารต้านอนุมูลอิสระในสูตรที่มีวิตามินซี แต่อิทธิพลของ BNCF จะแตกต่างกันไปตามส่วนประกอบที่ออกฤทธิ์ทางชีวภาพ ผลการศึกษานี้ชี้ให้เห็นถึงศักยภาพของ BCNF ในการเป็นสารให้โครงสร้างและสารให้ประโยชน์เชิงหน้าที่ในผลิตภัณฑ์เยลลี่เสริมสุขภาพ

สาขาวิชาเทคโนโลยีชีวภาพ
ปีการศึกษา 2567

ลายมือชื่อนักศึกษา.....
ลายมือชื่ออาจารย์ที่ปรึกษา.....
ลายมือชื่ออาจารย์ที่ปรึกษาร่วม.....

WAWAN AGUSTINA: OPTIMIZATION OF THAI TEA FERMENTATION TO PRODUCE BACTERIAL CELLULOSE FOR APPLICATION IN JELLY CANDY. THESIS ADVISOR: ASSOC. PROF. APICHAT BOONTAWAN, Ph.D., 328 PP.

Keywords: Bacterial Cellulose Nanofibrils (BCNF)/Kombucha Fermentation/Thai Red Tea/CCD-RSM Optimization/Nutraceutical/Jelly Candy/Bioactive Compounds Profile/Gastrointestinal Simulation

Cellulose is a renewable, biodegradable polymer with broad applications in food and pharmaceuticals. Bacterial cellulose (BC), produced by fermentation (e.g., *Komagataeibacter xylinum*), is valued for its purity, flexibility, and mechanical strength. In food systems, BC can serve as a low-calorie thickener, stabilizer, fat replacer, and flavor carrier, thus supporting the development of functional and health-oriented products. However, high production cost limits its use, prompting further exploration of cost-effective substrates, such as tea. Therefore, this study investigates BC production from Thai tea kombucha, focusing on its yield, physicochemical and mechanical properties, and nanofibril (BCNF) production via high-pressure microfluidization. The resulting BCNF is then applied in jelly candy as a model nutraceutical delivery system. The research comprises four main studies as follows.

Study 1 evaluated Thai tea kombucha as a low-cost and culturally relevant medium for BC production under static conditions at 30 °C for 15 days using a commercial SCOBY. Among four tea varieties tested—Chinese black, Assamica black, green, and red—Thai red tea (RTC) produced the highest wet BC yield (168.00 ± 2.93 g/L) and was selected for further optimization. Its yield was enhanced through additives such as ethanol (RTC-EtOH) (218.36 ± 12.85 g/L) and a sucrose-glucose combination (RTC-SGlu) (259.54 ± 8.92 g/L). Additional optimization of pH, tea concentration, harvest frequency, and cultivation methods showed that unadjusted pH (~5.20), 2% tea, biweekly harvests, and static cultivation gave the best results. Its property characterization (SEM, FTIR, XRD, TGA, nanoindentation) confirmed RTC kombucha as a promising medium for BC production.

Study 2 applied a response surface methodology (RSM) with a central composite design (CCD) model to optimize BC production from Thai red tea kombucha. A total of 34 experiments were conducted to evaluate the effects of the sucrose-glucose ratio, tea concentration, and ethanol level. The model generated 53 optimized formulations, three of which were validated. The recommended formulation (RTC-V1)

achieved a wet BC yield of 621.71 ± 24.06 g/L, a 238% increase over the RTC-SGlu formulation. Further characterization on the obtained BC properties confirmed high crystallinity (83.23–85.97%), thermal stability, and strong mechanical properties, confirming the effectiveness of RSM-CCD in maximizing the BC production.

Study 3 examined the effects of high-pressure microfluidization (HPM, at 10,000 psi, for up to 20 cycles) on BC. The resulting BC nanofibril (BCNF) showed reduced fiber diameter (from ~37 nm to ~25 nm), decreased WHC (from 96.6 to ~31.0 g water/g cellulose), reduced particle size, and improved particle uniformity. SEM, XRD, and TGA analyses confirmed structural and thermal modifications, demonstrating HPM's role in tailoring BC properties for wider applications.

Study 4 incorporated BCNF into jelly candy along with bioactive ingredients (vitamins C, E, butterfly pea, and tomato extract). BCNF impacted jelly candy texture, especially firmness and chewiness. Vitamin E yielded the firmest texture, while tomato extract and vitamin C softened it. In simulated digestion experiment, BCNF-enhanced jellies improved antioxidant retention in vitamin C formulations, though the effects varied across bioactive ingredients. These findings highlight BCNF's potential as a structural and functional component in nutraceutical jelly candy products.

School of Biotechnology
Academic Year 2024

Student's Signature .....
Advisor's Signature .....
Co-Advisor's Signature .....

ACKNOWLEGEMENT

First and foremost, I am deeply grateful to Allah SWT for His endless blessings, guidance, and strength, which have sustained me throughout this journey and enabled me to complete this work.

I sincerely thank my advisor, Assoc. Prof. Apichat Boontawan, Ph.D., for his exceptional guidance, unwavering support, and for providing all the necessary resources to carry out this research. His mentorship has been instrumental in shaping the direction of this work and has significantly contributed to both my academic development and personal growth.

My heartfelt thanks also go to my co-advisor, Dr. Chaiwut Gamonpilas, for his valuable guidance, expertise, and continuous support throughout this project.

I am also deeply thankful to Prof. Montarop Yamabhai, Ph.D., Assoc. Prof. Sunanta Tongta, Ph.D., Assoc. Prof. Prakit Sukyai, Assoc. Prof. Kaemwich Jantama, Ph.D., and Dr. Kanjana Thumanu for their valuable feedback, insightful comments, and constructive suggestions, all of which have significantly strengthened the quality of this thesis.

My heartfelt appreciation extends to all the lecturers (*Ajarn*) at Suranaree University of Technology (SUT) whose dedication and encouragement have played an important role in my academic journey.

I would like to express my sincere gratitude to Badan Riset dan Inovasi Nasional (BRIN) for giving me the opportunity to continue my doctoral studies. I am also deeply thankful to Suranaree University of Technology (SUT) for awarding me the doctoral scholarship that made this journey possible. My special appreciation goes to the Center for International Affairs (CIA-SUT), the Institute of Agricultural Technology, and the

School of Biotechnology for their unwavering support, kind assistance, and warm hospitality throughout my time at SUT.

I am especially grateful to the members and staff of the Biorefinery Laboratory—including Chakapong Wongsalee, Patawee Aupalikit, and others—as well as Labs F3, F10, and F11, for their technical support, collaboration, and kindness, all of which were essential in carrying out this research.

To my friends at SUT, thank you for your friendship, encouragement, and the many shared moments that made this journey both meaningful and memorable.

To my parents, I am forever thankful for your unconditional love, prayers, and unwavering support. To my beloved wife, I deeply appreciate your patience, understanding, and constant encouragement. To my son, your presence has brought light, joy, and motivation throughout this journey.

To my extended family, thank you for always believing in me. Your support has been a steady source of strength.

Finally, I would like to express my heartfelt thanks to everyone who has supported me along the way, even if I cannot mention each one by name.

Alhamdulillah, I am eternally grateful for Allah SWT's grace, and for the support and kindness of all the individuals and institutions who have walked beside me on this path.

WAWAN AGUSTINA

TABLE OF CONTENTS

TABLE OF CONTENTS (Continued)

Page

TABLE OF CONTENTS (Continued)

Page

TABLE OF CONTENTS (Continued)

Page

TABLE OF CONTENTS (Continued)

Page

TABLE OF CONTENTS (Continued)

Page

LIST OF TABLES

Table **Page**

LIST OF TABLES (Continued)

LIST OF TABLES (Continued)

LIST OF TABLES (Continued)

LIST OF FIGURES

LIST OF FIGURES (Continued)

LIST OF FIGURES (Continued)

LIST OF FIGURES (Continued)

LIST OF FIGURES (Continued)

LIST OF FIGURES (Continued)

LIST OF ABBREVIATIONS

BC	=	Bacterial Cellulose
BCNF/s	=	Bacterial cellulose nanofibril/s
BF	=	Code for butterfly flower powder extract
BTC	=	Code for black tea *Chatramue* brand
GTC	=	Code for Thai green tea *Chatramue* brand
CI	=	Crystallinity index
HPM	=	High-pressure microfluidization
JC	=	Jelly candy
ND	=	Not detected
PC	=	Pure coffee
RBTH	=	Code for Chinese black tea *Three horse* brand
RTC	=	Code for Thai red tea *Chatramue* brand
RTC-SD	=	RTC-Sucrose-dextrose
RTC-SF	=	RTC-Sucrose-fructose
RTC-SGlu	=	RTC-Sucrose-glucose
RTC-SGly	=	RTC-Sucrose-glycerol
SCOBY	=	symbiotic culture of bacteria and yeast
SPI	=	Soy protein isolate
TFC	=	Total Flavonoid content
TPC	=	Total Phenolic content
TOM	=	Code for tomato powder extract
VC	=	Vitamin C
VE	=	Vitamin E
YE	=	Yeast extract
XRD	=	X-ray diffraction

CHAPTER 1

INTRODUCTION

1.1 Rationale for the Research

Technological developments are accompanied by an increase in various material needs, both as raw materials and as intermediate products. One of the most needed materials today is cellulose-based products such as nanocellulose and various derivatives. Although it had decreased in the 20th century, the use of cellulose is now rising, owing to its natural abundance, renewability, biodegradability, and inherent biocompatibility, especially with the development of nanotechnology and characterization techniques such as isolating, modifying, and characterizing cellulose (Jiang et al. 2021).

Cellulose has been known for a long time—around 150 years ago—as a renewable and biodegradable polymer (Börjesson and Westman 2015). Current technological developments have succeeded in changing or modifying cellulose polymers into various derivative products, and these products are widely used in various applications such as coatings, films, membranes, new building materials, drilling techniques, pharmaceuticals, and food products (Börjesson and Westman 2015). In general, cellulose is one of the main components of lignocellulosic, which is mostly part of the plant cell wall along with other components such as hemicellulose, lignin, pectin, and wax (Mulyadi 2019). The composition of cellulose can reach one-third of the plant tissue and is the main component of several natural fibers such as cotton, flax, hemp, jute, and others (Moran et al. 2008). Apart from plant tissue sources, cellulose can also be obtained from other sources such as tunicates, algae, and bacteria. According to Kargarzadeh et al. (2017), several sources of cellulose other than

plants are (1) tunicates, namely a group of invertebrates from marine animals, especially from the subphylum of *Tunicate* group; (2) several types of algae such as green, red, gray, and brown algae; and (3) several species of bacteria that can produce cellulose, such as the bacteria *Gluconacetobacter xylinus*.

Bacteria may create cellulose in a fermentation process, such as when making kombucha. Kombucha is a fermented beverage with a long list of health advantages. As a by-product of kombucha production, a white pellicle layer (cellulose) known as bacterial cellulose (BC) is produced. Bacteria like *Acetobacter xylinum* can produce BC during their metabolism (Jasmania 2018). BC has a unique structure, a better degree of purity, and a higher mechanical property, to name a few advantages (Klemm et al. 2005). The unique characteristics and its potential application are the advantages of BC such as biodegradability and high purity (Ludwicka et al. 2020), high flexibility, high water holding capacity, hydrophilicity, high crystallinity, moldability, mechanical stability, etc. (Gorgieva and Trček 2019; Ullah et al. 2019; Lin et al. 2020; Choi et al. 2022).

BC has been used for many applications, including in the food industry. In the food industry, cellulose can be utilized as a low-calorie carbohydrate alternative, thickener, flavor carrier, and suspension stabilizer (Peng et al. 2011). A study reported as well on the application of BC in food industries such as food packaging, dietary food, thickening agents, and traditional desserts like nata de coco (Reiniati 2017), fat replacers, meat analogs, stabilizers of Pickering emulsions (PEs), rheology modifiers, and immobilizers of probiotics and enzymes (Azeredo et al. 2019a). Nanocellulose can extend food shelf life and improve food quality by acting as a carrier for active ingredients such as antioxidants and antimicrobials (Peng et al. 2011). So, in the nutraceutical product, there are such things as an emulsifier, the immobilization of bacterial and mammalian cells, the immobilization of enzymes, and the immobilization of bioactive agents (Khan et al. 2018).

BC has been produced and marketed commercially. One biotechnology company, *Polybion*, has completed the construction of the world's first BC biomanufacturing factory (www.prnewswire.com 2022). Even though it has been manufactured commercially, the synthesis of BC is claimed to be expensive due to the use of expensive medium components (Revin et al. 2018; El-Gendi et al. 2022; Kamal et al. 2022). Some studies have been reported about the effort of using low-cost substrates for BC production, such as agricultural waste or residual biomass (Waghmare et al. 2018; Akintunde et al. 2022) and industrial waste and by-product streams (Tsouko et al. 2015).

In the kombucha production process, BC is a by-product that has not been used optimally so far. This by-product can increase its value by being made into an intermediate product or a final product. Apart from only producing BC as a by-product, the kombucha fermentation method is actually very possible to apply to produce BC as the main product. BC production by applying this method can be an alternative for producing BC with low production costs. The substrate used in BC production media through kombucha fermentation generally only consists of sugar (sucrose), tea, water, and the addition of microbial cultures.

Thailand is well known for producing tea (Pongpruttikul and Yamsa-ard 2022). Thailand produces some types of tea, which are classified into four major groups based on the production methods and product used: green tea, black tea, oolong tea, and chewing tea (P. Winyayong 2007). Different types of teas show different nutritional or compositional values, such as protein, water content, ash, volatiles, caffeine, and minerals (Czernicka et al. 2017). As it is known, production of BC is affected by the nutritional value of the medium; thus, different types of tea may affect the yield and characteristics of BC. Therefore, an investigation of the effect of the tea on the yield and characteristics of BC is necessary. Once the tea is selected, it must also be selected for other factors such as the best carbon source, additives, initial pH of the medium, tea concentration, fermentation time, and cultivation technique. To get the optimal

conditions for BC production, the medium composition and environmental conditions must also be optimized.

Optimization of BC production is essential to improve yield and process efficiency, particularly when using alternative substrates or modified culture conditions. Response Surface Methodology (RSM) is a widely used statistical approach that enables the evaluation of multiple variables and their interactions in a systematic and efficient manner. Several previous studies have successfully applied RSM to optimize BC production, such as from agro-industrial waste materials (Singh et al. 2017), waste fig substrates (Yilmaz and Goksungur 2024), and by modifying the composition of the Hestrin–Schramm (HS) medium to enhance culture performance (Aswini et al. 2020). In this study, RSM was employed to optimize the production conditions of BC, based on selected key factors known to influence microbial cellulose synthesis.

Once the optimum production conditions were achieved, the next phase of this study focused on modifying BC. Although BC is a highly pure, biocompatible, and biodegradable biopolymer with excellent native properties, its structure often requires further modification to meet specific functional and industrial demands. Various physical, chemical, and enzymatic techniques have been explored to tailor its morphology and performance. Among these, high-pressure homogenization (HPH) and, in particular, high-pressure microfluidization (HPM) are effective physical methods used to reduce fiber size and alter surface characteristics, thereby improving material functionality (Wang et al. 2015; Mert 2020). These treatments can significantly influence properties such as crystallinity, surface area, and mechanical strength, with HPM offering particular promise, though its application to BC remains relatively underexplored.

In this study, HPM was employed as a mechanical modification method with the aim of investigating how the structural changes in BC affect its performance when incorporated into a food matrix. The resulting BC nanofibers (BCNFs) were integrated into a jelly candy (JC) formulation to assess their influence on product characteristics

such as color and texture. In addition, the jelly candies were analyzed to evaluate the BCNFs' potential role in preserving the bioaccessibility of bioactive compounds—specifically total phenolic content (TPC), total flavonoid content (TFC), and antioxidant activity—during simulated gastrointestinal digestion. This approach enabled a deeper understanding of how HPM-treated BC behaves when mixed into food systems, highlighting its potential as a functional ingredient.

1.2 Hypothesis of the Research

This study aims to explore the following hypothesis:

1) The use of different types of tea, carbon source combinations, and variations in additives such as ethanol, yeast extract, vitamin C, soy protein isolate, and puree coffee will affect the yield and characteristics of the BC produced.

2) The use of different pH, harvesting times, tea concentrations, and cultivation methods will affect the yield and characteristics of the BC produced.

3) Response surface methodology (RSM) can be used for optimization of the best formulation to increase the yield of BC production.

4) The treatment methods of the high-pressure microfluidizer will result in different characteristics of the BCNFs produced.

5) BC can be used in the formulation of jelly candy (JC) and can affect its properties.

1.3 Objective of the Research

The research aims to achieve the following objectives:

1) To obtain the best types of tea, carbon sources, and additives on the yield of BC production.

2) To obtain the best pH of culture medium, harvesting time, tea concentration, and cultivation methods on the yield BC production.

3) To obtain the optimum condition for BC production using response surface methodology (RSM).

4) To obtain BCNFs from BC under different treatments of high pressure microfluidizer.

5) To develop a jelly candy (JC) formulation containing BC and bioactive ingredients

1.4 Expected Results of the Research

The expected results from this study are:

1) Knowledge on the best type of tea, carbon source combination, and additive type for the yield and characteristics of produced BC.

2) Knowledge on the effects of pH, harvesting time, tea concentration, and cultivation methods on the yield and characteristics of the produced BC.

3) Obtaining the best formulation for increasing the yield of BC using response surface methodology (RSM).

4) Knowledge on the effect of high-pressure microfluidizer treatment on the characteristics of BCNFs.

5) A prototype of a jelly candy product containing BC and bioactive compounds.

1.5 Scope of the Research

BC was produced using the kombucha fermentation method. The microbial starter used in this study was a symbiotic culture of bacteria and yeast (SCOBY) purchased online from Neo Cold Brew Thailand, a local supplier of kombucha cultures

and related products. The SCOBY was used directly after purchase and regenerated through standard cultivation methods, without further microbial identification.

Several experiments were conducted to investigate the effects of different types of tea, additives, carbon source combinations, initial pH levels, fermentation time, tea concentrations, and cultivation methods on the yield and characteristics of BC. Optimization of BC production was performed using response surface methodology (RSM) to determine the best production conditions based on these variables.

After optimization, BC was produced under the best conditions and further used to study the effects of mechanical treatment for the production of bacterial cellulose nanofibers (BCNFs). BCNFs were obtained from BC pulp using a high-pressure microfluidizer method, and their characteristics were examined. The BC pulp and BCNFs were first applied in the development of a JC formulation to identify the best texture and color properties, aiming to achieve a texture similar to the control sample. The optimized JC formulation was combined with selected bioactive ingredients to assess the role of BC as an effective delivery carrier. Subsequently, simulated gastrointestinal digestion was conducted to evaluate the impact of digestive processes on the bioaccessibility of bioactive compounds within the JC matrix.

1.6 Organization of the Research

The research comprises seven (7) chapters, structured as follows:

1) Chapter 1: Research Principles and Justification, including Background Information, Research Hypothesis, Research Objectives, Expected Results of the Research, and Research Scope.

2) Chapter 2: Literature Review including overview of the Kombucha (Tea in Thailand and Kombucha fermentation), BC (BC biosynthesis, BC production methods, Factors affecting BC production, Production of BCNFs, and Application of BC in nutraceutical), and Response Surface Methodology (RSM).

3) Chapter 3: Investigation of Factors Affecting Bacterial Cellulose Production and Characteristics from Thai Tea Kombucha, including Tea Varieties, Carbon Sources, Additives, Initial pH, Harvesting Time, Tea Concentration, and Cultivation Methods

4) Chapter 4: Study to optimize BC production from Thai red tea kombucha using central composite design (CCD) in response surface methodology (RSM)

5) Chapter 5: Study to explore the effect of High-Pressure Micro-fluidization on the Characteristics of BC Produced from Thai Red Tea Kombucha

6) Chapter 6: Study to explore the effect of high-pressure micro-fluidization on the characteristics of BC produced from Thai red tea kombucha

7) Chapter 7: Conclusion and Recommendation

1.7 References

Akintunde MO, Adebayo-Tayo BC, Ishola MM, et al (2022) Bacterial Cellulose Production from agricultural Residues by two Komagataeibacter sp. Strains. Bioengineered 13:10010–10025. https://doi.org/10.1080/21655979.2022.2062970

Aswini K, Gopal NO, Uthandi S (2020) Optimized culture conditions for bacterial cellulose production by Acetobacter senegalensis MA1. BMC Biotechnol 20:1–16. https://doi.org/10.1186/s12896-020-00639-6

Azeredo HMC, Barud H, Farinas CS, et al (2019) Bacterial Cellulose as a Raw Material for Food and Food Packaging Applications. Front. Sustain. Food Syst. 3:1–14

Börjesson M, Westman G (2015) Crystalline Nanocellulose — Preparation, Modification, and Properties. In: Cellulose - Fundamental Aspects and Current Trends Author. IntechOpen, pp 159–191

Choi SM, Rao KM, Zo SM, Shin EJ (2022) Bacterial Cellulose and Its Applications. Polymers (Basel) 14:1–44. https://doi.org/https://

doi.org/10.3390/polym14061080

Czernicka M, Zaguła G, Bajcar M, et al (2017) Study of nutritional value of dried tea leaves and infusions of black, green and white teas from Chinese plantations. Rocz Panstw Zakl Hig 68:237–245

El-Gendi H, Taha TH, Ray JB, Saleh AK (2022) Recent advances in bacterial cellulose: a low-cost effective production media, optimization strategies and applications. Cellulose 29:7495–7533

Gorgieva S, Trček J (2019) Bacterial cellulose: Production, modification and perspectives in biomedical applications. Nanomaterials 9:1–20. https://doi.org/10.3390/nano9101352

Jasmania L (2018) Preparation of nanocellulose and its potential application. For Res 7:014–021. https://doi.org/10.17352/2455-3492.000026

Jiang J, Zhu Y, Jiang F (2021) Sustainable isolation of nanocellulose from cellulose and lignocellulosic feedstocks: recent progress and perspectives. Carbohydr Polym 118188. https://doi.org/10.1016/j.carbpol.2021.118188

Kamal T, Ul-Islam M, Fatima A, et al (2022) Cost-Effective Synthesis of Bacterial Cellulose and Its Applications in the Food and Environmental Sectors. Gels 8:552

Kargarzadeh H, Ioelovich M, Ahmad I, et al (2017) Methods for Extraction of Nanocellulose from Various. In: Kargarzadeh H, Ahmad I, Thomas S, Dufresne. A (eds) Handbook ofNanocellulose and Cellulose Nanocomposites. Wiley-VCHVerlag GmbH& Co. KGaA, pp 1–49

Khan A, Wen Y, Huq T, Ni Y (2018) Cellulosic Nanomaterials in Food and Nutraceutical Applications: A Review. J Agric Food Chem 66:8–19. https://doi.org/10.1021/acs.jafc.7b04204

Klemm D, Heublein B, Fink H-P, Bohn A (2005) Cellulose: Fascinating Biopolymer and Sustainable Raw Material. Angew Chemie Int 44:3358–3393. https://doi.org/https://doi.org/10.1002/anie.200460587

Lin D, Liu Z, Shen R, et al (2020) Bacterial cellulose in food industry: Current research and future prospects. Int J Biol Macromol 158:1007–1019. https://doi.org/10.1016/j.ijbiomac.2020.04.230

Ludwicka K, Kaczmarek M, Białkowska A (2020) Bacterial nanocellulose—a biobased polymer for active and intelligent food packaging applications: Recent advances and developments. Polymers (Basel) 12:1–23. https://doi.org/10.3390/polym12102209

Mert ID (2020) The applications of microfluidization in cereals and cereal-based products: An overview. Crit Rev Food Sci Nutr 60:1007–1024. https://doi.org/10.1080/10408398.2018.1555134

Moran JI, Alvarez VA, Cyras VP, Vazquez A (2008) Extraction of cellulose and preparation of nanocellulose from sisal fiber. Cellulose 149–159. https://doi.org/10.1007/s10570-007-9145-9

Mulyadi I (2019) Isolasi dan Karakterisasi Selulosa : Review. J Santika UNPAM 1:177–182. https://doi.org/10.32493/jsmu.v1i2.2381

P. Winyayong (2007) Current Status and Future Prospect for Tea Production in Thailand. In: The 3rd International Conference on O-CHA (Tea) Culture and Science. The Organizing Committee of the 3rd International Conference on O-CHA (tea) Culture and Science, Shizouka city, pp MI-S-04

Peng BL, Dhar N, Liu HL, Tam KC (2011) Chemistry and applications of nanocrystalline cellulose and its derivatives: A nanotechnology perspective. Can. J. Chem. Eng. 89:1191–1206

Pongpruttikul P, Yamsa-ard S (2022) Market Opportunities and Accessibility for Consumers of Thai Tea : Trends, Trade, Consumer Behaviors, and Marketing Strategy in ASEAN. J Manag Sci Chiangrai Rajabhat Univ 17:23–42

Reiniati I (2017) Bacterial Cellulose Nanocrystals : Production and Application. The University of Western Ontario

Revin V, Liyaskina E, Nazarkina M, et al (2018) Cost-effective production of bacterial cellulose using acidic food industry by-products. Brazilian J Microbiol 49:151–159. https://doi.org/10.1016/j.bjm.2017.12.012

Singh O, Panesar PS, Chopra HK (2017) Response surface optimization for cellulose production from agro industrial waste by using new bacterial isolate Gluconacetobacter xylinus C18. Food Sci Biotechnol 26:1019–1028. https://doi.org/10.1007/s10068-017-0143-x

Tsouko E, Kourmentza C, Ladakis D, et al (2015) Bacterial cellulose production from industrial waste and by-product streams. Int J Mol Sci 16:14832–14849. https://doi.org/10.3390/ijms160714832

Ullah MW, Manan S, Kiprono S, Islam MU (2019) Synthesis , Structure , and Properties of Bacterial Cellulose. In: Huang J, Dufresne A, Lin N (eds) Nanocellulose: From Fundamentals to AdvancedMaterials, first. Wiley-VCHVerlag GmbH& Co. KGaA, pp 81–114

Waghmare PR, Patil SM, Jadhav SL, et al (2018) Utilization of agricultural waste biomass by cellulolytic isolate Enterobacter sp. SUK-Bio. Agric Nat Resour 52:399–406. https://doi.org/10.1016/j.anres.2018.10.019

Wang Y, Wei X, Li J, et al (2015) Study on nanocellulose by high pressure homogenization in homogeneous isolation. Fibers Polym 16:572–578. https://doi.org/10.1007/s12221-015-0572-1

www.prnewswire.com (2022) Polybion Completes Development of World's First Bacterial Cellulose Biomanufacturing Facility. https://www.prnewswire.com/news-releases/polybion-completes-development-of-worlds-first-bacterial-cellulose-biomanufacturing-facility-301501949.html. Accessed 6 Feb 2022

Yilmaz M, Goksungur Y (2024) Optimization of Bacterial Cellulose Production from Waste Figs by Komagataeibacter xylinus. Fibers 12:1–18. https://doi.org/10.3390/fib12030029

CHAPTER 2

LITERATURE REVIEWS

2.1 Kombucha

Kombucha is a type of fermented beverage product that is quite popular in the world community or international market. It originally came from Manchuria (northeast China) during the Tsin (Ling Chi) dynasty around 220 BCE and is believed to have arrived in Japan in 414 CE (Chakravorty et al. 2019). The name kombucha comes from the name of a Japanese physician and is now used to refer to slightly fermented teas (Chakravorty et al. 2019). Kombucha is usually made from tea-containing drinks such as black tea or green tea with the addition of sucrose and then fermented using a starter known as the SCOBY. In its development, kombucha can be made using various other ingredients, such as spice teas and other herbal teas.

2.1.1 Tea in Thailand

Tea is a popular and well-known beverage among the general population. Apart from water, tea is one of the most extensively consumed drinks in the world (Suteerapataranon et al. 2009). In general, the term "tea" refers to products derived from the leaves of plants belonging to the camellia family. The tea cultivars discovered and commercially produced in Thailand include *Camellia sinensis* var. *Assamica* and *Camellia sinensis* var. *Sinensis*, generally known as Chinese cultivars (Theppakorn et al. 2014).

The parts taken from the tea plant are the leaves, especially the top two leaves, and the shoots. The leaves are then processed into a variety of dried tea leaves, including black tea, green tea, oolong tea, and white tea. Drying, complete oxidation, and withering are the steps in the preparation of black tea. Green tea bypasses the oxidation process and results in a light green or golden tint. Oolong tea

is a mix of colors and flavors between black tea and green tea. Meanwhile, white tea is only withered and dried by steaming (Commins and Sampanvejsobha 2008). Assam tea is often utilized for green and black tea manufacture, while Chinese tea is mostly used for green and oolong tea production (Theppakorn et al. 2014). Assam tea is also commonly used to make red tea (Pongpruttikul and Yamsa-ard 2022).

Thailand is the 15th of the world's largest tea producers in the world with the production of 58,803.00 metric ton in 2019 (NationMaster.com 2023). Thai tea products such as black tea and green tea have gained popularity in the last three years, particularly with buyers from Western and Asian nations (Pongpruttikul and Yamsa-ard 2022). There are several commercial tea products available on the Thai market with different types, packing sizes, and prices, such as green tea, oolong tea, white tea, red tea, black tea, and barley tea (Teepprasarn 2015).

Tea contains nutrients and active components such as polyphenols, amino acids, vitamins, proteins, carbs, trace elements, and alkaloids such as caffeine (1,3,7-trimethylxanthine), theobromine, and theophylline that are beneficial to health (Fatima and Rizvi 2011). Various types of tea are made differently and may contain different ingredients. Aside from black and green tea, red Thai tea is a popular form of tea in Thailand. Red Thai tea is made with black tea and other herbs and spices, including star anise, cardamom, and tamarin seed (Devje 2022). Thai tea is a chilled drink made from strongly brewed Assam tea that has been sweetened with sugar and condensed milk. Additional ingredients may include orange blossom water, star anise, crushed tamarind seed, red and yellow food coloring, and sometimes other spices (Teapedia.org 2015). The nutrition facts of black tea, green tea, and spices used as additives in red Thai tea are demonstrated in **Table 2.1.**

Table 2.1 Nutritional value of green tea, black tea, and some spices used for additive in red Thai tea

Nutrient	Nutritional value per 100g						
	Black tea	Green tea	Star anise	Cardamom	Cinnamon	Cloves	Vanilla Extract*
Net carbohydrates	0.3g	7.16g	35.42g	40.47g	27.49g	31.63g	12.65g
Protein	0g	0g	17.6g	10.76g	3.99g	5.97g	0.06g
Fats	0g	0.18g	15.9g	6.7g	1.24g	13g	0.06g
Carbs	0.3g	7.16g	50.02g	68.47g	80.59g	65.53g	12.65g
Calories	1kcal	30kcal	337kcal	311kcal	274kcal	274kcal	288kcal
Fiber	0	0	14.6g	28g	53.1g	33.9g	0
Fructose	0	3.59g	0	0	1.11	1.07g	0
Sugar	0	6.87g	0	0	2.17g	2.38g	12.65g
Calcium	0	3mg	646mg	383mg	1002mg	632mg	11mg
Iron	0.02mg	0.02mg	36.96mg	13.97mg	8.32mg	11.83mg	0.12mg
Magnesium	3mg	1mg	170mg	229mg	60mg	259mg	12mg
Phosphorus	1mg	0	440mg	178mg	64mg	104mg	6mg
Potassium	37mg	5mg	1441mg	1119mg	431mg	1020mg	148mg
Sodium	3mg	2mg	16mg	18mg	10mg	277mg	9mg

Table 2.1 Nutritional value of green tea, black tea, and some spices used for additive in red Thai tea (Continued)

Nutrient	Nutritional value per 100g						
	Black tea	Green tea	Star anise	Cardamom	Cinnamon	Cloves	Vanilla Extract*
Zinc	0.02mg	0.01mg	5.3mg	7.47mg	1.83mg	2.32mg	0.11mg
Copper	0.01mg	0.01mg	0.91mg	0.38mg	0.34mg	0.37mg	0.07mg
Vitamin A	0	0	311IU	0	295IU	160IU	0
Vitamin E	0	0	0	0	2.32mg	8.82mg	0
Vitamin C	0	7.7mg	21mg	21mg	3.8mg	0.2mg	0
Vitamin B1	0	0.04mg	0.34mg	0.2mg	0.02mg	0.16mg	0.01mg
Vitamin B2	0.01mg	0	0.29mg	0.18mg	0.04mg	0.22mg	0.1mg
Vitamin B3	0		3.06mg	1.1mg	1.33mg	1.56mg	0.43mg
Vitamin B5	0.01mg	0	0.8mg	0	0.36mg	0.51mg	0.04mg
Vitamin B6	0		0.65mg	0.23mg	0.16mg	0.39mg	0.03mg
Vitamin K	0	0	0	0	0	141.8µg	0
Folate	5µg	0	10µg	0	6µg	25µg	0
Tryptophan	0	0	0	0	0.05mg	0.03mg	0
Threonine	0	0	0	0	0.14mg	0.18mg	0

Table 2.1 Nutritional value of green tea, black tea, and some spices used for additive in red Thai tea (Continued)

Nutrient	Nutritional value per 100g						
	Black tea	Green tea	Star anise	Cardamom	Cinnamon	Cloves	Vanilla Extract*
Isoleucine	0	0	0	0	0.15mg	0.24mg	0
Leucine	0	0	0	0	0.25mg	0.4mg	0
Lysine	0	0	0	0	0.24mg	0.37mg	0
Methionine	0	0	0	0	0.08mg	0.08mg	0
Phenylalanine	0	0	0	0	0.15 mg	0.23mg	0
Valine	0	0	0	0	0.22mg	0.34mg	0
Histidine	0	0	0	0	0.12mg	0.13mg	0
Saturated Fat	0	0	0.59g	0.68g	0.35g	3.95g	0.01g
Monounsaturated Fat	0	0	9.78g	0.87g	0.25g	1.39g	0.01g
Polyunsaturated fat	0	0	3.15g	0.43g	0.07g	3.61g	0

Source: (Foodstruct.com, 2022), (Nutrition-and-you.com, 2022)

2.1.2 Kombucha Fermentation

Kombucha tea is a traditional beverage product made from the fermentation of a tea and sugar solution using a kombucha starter, which contains bacteria such as *A. xylinum* and several other types of bacteria and other yeasts (Wistiana and Zubaidah 2015). The result of fermented kombucha tea is a suspension that can produce organic acids such as glucuronic acid, acetic acid, lactic acid, and folic acid, along with amino acids, vitamins, antibiotics, enzymes, and other products (Napitupulu and Lubis 2015).

Kombucha fermentation occurs in two stages: alcoholic fermentation and acetic acid fermentation. Yeast such as *S. cerevisiae* will break down sugar into alcohol, and acetic acid bacteria such as *A. xylinum* will oxidize the alcohol to acetic acid (Ardheniati and Amanto 2009). This continues until the sugar contained in the kombucha solution turns into organic acids needed by the body, such as acetic acid and others (Kustyawati and Ramli 2008). The resulting kombucha fermentation contains two phases: a floating biofilm and a sour liquid phase. The floating biofilm is known as BC, and the primary components of the liquid are acetic acid, gluconic acid, and ethanol, which are also present in the biofilm due to its high water absorption ability (Czaja et al. 2006).

In the kombucha fermentation process, BC can be produced as a by-product. This process can be simply illustrated in **Figure 2.1**. Bacteria can utilize several types of sugars, such as glucose and fructose, to be converted into various compounds or products, such as cellulose, gluconic acid, acetic acid, ethanol, and CO_2 (May et al. 2019).

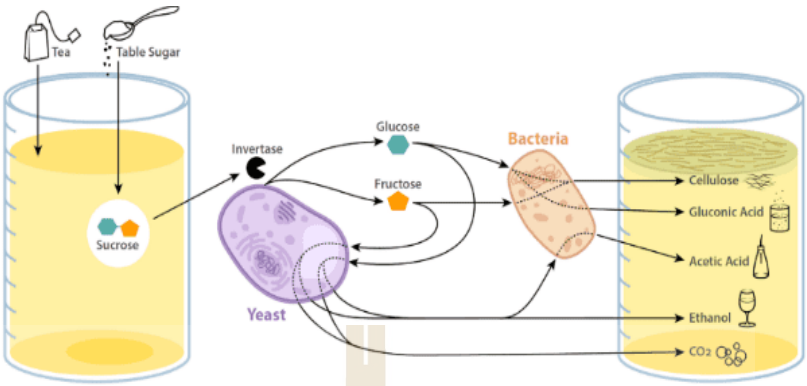

Figure 2.1 Formation of several types of compounds, including BC, in the fermentation of kombucha drinks (May et al. 2019)

2.2 Bacterial Cellulose

In general, cellulose is one of the main components of lignocellulosic materials and is mostly part of the plant cell wall along with other components such as hemicellulose, lignin, pectin, and wax (Mulyadi 2019). The composition of cellulose can reach one-third of the plant tissue and is the main component of several natural fibers such as cotton, flax, hemp, jute, and others (Moran et al. 2008). However, now cellulose has also been produced on a commercial scale using bacteria and is known as BC. The chemical structure of the cellulose polymer can be seen in **Figure 2.2.**

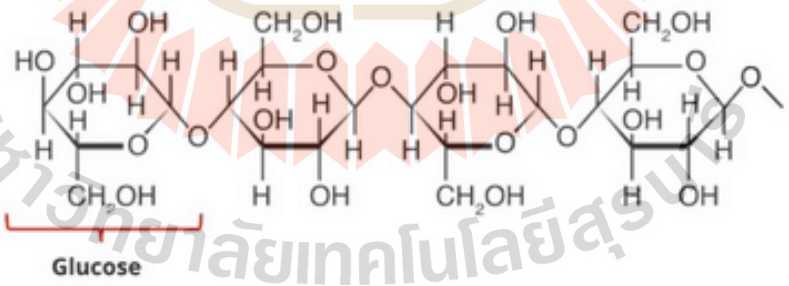

Figure 2.2 The structure of the cellulose chain composed of glucose monomers Source: (Amapex.net 2021)

BC, also known as bacterial nanocellulose (BNC), is cellulose synthesized by certain bacteria during the fermentation process. BC is produced as a metabolite from the activity of bacteria such as *A. xylinum* (Jasmania 2018). Bacteria use glucose or other carbohydrate foods to build cellulose through bacterial pathways (Dhali et al.

2021). Bacteria build cellulose (nanofiber) with nanoscale dimensions, with a nanometer diameter and length up to micrometers (Börjesson and Westman 2015). The diameter of BNCs usually ranges between 20 and 100 nm and is arranged in different types of nanofiber networks (Klemm et al. 2005). BC is called "bacteria nanocellulose" because the bacteria can only make cellulose on the nanoscale (Ho et al. 2022). Based on their length, BC can be classified as BCNFs (BC with longer whiskers) and BCNCs (BC with shorter whiskers) (Choi and Shin 2020).

Cellulose nanofibrils (CNFs) are the result of extraction from cellulose, which has a length ranging from 500–2000 nm and a width of about 20–50 nm with a flexible formation consisting of elementary nanofibrils (aggregates) composed of alternating crystalline and amorphous domains (Kargarzadeh et al. 2017). Meanwhile, crystalline nanocellulose (CNCs) is a type of nanocellulose that is also often referred to as nanocrystalline cellulose, nano whiskers, nanorods, and rod-like cellulose crystals (Kargarzadeh et al. 2017). CNCs have an elongated rod-like shape with less flexibility than CNFs due to their high crystallinity (Trache et al., 2020). CNCs are nanoparticles that range in size from 4 to 70 nm in width and 100 to 6,000 nm in length and have a crystallinity index of 54 – 88% (Naz et al. 2019).

BC is used in many applications due to its unique and good characteristics. Some of the unique properties of BC and its potential applications are demonstrated in **Table 2.2.**

2.2.1 Biosynthesis

Biosynthesis is a process in the cells of living organisms that is catalyzed by enzymes. The process transforms the substrate into a more complex product (bio.libretexts.org 2022). By using an envelope-spanning mechanism known as the BC complex synthase (BCS), bacteria may synthesize BC. The BCS gene cluster, which was initially discovered in *Gluconacetobacter* (Römling and Galperin 2015), encodes the BC complex synthase. In bacterial cultivation, gram-negative bacteria such as *Gluconacetobacter, Acetobacter, Agrobacterium, Achromobacter, Aerobacter,*

Sarcina, Azobacter, Rhizobium, Pseudomonas, Salmonella, and *Alcaligenes* frequently create extracellular BC (Chen et al. 2022).

Table 2.2 The unique characteristic of BC and Its potential application

Characteristics	Potential application	Reference
• Biodegradability • High purity • High Flexibility • High Water Holding Capacity • Hydrophilicity • High Crystallinity • Mouldability • Mechanical stability • High tensile strength	• Food packaging • Engineering of artificial skin, artificial blood vessels, wound dressing, nerve surgical covering, hemostatic material, electronic platforms, cartilage implants, and bone repair	(Ludwicka et al. 2020) (Gorgieva and Trček 2019)
• Thermostability • Biocompatibility • High degree of polymerization • Better biological adaptability	• A good prospect for a wide range of commercialization opportunities • Synthetic skin, cartilage, vessels, wound dressing, and delivery systems • Food industry	(Hussain et al. 2019) (Choi et al. 2022) (Lin et al. 2020)
• Highly porous structure • High permeability to liquids • Favorable for cell adhesion and proliferation	• Physics and chemistry, as well as medicine and mechanical engineering	(Volova et al. 2022)
• Considered as non-toxicity	• Food industry	(Dourado et al. 2017)

In conclusion, the BC production process can be summarized in two major stages: (1) the polymerization of β-1,4-glucan chains; and (2) the assembly and crystallization of these cellulose chains (Reiniati 2017). Additionally, Sutherland, (2001) outlines four key steps in the BC biosynthesis pathway: (1) activation of monosaccharides through the formation of sugar nucleotides; (2) polymerization into a repeating glucose chain; (3) elongation by the addition of glucose units; and (4) secretion of cellulose fibers through the bacterial cell membrane. The schematic representation of these biosynthetic pathways is illustrated in **Figure 2.3**.

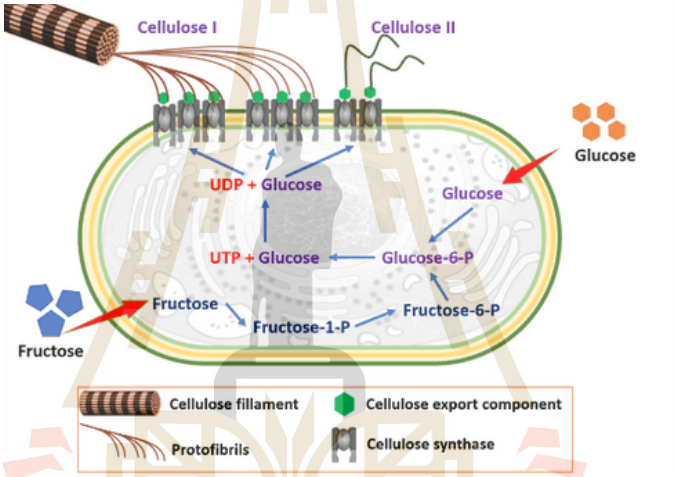

Figure 2.3 Schematic diagrams of BC biosynthesis by bacteria (Source: Modification of (Swingler et al. 2021))

2.2.2 Bacterial Cellulose Production

Bacterial nanocellulose (BNC) is cellulose produced during fermentation by certain bacteria. Utilizing glucose or other carbohydrates, bacteria employ bacterial processes to create cellulose (Dhali et al. 2021). The fermentation process to produce BC can be observed in the kombucha fermentation process, which produces a white layer on the surface of the broth. The general process of forming BC is illustrated in **Figure 2.4.**

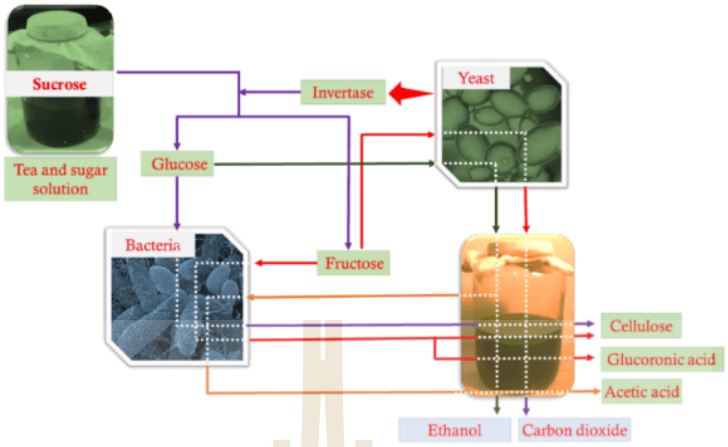

Figure 2.4 Schematic diagram of kombucha fermentation showing the production of BC and other compounds (source: modification of (May et al. 2019))

There are several cultivation methods that are commonly used in the process of producing BC, such as static cultivation, agitated cultivation (Azeredo et al. 2019a), and cultivation shaking methods (Ullah et al. 2019). Numerous factors, including the intended usage, morphology, and desirable BC properties, might affect the choice of the growing technique to be employed for the manufacture of BC (Zhong 2020). The cultivation method is discussed in more detail as follows:

1) Static Cultivation

The static cultivation method is a widely used and conventional approach for BC production (Ullah et al. 2019). In this method, a thick, white, jelly-like pellicle forms at the air–liquid interface of the fermentation vessel (Sharma et al. 2021). Despite its simplicity and broad application, static fermentation has several limitations, including long production times, high costs, uneven yields due to variable oxygen exposure among microbes, and depletion of carbon sources during fermentation (Swingler et al., 2021). Examples of BC production using this technique are presented in **Table 2.3.**

Table 2.3 Examples of some studies of BC production using static cultivation methods

Medium culture	Microorganisms / starter	Fermentation condition	Productivity	References
Hestrin-Schramm (HS) and its modification medium	*Gluconacetobacter hansenii* UCP1619	10 days, 30°C	51.8±0.6 g/L (ww)	(Costa et al. 2017)
Hestrin-Schramm (HS)	*G. xylinus* (ATCC No. 23768)	7–15 days, 28°C	-	(Badshah et al. 2018)
Hestrin-Schramm (HS)	*K. sucrofermentans* DSM 15973	7 days, 30°C	-	(Rovera et al. 2020)
Glycerol and Sunflower meal hydrolysate	*K. sucrofermentans* DSM 15973 strain	15 days, 30°C	Yield 0.6 g BC/g glycerol, 0.8 g/ (L.day)	(Efthymiou et al. 2022)

2) Agitated Cultivation

Ullah et al. (2019) mentioned that agitation cultivation can be used to produce BC in the form of granules and has a number of benefits over static and shaking cultivation, including a faster production rate, high cell density, and better cell contact with oxygen, thereby increasing productivity (Ullah et al. 2019). It has been suggested that agitated cultivation can boost production rates and the level of dissolved oxygen in the medium (Barja 2021a). BC produced in agitated cultivation has a different shape compared to that produced in static cultivation, which has shapes such as sphere-like, cocoon-like, or sometimes irregular clumps (Wang et al. 2019b).

Although agitation cultivation is believed to produce BC in a short time with high productivity, several studies report different results. The yield of BC produced by *G. xylinus* in static and agitated cultures was not significantly different (Ruka et al. 2015), as was the yield of BC produced by *Komagataeibacter* sp. CCUG73630 (Akintunde et al. 2022). Another study also reported the limitations of

agitated cultivation methods. Agitated bacteria can cause the mutation of bacteria into non-cellulosic bacteria, thereby reducing the productivity of BC (Barja 2021a; Choi et al. 2022). This method cannot be applied to all types of bacteria (Barja 2021a).

3) Shaking Cultivation

The shaking cultivation method is used for BC production in the form of pellets (Ullah et al. 2019). The expressions "shaking" and "agitated", although usually used synonymously to describe a bacterial culture state, are sometimes used in reports to denote different culture conditions. For example, the development of bacteria or microorganisms in an incubator with a rotator is usually referred to as "shaking", but the growth of bacteria or microorganisms in a reactor may be referred to as "agitation" (Ruka et al. 2015).

Ullah et al. (2019) have provided a detailed description of the shaking process, including the rate of shaking, which is typically expressed in rotations per minute (RPM), the time period of fermentation, which is typically 24 to 36 hours, and the BC product, which is in the form of small pellets with a variety of pellet shapes depending on the type of microbial strain, the incubation period, and the rate of shaking (Ullah et al. 2019). Shaken culture fermentation on BC synthesis was performed with *A. xylinum* bacteria in media containing pineapple waste under optimal conditions (pH 5, 120 rpm, 28°C) with the addition of microparticles, raising the BC yield to 15.19% (Pa et al. 2007).

2.2.3 Factor Affecting Bacterial Cellulose Production

Various factors can influence the fermentation process, including in the production of BC. Key parameters such as substrate type and concentration, fermentation duration, pH, temperature, and oxygen availability significantly affect both kombucha fermentation and BC yield (Villarreal-Soto et al. 2018a). Several nutrient sources, such as carbon, nitrogen, and caffeine, affect the fermentation substrate (Engström 2019). The surface area of the container and the depth of the culture medium are also important parameters (Engström 2019).

1) Microbial Starter

Microbial starters for BC production can be in the form of both monoculture and coculture (igem.org 2022). In the case of BC production using kombucha fermentation methods, the starter generally takes the form of a SCOBY. SCOBY is a cellulose biofilm generated by monosaccharide polymerization, and because of its similar form and look to the fruiting caps of macroscopic mushrooms, the SCOBY is also known as the tea mushroom (Kruk et al. 2021).

The SCOBY produced from kombucha production consists of many types of microorganisms from the genera of bacteria and yeast. A study of the composition of SCOBY starter cultures used by commercial kombucha brewers in North America showed that the most prevalent and abundant SCOBY taxa were the yeast genus *Brettanomyces* and the bacterial genus *Komagataeibacter* (Harrison and Curtin 2021). Some types of microorganisms found in kombucha starter, including bacteria such as *A. xylinum, A. aceti, A. pasteurianus, and Gluconobacter*, and yeasts, e.g. *Brettanomyces, B. bruxellensis, B. intermedius, Candida, C. fatama, Mycodicia, Saccharomyces, S. cerevisiae, S. cerevisiae* subsp. *Aceti, Schizo saccharomyces, Torula, Torulaspora delbrueckii, Torupsis, Zygosaccharomyces, Z. bailii, and Z. rouxii* (Greenwalt et al. 2000).

Different microbial species may produce BC with different yields and characteristics. Several selected bacteria grown in the same production media and conditions can produce BC with different yields (Angela et al. 2020). Furthermore, the inoculum concentration can affect the output of BC. According to research on different *Lactobacillus acidophilus* inoculum concentrations of 4%, 6%, 8%, and 10% (v/), a concentration of 6% (w/w) produces the best BC results of 1.843 g/L (dry weight) after 14 days fermentation (Jeff Sumardee et al. 2020).

2) Carbon Sources

Several studies have investigated the effect of different carbon sources on BC production during kombucha fermentation. While sucrose is the most

commonly used carbon source, alternative substrates such as honey have been studied for partial or complete substitution. Reported concentrations of sucrose range from 70 to 190 g/L, while honey has been tested in the range of 1% to 20% (v/v). Al-Kalifawi (2018) reported that 100 g/L sucrose resulted in the highest wet BC yield of 66 g/L, while 10% (v/v) honey yielded 41.64 g/L. Goh et al. (2012) observed that 9% (w/v) sucrose resulted in the highest BC yield after 8 days of fermentation; however, 10% was not tested in that study. Optimal conditions for BC production using kombucha have been reported as 1% tea and 10% sucrose, with a fermentation time of 18 days (Al-Kalifawi and Hassan 2014). A larger surface area was also found to enhance BC formation.

The use of a 5% dextrose concentration in kombucha fermentation produced the highest yield of BC compared to glucose, fructose, and sucrose (Trevino-Garza et al., 2020). The use of glycerol produced the highest yield of BC compared to sucrose, fructose, glucose, mannitol, and lactose in a fermentation using *K. rhaeticu* (De Souza et al. 2021). The study of *A. xylinum* BC production at the same concentration from several carbon sources with 5% sucrose as the control medium showed that mannitol, fructose, and glycerol yielded 5, 3.5, and 3 times higher, respectively, than sucrose, while glucose medium and lactose produced less BC compared to the production on sucrose medium Yodsuwan et al., 2012). The combination of sucrose and fructose (1:1) at a total of 2% w/v in the BC production medium using *G. persimmonis* GH-2 had the highest yield, followed by fructose : lactose and galactose : sucrose (Hungund et al. 2013).

3) Nitrogen Sources

Another substrate component that impacts the productivity of BC synthesis is nitrogen. Nitrogen is essential for cell formation and microbial growth during the fermentation process with microorganisms (Kim et al. 2021). Nitrogen is required for cell metabolism and accounts for 8–14% of the dry cell mass of bacteria (Yodsuwan et al. 2012). The utilization of an appropriate nitrogen source will boost BC

output (Engström 2019). The addition of a 0.1% (w/v) nitrogen source increased the productivity of BC by *Komagataeibacter* sp. bacteria, where beef extract produced the highest number of cellulose, followed by yeast extract, peptone, corn step liquor, and ammonium sulfate, respectively (Sutthiphatkul et al. 2020). The addition of some type of nitrogen source (at 0.5% concentration) to the HS medium in the fermentation to produce BC by *A. senegalensis* MA1 showed that yeast extract produced the highest yield of BC (Aswini et al. 2020).

4) Caffeine

Caffeine has been identified as a potential stimulator for BC production (Fontana et al. 1991). Black tea has a role as a source of caffeine in kombucha (Miranda et al. 2016). The presence of coffee ground (8 g/L) and sugarcane molasses increases the production of BC, but it can still be optimized (De Souza et al. 2021). The addition of coffee cherry husk (CCH) increased the yield of BC by more than three times (Rani and Appaiah 2013).

5) Trace Elements

The presence of trace elements in the medium has an impact on the yield of BC produced during fermentation. Almeida et al. reported that a number of trace elements were used during coconut water fermentation to produce BC (nata de coco). K (69%), Fe (84.3%), P (97.4%), SO_2^{-2} (64.9%), B (56.1%), NO_3^- (94.7%), and NH_4^+ (95.2%) are the most consumed ions in ripe coconut water fermentation. Na (94.5%) and Mg (67.7%) are the most consumed ions in green coconut water fermentation. Fermentation of cooked coconut water with the addition of KH2PO4, FeSO4, and NaH2PO4 was shown to produce the highest BC (6 g/L) (Almeida et al. 2013).

6) Environmental Conditions

Environmental elements including pH, temperature, the length of the fermentation process, and the presence of oxygen all have an impact on the formation of BC. When it comes to BC production, the surface area of the container

and the depth of the broth are also important aspects to consider (Goh et al. 2012; Al-Kalifawi 2018). The temperature range for BC production in the kombucha fermentation process is 20–50°C; also, 18 days of fermentation and a larger container surface area are ideal circumstances (Al-Kalifawi 2018). Similar results were found in another study, which asserted that fermentation in containers with larger surfaces results in the production of more BC from the same quantity of substrate (Goh et al. 2012). The pH of the production medium is another environmental factor that affects the amount of BC produced. According to some studies, the ideal pH for the production of BC is 4.5 for *A. senegalensis* MA1 (Aswini et al. 2020), 5 for *Bacillus* sp. strain SEE-12 (El-Naggar et al. 2022), and 5.45 for *G. sucrofermentans* B-11267 (Revin et al. 2018).

2.2.4 Production of Bacterial Cellulose nanofibrils (BCNFs)

BCNFs are products derived from BC. BCNF is a fiber with a diameter of 10–50 nm and a micrometer length that is flexible, contains crystalline and amorphous regions, and can be made by mechanical techniques (Zhang et al. 2022d). Several methods that can be used for the production of BCNF include high pressure homogenizer (HPH), hydrochloric acid hydrolysis, TEMPO ((2,2,6,6-tetramethylpiperidin-1-yl)oxidanyl) oxidation, or a combination of HPH and TEMPO oxidation (Li et al. 2018, 2021; Wu et al. 2021).

High-pressure homogenizer (HPH) is one of the general methods that is frequently used for BCNF production (Zhang et al. 2022d). A high-pressure microfluidizer (HPM) is a mechanical method that can be used for the manufacture of nanomaterials (Yang et al. 2019). A high-pressure microfluidizer works at a high pressure of more than 100 MPa (Zhou 2022). One use of these microfluidizer technologies is in the development of a drug nano delivery system (Ganesan et al. 2018). The schematic for the preparation of nanomaterials with microfluidizer technology is illustrated in **Figure 2.5**.

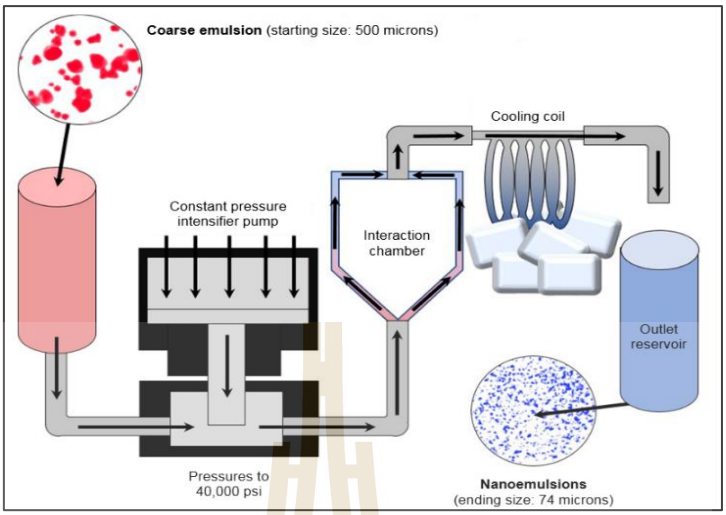

Figure 2.5 Schematic representation of the microfluidization process used to prepare the nano delivery system (Ganesan et al. 2018)

2.2.5 Application of BC in Nutraceutical

BC has been extensively researched and employed in the nutraceutical industry. Indeed, the phrases nutraceutical and functional food are still widely used interchangeably. Nonetheless, some literature defines the word nutraceutical. According to De Felice, nutraceuticals are "any substance that is a food or part of a food and provides medical or health benefits, including the prevention and treatment of disease" (DeFelice 1995). A nutraceutical is a substance derived by the isolation and purification of foodstuffs that is made in pharmaceutical form, is not related to food, and may obviously give physiological advantages or protection against chronic illness (Aronson 2017). Nutraceuticals are chemical or bioactive molecules with beneficial biological properties (Hoti et al. 2022).

Cellulosic nanoparticles can be used in nutraceuticals as emulsifiers, to immobilize bacterial and mammalian cells, to immobilize enzymes, and to immobilize bioactive compounds (Khan et al. 2018). Additionally, BC's inherent properties make it an intriguing candidate for use in nutraceuticals as a source of dietary fiber and meal replacement (Zhang et al. 2022c, b), immobilization agents (Jayani et al. 2020), and emulsifiers and Pickering emulsions (Z. Li et al., 2023). Following are the examples of the application of BC for nutraceutical.

1) BC for Dietary Fiber

A critical nutrient, dietary fiber, has been associated with reduced risks of obesity, diabetes, hypertension, coronary heart disease, cardiovascular disease, and stroke (Kushwaha and Maurya 2020), as well as enhanced digestive health (Guan et al. 2021). According to Shi et al. (2014), BC is a dietary fiber that has a number of benefits over other sources of dietary fiber, including high purity, the capacity to keep natural taste and color, and the capacity to be made in a variety of forms (Shi et al. 2014). According to studies, BC is used in foods like Nata de Coco, which is combined with other ingredients and processed into a fine powder for quick beverages. The instant drink's dietary fiber content ranged from 5.60 to 12.48% (Tangkanakul 2022). An ice cream product with a dietary fiber content of 2.39% was produced with the inclusion of 30% (w/w) wet BC and 1.4% (w/w) dry inulin in the creation of ice cream that was supplemented with dietary fiber (Xavier and Ramana 2022). In a different study, a meal replacement powder with a dietary fiber content of 15.09% was created by mixing buckwheat powder, fried cooked soybean powder, BC powder, konjac purified powder, and xylitol at a mass ratio of 80:60:20:3:1 (Zhang et al. 2022b).

2) BC for Immobilization Agents

BC and its derivative products have the potential to be used as cell immobilization agents, enzymes, and bioactive compounds (Khan et al. 2018). The purpose of immobilizing these samples is to prolong probiotic cell viability, enhance biocatalytic and enzyme processes, and protect enzymes from harmful environmental factors (Mitropoulou et al. 2013; Guzik et al. 2014; Maghraby et al. 2023).

The following research has looked into BC's potential as an immobilizing agent: The most efficient method for shielding bacteria from bile salts and digestive acids has been to employ BC to immobilize bacteria, such as *Lactobacillus* sp. (Fijałkowski et al. 2016). *L. acidophilus* 016 was a probiotic bacterium that was immobilized on BCNF and could last for up to 24 days, with 71% of the population surviving at 35°C (Jayani et al. 2020). Additionally, BC has been designed to

immobilize "ready-to-use" freeze-dried cultures of lactic acid bacteria, which are subsequently utilized in the fermentation of milk (Lappa et al. 2022). Lysozyme, an enzyme with antibacterial activity, has been immobilized using BC without significantly affecting its function. Additionally, the pH and temperature ranges for appropriate activity were widened, and the storage stability of enzymes was improved (Bayazidi et al. 2018).

3) BC for Emulsifier and Pickering Emulsions

Emulsions are dispersion systems composed of two immiscible liquids, usually water and oil, with the oil phase typically consisting of organic liquids (Chen et al. 2020). Pickering emulsions (PEs) are a specific kind of emulsion that is solely sustained by solid particles at the oil-water interface (Yang et al. 2017). The food sciences have recently been interested in pickling emulsions, a revolutionary technology (Chen et al. 2020). The use of BC in the creation of emulsifiers and PEs has been documented in a number of investigations. Particle stabilizers for high internal phase emulsions (HIPEs) have been made using BCNs and soy protein isolate (SPI) with an optimum BCNs/SPI ratio of 7:25, the findings demonstrated that BCNs considerably boosted the emulsifying ability (Liu et al. 2021). An increase in curcumin bioaccessibility to 30.54% was observed following encapsulation in curcumin-loaded HIPEs stabilized by BCNs and SPI colloidal particles, demonstrating high encapsulation efficiency and antioxidant activity (Shen et al. 2021).

4) BC for Personalized Nutrition

A fresh method for BC applications is personalized nutrition, which is founded on the idea that every individual is different and has distinct needs. In order to help an individual achieve personalized nutrition and healthy eating habits, personalized nutrition entails gathering genetic, phenotypic, medical, nutritional, and other significant facts about the individual that are pertinent (Chaudhary et al. 2021). Only a few publications are currently accessible that discuss the use of BC in the creation of individualized nutrition. Future applications of BC in the development of

customized nutrition can be guided by case studies in the production of low-fat 3D-printed cheese analogs and low-fat printable casein-based inks (Shahbazi et al. 2021b, a). Customized nutrition depending on a person's medical needs may be possible with the use of low-fat Pickering emulsions in 3D food printing (Shahbazi et al. 2021a). The use of 3D printing technology in the food industry has made edible components easily adjustable and capable of taking on a range of visually attractive designs (Shahbazi and Jäger 2021).

2.3 Response Surface Methodology (RSM)

Response surface methodology (RSM) is a group of mathematical and statistical methods used to plan experiments, adapt hypothesized models to data, and identify the best conditions to produce the most desired response (Khuri 2017). RSM is a technique for conducting design of experiments (DoE). According to Hadiyat (2012), RSM was originally introduced by Box and Wilson in 1951 as a version of DoE that not only examines the effect of experimental components but can also be used to determine the best points from multifactor experiments. DoE is a technique used to plan and analyze experiments, allowing a minimum number of experiments and varying several experimental parameters systematically and simultaneously (Whitford et al. 2018). Design of Experiment (DoE) is used to collect data and identify the principle of variables that influence process response, and RSM is used to determine the best parameter values to optimize process and equipment design (Hadiyat et al. 2022).

Central Composite Design (CCD) and Box-Behnken Design (BBD) are the two main design types used in RSM. Response surface design experiments using CCDs are the most popular. CCD is a factorial or fractional factorial design with a center point and a set of axial points (also known as star points) that allow curvature estimation, whereas BBD is a type of response surface design that excludes embedded factorial or fractional designs (support.minitab.com 2023). On CCD, the response data obtained is modeled with appropriate mathematical models such as average, linear, quadratic, 2-factor interaction (2FI), and cubic (Hidayat et al. 2020).

In practice, RSM is carried out using statistical software or programs such as SAS, MINITAB, STATISTICA, or Design Expert (Nassiri Mahallati 2020). Design-Expert is one such statistical program. It offers integrated design, robust parameter design, mix design, screening, characterization, and comparison testing (Tanco et al. 2008). It provides a test matrix to screen up to 50 variables and an analysis of variance (ANOVA) to ascertain its statistical significance. Tools for data visualization help identify abnormalities in the data and show how each factor affects the desired results (Comley 2009).

RSM is one of a common method used for optimizing production processes in fermentation techniques, including the production of BC. Studies have reported on the use of RSM in the production of BC, which primarily aims to increase the yield or productivity of BC. The process of cellulose production from *G. xylinus* C18 was optimized using RSM based on the CCD. The result showed that the maximum yield of BC (4.34 g/L) was reached at the best conditions, i.e., a sugarcane molasses concentration of 10.77% (w/v) supplemented with 12.47% (v/v) corn steep liquor, a temperature of 31°C, pH 6.5, and an incubation time of 172 h (Singh et al. 2017). A similar approach was applied to maximize BC production using *A. senegalensis* MA1. The ideal fermentation conditions were 50 ml/L of glycerol, 7.50 g/L of yeast extract at pH 6.0, and 7.76 g/L of polyethylene glycol 6000, which produced the maximum yield of 469.83 g/L (Aswini et al. 2020). Another study optimized the manufacture of nitrocellulose (NC) from BC to create a product with a high nitrogen content using the CCD of the RSM technique. The highest percentage nitrogen content of NC was 12.64% under the predicated ideal circumstances of mole ratio H_2SO_4/HNO_3 = 3:1 mol/mol, temperature = 35°C, and duration of 22 min (Roslan et al. 2019)

2.4 References

Akintunde MO, Adebayo-Tayo BC, Ishola MM, et al (2022) Bacterial Cellulose Production from agricultural Residues by two Komagataeibacter sp. Strains. Bioengineered 13:10010–10025. https://doi.org/10.1080/21655979.2022.2062970

Al-Kalifawi EJ, Hassan IA (2014) Factors Influence on the yield of Bacterial Cellulose of Kombucha (Khubdat Humza). Baghdad Sci J 11:1420–1428. https://doi.org/10.21123/bsj.11.3.1420-1428

Al-Kalifawi EJ (2018) Produce bacterial cellulose of kombucha (Khubdat Humza) from honey. J Genet Environ Resour Conserv 2:39–45

Almeida DM, Aparecida Prestes R, da Fonseca AF, et al (2013) Minerals consumption by Acetobacter xylinum on cultivation medium on coconut water. Brazilian J Microbiol 44:197–206. https://doi.org/10.1590/S1517-83822013005000012

Amapex.net (2021) Enzymatic hydrolysis of cellulosic biomass. https://amapex.net/enzymatic-hydrolysis-cellulosic-biomass/?lang=en. Accessed 8 Jun 2022

Angela C, Young J, Kordayanti S, et al (2020) Isolation and Screening of Microbial Isolates from Kombucha Culture for Bacterial Cellulose Production in Sugarcane Molasses Medium. KnE Life Sci 2020:111–127. https://doi.org/10.18502/kls.v5i2.6444

Ardheniati M, Amanto BS (2009) Kinetika fermentasi pada teh kombucha dengan variasi jenis teh berdasarkan pengolahannya Fermentation kinetics in kombucha tea with tea kind variation based on its processing. 7:48–55. https://doi.org/10.13057/biofar/f070106

Aronson JK (2017) Defining 'nutraceuticals': neither nutritious nor pharmaceutical. Br J Clin Pharmacol 83:8–19. https://doi.org/10.1111/bcp.12935

Aswini K, Gopal NO, Uthandi S (2020) Optimized culture conditions for bacterial cellulose production by Acetobacter senegalensis MA1. BMC Biotechnol 20:1–16. https://doi.org/10.1186/s12896-020-00639-6

Azeredo HMC, Barud H, Farinas CS, et al (2019) Bacterial Cellulose as a Raw Material for Food and Food Packaging Applications. Front. Sustain. Food Syst. 3:1–14

Badshah M, Ullah H, Khan AR, et al (2018) Surface modification and evaluation of bacterial cellulose for drug delivery. Int J Biol Macromol 113:526–533.

https://doi.org/10.1016/j.ijbiomac.2018.02.135

Barja F (2021) Bacterial nanocellulose production and biomedical applications. J Biomed Res 35:310–317. https://doi.org/https://doi.org/10.7555/JBR.35.20210036

Bayazidi P, Almasi H, Asl AK (2018) Immobilization of lysozyme on bacterial cellulose nanofibers: Characteristics, antimicrobial activity and morphological properties. Int J Biol Macromol 107:2544–2551. https://doi.org/10.1016/j.ijbiomac.2017.10.137

bio.libretexts.org (2022) Biosynthesis and Energy. https://bio.libretexts.org/Bookshelves/Microbiology/Microbiology_(Boundless)/05%3A_Microbial_Metabolism/5.12%3A_Biosynthesis/5.12B%3A_Biosynthesis_and_Energy. Accessed 15 Mar 2023

Börjesson M, Westman G (2015) Crystalline Nanocellulose — Preparation, Modification, and Properties. In: Cellulose - Fundamental Aspects and Current Trends Author. IntechOpen, pp 159–191

Chakravorty S, Bhattacharya S, Bhattacharya D, et al (2019) Kombucha: A promising functional beverage prepared from tea. In: Non-alcoholic Beverages: Volume 6. The Science of Beverages. Elsevier Inc., pp 285–327

Chaudhary N, Kumar V, Sangwan P, et al (2021) Personalized Nutrition and -Omics. Compr. Foodomics 495–507

Chen C, Ding W, Zhang H, et al (2022) Bacterial cellulose-based biomaterials: From fabrication to application. Carbohydr Polym 278:1–14. https://doi.org/10.1016/j.carbpol.2021.118995

Chen L, Ao F, Ge X, Shen W (2020) Food-grade pickering emulsions: Preparation, stabilization and applications. Molecules 25:. https://doi.org/10.3390/molecules25143202

Choi SM, Rao KM, Zo SM, Shin EJ (2022) Bacterial Cellulose and Its Applications. Polymers (Basel) 14:1–44. https://doi.org/https://doi.org/10.3390/polym14061080

Choi SM, Shin EJ (2020) The nanofication and functionalization of bacterial cellulose and its applications. Nanomaterials 10:. https://doi.org/10.3390/nano10030406

Comley J (2009) Design of experiments useful statistical tool in assay development or vendor disconnect! Drug Discov World 11:41–50

Commins T, Sampanvejsobha S (2008) Development of the tea industry in Thailand. Asian J Food Agro-Industry 1:1–16

Costa AFS, Almeida FCG, Vinhas GM, Sarubbo LA (2017) Production of Bacterial Cellulose by Gluconacetobacter hansenii Using Corn Steep Liquor As Nutrient Sources. Front Microbiol 8:1–12. https://doi.org/10.3389/fmicb.2017.02027

Czaja W, Krystynowicz A, Bielecki S, Brown RM (2006) Microbial cellulose - The natural power to heal wounds. Biomaterials 27:145–151. https://doi.org/10.1016/j.biomaterials.2005.07.035

De Souza KC, Trindade NM, De Amorim JDP, et al (2021) Kinetic study of a bacterial cellulose production by komagataeibacter rhaeticus using coffee grounds and sugarcane molasses. Mater Res 24:. https://doi.org/10.1590/1980-5373-MR-2020-0454

DeFelice SL (1995) The nutraceutical revolution: its impact on food industry R&D. Trends Food Sci Technol 6:59–61. https://doi.org/10.1016/S0924-2244(00)88944-X

Devje S (2022) What Is Thai Tea? Everything You Need to Know About This Sweet, Spiced Delight. https://www.healthline.com/nutrition/thai-tea#basics. Accessed 6 Feb 2023

Dhali K, Ghasemlou M, Daver F, et al (2021) Science of the Total Environment A review of nanocellulose as a new material towards environmental sustainability. Sci Total Environ 775:145871. https://doi.org/10.1016/j.scitotenv.2021.145871

Dourado F, Gama M, Rodrigues AC (2017) A Review on the toxicology and dietetic role of bacterial cellulose. Toxicol. Reports 4:543–553

Efthymiou MN, Tsouko E, Papagiannopoulos A (2022) Development of biodegradable films using sunflower protein isolates and bacterial nanocellulose as innovative food packaging materials for fresh fruit preservation. Sci Rep 12:1–13. https://doi.org/10.1038/s41598-022-10913-6

El-Naggar NEA, El-Malkey SE, Abu-Saied MA, Mohammed ABA (2022) Exploration of a novel and efficient source for production of bacterial nanocellulose, bioprocess optimization and characterization. Sci Rep 12:1–22. https://doi.org/10.1038/s41598-022-22240-x

Engström A (2019) Production of Bacterial Cellulose From Molasses By Kombucha Fermentation

Fatima M, Rizvi SI (2011) Health beneficial effects of black tea. Biomedicine 31:3–8

Fijałkowski K, Peitler D, Rakoczy R, Zywicka A (2016) Survival of probiotic lactic acid bacteria immobilized in different forms of bacterial cellulose in simulated gastric juices and bile salt solution. Lwt 68:322–328. https://doi.org/10.1016/j.lwt.2015.12.038

Fontana JD, Franco VC, De Souza SJ, et al (1991) Nature of plant stimulators in the production of Acetobacter xylinum ("tea fungus") biofilm used in skin therapy. Appl Biochem Biotechnol 28–29:341–351. https://doi.org/10.1007/BF02922613

Foodstruct.com. (2022). Encyclopedia of food & nutrition focused on comparison. https://foodstruct.com/

Ganesan P, Karthivashan G, Park SY, et al (2018) Microfluidization trends in the development of nanodelivery systems and applications in chronic disease treatments. Int J Nanomedicine 13:6109–6121. https://doi.org/10.2147/IJN.S178077

Goh WN, Rosma A, Kaur B, et al (2012) Fermentation of black tea broth (kombucha): I. effects of sucrose concentration and fermentation time on the yield of microbial cellulose. Int Food Res J 19:109–117

Gorgieva S, Trček J (2019) Bacterial cellulose: Production, modification and

perspectives in biomedical applications. Nanomaterials 9:1–20. https://doi.org/10.3390/nano9101352

Greenwalt CJ, Steinkraus KH, Ledford RA (2000) Kombucha, the fermented tea: microbiology, composition, and claimed health effects. J Food Prot 7:976–981. https://doi.org/doi: 10.4315/0362-028x-63.7.976

Guan ZW, Yu EZ, Feng Q (2021) Soluble dietary fiber, one of the most important nutrients for the gut microbiota. Molecules 26:1–15. https://doi.org/10.3390/molecules26226802

Guzik U, Hupert-Kocurek K, Wojcieszynska D (2014) Immobilization as a strategy for improving enzyme properties- Application to oxidoreductases. Molecules 19:8995–9018. https://doi.org/10.3390/molecules19078995

Hadiyat MA (2012) Response-surface dan Taguchi : Sebuah alternatif atau kompetisi dalam optimasi secara praktis. Pros Semin Nas Ind Madura 134–139

Hadiyat MA, Sopha BM, Wibowo BS (2022) Response Surface Methodology Using Observational Data: A Systematic Literature Review. Appl Sci 12:. https://doi.org/10.3390/app122010663

Harrison K, Curtin C (2021) Microbial composition of scoby starter cultures used by commercial kombucha brewers in North America. Microorganisms 9:1–21. https://doi.org/10.3390/microorganisms9051060

Hidayat IR, Zuhrotun A, Sopyan I (2020) Design-Expert Software sebagai Alat Optimasi Formulasi Sediaan Farmasi. Maj Farmasetika 6:99–120. https://doi.org/10.24198/mfarmasetika.v6i1.27842

Ho YS, Fahad Halim AFM, Islam MT (2022) The Trend of Bacterial Nanocellulose Research Published in the Science Citation Index Expanded From 2005 to 2020: A Bibliometric Analysis. Front Bioeng Biotechnol 9:1–18. https://doi.org/10.3389/fbioe.2021.795341

Hoti G, Matencio A, Pedrazzo AR, et al (2022) Nutraceutical Concepts and Dextrin-Based Delivery Systems. Int J Mol Sci 23:1–47.

https://doi.org/10.3390/ijms23084102

Hungund B, Prabhu S, Shetty C, et al (2013) Production of bacterial cellulose from gluconacetobacter persimmonis GH-2 using dual and cheaper carbon sources. J Microb Biochem Technol 5:31–33. https://doi.org/10.4172/1948-5948.1000095

Hussain Z, Sajjad W, Khan T, Wahid F (2019) Production of bacterial cellulose from industrial wastes: a review. Cellulose 26:2895–2911

igem.org (2022) Co-culture Modelling. https://2022.igem.wiki/calgary/production-co-culture-modelling. Accessed 6 Feb 2023

Jasmania L (2018) Preparation of nanocellulose and its potential application. For Res 7:014–021. https://doi.org/10.17352/2455-3492.000026

Jayani T, Sanjeev B, Marimuthu S, Uthandi S (2020) Bacterial Cellulose Nano Fiber (BCNF) as carrier support for the immobilization of probiotic, Lactobacillus acidophilus 016. Carbohydr Polym 250:116965. https://doi.org/10.1016/j.carbpol.2020.116965

Jeff Sumardee NS, Mohd-Hairul AR, Mortan SH (2020) Effect of inoculum size and glucose concentration for bacterial cellulose production by Lactobacillus acidophilus. IOP Conf Ser Mater Sci Eng 991:. https://doi.org/10.1088/1757-899X/991/1/012054

Kargarzadeh H, Ioelovich M, Ahmad I, et al (2017) Methods for Extraction of Nanocellulose from Various. In: Kargarzadeh H, Ahmad I, Thomas S, Dufresne. A (eds) Handbook ofNanocellulose and Cellulose Nanocomposites. Wiley-VCHVerlag GmbH& Co. KGaA, pp 1–49

Khan A, Wen Y, Huq T, Ni Y (2018) Cellulosic Nanomaterials in Food and Nutraceutical Applications: A Review. J Agric Food Chem 66:8–19. https://doi.org/10.1021/acs.jafc.7b04204

Khuri AI (2017) A General Overview of Response Surface Methodology. Biometrics Biostat Int J 5:87–93. https://doi.org/10.15406/bbij.2017.05.00133

Kim H, Song JE, Kim HR (2021) Comparative study on the physical entrapment of soy and mushroom proteins on the durability of bacterial cellulose bio-leather _ Enhanced Reader.pdf. Cellulose 28:3183–3200

Klemm D, Heublein B, Fink H-P, Bohn A (2005) Cellulose: Fascinating Biopolymer and Sustainable Raw Material. Angew Chemie Int 44:3358–3393. https://doi.org/https://doi.org/10.1002/anie.200460587

Kruk M, Trząskowska M, Ścibisz I, Pokorski P (2021) Application of the "scoby" and kombucha tea for the production of fermented milk drinks. Microorganisms 9:1–17. https://doi.org/10.3390/microorganisms9010123

Kushwaha R, Maurya NK (2020) Research Trends in Medicinal Plant Sciences, first. AkiNik Publications, New Delhi

Kustyawati ME, Ramli S (2008) Pemanfaatan Hasil Tanaman Hias Rosella Sebagai Bahan Minuman. In: Proceeding of National Seminar of Sciences ang Technology. Universitas Lampung, Lampung

Lappa IK, Kachrimanidou V, Alexandri M, et al (2022) Novel Probiotic/Bacterial Cellulose Biocatalyst for the Development of Functional Dairy Beverage. Foods 11:14. https://doi.org/10.3390/foods11172586

Li Q, Wang Y, Wu Y, et al (2018) Flexible Cellulose Nanofibrils as Novel Pickering Stabilizers: The Emulsifying Property and Packing Behavior. Food Hydrocoll. https://doi.org/10.1016/j.foodhyd.2018.09.039

Li Q, Wu Y, Fang R, et al (2021) Application of Nanocellulose as particle stabilizer in food Pickering emulsion: Scope, Merits and challenges. Trends Food Sci Technol 110:573–583. https://doi.org/10.1016/j.tifs.2021.02.027

Lin D, Liu Z, Shen R, et al (2020) Bacterial cellulose in food industry: Current research and future prospects. Int J Biol Macromol 158:1007–1019. https://doi.org/10.1016/j.ijbiomac.2020.04.230

Liu Z, Lin D, Shen R, Yang X (2021) Bacterial cellulose nanofibers improved the

emulsifying capacity of soy protein isolate as a stabilizer for pickering high internal-phase emulsions. Food Hydrocoll 112:106279. https://doi.org/10.1016/j.foodhyd.2020.106279

Ludwicka K, Kaczmarek M, Białkowska A (2020) Bacterial nanocellulose—a biobased polymer for active and intelligent food packaging applications: Recent advances and developments. Polymers (Basel) 12:1–23. https://doi.org/10.3390/polym12102209

Maghraby YR, El-Shabasy RM, Ibrahim AH, Azzazy HMES (2023) Enzyme Immobilization Technologies and Industrial Applications. ACS Omega 8:5184–5196. https://doi.org/10.1021/acsomega.2c07560

May A, Narayanan S, Alcock J, et al (2019) Kombucha: A novel model system for cooperation and conflict in a complex multi-species microbial ecosystem. PeerJ 2019:1–22. https://doi.org/10.7717/peerj.7565

Miranda B, Lawton NM, Tachibana SR, et al (2016) Titration and HPLC Characterization of Kombucha Fermentation: A Laboratory Experiment in Food Analysis. J Chem Educ 93:1770–1775. https://doi.org/10.1021/acs.jchemed.6b00329

Mitropoulou G, Nedovic V, Goyal A, Kourkoutas Y (2013) Immobilization technologies in probiotic food production. J Nutr Metab 2013:1–15. https://doi.org/10.1155/2013/716861

Moran JI, Alvarez VA, Cyras VP, Vazquez A (2008) Extraction of cellulose and preparation of nanocellulose from sisal fiber. Cellulose 149–159. https://doi.org/10.1007/s10570-007-9145-9

Mulyadi I (2019) Isolasi dan Karakterisasi Selulosa : Review. J Santika UNPAM 1:177–182. https://doi.org/10.32493/jsmu.v1i2.2381

Napitupulu MOW, Lubis L (2015) The Effect of Sugar Consentration and the Fermentation Time of Kombucha Coffee. J Rekayasa Pangan dan Pertan 3:316–322

Nassiri Mahallati M (2020) Advances in modeling saffron growth and development at

different scales. In: Saffron: Science, Technology and Health. INC, pp 139–167

NationMaster.com (2023) Thailand - Tea Production: Metric Tons - 1972 to 2019. https://www.nationmaster.com/nmx/timeseries/thailand-tea-production

Naz S, Ali JS, Zia M (2019) Nanocellulose isolation characterization and applications: a journey from non-remedial to biomedical claims. Bio-Design Manuf 2:187–212. https://doi.org/10.1007/s42242-019-00049-4

Nutrition-and-you.com. (2022). Welcome to nutrition facts information blog! https://www.nutrition-and-you.com/

Pa N, Chia Hui N, Idayu Muhamad I (2007) Shaken Culture Fermentation for Production of Microbial Cellulose From Pineapple Waste. In: In: International Conference and Exhibition of Waste to Wealth (W2W). Kuala Lumpur, Malaysia. Kuala Lumpur, Malaysia, pp 1–10

Pongpruttikul P, Yamsa-ard S (2022) Market Opportunities and Accessibility for Consumers of Thai Tea : Trends, Trade, Consumer Behaviors, and Marketing Strategy in ASEAN. J Manag Sci Chiangrai Rajabhat Univ 17:23–42

Rani MU, Appaiah KAA (2013) Production of bacterial cellulose by Gluconacetobacter hansenii UAC09 using coffee cherry husk. J Food Sci Technol 50:755–762. https://doi.org/10.1007/s13197-011-0401-5

Reiniati I (2017) Bacterial Cellulose Nanocrystals : Production and Application. The University of Western Ontario

Revin V, Liyaskina E, Nazarkina M, et al (2018) Cost-effective production of bacterial cellulose using acidic food industry by-products. Brazilian J Microbiol 49:151–159. https://doi.org/10.1016/j.bjm.2017.12.012

Römling U, Galperin MY (2015) Bacterial cellulose biosynthesis: diversity of operons, subunits, products and functions. Trends Microbiol 23:545–557. https://doi.org/10.1016/j.tim.2015.05.005.Bacterial

Roslan NJ, Jamal SH, Rashid JIA, et al (2019) Response Surface Methodology for

Optimization of Nitrocellulose from Bacterial Cellulose Nata De Coco for Potential Propellant Application. 1–15

Rovera C, Fiori F, Trabattoni S, et al (2020) Enzymatic hydrolysis of bacterial cellulose for the production of nanocrystals for the food packaging industry. Nanomaterials 10:1–11. https://doi.org/10.3390/nano10040735

Ruka DR, Simon GP, Dean KM (2015) Bacterial Cellulose and Its Use in Renewable Composites. In: Nanocellulose Polymer Nanocomposites. Scrivener Publishing LLC, pp 89–130

Shahbazi M, Jäger H (2021) Current Status in the Utilization of Biobased Polymers for 3D Printing Process: A Systematic Review of the Materials, Processes, and Challenges. ACS Appl Bio Mater 4:325–369. https://doi.org/10.1021/acsabm.0c01379

Shahbazi M, Jäger H, Ettelaie R (2021a) Application of Pickering emulsions in 3D printing of personalized nutrition. Part II: Functional properties of reduced-fat 3D printed cheese analogues. Colloids Surfaces A Physicochem Eng Asp 624:1–17. https://doi.org/10.1016/j.colsurfa.2021.126760

Shahbazi M, Jäger H, Ettelaie R, Chen J (2021b) Construction of 3D printed reduced-fat meat analogue by emulsion gels. Part I: Flow behavior, thixotropic feature, and network structure of soy protein-based inks. Food Hydrocoll 120:1–16. https://doi.org/10.1016/j.foodhyd.2021.106967

Sharma C, Bhardwaj NK, Pathak P (2021) Static intermittent fed-batch production of bacterial nanocellulose from black tea and its modification using chitosan to develop antibacterial green packaging material. J Clean Prod 279:123608. https://doi.org/10.1016/j.jclepro.2020.123608

Shen R, Lin D, Liu Z, et al (2021) Fabrication of Bacterial Cellulose Nanofibers/Soy Protein Isolate Colloidal Particles for the Stabilization of High Internal Phase Pickering Emulsions by Anti-solvent Precipitation and Their Application in the Delivery of Curcumin. Front Nutr 8:1–16.

https://doi.org/10.3389/fnut.2021.734620

Shi Z, Zhang Y, Phillips GO, Yang G (2014) Utilization of bacterial cellulose in food. Food Hydrocoll 35:539–545. https://doi.org/10.1016/j.foodhyd.2013.07.012

Singh O, Panesar PS, Chopra HK (2017) Response surface optimization for cellulose production from agro industrial waste by using new bacterial isolate Gluconacetobacter xylinus C18. Food Sci Biotechnol 26:1019–1028. https://doi.org/10.1007/s10068-017-0143-x

support.minitab.com (2023) What are response surface designs, central composite designs, and Box-Behnken designs? https://support.minitab.com/en-us/minitab/21/help-and-how-to/statistical-modeling/doe/supporting-topics/response-surface-designs/response-surface-central-composite-and-box-behnken-designs/. Accessed 5 Jun 2023

Suteerapataranon S, Butsoongnern J, Punturat P, et al (2009) Caffeine in Chiang Rai tea infusions: Effects of tea variety, type, leaf form, and infusion conditions. Food Chem 114:1335–1338. https://doi.org/10.1016/j.foodchem.2008.11.013

Sutherland IW (2001) Microbial polysaccharides from Gram-negative bacteria. 11:663–674

Sutthiphatkul T, Suwanposri A, Ochaikul D (2020) Optimization of Bacterial Cellulose Production from Wastewater of Noodle Processing by Komagataeibacter sp . PAP1 and Bio-Cellulose Paper Production. Walailak J Sci Tech 17:1241–1251

Swingler S, Gupta A, Gibson H, et al (2021) Recent Advances and Applications of Bacterial Cellulose in Biomedicine. Polymers (Basel) 13:1–29. https://doi.org/https://doi.org/10.3390/polym13030412

Tanco M, Viles E, Ilzarbe L, Álvarez MJ (2008) Dissecting DoE Software. SIX SIGMA FORUM Mag. 25–29

Tangkanakul P (2022) Designing Instant High Fiber Beverage with Nata de Coco. Food 32:270–278

Teapedia.org (2015) Thai Tea. https://teapedia.org/en/Thai_Tea. Accessed 6 Feb 2023

Teepprasarn W (2015) The Study of Unmet Needs of Instant Tea Product In Thai Consumers: New Opportunities for New Product In Thai Market. Thammasat University

Theppakorn T, Luthfiyyah A, Ploysri K (2014) Comparison of the Composition and Antioxidant Capacities of Green Teas Produced From the Assam and the Chinese Varieties Cultivated in Thailand. J Microbiol Biotechnol food Sci 3:364–370

Trache, D., Tarchoun, A. F., Derradji, M., Hamidon, T. S., Masruchin, N., Brosse, N., & Hussin, M. H. (2020). Nanocellulose : From Fundamentals to Advanced Applications. Frontiers in Microbiology, 8(May), 1–33. https://doi.org/10.3389/fchem.2020.00392

Ullah MW, Manan S, Kiprono S, Islam MU (2019) Synthesis , Structure , and Properties of Bacterial Cellulose. In: Huang J, Dufresne A, Lin N (eds) Nanocellulose: From Fundamentals to AdvancedMaterials, first. Wiley-VCHVerlag GmbH& Co. KGaA, pp 81–114

Villarreal-Soto SA, Beaufort S, Bouajila J, et al (2018) Understanding Kombucha Tea Fermentation: A Review. J. Food Sci. 83:580–588

Volova TG, Prudnikova S V., Kiselev EG, et al (2022) Bacterial Cellulose (BC) and BC Composites: Production and Properties. Nanomaterials 12:. https://doi.org/10.3390/nano12020192

Wang J, Tavakoli J, Tang Y (2019) Bacterial cellulose production , properties and applications with di ff erent culture methods – A review. Carbohydr Polym 219:63–76. https://doi.org/10.1016/j.carbpol.2019.05.008

Whitford WG, Lundgren M, Fairbank A (2018) Cell Culture Media in Bioprocessing. Elsevier Ltd.

Wistiana D, Zubaidah E (2015) Chemical and Microbiological Characteristics of Kombucha from Various High Leaf Phenols During Fermentation. J Pangan dan Agro Ind 3:1446–1457

Wu Y, Zhang X, Qiu D, et al (2021) Effect of surface charge density of bacterial cellulose nanofibrils on the rheology property of O/W Pickering emulsions. Food Hydrocoll 120:106944. https://doi.org/10.1016/j.foodhyd.2021.106944

Xavier JR, Ramana KV (2022) Development of slow melting dietary fiber-enriched ice cream formulation using bacterial cellulose and inulin. J Food Process Preserv 46:1–8. https://doi.org/10.1111/jfpp.15394

Yang Y, Chen Z, Zhang J, et al (2019) Preparation and Applications of the Cellulose Nanocrystal. Int J Polym Sci 2019:. https://doi.org/10.1155/2019/1767028

Yang Y, Fang Z, Chen X, et al (2017) An Overview of Pickering Emulsions : Solid-Particle Materials , Classification , Morphology , and Applications. Front Pharmacol 8:1–20. https://doi.org/10.3389/fphar.2017.00287

Yodsuwan N, Owatworakit A, Ngaokla A, et al (2012) Effect of Carbon and Nitrogen Sources on Bacterial Cellulose Production for Bionanocomposite Materials. Sch Sci Mae Fah Luang Univ Technol Instruments Cent (STIC), Mae 2005–2010

Zhang W, Li Y, Zhang L, et al (2022a) Preparation of meal replacement powder based on bacterial cellulose/konjac glucomannan and its influence on sugar metabolism. Lwt 169:113954. https://doi.org/10.1016/j.lwt.2022.113954

Zhang W, Zhang Q, Wang J, et al (2022b) Efficiency Assessment of Bacterial Cellulose on Lowering Lipid Levels In Vitro and Improving Lipid Metabolism In Vivo. 1–17

Zhang X, Wang D, Liu S, Tang J (2022c) Bacterial Cellulose Nanofibril-Based Pickering Emulsions: Recent Trends and Applications in the Food Industry. Foods 11:1–16. https://doi.org/10.3390/foods11244064

Zhong C (2020) Industrial-Scale Production and Applications of Bacterial Cellulose. Front. Bioeng. Biotechnol. 8:1–19

Zhou Y (2022) Research Progress in Preparation, Stability and Application of Nanoemulsion. J Phys Conf Ser 2152:. https://doi.org/10.1088/1742-6596/2152/1/012044

CHAPTER 3

PRE-OPTIMIZATION OF BACTERIAL CELLULOSE PRODUCTION: INVESTIGATING KEY FACTORS AFFECTING YIELD AND PROPERTIES

3.1 Abstract

Bacterial cellulose (BC) is a high-value biopolymer with broad applications in food, biomedical, and material sciences. However, its production is constrained by the high cost of traditional culture media. This study explores the use of Thai tea kombucha as a low-cost and culturally relevant medium for BC production, with the goal of identifying favorable conditions for subsequent process optimization. The study was conducted under static conditions at 30 °C for 15 days using a commercial SCOBY as the inoculum. Four types of tea—Chinese Black Tea (RBTH), *Assamica* Black Tea (BTC), Thai Green Tea (GTC), and Thai Red Tea (RTC)—were evaluated. Among them, RTC produced the highest wet BC yield (168.00 ± 2.93 g/L), making it the most promising substrate. To further explore yield enhancement, RTC-based media were supplemented with various additives (ethanol, pure coffee, yeast extract, soy protein isolate, and vitamin C) and different carbon source combinations. The highest yield was obtained with ethanol supplementation (RTC-EtOH, 218.36 ± 12.85 g/L) and the sucrose-glucose combination (RTC-SGlu, 259.54 ± 8.92 g/L), though not significantly different from RTC-sucrose-dextrose. Further investigation of basic fermentation parameters—including initial pH, tea concentration, cultivation duration, and harvesting frequency—revealed that unadjusted pH (~5.20), tea concentrations of 2%, and bi-weekly harvesting over four weeks yielded the best results (368.22 ± 28.33 g/L cumulative). Characterization of the resulting BC using SEM, FTIR, XRD, TGA/DTG, and nanoindentation confirmed acceptable physical and chemical properties, including good fiber structure, crystallinity, thermal stability, and mechanical strength. This

preliminary study establishes the suitability of Thai red tea kombucha as a viable fermentation medium. It provides essential baseline data to guide the statistical optimization in the next phase of research.

Keywords: Bacterial nanocellulose, Thai tea, kombucha, mechanical properties, nano-indentation

3.2 Introduction

Bacterial cellulose (BC) is a sustainable and multifunctional biomaterial distinguished by its exceptional mechanical strength, high crystallinity, purity, and biocompatibility (Lin et al. 2020). Unlike plant-derived cellulose, BC is extracellularly synthesized by *Komagataeibacter* spp. as a nanofibrillar network, free of lignin and hemicellulose contaminants (Gorgieva and Trček 2019). Its unique properties have enabled diverse applications in the food industry, where it serves as a food ingredient, fat replacer, dietary fiber, thickening agent, and stabilizer in emulsions (Reiniati 2017; Lin et al. 2020). BC has also been incorporated into functional foods and traditional desserts, as well as employed as a carrier for bioactive compounds such as antioxidants, probiotics, and enzymes (Khan et al. 2018; Azeredo et al. 2019a; Li et al. 2021).

Despite these advantages, commercial BC production remains limited due to the high costs associated with conventional media, which typically utilize purified glucose and refined nutrients (Revin et al. 2018; El-Gendi et al. 2022; Kamal et al. 2022). In response, research has focused on exploring low-cost substrates such as agricultural by-products, food industry residues, and waste biomass to reduce production costs (Tsouko et al. 2015; Waghmare et al. 2018; Akintunde et al. 2022). Among these, kombucha fermentation—employing a symbiotic culture of bacteria and yeast (SCOBY)—has gained attention as an eco-friendly, scalable, and cost-effective system for BC production (Dhali et al. 2021) (Mehrotra et al. 2023). Using simple ingredients like tea and sugar, kombucha fermentation can produce BC with properties comparable to those obtained from synthetic media. However, BC yield and quality in

this system are highly sensitive to multiple variables, including tea type, sugar composition, fermentation conditions, and microbial dynamics.

Thailand offers a wide diversity of tea products, such as black tea, green tea, and Thai red tea, that present promising substrates for BC production. Variations in tea processing methods lead to differences in nutrient composition, potentially influencing microbial metabolism and BC yield (Shevchuk et al. 2020; Deka et al. 2021). Thai red tea, often a blend of black tea with herbs, spices, and colorants, may introduce unique bioactive compounds not present in other teas. While some studies have investigated black and green teas for BC production, systematic comparisons across diverse Thai teas remain limited.

Beyond tea type, numerous studies have shown that additives and carbon source variations can further enhance BC yield and tailor its properties. Additives such as vitamin C (VC) act as antioxidants and metabolic cofactors, improving crystallinity and yield (Keshk 2014; Cielecka et al. 2021; Leonarski et al. 2021a). Nitrogen sources like yeast extract (YE) and soy protein isolate (SPI) supply essential nutrients for bacterial growth (Aswini et al. 2020; Almihyawi et al. 2024) (Wen et al. 2024). Ethanol can optimize metabolic pathways, increasing glucose utilization and cellulose biosynthesis (Kazemi et al. 2015; Agustin and Padmawijaya 2018; Montenegro-Silva et al. 2024). Similarly, coffee-based additives rich in phenolic compounds serve as stimulants and alternative carbon sources (De Souza et al. 2021; Jiménez-Sánchez et al. 2024).

The selection and combination of carbon sources also critically influence BC production. Different substrates are metabolized via distinct pathways, affecting both yield and productivity. Glucose and dextrose are quickly utilized through glycolysis, while fructose contributes via both glycolysis and the TCA cycle (Wang et al. 2018; Trevino-Garza et al. 2020). Glycerol not only serves as a carbon source but also promotes microbial viability as an osmoprotectant (Aswini et al. 2020). Various studies have reported that glycerol consistently enhances BC yield compared to other sugars,

while optimal sucrose concentrations and honey have also shown promising results (Kalifawi 2018; Trevino-Garza et al. 2020; De Souza et al. 2021; Amorim et al. 2024).

In addition to substrate composition, process parameters such as initial pH, fermentation time, tea concentration, and cultivation method play crucial roles in determining BC productivity and characteristics. Moderate acidity (around pH 5) generally favors BC synthesis, while extreme pH levels can inhibit microbial growth (Tsouko et al. 2015). Extended fermentation time allow thicker BC pellicle formation but may ultimately reduce quality due to nutrient depletion and microbial senescence (Lin et al. 2013). Tea provides essential bioactive compounds—including polyphenols, caffeine, and minerals—that stimulate microbial activity, but excessive concentrations may disrupt fermentation balance (Mann et al. 2017). Cultivation methods also influence production outcomes: static culture produces high-quality BC but at lower yields, whereas dynamic systems (agitation or shaking) often enhance yield and homogeneity at the potential cost of reduced mechanical properties (Wang et al. 2019b; Gao et al. 2020; Lahiri et al. 2021; Akintunde et al. 2022).

This study investigated key factors influencing BC productivity with the aim of identifying conditions conducive to further optimization. The variables examined include the type of Thai tea—Chinese Black Tea (RBTH), *Assamica* Black Tea (BTC), Thai Green Tea (GTC), and Thai Red Tea (RTC); various additives—vitamin C (VC) as a metabolic enhancer, yeast extract (YE) and soy protein isolate (SPI) as nitrogen sources, ethanol (EtOH) as a metabolic modulator, and pure coffee (PC) as a phenolic stimulant; combinations of carbon sources—sucrose (control), sucrose-glucose (S-Glu), sucrose-dextrose (SD), sucrose-fructose (SF), and sucrose-glycerol (SGLy); as well as initial pH, fermentation duration, tea concentration, and cultivation method. The findings are expected to contribute to the development of optimized and cost-effective strategies for enhanced BC production.

3.3 Materials and Methods

The materials used in this study include a commercial kombucha starter (SCOBY) from Neo Cold Brew Shop (Thailand), sucrose, various teas (red tea-vanilla flavor (*ChaTraMue*, RTC), green tea mix (*ChaTraMue*, GTC), black tea (*ChaTraMue*, BTC), and Chinese black tea (Three Horses brand No. 3, RBTH)), Various of additives (yeast extract (Merck), ethanol absolute anhydrous (Carlo Erba), commercial vitamin C (Bright Aromatic and Chemical, Thailand), commercial soy protein isolate (KME Mart, Thailand), and commercial pure coffee (Nescafe gold brand)), and various carbon sources (D-glucose (UniVAR, Merck), D-fructose (Carlo Erba), sucrose (ACI Labscan), dextrose monohydrate (KC, Bangkok Chemical), and glycerol (Merck). Other chemicals include sodium hydroxide (NaOH, Q RëC™) and hydrochloric acid 37% (HCl, Q RëC™). Water sources included reverse osmosis (RO) and deionized (DI) water.

Equipment used consisted of a cheesecloth, coffee filter, glass jar, funnel, autoclave (Biobase), laboratory glassware, biosafety cabinet (Cryste, Puricube Neo), analytical balance (AE Nimbus NBL 84E), incubator, pH meter (Oakton pH 700), refractometer, oven dryer (XUE058, France-Etuves), FT-IR (Bruker VERTEX 70), XRD (Bruker D8 Advance), SEM (Zeiss AURIGA, Germany), nanoindenter (NanoTest Vantage, Micro Materials Limited, UK), and HPLC (Hitachi Chromaster: RI detector 5450, column oven 5310, auto sampler 5260, and pump 5110).

3.3.1 Experimental Design

This study was designed to systematically evaluate the key factors influencing BC production in a kombucha-based fermentation system. The primary objective was to identify the most effective conditions for maximizing BC yield. In addition to measuring BC yield, selected physicochemical properties of the resulting BC were characterized, along with kombucha culture parameters to support a more comprehensive understanding of the fermentation process. The experimental framework consisted of four main studies, each targeting a different set of variables, as outlined below:

1) Effect of Different Thai Tea Types on BC Yield and Characteristics

This experiment aimed to evaluate the impact of different Thai tea substrates on BC production through kombucha fermentation. Four commercially available Thai teas with distinct compositions were selected, including traditionally used teas—such as Assam-type black tea and Chinese black tea—and flavored blends that are less common in conventional kombucha fermentation. The selection was guided by practical considerations, including local availability, affordability, and insights from previous scientific studies. Market surveys, both online and offline, indicated that some teas were more accessible and cost-effective, making them suitable candidates for reducing production costs. All samples were fermented under identical conditions to assess their influence on BC yield and properties. Detailed descriptions of the tea types and their compositions are provided in **Table 3.1.**

Table 3.1 Thai tea type variations and their compositions used as substrates in kombucha fermentation for BC production

Variation of tea	Samples Code	Composition of tea*
Chines Black Tea (Three Horses Brand No. 3)	RBTH	Dried Chinese tea leaves (100%).
Assamica Black Tea (ChaTraMue Brand)	BTC	Black tea powder (Assam) (100%).
Assamica Green Tea Mix (*ChaTraMue* Brand)	GTC	Green tea powder (Assam) (94%), sugar (5%), nature identical flavor, FD&C Yellow No. 5 (INS 102), FD&C Yellow No. 6 (INS 110), FD&C Blue No. 1 (INS 133)
Assamica Red Tea Powder-Vanilla Flavor (*ChaTraMue* Brand)	RTC	Red tea powder (Assam) 94%, sugar 5%, artificial flavors, FD&C Yellow No. 6 (INS 110)

**Based on product label information available on the packaging.*

The fermentation broth was characterized for pH, total soluble solids (°Brix), and sugar composition before and after fermentation using standard analytical methods. The BC produced was evaluated for wet and dry yield, water holding capacity (WHC), visual appearance, and color. Surface morphology was examined using scanning electron microscopy (SEM), and chemical functional groups were identified through Fourier-transform infrared spectroscopy (FTIR). Crystallinity and crystallite size were determined using X-ray diffraction (XRD), while thermal behavior was assessed by thermogravimetric analysis (TGA). Mechanical properties of the BC were measured using nanoindentation.

2) Effect of Different Types of Additives on BC Yield and Characteristics

This study examined the effects of five different additives—selected for their distinct nutritional and functional properties—on the productivity and characteristics of BC. Thai red tea (RTC), identified as the optimal substrate from the previous experiment, was used as the fermentation medium. The additives were chosen based on prior studies indicating their potential to enhance microbial growth, stimulate BC biosynthesis, or improve product quality. Each additive was incorporated at predetermined concentrations, as detailed in **Table 3.2**.

Table 3.2 Types of additives incorporated into the fermentation medium for BC production in Thai tea-based kombucha fermentation

Type of additive	Samples code	Concentration	References
Control*	RTC-C	-	-
Soy protein isolate	RTC-SPI	0.5% (w/v)	-
Ethanol	RTC-EtOH	1% (v/v)	(Kazemi et al. 2015; Cielecka et al. 2021; Fei et al. 2023)
Vitamin C	RTC-VC	0.5% (w/v)	(Keshk 2014)
Yeast extract	RTC-YE	0.5% (w/v)	(Aswini et al. 2020)
Puree coffee	RTC-PC	0.8% (w/v)	(De Souza et al. 2021)

**) The tea used in this study is based on a previous study, i.e. Thai red tea (ChaTraMue Brand)*

The objective of the study was to assess how these supplemental ingredients affect BC yield, structural attributes, and overall production efficiency, thereby providing insights for optimizing BC fermentation conditions. Each sample was fermented using the same set of conditions. The characterization parameters for both the fermentation broth and the BC in this experiment were consistent with those used in the previous experiment, including pH, total soluble solids (°Brix), sugar composition, wet and dry yield, WHC, surface morphology, chemical functional groups, crystallinity, thermal behavior, and mechanical properties. Due to the insignificant changes in color after purification, BC color analysis was not performed

3) Effect of Carbon Source Combinations on BC Yield and Characteristics

This study systematically evaluated five carbon source formulations to optimize BC production (**Table 3.3**) in Thai red tea fermentation as the selected tea for BC production. The experimental design leveraged distinct metabolic advantages of each component: while sucrose (hydrolyzed to glucose and fructose) served as the foundational carbon source, dextrose and glucose were included to boost UDP-glucose precursor supply for cellulose polymerization. Fructose supplementation targeted enhanced energy generation through TCA cycle activity, whereas glycerol provided dual benefits as both a carbon source and an osmoprotectant. The fermentation conditions were consistent across all samples.

The characterization parameters for both the fermentation broth and the BC in this experiment were consistent with those used in the previous study, including pH, total soluble solids (°Brix), sugar composition, wet and dry yield, WHC, surface morphology, chemical functional groups, crystallinity, thermal behavior, and mechanical properties. BC color analysis was not included in this experiment, as purification resulted in minimal variation.

Table 3.3 Carbon source combinations tested for BC production in in Thai tea-based kombucha fermentation.

Carbon source	Code	Total carbon source (g/100 ml)
Sucrose (S)*	RTC-C	10
Sucrose (S) + Fructose (F)	RTC-SF	5 + 5
Sucrose (S) + Dextrose (D)	RTC-SD	5 + 5
Sucrose (S) + Glycerol (Gly)	RTC-SGly	5 + 5
Sucrose (S) + Glucose (Glu)	RTC-SGlu	5 + 5

** Sucrose as control treatment*

4) Effect of Process Parameters: initial pH, Harvesting Time, Tea Concentration, and Cultivation Method on BC yield and WHC

This multifactorial study examined the influence of key fermentation parameters on BC yield, using the following experimental variations. This experiment utilized the optimal tea i.e. Thai red tea.

- **Effect of Different Initial pH on the BC Yield and WHC**

This experiment investigated the impact of different initial pH on BC yield and WHC. The pH of the fermentation medium was adjusted to target values of 5, 6, and 7 by adding either 0.1 N NaOH or 0.1 N HCl until the desired pH was reached. A control group was included without pH adjustment, maintaining the natural pH of the medium at approximately 5.2. Prior to and after fermentation, the broth of each sample was analyzed for pH and total soluble solids (°Brix). Additionally, the yield of BC and its WHC were measured for each treatment.

- **Effect of Different Harvesting Period on BC Yield and WHC**

This experiment investigated the effect of different harvesting periods on BC yield and WHC. Samples were divided into four harvesting groups: 1st week, 2nd week, 3rd week, and 4th week. After the initial harvest, the 1st, 2nd, and 3rd week samples were allowed to continue fermenting and were harvested again along

with the 4th week group. For the 1st, 2nd, and 3rd week samples, total BC yield was calculated by summing the *wet weight after purification* and the *dry weight after drying* from both the first and second harvests. The 4th week samples were harvested only once. Before and after fermentation, pH and °Brix values of the sample broths were measured. BC yield and WHC were subsequently determined for each treatment group. The experimental design related to the harvesting period variations is summarized in **Table 3.4.**

Table 3.4 Experimental design of harvesting period for BC production

Treatment	Harvesting time			
Harvest 1st week	7th day	-	-	28th day
Harvest 2nd week	-	14th day	-	28th day
Harvest 3rd week	-	-	21st day	28th day
Harvest 4th week	-	-	-	28th day

- **Effect of Different Tea Concentration on BC Yield and WHC**

To evaluate the impact of varying tea concentrations on BC yield and WHC, a study was conducted using concentrations of 1%, 2%, and 3% (w/v). Broth samples were analyzed for pH and total soluble solids (°Brix) both before and after fermentation. The resulting BC yield and WHC were also determined for each treatment.

- **Effect of Different Cultivation Methods on BC Yield and WHC**

The study on various cultivation methods, including static, shaking, and agitated cultures, was conducted to investigate their effects. Static cultivation served as the control method, while shaking cultivation was performed using an orbital shaker at 150 rpm, and agitated cultivation was conducted in a bottle with a magnetic stirrer at 150 rpm (Zywicka et al. 2015). Broth samples were analyzed

for pH and total soluble solids (°Brix) at both pre- and post-fermentation stages. The resulting BC yield and WHC were also measured for each treatment.

3.3.2 Bacterial Cellulose Production

1) Medium Preparation

In general, the fermentation medium was prepared as follows: a total of 20 g of sucrose and tea extract (at a concentration of 10 g/L) were added to a 480 mL glass jar. The tea extract was prepared by brewing 2 g of tea leaves in 180 mL of hot deionized water (~90 °C) for approximately 15 minutes. After brewing, the tea was filtered and combined with sucrose in the jar. The mixture was then adjusted to a final volume of approximately 180 mL using deionized water, stirred until homogeneous, covered, and sterilized by autoclaving (121 °C, 15 minutes, 1 psi). After sterilization, the medium was cooled to room temperature (~30–35 °C).

To study the effect of different tea types, the tea component was substituted with various tea variants (see **Table 3.1**) at the same concentration (10 g/L). Thai red tea (RTC) was identified as the most effective and was subsequently used in all following experiments using the same formulation (1% tea concentration), except in experiments investigating the effect of different tea concentrations. For the study on the harvesting period, the general formulation was also used prior to evaluating its impact.

For the additive effect study, selected additives were incorporated into the medium based on the formulations provided in **Table 3.2.** Yeast extract (YE), soy protein isolate (SPI), and peptone casein (PC) were added prior to sterilization, whereas ethanol (EtOH) and vitamin C (VC) were added after cooling, immediately before inoculation.

For the study on carbon source effects, the carbon sources were varied according to the combinations detailed in **Table 3.3.** The general formulation was also used as the base medium for experiments investigating the effects of initial

pH, fermentation time, and cultivation method. In the initial pH variation study, the pH was adjusted to 5, 6, and 7 using 0.1 N HCl or 0.1 N NaOH, while the control (unadjusted) had an initial pH of approximately 5.20. Acid or base was added dropwise prior to sterilization, with pH monitored concurrently.

To examine the effect of tea concentration, tea infusions were prepared at concentrations of 1%, 2%, and 3% using the same brewing method described in the general procedure. Each sample was adjusted to a final volume of approximately 180 ml.

2) Regeneration of Kombucha Starter

In the first experiment, designed to study the effect of different tea types, kombucha cultures were prepared using four types of tea: RTC, GTC, BTC, and RBTH. The kombucha cultures were prepared in accordance with the tea types used in the fermentation media. Each sterilized tea medium was inoculated with 20 mL of commercial kombucha starter, mixed thoroughly, covered with two layers of cheesecloth, and fermented for 14 days at approximately 30 °C. Based on the results, Thai red tea (RTC) was selected as the optimal tea. Therefore, in all subsequent experiments, kombucha cultures were consistently prepared using RTC and regenerated every two weeks to maintain experimental consistency. Kombucha culture regeneration was carried out separately for each experimental treatment or study design.

3) Kombucha Fermentation for BC Production

The sterilized media, prepared according to each experimental design, were inoculated with 20 mL (10% (v/v)) of regenerated kombucha starter and gently shaken to ensure thorough mixing. The jars were covered with two layers of cheesecloth and incubated for 15 days at approximately 30 °C. In the experiment examining different tea types, a control consisting of a 10% sucrose solution without tea was included under the same conditions. For all subsequent experiments, a medium containing Thai red tea (RTC) with 10% sucrose was used as the control for

BC production. Each experiment was conducted independently and simultaneously in triplicate, following its respective design.

4) Harvesting and Purification of BC

After around 15 days of fermentation, the BC was separated by lifting it using tweezers and drained for ±10 minutes. The BC was then heated in boiling water for about 30 minutes and drained for about 10 minutes. The BC is then heated (~90oC) in the alkaline solution (NaOH, 2%) for 120 minutes and rinsed with RO water, then soaked and changed repeatedly with RO water until the pH is neutral (Yanti et al. 2018; Aswini et al. 2020).

3.3.3 Culture Medium Characterization

The culture media were analyzed both before and after fermentation to assess key parameters, including °Brix, pH, and sugar composition (sucrose, glucose, and fructose), depending on the specific experimental design. °Brix was measured using a refractometer, while pH was determined with a pH meter. Sugar composition was analyzed using high-performance liquid chromatography (HPLC).

Sugar composition analysis was performed using an HPLC system (Hitachi Chromaster) equipped with a refractive index (RI) detector (model 5450), column oven (model 5310), auto sampler (model 5260), and pump (model 5110). Separation was achieved using an Aminex HPX-42A column with filtered deionized water (0.22 µm) as the mobile phase, operating at a flow rate of 0.6 mL/min. The column temperature was maintained at 45°C, with an acquisition time of 22 minutes and an injection volume of 20 µL. The standard solution for calibration was prepared by mixing sucrose, glucose, and fructose at a concentration of 60 g/L, resulting in a final concentration of 20 g/L for each sugar. A standard curve was constructed using a series of concentrations: 0, 3, 6, 9, 12, and 15 g/L. Samples were diluted by combining 0.1 mL of the sample with 0.9 mL of DI water in Eppendorf tubes. Both standard solutions and diluted samples were filtered through a 0.22 µm syringe filter prior to HPLC analysis. Before analyzing the standards and samples, the HPLC system was

stabilized to ensure a steady baseline. All measurements were conducted in triplicate to ensure accuracy and reliability.

3.3.4 Bacterial Cellulose Characterization

1) Yield and Water Holding Capacity

After the BC was purified and drained for about 10 minutes, it was weighed to determine the net wet weight. Further, for dry samples, the BC sample was dried using an oven at a temperature of 40°C until it reached a constant weight (Aswini et al. 2020). WHC was determined by calculating the mass of water lost during drying, expressed as the ratio of removed water to the dry weight of the cellulose (g of water per g of dry sample) (Schrecker and Gostomski 2005). The samples were made in three replications.

2) The Color of BC

The appearance of wet BC before and after purification was observed directly and measured using a colorimeter. Observation and analysis was carried out on the sample after it was boiled in RO water and after it was purified using NaOH and neutralization. The purified sample was then compared to the commercial nata de coco (NDC) as a control. The color investigation was determined with a portable digital colorimeter using the CIELAB color parameters L* (luminosity), a* (-green to +red), and b* (-blue to +yellow). The details of the method are mode measurement: RSEX, path length of cell: (-), port size: 0.375 inch, and scale: CIE Lab. The analysis was made in three repetitions.

3) Morphology Analysis Using Scanning Electron Microscope (SEM)

The surface morphology of BC was analyzed using a scanning electron microscope (SEM). After the BC samples were dried, the BC sheets were cut to a size of approximately 5×5 mm, positioned on a sample stage, and coated with gold. The fiber diameter was determined by analyzing SEM images with Image J software (Volova et al. 2022). The number of data points taken for fiber diameter analysis was 50.

4) Fourier Transform Infrared Spectroscopy Analysis

The functional group of the sample was analyzed using FT-IR spectroscopy. The spectral data was collected at a wavelength of around 400–4000 cm^{-1}. The resolution was 4 cm^{-1}, the background and sample scan times were 64, and the result spectrum was transmittance. The measurements were carried out at room temperature.

5) X-Ray Diffraction (XRD) Analysis

Crystal characteristics, primarily the 2θ diffraction peaks and crystallinity index (CI), were analyzed using a Bruker D8 Advance X-ray diffractometer. The measurements were conducted in Coupled Theta/2Theta scan mode with Continuous PSD Fast acquisition. A Cu Kα radiation source (λ = 1.5418 Å) was used, operating at 40 kV and 40 mA (power = 1600 W). The detector employed was a LYNXEYE 1D position-sensitive detector. Data were collected over a 2θ range of 10° to 60° with an increment of 0.0204°, a step count of 2446, and a time per step of 0.400 seconds, resulting in a total scan time of approximately 1035.2 seconds. Crystallinity index was calculated using **Equation 3.1**, and average crystallite size was determined by the Scherrer equation (**Equation 3.2**), with data processing performed in *OriginLab* and *Microsoft Excel*.

$$CI = \frac{Total\ Area\ of\ Crystalline\ Peak}{Total\ Area\ of\ Crystalline\ and\ AmporphousePeak}\ x\ 100\% \quad \text{.....(Eq. 3.1)}$$

$$d = \frac{K\lambda}{\beta \cos\theta} \quad \text{.....(Eq. 3.2)}$$

where *CI* is the crystallinity index, *d* is the crystallite size, *K* is the Scherrer constant (0.89), λ is the wavelength of the X-ray radiation (1.5418 Å for Cu Kα), β is the full width at half maximum (FWHM) of the diffraction peak in radians, and θ is the Bragg angle corresponding to the peak position (in radians, i.e., half of the 2θ value) (Sardjono et al. 2019).

6) Thermogravimetric (TGA/DTG) Analysis

The dynamic weight loss and thermal decomposition behavior of the BC samples were analyzed using a thermogravimetric analyzer (Mettler-Toledo, Model TGA/DSC1). The samples were heated on an alumina sampling pan from 28°C to 600°C at a rate of 10°C/min under nitrogen (N_2) gas purging with a flow rate of 30 mL/min. The TGA/DTG data was processed using *OriginLab* software, and the TDA/DTG graph was made in *MS Excel* software.

7) Mechanical Properties analysis Using Nanoindentation

A nanoindenter was used to evaluate the mechanical properties of BC films, including penetration depth at a maximum load of 50 mN, hardness, reduced modulus, elastic recovery parameter (ERP), and Young's modulus. Samples were prepared by cutting them into circular shapes with a diameter of 0.8 cm and mounted flat on a clear acrylic holder using white glue (adhesive latex), without additional treatment. Indentation tests were performed at loading and unloading rates of 0.40 mN/s, with a maximum load of 50 mN. Each BC film was measured at six different points to calculate average surface property values. Young's modulus was determined using the equation presented in **Equation 3.3.**

$$E = \frac{(1-v^2)}{\left(\frac{1}{E_r} - \frac{(1-v_i^2)}{E_i}\right)} \quad \text{.....(Eq. 3.3)}$$

Where E = Young's Modulus of the sample, ν = Poisson's ratio of BC sample (0.3), E_r = Reduced modulus of BC sample, ν_i = Poisson's ratio of the indenter (0.07) and E_i = Young's Modulus of the indenter (1141 GPa) (Roberts et al. 1994; Rabbani et al. 2022).

3.3.5 Statistical Analysis

Analysis of variance was carried out using Ms. Excel software. The differences between the mean values were analyzed using least significant difference (LSD) test and the significance level was set at $P < 0.05$.

3.4 Results and Discussion

3.4.1 Effect of Thai Tea Types on Bacterial Cellulose Yield and Characteristics

1) Tea Profile Composition

The term "tea" refers to products derived from the leaves of plants in the Camellia family. In Thailand, the commercially produced tea cultivars *include Camellia sinensis* var. *Assamica* and *Camellia sinensis* var. *Sinensis*, commonly known as Chinese cultivars (Theppakorn et al. 2014). The same fresh tea leaves can yield various types of dried tea depending on the processing method, including black, green, oolong, white, and Thai red tea. These processing methods result in distinct chemical compositions and nutritional (Naveed et al. 2018; Shevchuk et al. 2020; Deka et al. 2023). The general composition of the teas used in this study was obtained from the tea packaging labels, as detailed in **Table 3.1,** in the design experiment section.

Different types of tea have distinct nutritional compositions. For example, the dried Chinese black tea contains approximately 16.79–23.68% protein, 5.02–7.23% water, 2.67–2.90% volatiles, and 5.43–6.10% ash, while dried Chinese green tea contains 28.66–41.36% protein, 3.23–6.60% water, 2.41–2.67% volatiles, and 5.06–6.09% ash (Czernicka et al. 2017). Additionally, Chinese green tea generally has higher levels of Ca, K, Na, Mg, Zn, and Mn, but lower levels of Al and caffeine compared to black tea, with similar phosphorus content (Czernicka et al. 2017). Green tea infusion also contains higher total phenolic content (110.73±22.46 mg/100 mL) compared to black tea (69.36±16.66 mg/100 mL) (Klepacka et al. 2021). Moreover, dried green tea has higher levels of epigallocatechin (21.91–37.46 mg/g) and caffeine (21.3–47.47 mg/g) than dried black tea, which contains 3.5–8.3 mg/g of epigallocatechin and 20.58–24.22 mg/g of caffeine (Wang et al. 2022b).

Comprehensive data on the nutritional composition of Assam black and green teas remain limited. Nonetheless, a comparative study on carbohydrate content reported that Assam black tea contains approximately 6.87 ± 2.68 mg/g of

fructose, 1.04 ± 0.16 mg/g of maltose, 9.41 ± 1.75 mg/g of inositol, 6.83 ± 4.73 mg/g of sucrose, and 3.95 ± 1.19 mg/g of glucose—values slightly higher than those observed in Chinese black tea (Shevchuk et al. 2020). In addition to traditional teas, Thai red tea is widely consumed in Thailand. This type of tea is typically derived from black tea and blended with various spices, such as star anise, cardamom, and crushed tamarind seed, as well as food colorants (Devje 2022; Thegreencreator.com 2022).

The distinct nutritional profiles and bioactive compound compositions of different tea types may significantly influence BC production during kombucha fermentation. For example, caffeine has been identified as a potential stimulant for BC synthesis (Fontana et al. 1991). Black tea, in particular, serves as an important source of caffeine in kombucha fermentation and contributes to the overall metabolic activity of the microbial consortium involved (Miranda et al. 2016).

2) The Change of pH and Total Soluble Solid (TSS)

The changes in fermentation parameters, including pH and total soluble solids (TSS), were systematically evaluated in this study to monitor microbial activity and substrate utilization. Before inoculation, the pH of the tea-based media ranged from 5.02 to 5.37, depending on the type of tea used. After inoculation with the starter culture, the pH dropped to 3.05 to 3.57, due to the introduction of an acidic inoculum typically rich in organic acids from prior fermentation. After 15 days of fermentation, the pH further decreased to 2.33 to 2.70, primarily due to the microbial production of organic acids such as acetic acid and gluconic acid, which are commonly generated by acetic acid bacteria (Aswini et al. 2020; Lee et al. 2021). Other organic acids such as glucuronic, lactic, malic, tartaric, citric, and succinic acids may also be produced, contributing to the overall pH reduction (Neffe-Skocińska et al. 2017).

The extent of pH reduction can vary depending on the type of tea used, as different teas contain varying levels of polyphenols, caffeine, amino acids, and other bioactive compounds that affect microbial growth and metabolism. For instance, teas richer in polyphenols and free amino acids may support higher

metabolic activity, accelerating acid production. **Table 3.5** and **Figure 3.1** (left side) illustrate the progression of pH throughout the fermentation process.

Table 3.5 The change of pH and degree of °Brix during kombucha fermentation of different types of Thai tea for BC production.

Tea Sample	The Change of the pH			The Change of the °Brix		
	Medium	Before	after	Medium	Before	after
WT	5.31±0.01^{c}	3.05±0.00^{a}	2.33±0.03^{a}	10.50±0.00^{a}	10.40±0.00^{a}	10.40±0.00^{c}
RTC	5.15±0.01^{b}	3.53±0.00^{c}	2.47±0.02^{b}	10.80±0.00^{b}	10.60±0.00^{c}	8.57±0.10^{a}
BTC	5.02±0.00^{a}	3.57±0.00^{d}	2.53±0.02^{c}	10.90±0.00^{c}	10.50±0.00^{b}	8.50±0.15^{a}
GTC	5.37±0.01^{d}	3.53±0.00^{c}	2.70±0.03^{d}	10.80±0.00^{b}	10.47±0.05^{b}	9.30±0.09^{b}
RBTH	5.06±0.02^{a}	3.47±0.00^{b}	2.53±0.04^{c}	10.90±0.08^{c}	10.70±0.00^{d}	9.20±0.23^{b}

Different lowercase letters within a column indicate significant differences among the five tea samples (LSD test: P < 0.05).

TSS, expressed in °Brix, serves as an indicator of the sugar content in the fermentation medium. Prior to inoculation, TSS values ranged from 10.50 to 10.90 °Brix, depending on the tea base and sugar concentration. After fermentation, TSS decreased to a range of 8.57 to 10.40 °Brix. This reduction reflects microbial consumption of sugars during fermentation. Although ethanol and organic acid contents were not directly measured in this study, previous research has shown that such reductions are typically associated with the conversion of sugars into ethanol and organic acids by yeast and acetic acid bacteria (Muzaifa et al. 2022).

The rate of TSS reduction is also influenced by the tea composition. Teas with higher levels of fermentable sugars or compounds that stimulate yeast activity may experience a more rapid decline in TSS. For example, Zubaidah et al. (2019) reported that the TSS of snake fruit kombucha dropped from 13.30–14.08 °Brix to 12.43–12.97 °Brix, while cascara kombucha TSS declined from 10.97 °Brix on day two to 9.97 °Brix by day eight (Muzaifa et al. 2022). The decrease in TSS is mainly due to the hydrolysis of sucrose into glucose and fructose, which are then utilized for

microbial growth and secondary metabolite production (Sinamo et al. 2022). **Table 3.5** and **Figure 3.1** (right side) present the changes in TSS before and after fermentation.

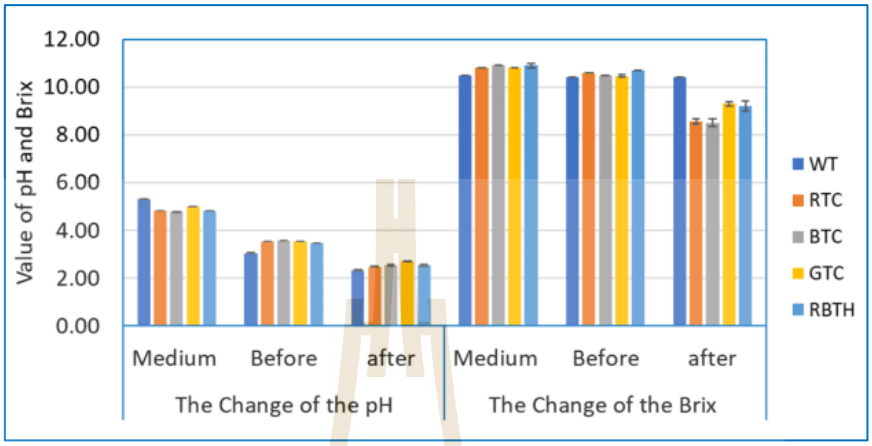

Figure 3.1 The change of pH and degree of °Brix during kombucha fermentation of different types of Thai tea for BC production.

3) **The Change of Sugar Composition**

Sugar composition, especially sucrose, glucose, and fructose, was evaluated before and after fermentation using HPLC. The result showed that there were changes in the concentration of the sugar components before and after fermentation, as is demonstrated in **Figure 3.2** and **Table 3.6.** The microbial (SCOBY) used the sucrose in the kombucha as a carbon source. Microbes often require carbon sources for growth and product formation, among other activities (Shu 2007). Numerous yeasts and bacteria, including *Saccharomyces cerevisiae*, *Schizosaccharomyces*, *Zygosaccharomyces rouxii*, *Torulaspora delbrueckii*, *Acetobcter xylinum*, and *Gluconobacter*, are found in SCOBY (Greenwalt et al. 2000). Before fermentation, the concentration of sucrose, glucose, and fructose was 9.03 to 9.58 %, 0.21 to 2.53 %, and 0.05 to 1.19 %, respectively. The presence of glucose and fructose prior to fermentation may be attributed to both the use of kombucha starter culture and the partial hydrolysis of sucrose during the autoclaving process. Ball (1953) reported that autoclaving a 3% sucrose solution resulted in the formation of approximately 0.7% to 0.9% glucose, indicating that thermal processing can induce sucrose breakdown. Similarly, de Lange (1989) demonstrated through a

semiquantitative test that sucrose in an autoclaved medium at pH 2 could be fully hydrolyzed into glucose and fructose. This hydrolysis was also found to occur, albeit to a lesser extent, at pH levels between 5 and 7.

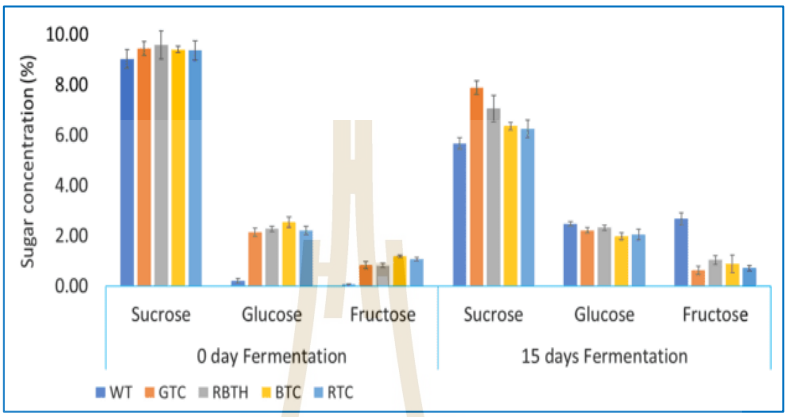

Figure 3.2 The change of sugar composition (sucrose, glucose, and fructose) of kombucha broth before and after fermentation

In the early stages of kombucha fermentation, microbial cells hydrolyze the sucrose into glucose and fructose. The subsequent metabolism of glucose and fructose yields carbon dioxide and ethanol (Wang et al. 2022a). In BC production, bacteria use some of the available glucose and fructose to synthesize cellulose. At the end of the fermentation, the concentration of sucrose decreases to the range of 5.67 to 7.88%. For all the different tea kombucha samples, there are significant differences in sucrose concentration before and after fermentation. Before fermentation, the concentration of sucrose in all the samples was not significantly different ($P > 0.05$). However, after fermentation, the concentrations of sucrose in the samples are different. **Table 3.6** provides details about the differences in concentrations of glucose and fructose before and after fermentation. Neffe-Skocińska et al. (2017) found that after 10 days of Kombucha fermentation at 30°C, the concentrations of glucose and fructose increased from 0.09% to 0.1% and from 0.07 to 0.87%, respectively, while the concentration of sucrose decreased from 9.97% to 0.74%.

Table 3.6 The change of sugar composition during kombucha fermentation with different types of teas

Sample	Before fermentation			After fermentation		
	Sucrose	Glucose	Fructose	Sucrose	Glucose	Fructose
WT*	$9.03\pm0.36^{a, B}$	$0.21\pm0.08^{a, A}$	$0.05\pm0.03^{a, A}$	$5.67\pm0.23^{a, A}$	$2.47\pm0.08^{c, B}$	$2.67\pm0.23^{c, B}$
GTC	$9.43\pm0.28^{a, B}$	$2.15\pm0.16^{b, A}$	$0.82\pm0.14^{b, A}$	$7.88\pm0.27^{d, A}$	$2.22\pm0.11^{b, A}$	$0.62\pm0.16^{a, A}$
BTC	$9.40\pm0.13^{a, B}$	$2.53\pm0.21^{c, B}$	$1.19\pm0.05^{d, A}$	$6.35\pm0.16^{b, A}$	$1.98\pm0.14^{a, A}$	$0.87\pm0.35^{ab, A}$
RBTH	$9.58\pm0.56^{a, B}$	$2.27\pm0.10^{b, A}$	$0.82\pm0.08^{b, A}$	$7.05\pm0.52^{c, A}$	$2.32\pm0.11^{bc, A}$	$1.03\pm0.18^{ab, A}$
RTC	$9.36\pm0.38^{a, B}$	$2.21\pm0.16^{b, A}$	$1.06\pm0.07^{c, B}$	$6.24\pm0.36^{b, A}$	$2.04\pm0.20^{a, A}$	$0.71\pm0.11^{ab, A}$

**Sample without tea as a control. Different lowercase letters within a column indicate significant differences among the five tea samples (LSD test: P, 0.05); different uppercase letters in the same row indicate the significant differences between the same sugar before and after fermentation (LSD test: P, 0.05).*

4) BC Productivity and Water Holding Capacity (WHC)

Figure 3.3 shows the BC production results from kombucha with various types of Thai tea. It showed that the generated BC has varying wet yields, dry yields, and WHC. The wet yields (g/L) of BC from WT, GTC, RBTH, BTC, and RTC are 61.25±10.25, 73.47±9.94, 74.82±16.14, 158.56±17.30, and 168.00±16.59, respectively. RTC and BTC produced the highest wet yields, significantly different from WT, GTC, and RBTH ($P<0.05$). The wet yields from WT, GTC, and RBTH are not significantly different from one another ($P > 0.05$). The dry yield results (g/L) of WT, GTC, RBTH, BTC, and RTC are 0.38±0.08, 0.87±0.08, 0.76±0.11, 1.49±0.08, and 1.36+0.10, respectively. The dry yield from WT is the lowest, and it is significantly different from GTC and RBTH ($P < 0.05$). GTC and RBTH are not significantly different from each other; however, they are significantly different from BTC and RTC. BTC and RTC have the highest dry yield, and both are not significantly different ($P > 0.05$).

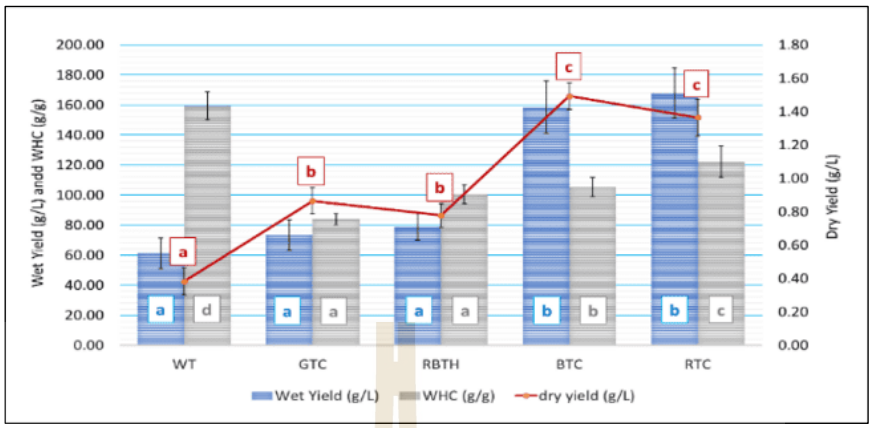

Figure 3.3 Wet yield (g/L), dry yield (g/L), and WHC (g water/g cellulose) from BC produced from kombucha with different types of Thai tea. Different lowercase letters indicate significant differences between the five BC sample (LSD test: $P < 0.05$).

The low BC yield observed in the WT (water treatment) sample is likely due to the lack of essential nutrients in the medium. As shown in **Table 3.6,** there was a marked decrease in sucrose content alongside an increase in glucose and fructose levels, indicating that while sucrose hydrolysis occurred, the conversion of available carbon into BC was inefficient. The absence of tea in the WT medium meant it lacked key compounds such as polyphenols, nitrogen, caffeine, and minerals, all of which are important for supporting microbial activity and efficient BC production. In the case of the GTC (green tea) sample, the relatively lower BC yield may be attributed to green tea's lower ash content, which suggests a limited supply of certain minerals essential for microbial growth and cellulose biosynthesis (Czernicka et al. 2017). Likewise, the RBTH sample exhibited reduced BC production compared to BTC, possibly because Chinese black tea contains lower amounts of sucrose, fructose, and glucose than Assam black tea (Shevchuk et al. 2020). Furthermore, the RBTH used in this study was grade 3, which included dried stems along with leaves, potentially influencing its overall nutrient composition. In contrast, the RTC sample had the highest BC yield, likely due to its richer nutritional profile. Unlike pure black tea, Thai red tea often contains added spices, which enhance its vitamin, mineral, and amino

acid content, creating a more favorable environment for microbial growth and BC production.

In the previous studies, several BC production results have been reported, including BC production in a 0.4% black tea solution with 20 g/L sucrose. The result was 17.63±0.50 g/L for wet yield and 3.06±0.21 g/L for dry yield after 10 days of fermentation (Hamed et al. 2023). Kombucha fermentation using a solution of 10 g/L black tea and 100 g/L sucrose for 14 days produced wet BC with a yield of 63.58 g/L (Al-Kalifawi and Hassan 2014). In green tea fermentation using kombucha culture with fermentation times of 7, 14, and 30 days, the dry weight yield of BC relative to the amount of sugar, where BC has not been purified with NaOH, is 0.9, 3.9, and 6.5 g/L (Charoenrak et al. 2023). Treviño-Garza et al. (2020) reported the results of wet-based BC produced from kombucha green tea using a microbial consortium coded Cor and CFr, producing between 195.39–301.81 g/L and 126.79–300.74 g/L. BC was made using coconut water with the addition of 10 g/L sucrose and 5 g/L yeast extract, using *G. xylinum* bacteria, and fermented for 14 days at 30°C. This production produces BC of 250.00±0.21 g/L (Gayathry 2015). In one study, BC was produced in Hestrin-Schramm medium using selected bacteria, *A. senegalensis* MA1. Fermentation was carried out at optimum conditions, namely pH 4.5 and temperature 33.5°C, for 30 days, and BC was produced with a wet weight of 469.83 g/L (Aswini et al. 2020). The amount of BC generated may be higher or lower than previously reported. These disparities in outcomes can be attributed to both internal and external factors. Several factors can influence BC productivity, including differences in nutrient source and concentration, as well as other conditions such as pH, temperature, volume, and container surface area (Al-Kalifawi and Hassan 2014; Villarreal-Soto et al. 2018b). However, in this situation, the BC findings of kombucha tea with BTC and RTC samples demonstrate high potential, and productivity may be increased through production optimization.

The WHC of BC from WT, GTC, RBTH, BTC, and RTC samples were 159.26±9.30, 83.99±3.73, 98.10±7.65, 105.21±6.36, and 122.20±10.33, respectively. The

WT sample has the highest WHC and is significantly different from all the other samples. The BC samples from the WT sample did not form BC sheets properly, and the dry yield was also very low. It may be due to the lack of nutrition content in the broth sample during kombucha fermentation. The WHC from GTC and RBTH are not significantly different from one another. However, they are significantly different and have a lower WHC than BTC and RTC samples. These results, in general, follow the reports from several previous studies, except for BC from the WT samples. The BC made from fermented coconut water (NDC) has a WHC value of around 87.14 g/g (Gayathry 2015). NDC produced with different pH, sucrose, and ammonium sulfate concentrations had WHC values ranging from 38.7±0.6 to 88.1±2.7 g/g (Jagannath et al. 2008). BC from distillery wastewater media had a WHC value of 98.5 g/g (Wu and Liu 2013). The WHC value of BC from those studies is comparable to the WHC value of BC samples from GTC and RBTH. The WHC of BC with different media fermentation of waste products from biodiesel and confectionery industries had WHC values ranging from 102 to 138 g/g (Tsouko et al. 2015). BC from kombucha fermentation with black tea media has a WHC of 114.01 g/g (Avcioglu et al. 2021). Those WHC values are comparable to the BC samples from BTC and RTC.

5) The Appearance and Colors of Bacterial Cellulose

The BC sample from the WT medium was quite thin, had a very high-water content, and had a very low dry weight. It also did not form a proper pellicle layer on the surface. Hence, we did not include the BC sample in the WT sample for further characterization. **Figure 3.4** displays the BC sample from the WT medium.

Figure 3.4 The appearance of BC from WT sample in a medium fermentation and after drained

The BC from various Thai tea kombucha fermentations has distinct hues. After harvesting, RTC produced red-orange BC, GTC produced green BC, and BTC and RBTH produced brownish white BC (**Figure 3.5.a**). Then, after boiling in RO water for 30 minutes at ±90oC, the color of BC slightly faded (**Figure 3.5.b**). The BC color becomes translucent white after purifying it with 2% sodium hydroxide and rinsing it with RO water until the pH is neutral (refer to **Figures 3.5.c and 3.5.d**). **Figure 3.5.e** displays the appearance of BC after oven drying at 40 °C until a consistent weight was achieved. We compared the characteristics of BC produced through the fermentation of kombucha tea with BC from commercial NDC. The studies of BC production using green tea reported a picture of BC with a greenish-white color (Fahim and Montazer 2020) and a brownish color (Treviño-Garza et al. 2020). The BC from kombucha fermentation using black tea has a brownish-white color (Sharma et al. 2021). None of the studies reported BC production using Thai red tea. In this study, the BC from green tea kombucha exhibited a more pronounced green color compared to previous studies, likely due to the presence of coloring agents such as FD&C Yellow No. 5 (INS 102), FD&C Yellow No. 6 (INS 110), and FD&C Blue No. 1 (INS 133). In some previous studies, the color of BC from black tea kombucha was similar to that of BC from black tea in this study. The BC from Red Thai Tea Kombucha might have a red-orange color due to the presence of the coloring agent FD&C Yellow No. 6 (INS 110).

The color of BC samples after boiling in RO water (P1) and after purification with NaOH (P2) was analyzed using the CIELAB Lab* system. L* indicates lightness (<50: dark, >50: light), a* represents red (+) to green (−), and b* represents yellow (+) to blue (−) (hunterlab.com, 2023). We then compared the four purified samples to the NDC control by calculating the ΔE value using **equation 3.4**. The summary results of the color analysis are shown in **Table 3.7**.

$$\Delta E = \sqrt{\Delta L^{*2} + \Delta a^{*2} + \Delta b^{*2}} \quad \text{.....(Eq. 3.4)}$$

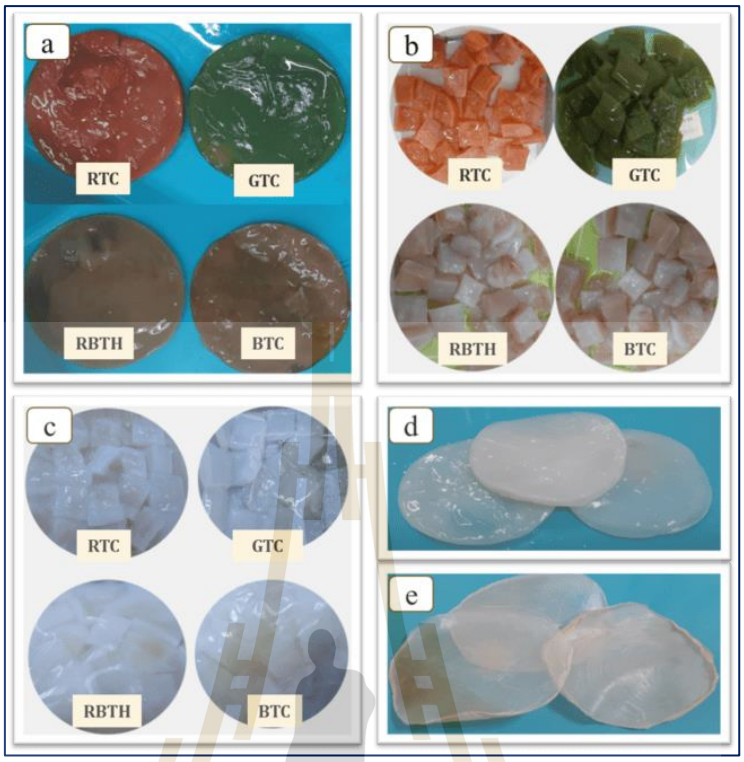

Figure 3.5 The appearance of BC (a) BC after harvesting, (b) sliced BC after harvesting and boiling in RO water, (c) sliced BC after purification using NaOH and RO water, (d) BC sheet after purification using NaOH and RO water, and (e) dried BC sheet.

Before purification, the BTC-P1 and RBTH-P1 samples had similar colors and were not significantly different (P<0.5). The L* and b* values in the RTC-P1 sample are not significantly different; however, the value of a* is greater and significantly different when compared to BTC-P1 and RBTH-P1 (P<0.5). The GTC-P1 sample exhibited significantly different L*, a*, and b* values than the RTC-P1, BTC-P1, and RBTH-P1 samples (P<0.5). After purification, the color values of the BTC-P2 and RBTH-P2 samples did not differ significantly (P<0.5). Sample RTC-P1 contains a* and b* values that are not significantly different, but L* values that are greater and significantly different from BTC-P2 and RBTH-P2 (P<0.5). The GTC-P2 sample shows significantly different L* and a* values, but the b* value is not statistically different when compared to the RTC-P1, BTC-P1, and RBTH-P1 samples (P<0.5). "We compared the ΔE values of four purified BC samples with the NDC as a control. According to Minaker et al. (2021),

a ***ΔE*** value between 0 and 1.0 is imperceptible to the human eye, while a ***ΔE*** between 1 and 2 is noticeable upon close inspection, and a ***ΔE*** between 2 and 10 is easily noticeable at a glance (Minaker et al. 2021). The BC samples BTC-P2 and RBTH-P2 have ***ΔE*** values below 2, indicating a subtle difference visible only upon close observation. In contrast, the ***ΔE*** values for RTC-P2 and GTC-P2 are 3.18 and 8.78, respectively, making them readily distinguishable.

Table 3.7 Summary of BC color investigation of kombucha with various types of tea before and after purification.

Samples Code	Results			
	L*	a*	b*	**ΔE*** **
Before purification				
RTC-P1	42.53±2.07^{b}	11.16±0.87^{c}	9.2 ±1.01^{a}	-
BTC-P1	42.45±3.40^{b}	2.36±1.14^{b}	7.41±2.30^{a}	-
RBTH-P1	41.80±0.53^{b}	3.29±0.22^{b}	9.09±0.62^{a}	-
GTC-P1	28.37±0.99^{a}	-5.52±0.68^{a}	12.02±1.07^{b}	-
After purification				
NDC**	47.96±1.16^{b}	-1.62±0.22^{a}	-10.38±0.31^{a}	control
RTC-P2	51.07±2.98^{c}	-1.95±0.09^{a}	-9.79±0.57^{ab}	3.18
BTC-P2	46.64±3.24^{b}	-1.81±0.17^{a}	-9.02±0.45^{b}	1.90
RBTH-P2	47.34±2.64^{b}	-1.77±0.10^{a}	-8.72±0.38^{bc}	1.78
GTC-P2	39.27±0.78^{a}	-1.06±0.43^{b}	-9.24±0.99^{b}	8.78

Different lowercase letters within a column indicate significant differences among the five BC samples (LSD test: P < 0.05).

Previous research has provided limited information on the color of BC or NDC before drying. One study investigated how different carbon sources—glucose, sucrose, mannitol, and fructose—affected the color of wet BC, reporting L*, a*, and b* values ranging from 24.7 to 48.48, -4.29 to 0.95, and -21.59 to 1.67, respectively (Shim and Kim 2019). These values are similar to those found in this study.

Other research has focused on the color of BC after drying. For example, Amorim (2022) reported that untreated BC had L*, a*, and b* values of 51.5±3.5, 14.8±0.6, and 31.5±2.1, respectively, while alkaline-treated BC had values of 83.6±1.0, 1.5±0.4, and 13.1±0.7 (Amorim et al. 2022).

6) Morphology Analysis

The morphology of BC samples produced from kombucha fermentation media with various types of tea, along with commercial NDC samples, was analyzed using SEM. **Figures 3.6.(a.1)** to **3.6(e.2)** present each sample at magnifications of 10,000x and 30,000x. Higher magnifications of 50,000x and 100,000x were applied to the RTC samples (**Figure 3.6.(e.3)** and **3.6.(e.4**)) to observe the cellulose fiber arrangement in greater detail. Fiber diameters were measured using ImageJ software, and their size distribution is illustrated in **Figure 3.7.**

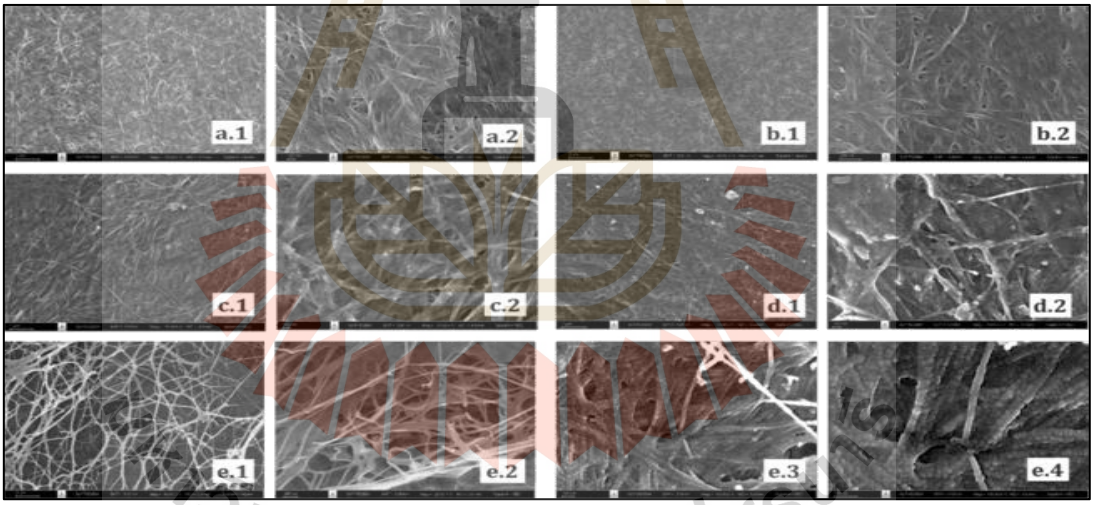

Figure 3.6 The SEM images of BC samples: (a) NDC; (b) GTC; (c) BTC; (d) RBTH; and (e) RTC. The images are shown at varying magnifications: (1) 10,000x; (2) 30,000x; (3) 50,000x; and (4) 100,000x.

Overall, the BC samples exhibit a consistent fiber pattern, aligning with the findings of Brandes et al. (2020), Nguyen and Nguyen (2022), and Illa et al. (2019) (Illa et al. 2019; Brandes et al. 2020; Nguyen and Nguyen 2022). However, in the samples of **Figure 3.6.c** (BTC) and **3.6.d** (RBTH), residues or insoluble materials persist after alkali purification, as also reported by Amorim et al. (2023) (Amorim et al. 2023).

This residual material obscures the fiber arrangement, particularly in **Figures 3.6.c.2** and **3.6.d.2**. In the RTC samples, magnified at 50,000x and 100,000x, the detailed arrangement of cellulose fiber units is more distinctly observed.

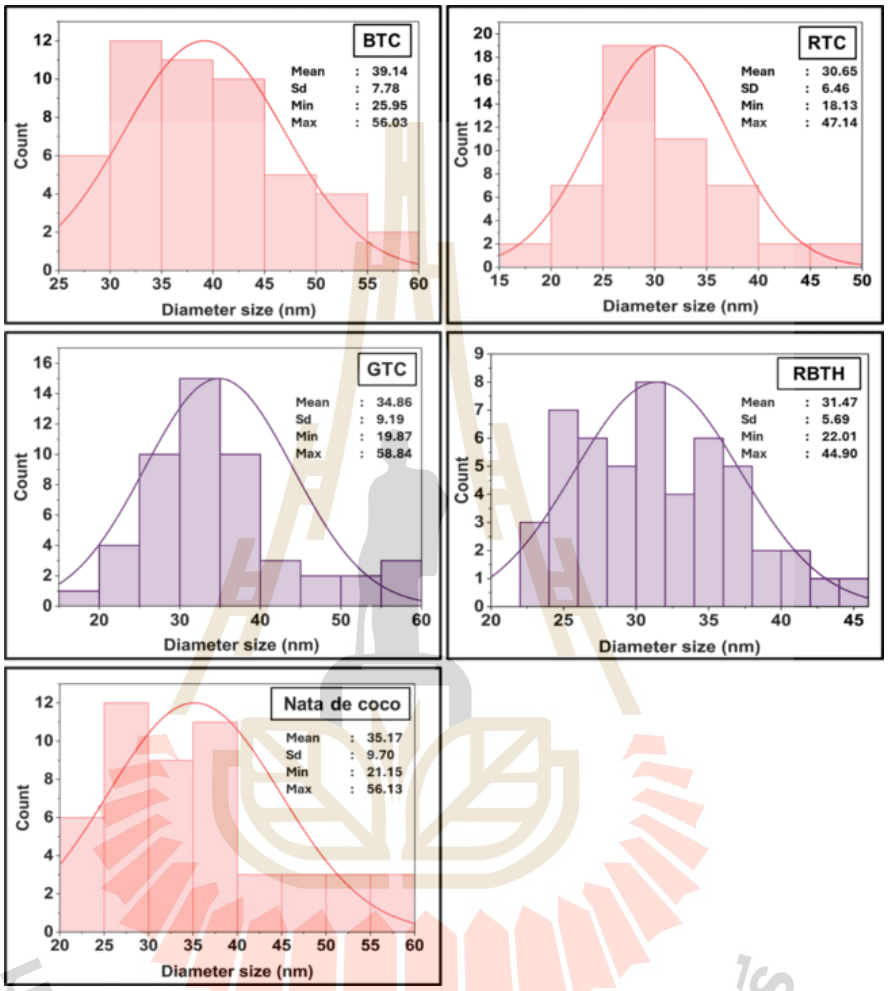

Figure 3.7 Graph of poly distribution diameter size of BC samples from NDC, RTC, GTC, BTC, and RBTH.

The polydistribution graphs of BC fiber diameters (**Figure 3.7**) revealed that fiber sizes range from 18.13±6.46 nm to 58.84±9.19 nm, with average diameters between 30.65±6.46 nm and 39.14±7.78 nm. The diameters of RTC, GTC, BTC, and RBTH are 30.65±6.46, 34.86±9.19, 39.14±7.78, and 31.47±5.70 nm, respectively. The fiber diameters of BC produced from kombucha tea are comparable to those of NDC (35.17±9.70). These results are consistent with the findings of Illa et al. (2019), who reported that BC produced by *K. hansenii* 23769 (ATCC) and an isolated

cellulose-producing strain from grape juice (GBHS) exhibited fiber diameters ranging from 10 to 60 nm (Illa et al. 2019). Specifically, oven-dried BC from the ATCC strain had an average diameter of 28.9±5.6 nm, while the GBHS strain had an average diameter of 28.6±6.7 nm. Similarly, BC produced by *A. pasteurianus* MGC-N8819 using lotus rhizome as a culture medium showed fiber diameters ranging from 28±1.5 nm to 57±1.2 nm (Nie et al. 2022). Furthermore, BC produced by *K. saccharivorans* MD1 using HS medium supplemented with palm date exhibited fiber diameters ranging from 10 to 90 nm (Abol-Fotouh et al. 2020).

7) Fourier Transform Infrared Spectroscopy

Figure 3.8 presents the FTIR spectra of BC samples obtained from different tea-based kombucha fermentations. Overall, all BC samples exhibit similar spectral bands. However, a noticeable difference is observed in the BC sample from GTC, which displays a distinct peak at approximately 1725.95 cm^{-1}.

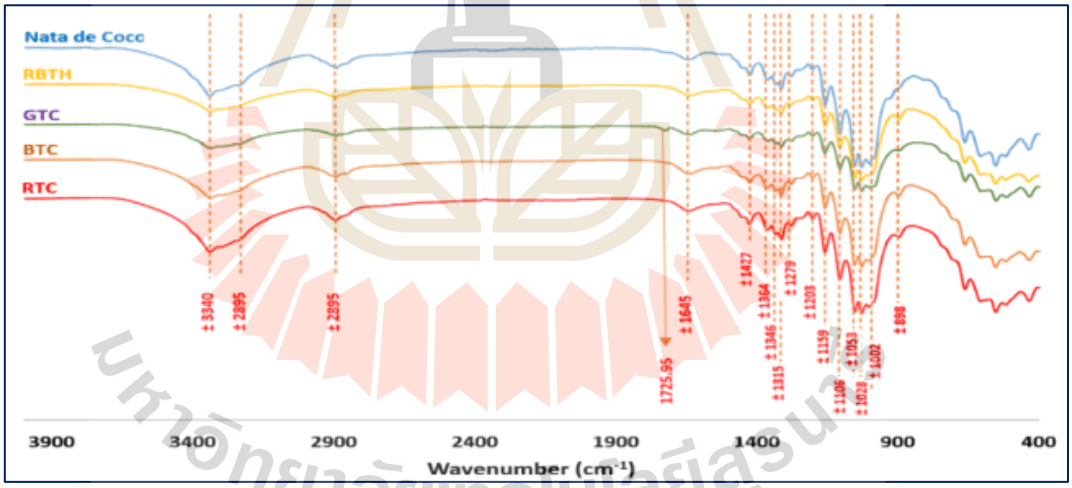

Figure 3.8 FTIR spectra of BC produced from different Thai tea kombucha fermentations

The FTIR spectra analysis is divided into two regions: the feature region and the fingerprint region. The feature region corresponds to high-frequency wavenumbers between 4000 and 1330 cm^{-1}. Meanwhile, the fingerprint region covers wavenumbers between 1330 and 500 cm^{-1} (Liu et al. 2023). The FTIR spectra of the BC

samples reveal the following key features: In the first spectral region, peaks were observed at wavenumbers around 3340, 3232, and 2895 cm^{-1}. The strong, broad bands at wavenumbers of approximately 3340 and 3232 cm^{-1} indicate the presence of O-H stretching, while the band near 2895 cm^{-1} corresponds to C-H stretching vibrations (Amorim et al. 2023). In the second spectral region, we observed a weak peak at around 2330 cm^{-1}, suggesting the presence of functional groups associated with triple bonds, specifically C≡C and C≡N (Srivastava and Mathur 2022). The third region in our FTIR spectra was observed between 1350 cm^{-1} and 2000 cm^{-1}, with absorption peaks at 1364 cm^{-1}, 1427 cm^{-1}, 1644 cm^{-1}, and 1725 cm^{-1}. The bands at 1360–1363 cm^{-1} correspond to C-H symmetric bending vibrations, while the peak at 1427 cm^{-1} represents CH_2 symmetric bending, and the peak at 1644 cm^{-1} indicates C=O stretching vibrations for the glucose carbonyl group (Liu et al. 2023). **Figure 3.8** also shows a peak at 1725 cm^{-1}, which appears exclusively in the FTIR spectrum of the BC sample from green tea kombucha (GTC). This peak may correspond to carbonyl stretching vibrations typically associated with aldehydes (1720–1740 cm^{-1}), ketones (1705–1725 cm^{-1}), or carboxylic acids (1700–1725 cm^{-1}) (Yao et al. 2015). The presence of this peak in the GTC sample could be attributed to specific compounds originating from green tea or intermediate metabolites produced during fermentation. Alternatively, it may indicate residual compounds or impurities that were not fully removed during purification. Further analysis would be required to determine the exact origin of this absorption peak.

In the fingerprint region, several peaks were observed at 1336 cm^{-1}, 1315 cm^{-1}, 1279 cm^{-1}, 1203 cm^{-1}, 1159 cm^{-1}, 1106 cm^{-1}, 1053 cm^{-1}, 1028 cm^{-1}, 1002 cm^{-1}, and 898 cm^{-1}. According to Liu et al. (2023), the peak at 1336 cm^{-1} corresponds to OH in-plane bending, while the peak at 1315 cm^{-1} is attributed to CH_2 wagging at C-6. The peak at 1159 cm^{-1} represents C-O-C antisymmetric bridge stretching vibrations, and the one at 1106 cm^{-1} is associated with ring asymmetric stretching vibrations. The 1053 cm^{-1} peak corresponds to C-O-C and C-O-H stretching vibrations of the sugar ring,

and the 1028 cm^{-1} peak represents C-O stretching vibrations (Liu et al. 2023). The band observed at 898–894 cm^{-1} may be associated with stretching vibrations of the C-O-C bond in the β-1,4-glycosidic linkages, indicating an amorphous absorption band (Ciolacu et al. 2011).

8) X-Ray Diffraction (XRD) Analysis

Figure 3.9 presents the X-ray diffraction (XRD) patterns of various BC samples, with a commercial NDC product used as a reference. It shows that the three distinctive peaks appear consistently in all samples at 2θ values of approximately 14.78°, 16.89°, and 22.90°. This indicates the crystalline structure of all the BC samples (Said Azmi et al. 2023). These XRD profiles are consistent with those reported for BC by Said Azmi et al. (2023), Jittaut et al. (2023), and Revin et al. (2018) (Revin et al. 2018; Jittaut et al. 2023; Said Azmi et al. 2023). While the X-ray patterns confirm the same cellulose chemical structure across all samples, they reveal variations in diffraction intensities. The highest intensity peak at around 23° corresponds to cellulose type I (Said Azmi et al. 2023; Hossen et al. 2024). Gaspar et al. (2014) identified that the peaks at 2θ values of 14.7°, 16.8°, and 22.7° correspond to the 100, 110, and 200 crystallographic planes of monolithic cellulose type I. This is typical of native cellulose (Gaspar et al. 2014). The variation in relative peak intensity likely reflects small differences in chain orientation among the samples (Said Azmi et al. 2023). This finding suggests that BC produced from different tea kombucha fermentations maintains a well-ordered crystalline structure, essential for its mechanical strength and WHC.

The data from the XRD analysis were then used to calculate the crystallinity index (CI) and crystallite size of BC samples. The CI of BC samples from BTC, GTC, RBTH, and RTC were 84.17%, 86.50%, 83.01%, and 85.36%, respectively, closely matching the CI of NDC, which was 86.66%. These results align with other studies, such as BC from pineapple peel waste fermentation with a CI of 87% (Sardjono et al. 2019), BC from pineapple waste solution fermentation at 82.2% (Pham and Tran

2023), BC produced from citrus processing waste or discarded fruits with a CI of 86.9% (Andritsou et al. 2018), and BC from HS-medium with varying carbon sources, which exhibited crystallinity ranging from 57% to 85% (Heydorn et al. 2023). BC can exhibit a high crystallinity index (CI), typically ranging from 84% to 90%, due to the absence of non-cellulosic components that may disrupt the crystalline structure (Cazón and Vázquez 2021). Further analysis of the average crystallite size of the BC samples revealed values of 2.60, 2.13, 3.34, 3.15, and 3.54 nm for BTC, RBTH, GTC, RTC, and NDC, respectively. For comparison, BC produced by *G. xylinus* InaCC B404 in HS medium was reported to have a crystallite size of 3.06 nm (Agustin et al. 2021). Additionally, BC derived from black tea kombucha after 3 and 5 days of fermentation showed crystallite sizes of 3.29 nm and 4.80 nm, respectively (Balistreri et al. 2024).

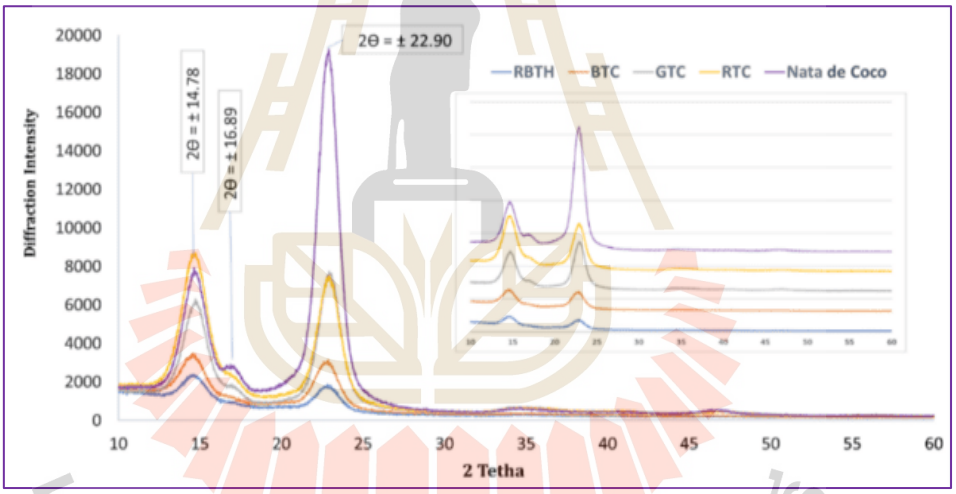

Figure 3.9 XRD spectra of BC produced from different types of tea kombucha fermentation

Differences in diffraction intensity and crystallite size (2.13–3.54 nm) suggest slight variations in molecular structure, likely influenced by fermentation conditions and tea type. The GTC sample had the highest CI (86.50%) and a larger crystallite size (3.34 nm), indicating improved crystallinity. Overall, the XRD results confirm that BC from kombucha tea fermentations has a highly crystalline structure, similar to commercial NDC. This makes it suitable for applications like food packaging,

biomedical materials, and nanocomposites. Further research on fermentation conditions could help enhance BC properties for specific uses.

9) Thermogravimetric (TGA/DTG) Analysis

Figure 3.10 presents the thermogravimetric (TG) and differential thermal degradation (DTG) curves of BC samples, obtained through thermogravimetric analysis (TGA). The thermal degradation of all BC samples occurred in two distinct stages. The first stage (28–240°C) involved weight loss ranging from 2.25% to 7.52%, primarily due to moisture evaporation and the loss of low-molecular-weight compounds. The second stage (240–600°C) showed a significant weight loss between 67.69% and 73.61%, corresponding to cellulose decomposition. At 600°C, the residue weight varied from 23.07% to 27.36%, as detailed in **Table 3.10.**

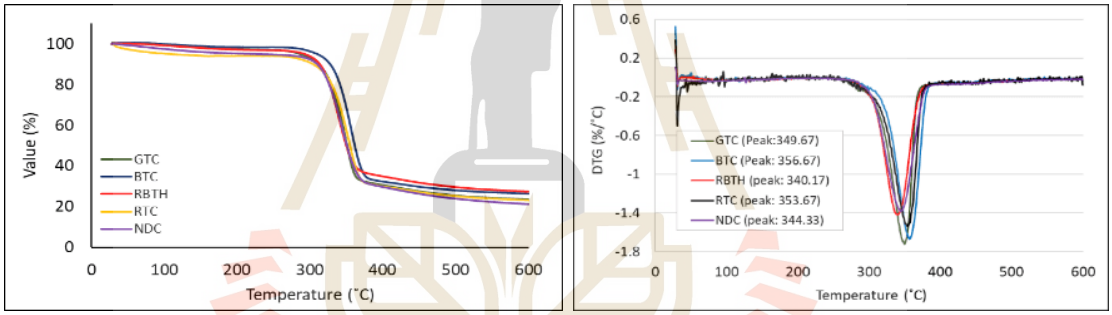

Figure 3.10 TGA (left) and DTG (right) thermographs of BC samples produced from kombucha fermentation using different types of tea

In the first stage, weight loss ranged from 2.25% (BTC) to 7.52% (NDC), with RTC showing a relatively high loss (6.03%), likely due to differences in residual moisture or volatile content. The second stage exhibited the most substantial degradation, with weight loss ranging from 67.69% (NDC) to 73.61% (GTC). At 600°C, the residual weight varied between 23.01% (RTC) and 27.36% (RBTH), indicating differences in thermal stability and carbonization potential among samples.

DTG curves provide further insight into the degradation behavior, with peak degradation temperatures (T_{max}) occurring between 340.17°C (RBTH) and 356.67°C (BTC). BTC exhibited the highest DTG T_{Max}, suggesting superior thermal

stability, while RBTH had the lowest T_{max}, indicating decomposition at a slightly lower temperature. RTC recorded a DTG T_{Max} of 353.67°C, closely resembling BTC, further confirming its thermal resistance. These variations in DTG T_{Max} can be attributed to differences in cellulose crystallinity, molecular structure, and residual compounds from the fermentation process.

Table 3.8 The details of data decomposition during the TGA process of BC samples from kombucha fermentation with different types of tea

Samples	First stage weight loss (%)	Second stage weight loss (%)	Residue (%)	DTG Peak range (°C)	DTG T_{Max} (°C)
GTC	3.45	73.61	23.51	255 – 379	349.67
BTC	2.25	71.99	26.37	255 – 382	356.67
RBTH	3.06	69.55	27.36	252 – 386	340.17
RTC	6.03	71.01	23.01	265 – 381	353.67
NDC	7.52	67.69	24.76	255 – 387	344.33

The findings align with previous research. BC produced by *G. xylinus* AGR 60 showed a first-stage mass loss of 6.2%, a second-stage loss of 64.0%, and a residue of 22.8% at 600°C, with DTG a T_{Max} of 339.6°C (Jenkhongkarn and Phisalaphong 2023). Similarly, BC from *A. xylinum* AGR60 exhibited a first-stage loss of about 6%, a second-stage loss of 74%, and a residue weight of approximately 20% at 700°C, with major decomposition occurring between 300 and 360°C (Potivara and Phisalaphong 2019). Our results are consistent with these studies, where the initial weight loss is attributed to dehydration and volatilization of low-molecular-weight components or residual water in the BC matrix (Teixeira et al. 2019; Mohamad et al. 2022a). The significant weight loss in the second stage corresponds to the decomposition of β-glucan chains and oxidation of cellulosic materials into carbonaceous residue (Mohammadkazemi et al. 2015; Mohamad et al. 2022a). Additionally, the minor weight

loss between 400°C and 600°C is associated with the degradation of carbonaceous residues (De Araújo Júnior et al. 2016; Teixeira et al. 2019).

The TGA results confirm that BC derived from kombucha fermentation exhibits good thermal stability, making it suitable for applications requiring heat resistance, such as food packaging and biomedical materials. BTC and RTC demonstrated the highest thermal stability, with RTC emerging as a promising alternative due to its comparable performance and lower production cost.

10) Mechanical Properties Analysis Using Nanoindentation

Nanoindentation analysis was conducted to assess the nanoscale mechanical properties of BC samples. This highly precise and sensitive technique enables the measurement of local mechanical responses—such as hardness and elastic modulus—at both the micro- and nanoscale. Such detailed evaluation is essential for applications that require materials with excellent mechanical strength, flexibility, and structural integrity, including advanced food packaging, biomedical devices, and nanocomposites.

The BC samples used in this analysis were obtained from kombucha fermentation using Thai Red Tea (RTC) and Thai Black Tea (BTC), selected for their potential as cost-effective and efficient sources of BC. These tea types also offer distinct chemical profiles, providing a meaningful basis for comparing the resulting BC properties. The full results of the nano-indentation analysis are presented in **Table 3.9.**

The data show no significant differences ($P > 0.05$) in the mechanical properties of BC from BTC and RTC. This indicates that both types of tea produce BC with similar properties at the nanoscale. The similarity may be due to the comparable composition of the fermentation medium, suggesting that the type of tea does not greatly affect the mechanical characteristics of the BC. The microbial activity during kombucha fermentation seems to create a uniform cellulose network, leading

to similar properties in both BTC and RTC samples. In contrast, Nata de Coco (NDC) shows significant differences ($P < 0.05$) in some properties compared to BTC and RTC. For example, the reduced modulus is lower in NDC (4.14 GPa) than in BTC and RTC (around 4.94 GPa), and the Young's modulus for NDC is also lower (3.78 GPa) compared to BTC (4.52 GPa) and RTC (4.51 GPa). Since the drying process is the same for all samples, these differences may be due to variations in the fermentation medium, the bacterial strain used, or the purification process. These factors can affect the density and arrangement of the cellulose in the final BC product.

Table 3.9 Mechanical properties data analysis using nano-indenter of BC from kombucha fermentation of BTC, RTC, and commercial product (NDC)

Sample	MD (nm)	Pl (nm)	ML (mN)	H (GPa)	RM (GPa)	ERP	CC (nm/mN)	PW (nJ)	EW (nJ)	YM (GPa)
BTC	3440.51 ±289.23^{a}	3011.45 ±270.30^{a}	50.10 ±0.00^{a}	0.22 ±0.04^{b}	4.94 ±0.70^{b}	0.14 ±0.01^{b}	11.42 ±0.63^{b}	56.11 ±6.39^{a}	20.48 ±1.16^{a}	4.52 ±0.64^{b}
RTC	3412.25 ±259.56^{a}	2980.18 ±253.91^{a}	50.10 ±0.00^{a}	0.22 ±0.05^{b}	4.94 ±0.56^{b}	0.15 ±0.01^{b}	11.50 ±0.22^{b}	54.41 ±4.64^{a}	20.80 ±0.47^{a}	4.51 ±0.51^{b}
NDC	3612.65 ±162.08^{a}	3123.34 ±148.57^{a}	50.10 ±0.00^{a}	0.20 ±0.02^{a}	4.14 ±0.31^{a}	0.16 ±0.00^{a}	13.02 ±0.41^{a}	59.92 ±4.09^{b}	22.90 ±0.80^{b}	3.78 ±0.28^{a}

MD: maximum depth, Pl: plastic, ML: maximum load, H: hardness, RM: reduced modulus, ERP: elastic recovery parameters, CC: contact compliance, PW: plastic work, EW: elastic work, and YM: Young's Modulus. The different lowercase letters within the same column indicate statistically significant differences ($P < 0.05$).

Several factors can influence BC's mechanical properties, including cultivation methods (Krystynowicz et al. 2002), bacterial strains (Zeng et al. 2014; Chen et al. 2018a), NaOH concentration during purification (Suryanto et al. 2019; Chen et al. 2021), carbon sources (Chibrikov et al. 2023), nutrient composition (Betlej et al. 2020), and drying methods (Zeng et al. 2014). The mechanical properties of BC are closely related to its network structure, such as porosity, including intrafibrillar and interfibrillar spaces (Wang et al. 2023b). The Young's modulus values for BTC (4.52 GPa) and RTC

(4.51 GPa) are consistent with previous studies. For example, BC produced from different *Komagataeibacter* strains shows a range of 1.10 to 5.56 GPa (Chen et al. 2018a), and BC from *A. xylinum* AGR60 in coconut water reaches 9.14 GPa (Potivara and Phisalaphong 2019). Our results for BTC, RTC, and NDC fall within these ranges, suggesting that different fermentation conditions can still produce high-quality BC. However, other studies, like Zeng et al. (2014), report different ranges, with Young's modulus between 198 to 659 MPa and hardness between 19 and 39 MPa for BC from different strains and drying methods (Zeng et al. 2014). Research using nano-indentation for BC is limited, with Zeng et al. (2014) being one of the few studies found. Most other studies use conventional methods like tensile strength tests, making it difficult to directly compare our results. Still, our study adds valuable new data by using nano-indentation to measure BC's properties. This method could be very useful for BC research, but more studies are needed to confirm our findings.

3.4.2 Effect of Different Types of Additives on Bacterial Cellulose Yield and Characteristics

1) The Change of pH and Total Soluble Solid (TSS)

The study examined changes in pH and TSS throughout the fermentation process. Initially, before inoculation, the pH of the medium ranged from 3.33 to 5.90. After adding the starter culture, the pH dropped slightly, ranging from 3.18 to 4.42. By the end of the 15-day fermentation, the pH further decreased, ranging from 2.34 to 3.37. Among the additives, the medium with vitamin C (VC) showed the lowest pH, while the soy protein isolate (SPI) maintained the highest pH. The changes in pH over time are detailed in **Table 3.10** and shown in **Figure 3.11** (left).

The initial pH decrease following inoculation is primarily due to the starter culture's naturally lower pH. Organic acids like acetic and gluconic acid, produced as fermentation progresses, contribute to a further reduction in pH (Aswini et al. 2020; Lee et al. 2021). Additional organic acids such as glucuronic, lactic, malic, tartaric, citric, and succinic acids may also be formed during this process (Neffe-

Skocińska et al. 2017). Neffe-Skocińska et al. (2017) observed a similar pH shift, noting a decrease from 3.04 to 2.63 after 10 days of kombucha fermentation. In a study using HS medium supplemented with vitamin C, the pH decreased from 6.0 to a range of 3.9 to 4.9 after one week of fermentation with six different *G. xylinus* strains (Keshk 2014). This result highlights the typical pattern of acid production during kombucha fermentation.

In addition of pH observation, we also monitored the total soluble solids (TSS) of the fermentation broth. Initially, before adding the inoculum, TSS values ranged from 9.97 to 10.90 °Brix. After inoculation, TSS levels varied from 9.50 to 10.70 °Brix. Following fermentation, TSS values declined to a range of 8.57 to 9.60 °Brix, as shown in **Figure 3.11** (right) and **Table 3.10** TSS is an important measure that reflects the sugar concentration in a solution (Muzaifa et al. 2022). A decrease in TSS during fermentation is common. A study conducted by Zubaidah et al. (2019) reported a reduction in TSS for various snake fruit kombucha from 13.30–14.08 °Brix to 12.43–12.97 °Brix (Zubaidah et al. 2019). Similarly, a study reported a drop in TSS for cascara kombucha from 10.97 °Brix on the second day to 9.97 °Brix by the eighth day (Muzaifa et al. 2022). This decline in sugar levels is attributed to the activity of microorganisms, which convert sugars into glucose and other compounds that are then utilized for their growth and metabolic processes (Sinamo et al. 2022).

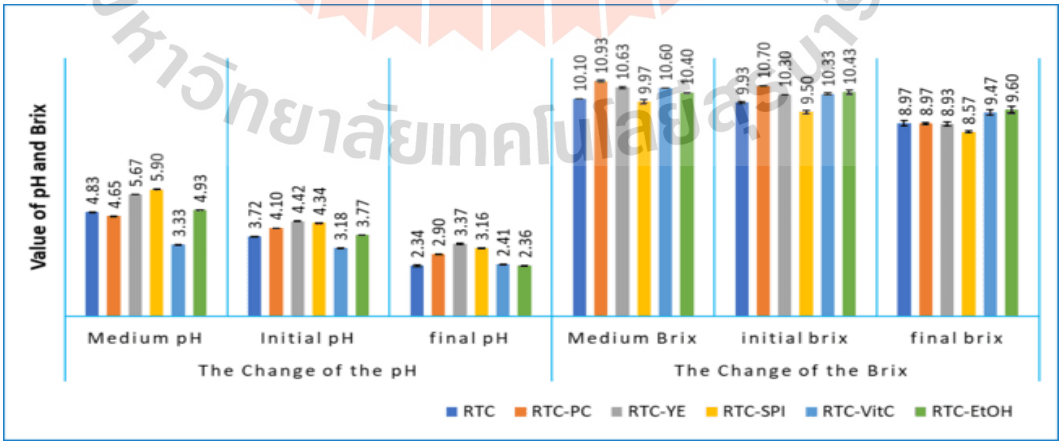

Figure 3.11 Changes in pH and °Brix before and after RTC kombucha fermentation with different type of additives

Table 3.10 Changes in pH and °Brix before and after RTC kombucha fermentation with different type of additives

Samples	The Change of the pH			The Change of the °Brix		
	Medium	Before	after	Medium	Before	after
RTC	4.83±0.01^{c}	3.72±0.00^{b}	2.34±0.04^{a}	10.10±0.00^{b}	9.93±0.05^{b}	8.97±0.13^{b}
RTC-PC	4.65±0.02^{b}	4.10±0.00^{d}	2.90±0.01^{c}	10.93±0.05^{e}	10.70±0.00^{e}	8.97±0.00^{b}
RTC-YE	5.67±0.00^{e}	4.42±0.00^{f}	3.37±0.02^{e}	10.63±0.05^{d}	10.30±0.00^{c}	8.93±0.10^{b}
RTC-SPI	5.89±0.01^{f}	4.34±0.00^{e}	3.16±0.02^{d}	9.97±0.09^{a}	9.50±0.08^{a}	8.57±0.05^{a}
RTC-VC	3.33±0.01^{a}	3.18±0.01^{a}	2.41±0.01^{b}	10.60±0.00^{d}	10.33±0.05^{c}	9.47±0.13^{c}
RTC EtOH	4.93±0.00^{d}	3.77±0.00^{c}	2.36±0.01^{a}	10.40±0.00^{c}	10.43±0.09^{cd}	9.60±0.15^{d}

Different lowercase letters within a column indicate significant differences among the five tea samples (LSD test: P < 0.05).

2) The Change of Sugar Composition

Sugar composition, especially sucrose, glucose, and fructose, was evaluated using HPLC. The result showed that there were changes in the concentration of the sugar components before and after fermentation, as is demonstrated in **Figure 3.12** and **Table 3.11**. The SCOBY used the sucrose in the kombucha as a source of carbon. The SCOBY utilized sucrose in the kombucha as a carbon source, essential for microbial growth and product formation (Shu 2007). It contains various yeasts and bacteria, including *Saccharomyces cerevisiae, Zygosaccharomyces rouxii, Schizosaccharomyces, Torulaspora delbrueckii, A. xylinum, and Gluconobacter* (Greenwalt et al. 2000). Before fermentation, the concentration of sucrose, glucose, and fructose was 9.03 to 9.58%, 0.21 to 2.53%, and 0.05 to 1.19%, respectively. The presence of glucose and fructose prior to fermentation may be attributed to both the use of kombucha culture and the hydrolysis of sucrose during the autoclaving process. Ball (1953) reported that autoclaving a 3% sucrose solution resulted in partial hydrolysis, yielding approximately 0.7–0.9% glucose. Similarly, de Lange (1989) demonstrated that autoclaving sucrose solutions at pH 2 could lead to complete hydrolysis into glucose and fructose, as confirmed by semi-quantitative analysis.

Notably, sucrose hydrolysis was also observed at pH values ranging from 5 to 7, albeit to a lesser extent.

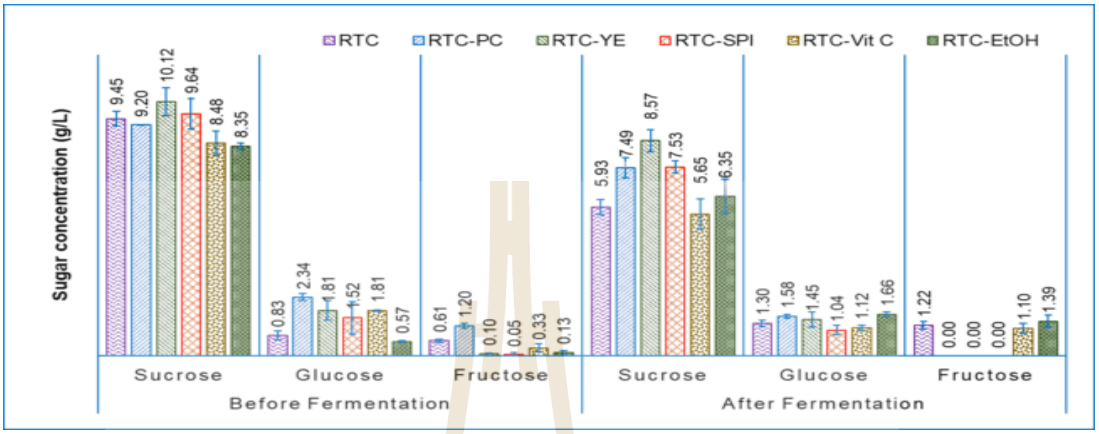

Figure 3.12 Changes in sugar composition (sucrose, glucose, and fructose) in RTC kombucha broth before and after fermentation with different types of additives.

In the early stage of kombucha fermentation, microorganisms hydrolyze sucrose into glucose and fructose, which are metabolized into carbon dioxide and ethanol (Wang et al. 2022a). In BC production, bacteria utilize these sugars for cellulose synthesis. At the end of the fermentation, the concentration of sucrose decreases to the range of 5.65 to 8.57%. For all the different additives, there are significant differences in sucrose concentration before and after fermentation. Before fermentation, the concentration of sucrose in all the samples was not significantly different ($P > 0.05$). However, after fermentation, the concentrations of sucrose in the samples are different. **Table 3.11** provides details about the differences in concentrations of sucrose, glucose and fructose before and after fermentation. Research by Neffe-Skocińska et al. (2017) revealed that over 10 days of Kombucha fermentation at 30°C, the glucose concentration rose from 0.09% to 0.1%, and fructose levels increased from 0.07% to 0.87%. Meanwhile, the sucrose concentration significantly dropped from 9.97% to 0.74%.

Table 3.11 Changes in sugar composition in RTC kombucha broth with different types of additives before and after fermentation

Samples	Before fermentation			After fermentation		
	Sucrose	Glucose	Fructose	Sucrose	Glucose	Fructose
RTC	$9.45\pm0.29^{b,B}$	$0.83\pm0.08^{a,A}$	$0.61\pm0.07^{c,A}$	$5.93\pm0.30^{a,A}$	$1.89\pm0.12^{b,B}$	$1.22\pm0.16^{bc,B}$
RTC-PC	$9.20\pm0.02^{b,B}$	$2.34\pm0.14^{c,B}$	$1.20\pm0.10^{d,B}$	$7.49\pm0.41^{c,A}$	$1.02\pm0.07^{c,A}$	$0.00\pm0.00^{a,A}$
RTC-YE	$10.12\pm0.56^{c,B}$	$1.81\pm0.39^{b,A}$	$0.10\pm0.01^{a,B}$	$8.57\pm0.45^{d,A}$	$2.36\pm0.30^{bc,B}$	$0.00\pm0.00^{a,A}$
RTC-SPI	$9.64\pm0.61^{b,B}$	$1.52\pm0.64^{b,A}$	$0.05\pm0.08^{a,A}$	$7.53\pm0.23^{c,A}$	$2.22\pm0.20^{a,B}$	$0.00\pm0.00^{a,B}$
RTC-VC	$8.48\pm0.07^{a,B}$	$1.81\pm0.03^{b,B}$	$0.33\pm0.17^{b,A}$	$5.65\pm0.60^{a,A}$	$0.92\pm0.10^{ab,A}$	$1.10\pm0.21^{b,A}$
RTC-EtOH	$8.35\pm0.08^{a,B}$	$0.57\pm0.04^{a,A}$	$0.13\pm0.09^{a,A}$	$6.35\pm0.68^{ab,A}$	$1.92\pm0.10^{c,B}$	$1.39\pm0.23^{c,B}$

Different lowercase letters within a column indicate significant differences among the five tea samples (LSD test: $P < 0.05$); different uppercase letters in the same row indicate the significant differences between the same sugar before and after fermentation (LSD test: $P < 0.05$).

3) The Appearance of Bacterial Cellulose

The appearance of BC produced from Thai red tea kombucha fermentation with different uses of additives are presented in **Figure 3.13.** The appearance of BC before purification exhibited distinct color variations depending on the additive used (**Figure 3.13(a)** and **3.13(b)**). As previously reported, BC from the Thai red tea kombucha showed a characteristic red-orange color. RTC-EtOH exhibited a similar red-orange hue to the control. RTC-VC resulted in a noticeably lighter orange shade. In contrast, BC from RTC-SPI, RTC-PC, and RTC-YE displayed significantly lighter colors, ranging from pale white to white-orange, indicating a reduced uptake or masking of natural tea pigments and artificial colorant.

The color variations observed in BC are influenced by the interaction of natural pigments from tea, artificial colorants, and fermentation additives. Thai red tea, in particular, is made from black tea and contains added artificial flavors and colorants. Tea leaves, rich in catechin polyphenols, undergo chemical transformations during black tea processing (Deka et al. 2021; Ito and Yanase 2022). Oxidase enzymes convert catechins into reddish-orange theaflavins and brown

thearubigins, the key pigments in black tea (Izawa et al. 2010; Deka et al. 2021; Ito and Yanase 2022). These water-soluble pigments easily incorporated into the BC matrix during fermentation. Additionally, FD&C Yellow No. 6 (INS 110), an artificial orange-red colorant in Thai red tea, enhances the coloration. The combination of natural and synthetic pigments gives the control BC its distinctive red-orange hue.

Figure 3.13 The appearance of BC sample from RTC kombucha fermentation with different type of additives: In fermentation process (a), before purification (b), after purification with sodium hydroxide (c), and after oven drying (d).

RTC-EtOH results suggest that ethanol had minimal impact on pigment absorption in BC. Color differences likely stem from interactions between tea pigments, additives, and microbial activity. In control and ethanol-treated samples, pigments remained more available, giving BC a red-orange hue. In contrast, SPI, YE, and PC-treated samples appeared lighter, possibly due to these additives affecting pigment solubility or binding. Interactions between tea polyphenols and artificial colorants may further reduce pigment absorption, as polyphenols form complexes with these

additives through hydrophobic, electrostatic, and hydrogen bonding (Shahidi and Dissanayaka 2023). Covalent interactions, which can occur during processes like heating and enzymatic reactions, may also contribute to reduced pigment incorporation in these additives-treated samples (Zhang et al. 2024).

After purification with 2% sodium hydroxide and drying in the oven at 40°C, the BC exhibits a consistent white, opaque color (**Figure 3.13(c)** and **3.13(d)**). This post-purification color aligns with the findings reported in most BC studies. Sodium hydroxide plays a vital role in BC purification by effectively removing tannins, polyphenols, residual bacteria, yeast cells, and proteins present in trace amounts within the kombucha pellicle (Amarasekara et al. 2020). It also facilitates the elimination of residual organic compounds, nucleic acids, and proteins produced by microbes during the fermentation process (Kamal et al. 2020).

4) BC Productivity and Water Holding Capacity

BC generated through kombucha fermentation exhibited distinct variations in wet yields, dry yields, and WHC based on the type of additives used, as depicted in **Figure 3.14**. The wet yields ranged from 61.73 ± 9.58 g/L for RTC-YE to 218.36 ± 12.85 g/L for RTC-EtOH. In a similar vein, the dry yields varied from 1.06 ± 0.10 g/L for RTC-YE to 2.18 ± 0.22 g/L for RTC-EtOH. The WHC of the samples varied between 57.49 ± 3.96 g water/g cellulose for RTC-YE and 109.31 ± 8.08 g water/g cellulose for RTC. Notably, the addition of certain additives, such as vitamin C and ethanol, significantly increased the wet productivity of BC compared to the RTC-C, with RTC-VC and RTC-EtOH showing significantly different results ($P < 0.05$). Conversely, the use of PC, SPI, and YE led to significantly lower wet yields compared to the control.

The dry yield of BC generally improved with the incorporation of most additives, except for YE, which produced the lowest dry yield among all samples. The highest dry yields were recorded for RTC-VC and RTC-EtOH, which did not differ significantly from each other ($P > 0.05$). Furthermore, WHC was highest in the RTC control, followed by RTC-EtOH, RTC-VC, RTC-SPI, RTC-PC, and RTC-YE, respectively. The

RTC-PC and RTC-SPI samples displayed similar outcomes across all measured parameters, with no significant differences observed ($P > 0.05$).

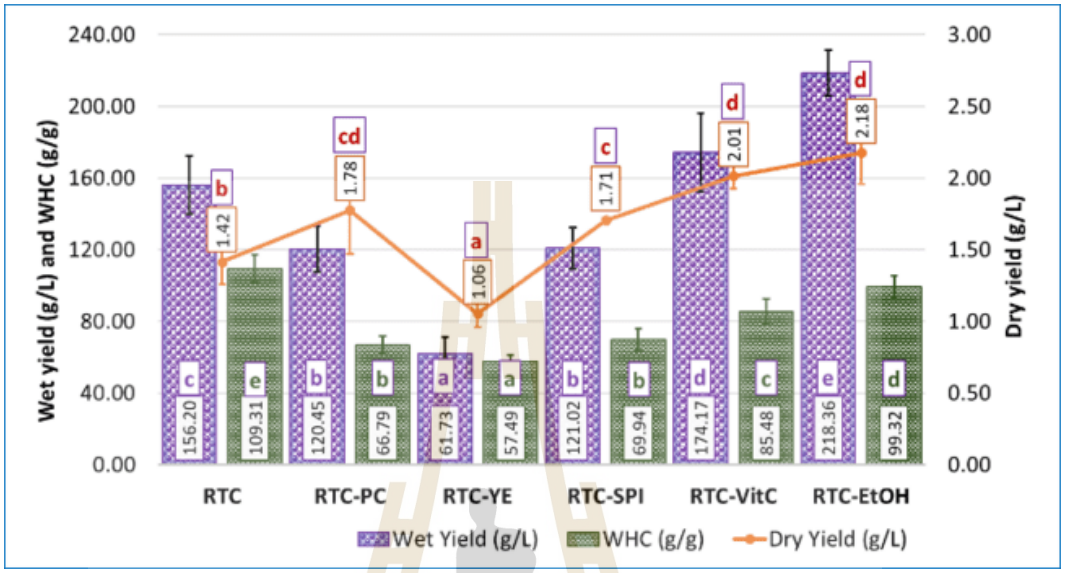

Figure 3.14 Wet yield (g/L), dry yield (g/L), and WHC (g water/g cellulose) from BC produced from RTC kombucha with different types additives.

Previous studies have reported varying effects of additives, including coffee grounds, yeast extract, vitamin C, and ethanol, on BC production. Some studies indicate that vitamin C can both enhance and reduce BC productivity. For instance, Keshk (2014) found that adding 0.5% (w/w) vitamin C increased BC production from 0.25 g/30 mL to 0.47 g/30 mL. Similarly, tropical fruits rich in vitamin C, such as mango, guava, and creole cherry, were shown to enhance BC production (Perna Manrique et al. 2018). Another study reported that a medium containing molasses with 0.5% ascorbic acid produced BC approximately three times higher than a control HS medium using *G. sucrofermentans* (Atykyan et al. 2020). In contrast, the addition of vitamin C to the medium of BC production using *K. hansenii* SI1 and *K. xylinus* PTCC 1734 resulted in lower BC productivity (Raiszadeh-Jahromi et al. 2020; Cielecka et al. 2021). In contrast, ethanol supplementation has consistently shown a significant increase in BC production. For example, the addition of 1% ethanol to the growth medium increased BC production by 57.7% using *G. xylinus* PTCC (Kazemi et

al. 2015). Similarly, a 1% ethanol supplementation in HS medium led to a 279% increase in BC production by *K. medellinensis* (Molina-Ramírez et al. 2018b). Moreover, in another study using *K. nataicola*, the addition of 1% ethanol increased BC yield by 48 ± 3% compared to the control (Fei et al. 2023).

The addition of 0.5% vitamin C and 1% ethanol in this study resulted in a notable increase in BC production. Compared to the control, the wet yield increased by 11.50% with vitamin C and 39.79% with ethanol, while the dry yield rose by 42.23% and 53.72%, respectively. These results align with previous studies suggesting that ethanol and vitamin C can enhance BC synthesis through different metabolic and regulatory mechanisms.

Ethanol has been shown to serve as an alternative energy source, reducing the reliance on glucose for ATP production and allowing more glucose to be diverted toward cellulose biosynthesis. Ethanol is metabolized via pyrroloquinoline quinone-dependent alcohol dehydrogenase (PQQ-ADH), which is linked to the electron transport chain and leads to increased ATP generation. Elevated ATP levels inhibit glucose-6-phosphate dehydrogenase, thereby decreasing flux through the pentose phosphate pathway and promoting the conversion of glucose into UDP-glucose, a direct precursor for cellulose synthesis (Montenegro-Silva et al. 2024). In addition, ethanol has been reported to upregulate genes involved in glucokinase activity, UDP-glucose biosynthesis, and BC production, while also enhancing cellular stress tolerance by promoting the expression of genes related to protein synthesis, iron uptake, and general metabolic stability (Ryngajłło et al. 2019).

In contrast, the stimulatory effect of vitamin C appears to be primarily associated with its role in reducing gluconic acid accumulation in the culture medium. By limiting gluconic acid production, vitamin C creates a more favorable pH environment and supports better bacterial growth and metabolic activity, which ultimately contributes to increased BC yield (Keshk 2014).

The WHC of BC resulted from RTC-C, RTC-PC, RTC-YE, RTC-SPI, RTC-VC, and RTC-EtOH was found to be 109.31±8.08, 66.79±4.74, 57.49±3.96, 69.94±6.11, 85.48±7.19, and 99.32±5.98 g water/g cellulose, respectively. The addition of various additives significantly reduced WHC values compared to the control sample, RTC-C ($P < 0.05$). Among the samples, those supplemented with nitrogen sources (RTC-YE and RTC-SPI) and RTC-PC exhibited the lowest WHC values, with RTC-YE showing the minimum WHC. The variation in the WHC of BC samples with different additives can be attributed to the structural and compositional changes induced during fermentation. A study reported that the addition of a higher concentration single sugar-linked glucuronic acid-based oligosaccharide (SSGO) to the synthetic medium resulted in a lower WHC value of BC (Ul-Islam et al. 2012).

The addition of SPI, YE, and PC are known to affect the metabolic activity of cellulose-producing bacteria, leading to a denser BC matrix with reduced porosity. This structural compactness limits the availability of hydrophilic sites for water retention, thereby decreasing WHC. In contrast, samples containing vitamin C and ethanol retained relatively higher WHC. BC from media containing vitamin C and ethanol holds more water likely because these additives make the BC structure more hydrophilic and better at forming hydrogen bonds with water. In addition, BC with Vitamin C, has smaller BC fiber among others thus increase the surface area. The higher surface area the higher the three-dimensional nanofibril structure the more water molecules trapped on the matrix (Ul-Islam et al. 2012). Ethanol, on the other hand, reduces the crystallinity of BC, making the cellulose network looser and exposing more hydrophilic sites.

These findings align with previous studies. For instance, Gayathry (2015) reported a WHC of approximately 87.14 g/g for BC produced from fermented coconut water (NDC) (Gayathry 2015). WHC values for NDC varied between 38.7±0.6 and 88.1±2.7 g/g when different pH levels, sucrose concentrations, and ammonium sulfate were used during production (Jagannath et al. 2008). Similarly, BC synthesized

using distillery wastewater achieved a WHC of 98.5 g/g (Wu and Liu 2013). WHC values ranging from 102 to 138 g/g were observed for BC produced in fermentation media derived from biodiesel and confectionery industry waste (Tsouko et al. 2015). Higher WHC values have also been documented, such as 114.01 g/g for BC produced via kombucha fermentation using black tea as the substrate (Avcioglu et al. 2021). BC synthesized from co-cultures of *K. hansenii* and *Rhizobium sp.* showed WHC values of 115 to 130 g/g (Almihyawi et al. 2024), higher compare to this study. These studies collectively highlight the variability of WHC based on fermentation conditions, bacterial strains, and additive use.

5) Morphology analysis

The morphology of BC samples produced from RTC kombucha fermentation with various types of additives was examined using scanning electron microscopy (SEM). Each sample was magnified 10,000 and 30,000 times (**Figures 3.15 (a.1 - f.2)**). The distribution size of the diameter of dried BC fiber was observed using ImageJ application and the results is depicted in **Figure 3.16**.

Based on the visual image, while there are similarities in the basic fiber form, differences in the finer details of structure suggest that the fiber morphology is not identical across all the samples. Overall, the BC samples exhibit a consistent fiber pattern, consistent with the findings of the previous studies (Illa et al. 2019; Brandes et al. 2020; Nguyen and Nguyen 2022). The BC sample of RTC-SPI (**Figure 3.15(b.1 an b.2)**) showed residues or insoluble materials persisting after alkali purification, likely due to the attachment of protein molecules to the fiber. This attachment of residual materials to BC fibers was also reported by Amorim et al. (2023) (Amorim et al. 2023).

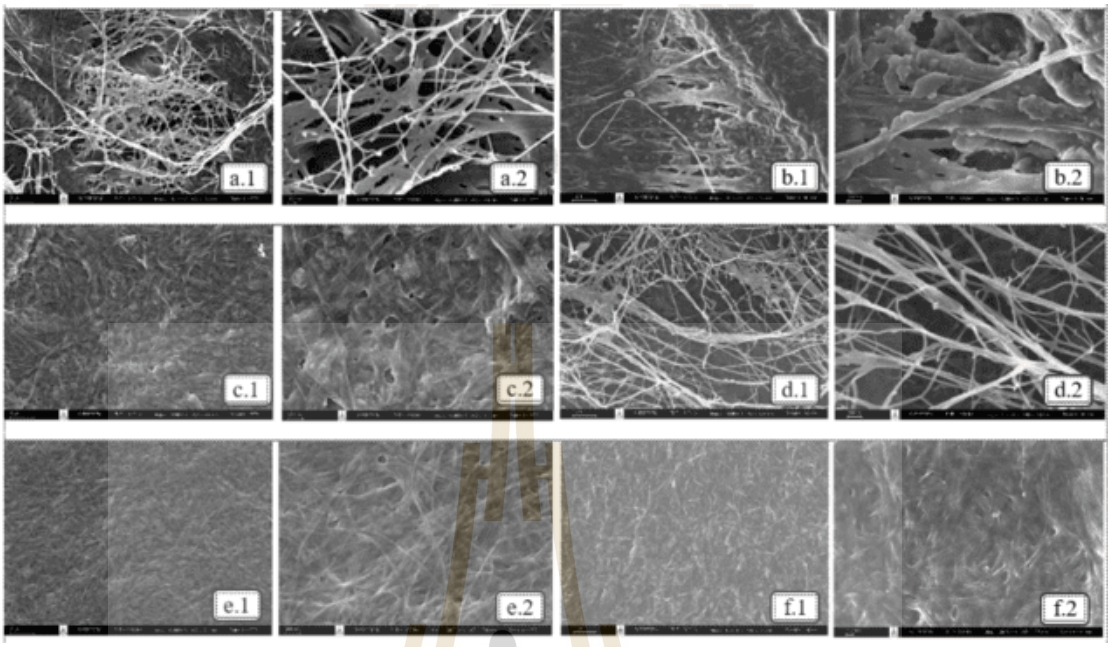

Figure 3.15 SEM image of BC (a) RTC-control; (b) RTC-SPI; (c) RTC-YE; (d) RTC-PC; (e) RTC-VC; (f) RTC-EtOH: (1) magnification of 10000 x; (2) magnification of 30,000x.

The polydispersity graphs of BC fiber diameters (**Figure 3.16**) indicate that the fiber sizes range from 13.74 nm to 68.44 nm, with average diameters varying between 25.49 ± 6.92 nm and 45.98 ± 9.38 nm. The average diameters of RTC-EtOH, RTC-SPI, RTC-YE, RTC-VC, RTC-PC, and RTC-C are 45.98 ± 9.38 nm, 40.92 ± 10.90 nm, 33.85 ± 4.91 nm, 25.50 ± 4.92 nm, and 29.70 ± 5.17 nm, respectively. Among the additives, VC produced BC with the smallest fiber diameters, while ethanol resulted in the largest. Sample with SPI, YE, and PC produced BC fibers with diameters larger than the RTC control but smaller than those in the RTC-EtOH sample. These findings demonstrate the significant role of additives in influencing BC fiber morphology.

The mechanisms by which additives affect BC fiber diameter remain unexplored. Among all the treatments, ethanol had the most significant impact on BC fiber morphology by markedly increasing fiber diameters. This observation supports previous findings by Fatima et al. (2023) who reported that ethanol concentrations of 1.5% and 3% led to increased fiber diameters ranging from 64.1–82.3 nm and 71.6–

88.6 nm, respectively. The underlying mechanism is thought to involve ethanol's disruption of hydrogen bonding during cellulose assembly, which interferes with the orderly formation of microfibrils and promotes the development of thicker fibers.

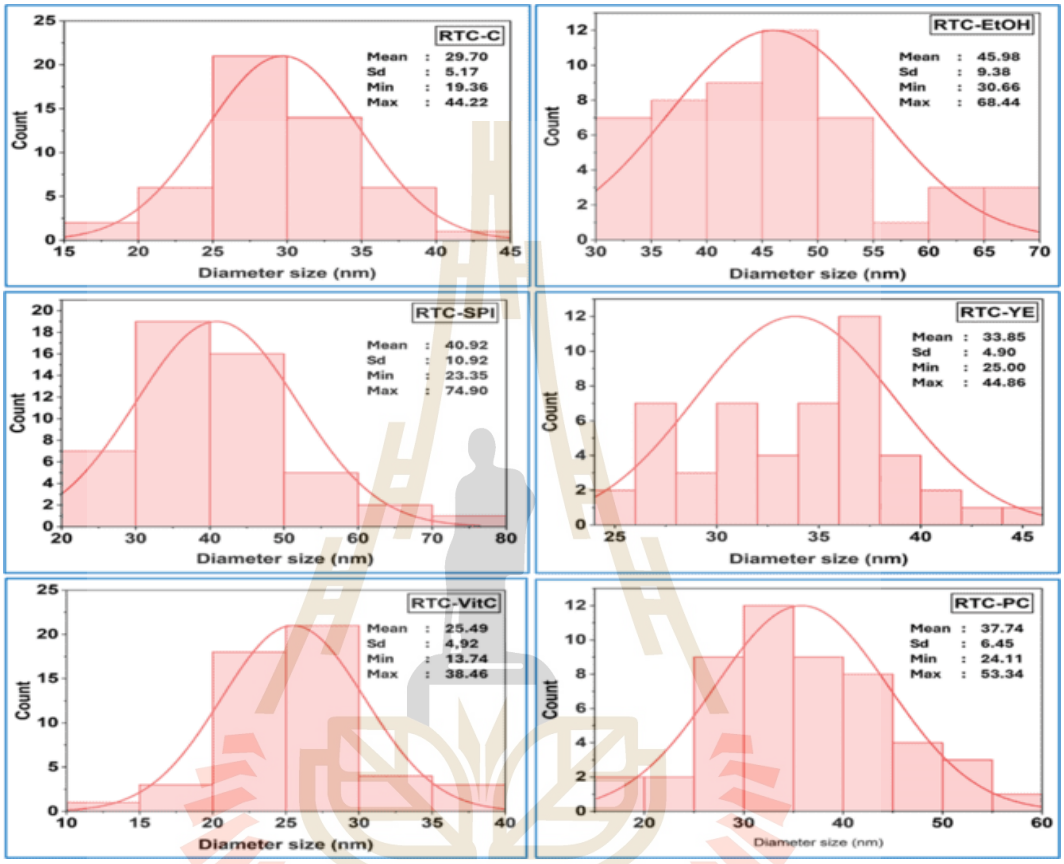

Figure 3.16 Graph of poly distribution size of BC samples diameter from RTC kombucha fermentation with various types of additives.

In contrast, the addition of VC resulted in the production of considerably thinner fibers. This effect may be linked to vitamin C's function as an antioxidant, which helps create a more favorable oxidative environment for bacterial metabolism during fermentation. By minimizing oxidative stress, VC can support enzymatic activity and stabilize the cellulose biosynthesis process. Moreover, it may enhance glucose metabolism and influence the crystallization and polymerization behavior of cellulose chains. Keshk (2014) reported that VC supplementation not only boosted BC yield but also altered its crystalline structure, suggesting that it plays a role in fine-tuning fiber assembly and promoting the formation of finer nanofibrils.

In comparison, samples containing YE, SPI, and PC exhibited moderately increased fiber diameters. This may be attributed to the nutritional contributions of nitrogen sources, peptides, and polyphenols present in these additives. Nitrogen-rich compounds such as YE and SPI are known to support microbial growth and biosynthetic activity, which can indirectly affect fiber thickness and structure (Said Azmi et al. 2023). Additionally, bioactive compounds in PC may interact with microbial cells or enzymes, subtly modifying the organization and bundling of cellulose fibrils.

Consistent with these observations, Illa et al. (2019) reported BC fiber diameters ranging from 10 to 60 nm, produced by *K. hansenii* 23769 (ATCC) and a cellulose-producing strain isolated from grape juice, with average diameters of 28.9 ± 5.6 nm and 28.6 ± 6.7 nm, respectively (Illa et al. 2019). The study highlighted the influence of microbial strain and cultivation medium on fiber dimensions. Similarly, Abol-Fotouh et al. (2020) showed that BC fibers produced by *K. saccharivorans* MD1 cultivated in HS medium with palm date supplementation ranged from 10 to 90 nm, illustrating how nutrient supplementation can modulate bacterial activity and BC properties (Abol-Fotouh et al. 2020).

Yilmaz and Goksungur (2024) further demonstrated that BC nanofibers derived from HS medium exhibited fiber diameters between 18 and 69 nm, averaging 36 nm. BC fibers from a waste fig medium had larger diameters, ranging from 23 to 90 nm, with an average of 44 nm. The larger fiber diameters in the waste fig medium may result from its complex composition, which could enhance nutrient availability and alter the cellulose biosynthesis pathway. In summary, the BC fiber diameters obtained from Thai red tea kombucha with different additives are consistent with those reported in earlier studies. These results confirm that the type and concentration of additives play a significant role in shaping BC fiber morphology.

6) Fourier Transform Infrared Spectroscopy Analysis

Figure 3.17 presents the FTIR spectra of BC samples produced from RTC kombucha fermentation with various additives, alongside the spectra of a BC sample from NDC for comparison. Overall, all BC samples exhibit similar spectral bands, but the intensity of these bands varies among the samples.

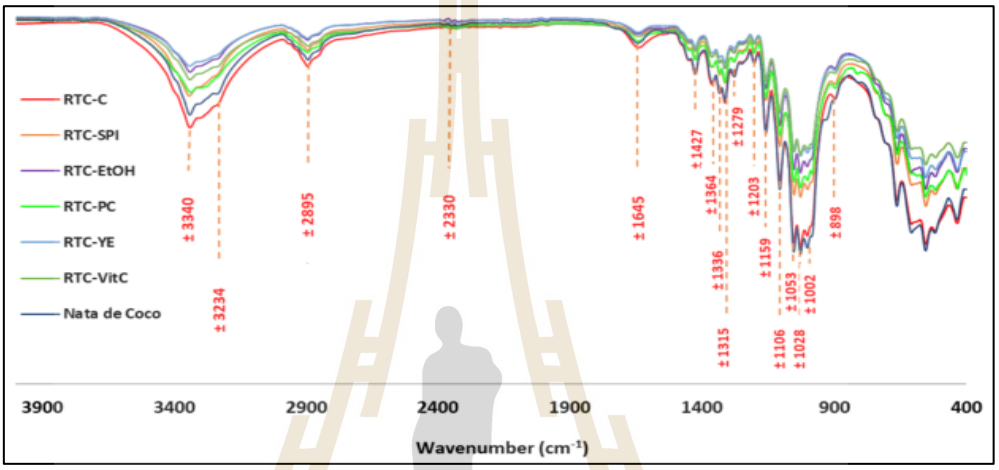

Figure 3.17 FTIR spectra of BCs from RTC kombucha fermentation with various types of additives

The FTIR spectra analysis of BC samples are divided into two main regions: the feature region and the fingerprint region. The feature region encompasses high-frequency wavenumbers between 4000 and 1330 cm^{-1}, while the fingerprint region spans 1330 to 500 cm^{-1} (Liu et al. 2023). In the feature region, key peaks were observed at wavenumbers around 3340 cm^{-1}, 3234 cm^{-1}, and 2895 cm^{-1}. The broad, intense bands at 3340 cm^{-1} and 3234 cm^{-1} indicate O-H stretching vibrations, while the peak near 2895 cm^{-1} corresponds to C-H stretching (Amorim et al. 2023). Additionally, a weak peak around 2330 cm^{-1} suggests the presence of triple-bond functional groups, such as C≡C and C≡N (Srivastava and Mathur 2022).

Another significant region, between 1350 and 2000 cm^{-1}, revealed absorption peaks at 1364 cm^{-1}, 1427 cm^{-1}, and 1644 cm^{-1}. The band at 1364 cm^{-1} corresponds to C-H symmetric bending, while the peak at 1427 cm^{-1} represents CH_2 symmetric bending. The 1644 cm^{-1} peak is associated with C=O stretching vibrations

from the glucose carbonyl group (Liu et al. 2023). In the fingerprint region, several distinct peaks were detected at 1336 cm^{-1}, 1315 cm^{-1}, 1279 cm^{-1}, 1203 cm^{-1}, 1159 cm^{-1}, 1106 cm^{-1}, 1053 cm^{-1}, 1028 cm^{-1}, 1002 cm^{-1}, and 898 cm^{-1}. The peak at 1336 cm^{-1} corresponds to OH in-plane bending, and the one at 1315 cm^{-1} is linked to CH_2 shifting at the C-6 position. The band at 1159 cm^{-1} is attributed to C-O-C antisymmetric bridge stretching, while the peak at 1106 cm^{-1} corresponds to ring asymmetric stretching. Peaks at 1053 cm^{-1} and 1028 cm^{-1} are associated with C-O-C and C-O-H stretching vibrations in the sugar ring, as well as C-O stretching, respectively (Liu et al. 2023). The peak between 898 and 894 cm^{-1} is linked to C-O-C stretching in β-1,4-glycosidic linkages, indicating the presence of an amorphous absorption band (Ciolacu et al. 2011).

The impact of additives on the FTIR spectra of BC is primarily reflected in variations in band intensity, rather than shifts in peak positions. Additives such as phenolic compounds (PC, e.g., caffeine), ethanol (EtOH), yeast extract (YE), vitamin C (VC), and soy protein isolate (SPI) can disrupt the hydrogen-bonding network within the BC matrix, as evidenced by the reduced intensity of the O–H stretching region (~3300–3400 cm^{-1}) (Moura et al. 2019; Feng et al. 2021; Wang et al. 2023, 2024; Liu et al. 2025). This suggests diminished hydroxyl group interactions and potentially increased hydrophobicity. As reported by Fornaro et al. (2015), hydrogen bonding significantly influences IR spectra by modifying both the frequency and intensity of bands associated with vibrational modes of directly involved functional groups. The observed spectral changes, particularly with ethanol treatment, support its role in weakening hydrogen bonding in the cellulose matrix.

A distinct peak at approximately 1645 cm^{-1}, observed across all samples, is attributed to the H–O–H bending vibration of water adsorbed by the hydroxyl-rich cellulose network (Zheng et al. 2019). Its consistent presence indicates that moisture remains associated with the BC structure regardless of the additive. However, variations in its intensity among different treatments reflect differences in

water retention capacity or the interaction of functional groups introduced by each additive, affecting the hydration behavior of the BC matrix.

7) X-Ray Diffraction (XRD) Analysis

Figure 3.18 illustrates the X-ray diffraction (XRD) patterns of different BC samples, highlighting three prominent peaks consistently observed at 2θ values of approximately 14.78°, 16.89°, and 22.90°. These peaks confirm the crystalline structure characteristic of BC (Said Azmi et al. 2023). The XRD profiles align closely with those previously reported for BC (Revin et al. 2018; Jittaut et al. 2023; Said Azmi et al. 2023). Despite the uniformity in chemical structure indicated by the XRD patterns, variations in diffraction peak intensities are evident among the samples. The most intense peak near 23°, is associated with cellulose type I (Said Azmi et al. 2023; Hossen et al. 2024). According to Gaspar et al. (2014), the peaks at 2θ values of 14.7°, 16.8°, and 22.7° correspond to the 100, 110, and 200 crystallographic planes, typical of monolithic cellulose type I found in native cellulose (Gaspar et al. 2014). The peak appeared at around 22.90° (2θ) indicate that the celluloses are crystalline in nature (Samuel and Adefusika 2019). Differences in relative peak intensity among the samples likely reflect subtle variations in cellulose chain orientation (Said Azmi et al. 2023).

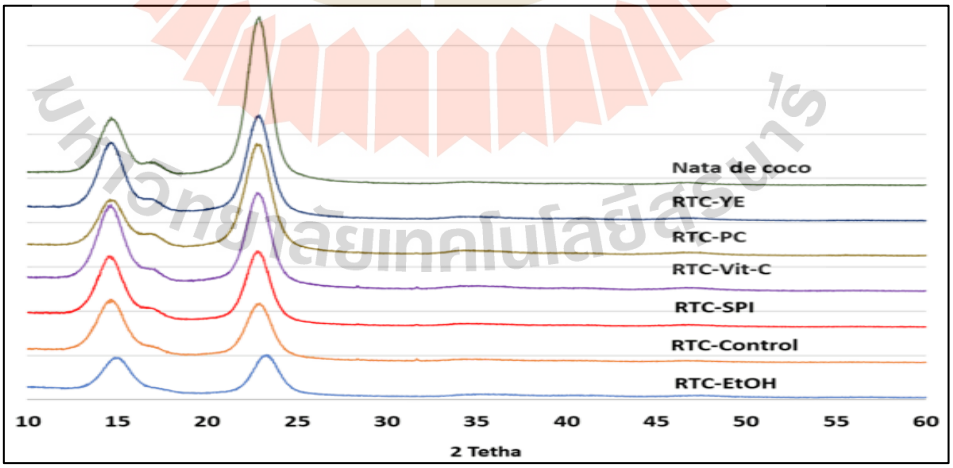

Figure 3.18 XRD spectra of BC from Thai red tea kombucha with different type of additives

The XRD data was used to calculate the crystallinity index (CI) and crystallite size of the BC samples, with the CI values presented in **Table 3.12**. The CI was determined using the Segal peak height method, yielding values ranging from 80.22% to 87.65%. All BC samples, except for RTC-EtOH, closely resembled the CI of NDC, which was 86.66%. The RTC-EtOH sample exhibited the lowest CI, likely due to the absence of, or a very subtle, peak around 16.89° (2θ). Several factors are known to influence the crystallinity of BC. These include the type of carbon and nitrogen sources, the use of various additives, the bacterial strain, fermentation conditions (such as temperature and duration), and post-production treatments (Zeng et al. 2011; Thielemans et al. 2023). Some previous studies reported that the effect of ethanol lead to decrease of crystallinity index of BC (Zeng et al. 2011; Cielecka et al. 2021; Wang et al. 2021). This reduction in crystallinity suggests that the cellulose structure becomes more disordered and less compact, possibly as a result of hydrogen bond disruption caused by ethanol treatment (Wang et al. 2021).

The CI results of BC in this study are consistent with findings from various other studies. For example, BC produced from pineapple peel waste fermentation achieved a CI of 87% (Sardjono et al. 2019), while BC fermented from pineapple waste solution had a CI of 82.2% (Pham and Tran 2023). BC derived from citrus processing waste or discarded fruits exhibited a CI of 86.9% (Andritsou et al. 2018), and BC produced in a HS-medium with different carbon sources showed a crystallinity ranging from 57% to 85% (Heydorn et al. 2023). Other studies have reported slightly lower CI values, such as BC produced using crude distillery effluent, which had a CI of 80.2% (Gayathri and Srinikethan 2019), and BC derived from wastewater of Arenga starch production, which had a CI of approximately 79.6% (Rahmayetty and Sulaiman 2023).

Table 3.12 Crystallinity index and average crystallite size of dried BC from Thai red tea kombucha fermentation with different type of additives.

Sample	Crystallinity Index (%)	Average Crystallite Size (nm)
RTC-C	85.36	3.512
RTC-PC	86.48	3.162
RTC-YE	87.65	3.356
RTC-SPI	85.30	3.302
RTC VC	85.71	3.286
RTC-EtOH	80.22	3.165
NDC	86.66	3.544

XRD analysis was performed once; therefore, variance data are not available

Further analysis is the average of the crystallite size of BC samples as shown in **Table 3.12**. The size of the crystallite ranging from 3.162 to 3.512 nm, slightly lower than crystallite size of NDC, 3.544 nm. This results in accordance with some of previous studies. BC produced by *G. xylinus* InaCC B404 in HS medium has a crystallite size of 3.06 nm (Agustin et al. 2021). In comparison, BC produced from black tea kombucha after 3 and 5 days of fermentation has crystallite sizes of 3.29 nm and 4.80 nm, respectively (Balistreri et al. 2024). However many studies reported the higher of crystallite size such as 4.9 and 4.76 nm (Sardjono et al. 2019), 5.6 nm (Jia et al. 2017), and 8.36 nm (Gayathri and Srinikethan 2019).

8) Thermogravimetric Analysis (TGA/DTG)

Figure 3.19 presents the thermogravimetric (TG) and derivative thermogravimetric (DTG) curves of the BC samples, analyzed using thermogravimetric analysis (TGA). **Table 3.13** shows the data of the decomposition change during analysis process. The data reveal the thermal stability and decomposition behavior of BC samples, including RTC-C, RTC-PC, RTC-YE, RTC-SPI, RTC-VC, and RTC-EtOH. The data from NDC was included for comparison. TGA and DTG analyses are crucial for studying BC applications. They help assess the purity, composition, drying behavior, and ignition

temperatures of materials. Additionally, these analyses provide insights into the thermal stability of BC, which is important for evaluating the effectiveness of chemical treatments that enhance bonding between natural fibers and polymer or synthetic fiber matrices (Nurazzi et al. 2021).

The first-stage weight loss, ranging from 1.42% to 7.52%, corresponds to the dehydration and volatilization of low-molecular-weight components or residual water in the BC matrix (Teixeira et al. 2019; Mohamad et al. 2022a). RTC-PC showed the lowest first-stage weight loss (1.42%), likely due to reduced moisture retention from the additive. This result relatively close result to previous result i.e. 1-2% (Gismatulina and Budaeva 2024) and 5-9% (Mohamad et al. 2022a).

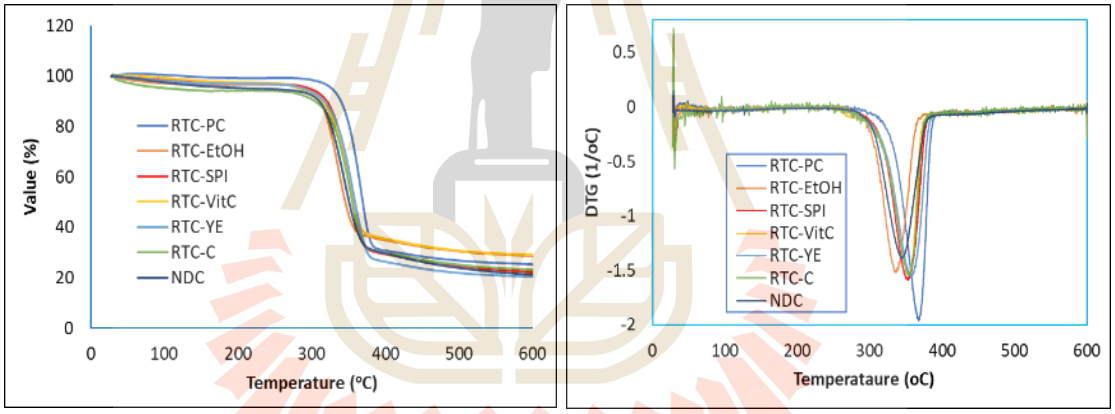

Figure 3.19 TGA (left) and DTG (right) thermographs of BC samples from RTC kombucha fermentation with different types of additives.

The second-stage weight loss, corresponding to the thermal decomposition of cellulose, ranged from 68.13% (RTC-EtOH) to 76.48% (RTC-YE), reflecting variations in thermal stability influenced by the additives. Nitrogen-based additives (RTC-PC, RTC-YE, RTC-SPI) generally showed higher second-stage losses, indicating enhanced cellulose decomposition under thermal stress. Residual weights at 600°C varied between 20.37% (RTC-YE) and 29.08% (RTC-VC), suggesting differences in the formation of thermally stable by-products. This stage represents the most significant weight loss, primarily driven by the breakdown of β-glucan chains and the

oxidation of cellulosic materials into carbonaceous residues (Mohammadkazemi et al. 2015; Mohamad et al. 2022a).

Table 3.13 The details of data decomposition during the TGA process of BC samples from RTC kombucha fermentation with different types of additives

Samples	First stage weight loss (%)	Second stage weight loss (%)	Residue (%)	DTG Peak range (°C)	DTG T_{Max} (°C)
RTC-C	6.03	71.06	23.07	255 – 379	353.67
RTC-PC	1.42	73.90	25.30	285 – 396	347.50
RTC-YE	3.09	76.48	20.37	270 – 389	356.67
RTC-SPI	2.94	74.81	22.21	271 – 384	352.67
RTC VC	2.60	68.27	29.08	258 – 378	354.17
RTC-EtOH	3.25	68.13	28.52	270 – 380	347.50
NDC	7.52	67.69	24.76	255 – 387	343.67

The findings of this study are consistent with previous research. For instance, BC produced by *G. xylinus* AGR 60 exhibited a first-stage mass loss of 6.2%, a second-stage mass loss of approximately 64.0%, and a residue of around 22.8% at 600°C, with a DTG T_{Max} of 339.6°C (Jenkhongkarn and Phisalaphong 2023). Similarly, BC from *A. xylinum* AGR 60 showed a first-stage mass loss of about 6%, a second-stage loss of approximately 74%, and a residue weight of around 20% at 700°C, with major thermal decomposition occurring between 300°C and 360°C (Potivara and Phisalaphong 2019).

The DTG peak temperature range (255–396°C) and maximum degradation temperatures (DTG T_{Max}: 343.67–356.67°C) show slight variations in the thermal degradation profiles, with RTC-YE exhibiting the highest DTG T_{Max} (356.67°C). These differences highlight the influence of additives on the thermal behavior of BC. The results align with previous studies, which report DTG peak ranges of 186–363°C and 199–347°C for BC treated by freeze-drying and hot-press drying, respectively, with

DTG T_{Max} values of 343.6°C and 313.4°C (Mohamad et al. 2022a). Additionally, BC produced by *G. xylinus* shows a DTG T_{Max} at 328.36°C (Jia et al. 2017).

9) Mechanical Properties Analysis Using Nanoindentation

Nanoindentation analysis was utilized to evaluate the nanoscale mechanical properties of BC samples. This highly precise technique measures local mechanical responses at micro- and nanoscale levels, making it essential for applications requiring durability and flexibility. BC samples selected for this analysis included RTC-EtOH and RTC-VC, chosen for their higher productivity, alongside control (RTC-C) and NDC samples for comparison. Detailed results are presented in **Table 3.14**.

The data show that in general, mechanical properties of RTC-EtOH and RTC-VC are quite different in many parameters such as maximum depth, plastic, reduced modulus, elastic recovery parameter, elastic work, and young's modulus. This indicates that both types of additives produce BC with quite different mechanical properties at the nanoscale. The differences in the mechanical properties of both could be attributed to the effects of the additives used during the fermentation process. Ethanol (EtOH) and vitamin C influence BC structure differently, impacting its mechanical behavior. Compare to RTC-C and NDC, some parameters show significantly different value, while others parameters are not significantly different.

The mechanical properties of BC are influenced by various factors, including cultivation methods, bacterial strains, purification processes, carbon sources, nutrient composition, and drying methods. Different cultivation techniques and bacterial strains affect the structure and quality of BC, impacting its strength and crystallinity (Krystynowicz et al. 2002; Zeng et al. 2014; Chen et al. 2018a). The purification process, particularly the concentration of NaOH used, determines the removal of impurities, influencing fiber quality (Suryanto et al. 2019; Chen et al. 2021). Additionally, the type of carbon source and nutrients, such as nitrogen, used during fermentation can affect BC's yield and mechanical properties (Betlej et al. 2020; Chibrikov et al. 2023). Drying methods also play a crucial role, in altering porosity and

density, which directly impact BC's flexibility, strength, and network structure, including intrafibrillar and interfibrillar spaces (Zeng et al. 2014; Wang et al. 2023b). These combined factors determine the unique mechanical characteristics of BC.

Another important factor to consider, complementing the earlier discussion, is the CI which plays a crucial role in determining the mechanical properties of BC. Research has shown that a higher CI generally results in increased stiffness and hardness while reducing ductility (Dusunceli and Colak 2008). Additionally, an increase in crystallinity has been linked to a higher Young's modulus (Adekoya et al. 2022). In this study, RTC-EtOH, with a CI of 80.22%, exhibited lower stiffness and hardness compared to RTC-VC, which had a CI of 85.71%. The Young's modulus (YM) of RTC-EtOH was 4.03 GPa, whereas RTC-VC displayed a higher YM of 4.47 GPa. Although the difference in hardness (H) was not statistically significant, RTC-EtOH showed a lower hardness value (0.20 GPa) compared to RTC-VC (0.23 GPa). Furthermore, the reduced CI in RTC-EtOH contributed to greater plasticity, as evidenced by its higher contact compliance (CC: 12.24 nm/mN) compared to RTC-VC (11.66 nm/mN). The plastic work (PW: 55.32 nJ) and elastic work (EW: 22.00 nJ) of RTC-EtOH were also higher than those of RTC-VC (PW: 52.73 nJ, EW: 20.90 nJ), indicating an increased energy absorption capability. Further supporting the notion that higher crystallinity contributes to enhanced stiffness and mechanical strength (Dusunceli and Colak 2008).

Young’s modulus values for RTC-EtOH were lower than those of RTC-VC and RTC-C but comparable to the NDC sample. Generally, these values align with previous studies. For instance, BC produced from various *Komagataeibacter* strains exhibits a Young's modulus range of 1.10 to 5.56 GPa (Chen et al. 2018a), while BC derived from *A. xylinum* AGR60 grown in coconut water reaches 9.14 GPa ((Potivara and Phisalaphong 2019).. The values observed for RTC-EtOH, RTC-VC, and RTC-C are within these ranges, indicating that different fermentation conditions can still yield high-quality BC. However, other studies, such as Zeng et al. (2014), report lower values,

with Young's modulus ranging from 198 to 659 MPa and hardness between 19 and 39 MPa, depending on the strain and drying methods used (Zeng et al. 2014).

Table 3.14 Mechanical properties data analysis using nano-indenter of BC from kombucha fermentation of RTC-C, RTC-EtOH, RTC-VC, and NDC.

Sample	MD (nm)	Pl (nm)	ML (mN)	H (GPa)	RM (GPa)	ERP	CC (nm/mN)	PW (nJ)	EW (nJ)	YM (GPa)
RTC-EtOH	3570.13 ±50.11^{b}	3110.31 ±48.59^{b}	50.10 ±0.00^{a}	0.20 ±0.01^{a}	4.41 ±0.09^{a}	0.15 ±0.00^{a}	12.24 ±0.09^{b}	55.32 ±1.14^{b}	22.00 ±0.16^{b}	4.03 ±0.08^{a}
RTC-VC	3308.46^{a} ±145.22	2870.18 ±121.85^{a}	50.10 ±0.00^{a}	0.23 ±0.02^{a}	5.04 ±0.51^{c}	0.15 ±0.01^{a}	11.66 ±0.82^{a}	52.73 ±3.34^{ab}	20.90 ±1.30^{a}	4.61 ±0.47^{b}
RTC-C	3412.25 ±259.56^{ab}	2980.18 ±253.91^{b}	50.10 ±0.00^{a}	0.22 ±0.05^{a}	4.94 ±0.56^{b}	0.15 ±0.01^{a}	11.50 ±0.22^{a}	54.41 ±4.64^{a}	20.80 ±0.47^{a}	4.51 ±0.51^{b}
NDC	3612.65 ±162.08^{bc}	3123.34 ±148.57^{b}	50.10 ±0.00^{a}	0.20 ±0.02^{a}	4.14 ±0.31^{a}	0.16 ±0.00^{a}	13.02 ±0.41^{c}	59.92 ±4.09^{bc}	22.90 ±0.80^{c}	3.78 ±0.28^{a}

MD: maximum depth, Pl: plastic, ML: maximum load, H: hardness, RM: reduced modulus, ERP: elastic recovery parameters, CC: contact compliance, PW: plastic work, EW: elastic work, and YM: Young's Modulus. The different lowercase letters within the same column indicate statistically significant differences ($P < 0.05$).

3.4.3 Effect of Carbon Source Combinations on Bacterial Cellulose Yield and Characteristics

1) The Change of pH and Total Soluble Solid (TSS)

This study investigated how various carbon sources influenced pH changes during a 15-day kombucha fermentation. The initial pH values of the media before inoculation ranged from 4.57 to 4.84, showing some statistically significant differences among groups. After inoculation with the kombucha culture, the pH dropped immediately to a range of 3.61 to 3.66, which can be attributed to the naturally acidic nature of the starter itself. Over the course of fermentation, the pH continued to decrease significantly, with final values ranging from 2.17 to 2.66 by day 15.

The reduction in pH is primarily due to microbial metabolism, particularly the activity of acetic acid bacteria (AAB) and yeasts that convert sugars into organic acids. As fermentation progresses, these microorganisms produce compounds such as acetic acid and gluconic acid, both of which contribute to the acidification of the medium (Aswini et al. 2020; Lee et al. 2021). Other minor acids like glucuronic, lactic, malic, citric, tartaric, and succinic acids may also be formed, further lowering the pH (Neffe-Skocińska et al. 2017).

The choice of carbon source significantly influenced the final pH levels, reflecting distinct metabolic behaviors during fermentation. RTC-SGlu (sucrose-glucose) and RTC-SD (sucrose-dextrose) yielded the lowest final pH values (2.17 ± 0.01 and 2.21 ± 0.01, respectively; $P > 0.05$), indicating pronounced acid production. This aligns with the rapid fermentability of glucose and dextrose, which are readily metabolized by microbial communities to support efficient growth and acid generation. In contrast, RTC-SGly (sucrose-glycerol) exhibited the highest final pH (2.66 ± 0.00), suggesting limited acidification due to the slower assimilation of glycerol by acetic acid bacteria (AAB) and yeasts. RTC-SF (sucrose-fructose) demonstrated intermediate acidification (pH 2.46 ± 0.01), likely attributable to fructose's preferential uptake over

sucrose, which requires prior hydrolysis. The control (RTC-C, pH 2.52 ± 0.04) displayed a typical fermentation profile but with marginally lower acid production compared to glucose- or dextrose-amended groups, underscoring the metabolic advantage of monosaccharide supplementation.

These findings are consistent with previous research showing that pH consistently declines during kombucha fermentation due to the production of organic acids. For example, Neffe-Skocińska et al. (2017) observed a pH drop from 3.04 to 2.63 after 10 days of fermentation. Yilmaz and Goksungur (2024) also reported final pH values between 3.51 and 4.54 when using *K. xylinus* with different initial pH levels (4.0–7.0), emphasizing the influence of starting conditions. Other studies have reported similar final pH ranges after 14 days of kombucha fermentation, such as 3.36 to 3.82 (Vohra et al. 2019) and 2.91 to 3.74 (Zhao et al. 2018). Chong et al. (2024) documented a pH decrease from 3.19–3.27 to 2.72–2.79 within 10 days when using black, green, and oolong teas. These comparisons highlight a consistent trend of acid production in kombucha systems.

In this study, **Table 3.** summarizes pH values before and after inoculation, as well as at the end of fermentation, showing statistically significant differences across treatments. **Figure 5.1** (left side) illustrates the progression of acidification over 15 days. The sharp pH decline observed in RTC-SGlu compared to the more gradual decrease in RTC-SGly clearly demonstrates how different carbon sources affect the rate and extent of acid production during fermentation.

For the TSS observation, initial values ranged from 9.70±0.00 to 10.70±0.00 °Brix before inoculation. After adding the inoculum, the TSS remained relatively stable, ranging from 9.70±0.00 to 10.60±0.00 °Brix. However, by the end of the fermentation process, TSS values decreased significantly, reaching a range of 7.87±0.05 to 8.60±0.00 °Brix, as presented in **Table 3.15** and illustrated in **Figure 3.20** (right).

Table 3.15 Changes in pH and °Brix degree during RTC kombucha fermentation with different carbon source combinations.

Samples	The Change of the pH			The Change of the °Brix		
	Medium	Before	after	Medium	Before	after
RTC-C	4.84±0.00^{d}	3.65±0.00^{c}	2.52±0.04^{c}	10.70±0.00^{d}	10.60±0.00^{c}	8.57±0.05^{c}
RTC-SD	4.76±0.00^{b}	3.62±0.00^{b}	2.21±0.01^{a}	10.10±0.00^{b}	10.10±0.00^{b}	8.33±0.09^{a}
RTC-SF	4.57±0.00^{a}	3.61±0.00^{a}	2.46±0.01^{b}	10.50±0.00^{c}	10.40±0.00^{a}	7.87±0.12^{b}
RTC-SGlu	4.76±0.00^{b}	3.62±0.00^{a}	2.17±0.01^{a}	10.70±0.00^{d}	10.40±0.00^{b}	8.40±0.08^{a}
RTC-Sgly	4.78±0.00^{c}	3.66±0.00^{c}	2.66±0.00^{d}	9.70±0.00^{a}	9.70±0.00^{c}	8.60±0.00^{d}

Different lowercase letters within a column indicate significant differences among the five tea samples (LSD test: P < 0.05)

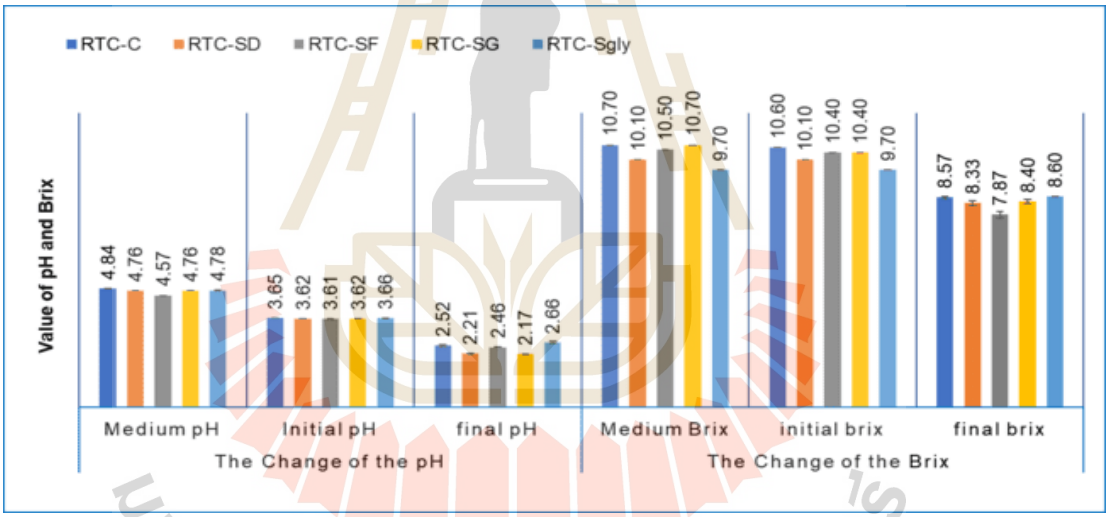

Figure 3.20 Changes in pH and °Brix degree during RTC kombucha fermentation with different carbon source combinations.

The reduction in TSS during fermentation is mainly driven by microbial activity. In kombucha, yeasts break down complex sugars into simpler ones like glucose and fructose. These are then further metabolized by acetic acid bacteria into organic acids and other by-products (Muzaifa et al. 2022), resulting in a decrease in soluble sugar concentration and, consequently, °Brix values.

The extent of TSS reduction varied depending on the carbon source, reflecting differences in sugar utilization efficiency. RTC-SF showed the greatest decline, from 10.40±0.00 to 7.87±0.12 °Brix, indicating a strong microbial preference and rapid metabolism. RTC-SD (dextrose) and RTC-SGlu had similar final values—8.33±0.09 and 8.40±0.08 °Brix, respectively—suggesting that both monosaccharides were efficiently utilized. The RTC-C dropped from 10.60±0.00 to 8.57±0.05 °Brix, reflecting normal microbial activity without added sugars. Meanwhile, RTC-SGly showed the smallest reduction, ending at 8.60±0.00 °Brix, possibly due to slower or more selective microbial metabolism of glycerol.

The structural similarity between dextrose and glucose likely accounts for their comparable fermentation behavior. In contrast, the more complex structure or lower fermentability of glycerol may have limited its consumption. These results are consistent with earlier studies (e.g., Zubaidah et al. 2019; Muzaifa et al. 2022), which highlight the influence of carbon source composition on microbial activity and sugar conversion during kombucha fermentation (Sinamo et al. 2022).

These findings are consistent with previous kombucha studies. For example, (Zubaidah et al. 2019) reported a TSS decrease from 13.30–14.08 °Brix to 12.43–12.97 °Brix in snake fruit kombucha, while (Muzaifa et al. 2022). observed a reduction in cascara kombucha from 10.97 °Brix on day two to 9.97 °Brix on day eight. Such comparisons reinforce the role of microbial metabolism in altering sugar profiles and show that the degree of TSS reduction varies by both fermentation duration and substrate type (Sinamo et al. 2022).

2) The Change of Sugar Composition

The sugar profile, including sucrose, glucose, fructose, and glycerol, was analyzed before and after fermentation using high-performance liquid chromatography (HPLC). Significant changes in sugar concentrations were observed following fermentation, as illustrated in **Figure 3.21** and detailed in **Table 3.16**.

Sucrose served as the primary carbon source for the SCOBY, promoting microbial growth and the synthesis of various metabolites, including BC (Shu 2007).

Before fermentation, the sucrose content in the control sample was 9.05 ± 0.18%, whereas in the sugar combination samples it ranged from 4.41% to 4.75%. Glucose levels ranged from 0.82% to 5.16%, and fructose from 0.00% to 4.92%. Glycerol was detected only in the RTC-SGly sample, at 5.40 ± 0.23%.

The presence of glucose and fructose in samples without added glucose or dextrose likely results from sucrose hydrolysis during autoclaving, as well as from enzymatic activity by the kombucha culture. Similar findings were reported by Ball (1953), who observed that autoclaving a 3% sucrose solution produced 0.7–0.9% glucose. Additionally, de Lange (1989) showed that sucrose can be completely hydrolyzed into glucose and fructose at pH 2 during autoclaving, with partial hydrolysis occurring at pH 5–7. These results align with observations discussed in the previous experiments of this study.

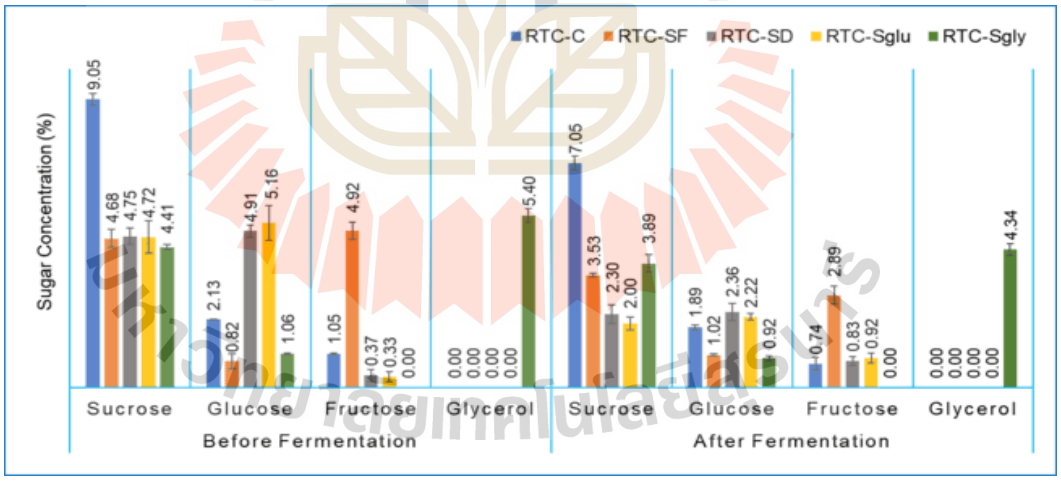

Figure 3.21 Change of sugar composition of RTC kombucha broth with different types of carbon sources combinations before and after fermentation

During kombucha fermentation, normally, sucrose serves as the primary carbon source. It is enzymatically hydrolyzed by yeasts into glucose and fructose through the action of invertase (Gao et al. 2019; Lee 2023). These simpler

sugars especially glucose are metabolized preferentially, providing energy and substrates for microbial activity (Gao et al. 2019). Under anaerobic conditions, yeasts convert glucose and fructose into ethanol and carbon dioxide (Wang et al. 2022a). Subsequently, acetic acid bacteria oxidize ethanol into acetic acid in the presence of oxygen, contributing to the characteristic tartness of kombucha (Wang et al. 2022a). If glucose, dextrose, and fructose are already present in the fermentation medium, microorganisms prioritize these simpler carbon sources over sucrose because they can be directly metabolized without enzymatic hydrolysis. This metabolic preference is demonstrated by the higher consumption of dextrose, glucose, and fructose compared to sucrose in various carbon source combinations. These results underline the efficiency of microbial metabolism in utilizing readily available simple sugars when presented in the fermentation medium.

All kombucha samples showed a significant reduction in sucrose levels post-fermentation, primarily due to invertase-mediated hydrolysis and microbial uptake. The largest decrease occurred in the control (RTC-C), where sucrose dropped from 9.05% to 7.05%. Despite overall sucrose consumption, the relatively high residual level in RTC-C suggests slower fermentation in the absence of added monosaccharides. Since sucrose requires hydrolysis before utilization, the lack of readily available simple sugars likely delayed microbial activity. In contrast, RTC-SGlu and RTC-SD exhibited similar and more efficient sugar consumption, with glucose levels falling from 5.16% to 2.22% in RTC-SGlu and from 4.91% to 2.36% in RTC-SD. The absence of a significant difference ($P > 0.05$) supports their metabolic equivalence and highlights the microbial preference for readily assimilable monosaccharides over disaccharides like sucrose.

In the RTC-SF sample, a substantial reduction in fructose concentration was observed—from 4.92% to 2.89%—indicating its active involvement in microbial metabolism. However, the remaining fructose suggests a relatively slower utilization rate compared to glucose, aligning with previous findings that yeasts tend to metabolize glucose more efficiently than fructose (Wang et al. 2022a). The RTC-SGly

sample exhibited a modest decrease in glycerol levels, from 5.40% to 4.34%, implying partial microbial usage. Glycerol is generally considered a secondary carbon source in kombucha fermentation, as it enters metabolic pathways differently and is not a primary substrate for most SCOBY microbes. The persistence of elevated glycerol levels post-fermentation suggests limited microbial affinity under the given conditions, potentially due to its lower energy yield and the availability of more favorable sugars.

These findings are consistent with those of Neffe-Skocińska et al. (2017), who reported a substantial decrease in sucrose concentration—from 9.97% to 0.74%—over a 10-day kombucha fermentation, highlighting the active hydrolysis of sucrose. Although the reduction observed in our study was less pronounced, the overall trend of sucrose consumption aligns with their results. However, due to the limited number of studies directly examining the effect of added monosaccharides on sucrose reduction in kombucha fermentation, direct comparisons remain challenging. Nonetheless, available evidence supports the idea that the presence of readily fermentable monosaccharides can accelerate fermentation by providing immediate energy sources, whereas reliance solely on sucrose may lead to slower sugar utilization.

Table 3.16 The change of sugar composition during RTC kombucha fermentation with different types of carbon source combinations

Samples	Before fermentation				After fermentation			
	Sucrose	Glucose	Fructose	Glycerol	Sucrose	Glucose	Fructose	Glycerol
RTC-C	9.05±0.18 (b, B)	2.13±0.02 (b, B)	1.05±0.03 (c, A)	ND	7.05±0.21 (d, A)	1.89±0.08 (b, A)	0.74±0.20 (b, A)	ND
RTC-SF	4.68±0.29 (a, B)	0.82±0.23 (a, A)	4.92±0.28 (d, B)	ND	3.53±0.06 (b, A)	1.02±0.03 (a, A)	2.89±0.28 (c, A)	ND
RTC-SD	4.75±0.26 (a, B)	4.91±0.20 (c, B)	0.37±0.20 (b, A)	ND	2.30±0.29 (a, A)	2.36±0.27 (bc, A)	0.83±0.13 (b, B)	ND
RTC-SG	4.72±0.51 (a, B)	5.16±0.54 (c, B)	0.33±0.16 (b, A)	ND	2.00±0.20 (a, A)	2.22±0.10 (b, A)	0.92±0.16 (b, B)	ND
RTC-SGly	4.41±0.07 (a, B)	1.06±0.03 (a, A)	0.00±0.00 (a, A)	5.40±0.23 (B)	3.89±0.29 (c, A)	0.92±0.08 (a, A)	0.00±0.00 (a, A)	4.34±0.18 (A)

Different lowercase letters within a column indicate significant differences among the five tea samples (LSD test: P < 0.05); different uppercase letters in the same row indicate the significant differences between the same sugar before and after fermentation (LSD test: P < 0.05). ND = not detected.

3) The appearance of Bacterial cellulose

The appearance of BC produced from Thai red tea kombucha fermentation with different uses of carbon sources combinations are presented in **Figure 3.22.**

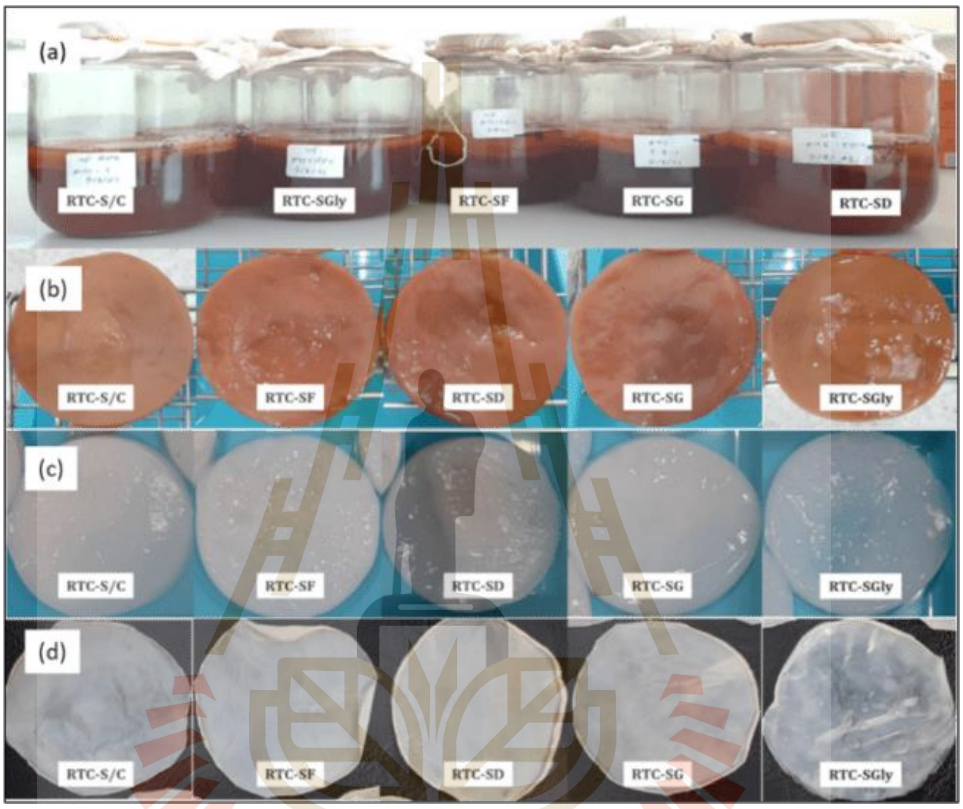

Figure 3.22 BC appearance at different stages of RTC kombucha fermentation with various carbon source combinations: (a) during fermentation, (b) before purification, (c) after purification with sodium hydroxide, and (d) after oven drying.

The appearance of BC before purification shows red-orange colors with the BC from RTC-SD, RTC-SGlu, and RTC SF show slightly darker compare to RTC-C and RTC-Gly (**Figure 3.22(a) and (b)**). The red-orange color of the BC samples produced during Thai red tea kombucha fermentation can be attributed likely to the combined effect of natural tea pigments, artificial colorants. Thai red tea, made from black tea with added artificial flavor and FD&C Yellow No. 6 (INS 110), contributes to the color. Black tea leaves contain catechins, which, through oxidation, are converted

into theaflavins (reddish-orange pigments) and thearubigins (brown pigments) during processing (Deka et al. 2021; Ito and Yanase 2022). These pigments are water-soluble and can be absorbed into the BC matrix during fermentation. Additionally, the presence of FD&C Yellow No. 6 enhances the orange-red hue of the BC samples (Izawa et al. 2010; Deka et al. 2021; Ito and Yanase 2022). The same results were also reported in the previous chapter of this thesis.

In the next steps, after purification using sodium hydroxide solution (2% w/v) the BC exhibits a similar white color (**Figure 3.22(c)**) and after drying in the oven at 40°C showed consistent white, opaque color (**Figure 3.22(d)**). This post-purification color aligns with findings reported in most BC studies. Sodium hydroxide plays a vital role in BC purification by effectively removing tannins, polyphenols, residual bacteria, yeast cells, and proteins present in trace amounts within the kombucha pellicle (Amarasekara et al. 2020). It also facilitates the elimination of residual organic compounds, nucleic acids, and proteins produced by microbes during the fermentation process (Kamal et al. 2020).

4) BC Productivity and Water Holding Capacity

Figure 3.23 presents the wet yield, dry yield, and WHC of BC produced from Thai red tea kombucha (RTC) using various carbon source combinations: RTC-C, RTC-SF, RTC-SD, RTC-SGlu, and RTC-SGly. The wet yields of BC for these treatments were 167.44 ± 24.00, 193.87 ± 36.68, 234.87 ± 39.10, 259.54 ± 8.92, and 74.53 ± 8.95 g/L, respectively, while the corresponding dry yields were 1.72 ± 0.19, 1.88 ± 0.23, 2.20 ± 0.54, 2.59 ± 0.16, and 0.66 ± 0.03 g/L. The WHC values were 109.31 ± 4.65, 101.92 ± 9.12, 105.79 ± 25.13, 99.07 ± 2.85, and 112.44 ± 17.49 g water/g cellulose, respectively.

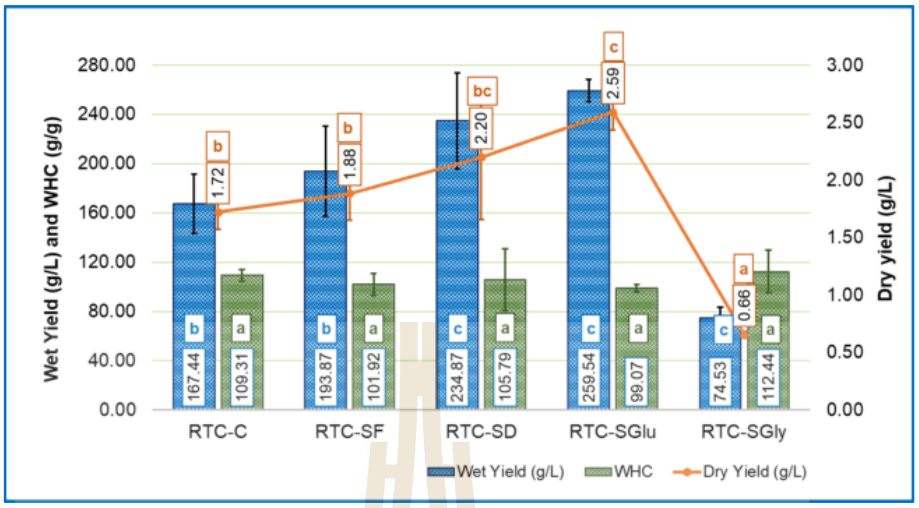

Figure 3.23 Wet yield (g/L), dry yield (g/L), and WHC (g water/g cellulose) of BC produced from RTC kombucha using different combinations of carbon sources.

Among the treatments, RTC-SGlu resulted in the highest wet and dry BC yields, significantly exceeding those of RTC-C, RTC-SF, and RTC-SGly ($P < 0.05$), though not significantly different from RTC-SD ($P > 0.05$). This enhancement can be attributed to the efficient microbial metabolism of glucose, which serves as a direct substrate for the biosynthesis of cellulose. As reported by Gao et al. (2019), simple sugars such as glucose and fructose are metabolized more efficiently than disaccharides like sucrose, accelerating the formation of cellulose precursors like UDP-glucose. In treatments such as RTC-SD and RTC-SGlu, sucrose likely underwent enzymatic hydrolysis by invertase into glucose and fructose, with glucose being preferentially utilized by the microbial consortium for cellulose biosynthesis (Wang et al. 2022a). As shown in **Table 3.16**, the higher consumption of carbon sources, particularly sucrose and glucose, in RTC-SD and RTC-SGlu likely contributed to the enhanced cellulose production observed in these treatments.

RTC-SF showed moderate increases in yield compared to the control, although the difference was not statistically significant. The use of fructose in combination with sucrose may have supported BC formation, as fructose is also metabolizable, though generally less efficiently than glucose (Gao et al. 2019). The

control group (RTC-C), containing sucrose alone, had lower yields, suggesting that additional monosaccharides improve sugar utilization and enhance BC biosynthesis.

In contrast, RTC-SGly showed the lowest wet and dry yields. This suggests that glycerol is a less favorable carbon source under the tested conditions, possibly due to slower metabolic conversion into cellulose precursors or inhibitory effects at the concentration used. While previous studies have reported high BC production with glycerol under optimized conditions (Keshk and Sameshima 2005; Tabaii and Emtiazi 2016; Agustin et al. 2018; Thorat and Dastager 2018; Amorim et al. 2019; Ho Jin et al. 2019), differences in bacterial strains, pH, and medium composition may explain the lower performance in this study.

These results align with those from Treviño-Garza et al. (2020), who found that glucose yielded the highest BC production, followed by dextrose, fructose, and sucrose in kombucha systems. Specifically, wet and dry yields reached 301.81 g/L and 11.19 g/L with glucose and 300.74 g/L and 12.12 g/L with dextrose. Similarly, (Amorim et al. (2024) reported that glucose supported higher BC yields than other carbon sources such as raffinose and glycerol. Thorat and Dastager (2018) also observed that *K. rhaeticus* produced maximum BC (~8.7 g/L) at 3% glycerol, but yields dropped at concentrations above 4%. In addition, Adnan et al. (2015) reported that the highest BC yield was obtained at a glycerol concentration of 2%, while yields decreased at concentrations of 3% and above.

Regarding WHC, no statistically significant differences were observed among the treatments, indicating that carbon source type primarily affects BC yield but not its water-holding functionality. WHC is influenced more by the nanofiber structure, porosity, and surface area of the dried BC, which remained comparable under similar culture conditions. The WHC values in this study (99.07–112.44 g water/g cellulose) are consistent with literature reports. Wu and Liu (2013) observed a WHC of 98.5 g/g in BC from distillery wastewater, while Avcioglu et al. (2021) reported values of ~114 g/g in kombucha using black tea. Other studies noted WHC ranges from 90 to

200 g/g depending on the bacterial strain, fermentation time, and drying method (Tsouko et al. 2015; Treviño-Garza et al. 2020; Almihyawi et al. 2024; U˘gurel and Ö˘güt 2024).

In summary, this study demonstrates that the choice of sugar significantly affects BC yield, with glucose and dextrose promoting the highest productivity. Fructose and sucrose supported moderate yields, while glycerol was least effective under the tested conditions. However, WHC was not significantly impacted, suggesting that yield improvements can be achieved without compromising the BC's functional properties.

5) Morphology Analysis Using SEM

Figure 3.24 presents SEM images showing the surface morphology of BC produced using different carbon sources. These images were captured at magnifications of 10,000x and 30,000x for all samples. Additionally, magnification at 50,000x was applied to RTC-C and RTC-SGlu to provide a more detailed view of their fiber structures. Overall, the BC samples exhibit a consistent fiber pattern, consistent with the findings of the previous studies (Illa et al. 2019; Brandes et al. 2020; Nguyen and Nguyen 2022).

The RTC-C sample exhibits a dense and compact fibril network at 10,000x, with higher magnifications (30,000x and 50,000) revealing tightly packed and uniform cellulose fibrils. For RTC-SF, the structure is less dense at 10,000x, with more visible voids and irregular fibril arrangements at 30,000x. RTC-SD displays a highly interconnected and dense network at 10,000x, while the fibrils are smooth and regularly arranged at higher magnifications, indicating uniform cellulose synthesis. The RTC-SGlu sample shows a tightly interwoven fibril network at 10,000x, with well-organized and continuous fibrils visible at higher magnifications, suggesting high-quality BC formation. In contrast, RTC-SGly demonstrates a disrupted network with larger gaps between fibrils at 10,000x, and irregular shapes and uneven fibril distributions are observed at 30,000, indicating less effective cellulose production. Overall, the images

highlight the significant influence of the carbon source on BC morphology, with RTC-SG and RTC-SD producing denser and more organized fibril networks, while RTC-SGly results in a looser and less uniform structure. The denser fibril networks observed in RTC-SD and RTC-SGlu are likely due to the thicker BC layers formed before drying, while the thinner network in RTC-SGly reflects a less compact structure. This difference aligns with the wet yield results, where BC from RTC-SD and RTC-SGlu had the highest wet yields, whereas RTC-SGly had the lowest. These findings suggest that the initial wet thickness of BC significantly influences its final structure and density. Some impurities are visible in the SEM images especially in RTC-C sample, likely representing residues or insoluble materials remaining after alkali purification.

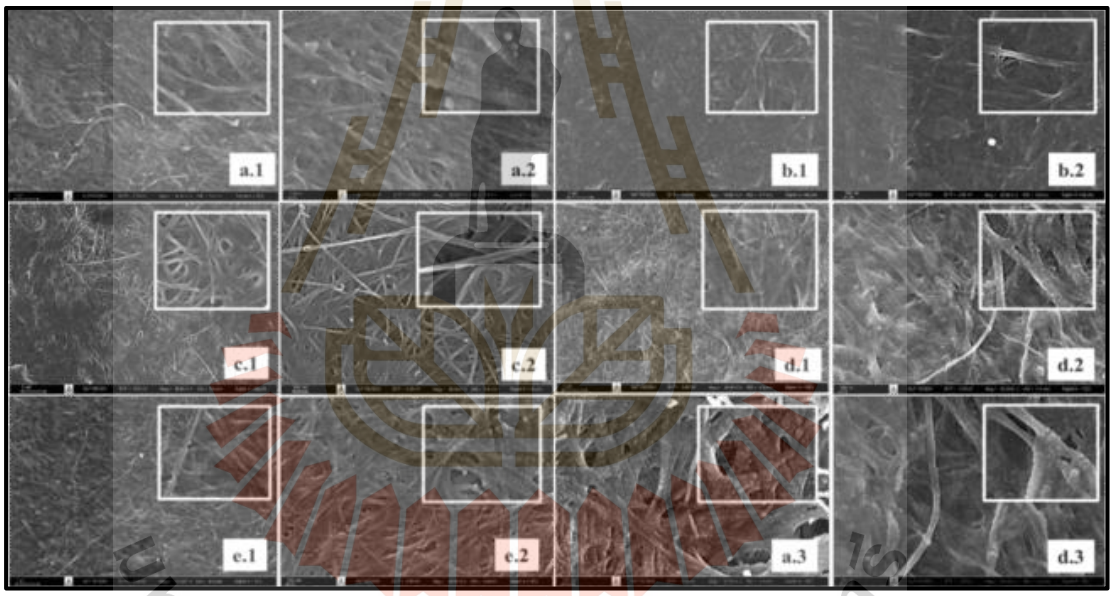

Figure 3.24 SEM image of BC (a) RTC-control; (b) RTC-SF; (c) RTC-SD; (d) RTC-SG; and (e) RTC-SGly; (1) magnification of 10000 x; (2) magnification of 30,000x; (3) magnification 50.000x.

The analysis following SEM imaging focused on the polydispersity of BC fiber diameters, as shown in **Figure 3.25.** The polydispersity graphs reveal that fiber diameters ranged from 19.35 nm (RTC-C) to 63.28 nm (RTC-SD), with average diameters varying between 29.70 ± 5.17 nm (RTC-C) and 40.39 ± 8.65 nm (RTC-SD). Compared to RTC-C, the use of sugar combinations resulted in slightly larger BC fiber

diameters. Among the sugar combination samples, the average diameters ranged from 34.34 ± 7.56 nm (RTC-SG) to 40.39 ± 8.65 nm (RTC-SD). These findings suggest that, although sugar combinations slightly increased fiber size, the effect was not as pronounced as the variations caused by different additives discussed in the previous section. Overall, the use of different carbon source combinations had a relatively minor impact on BC fiber diameter.

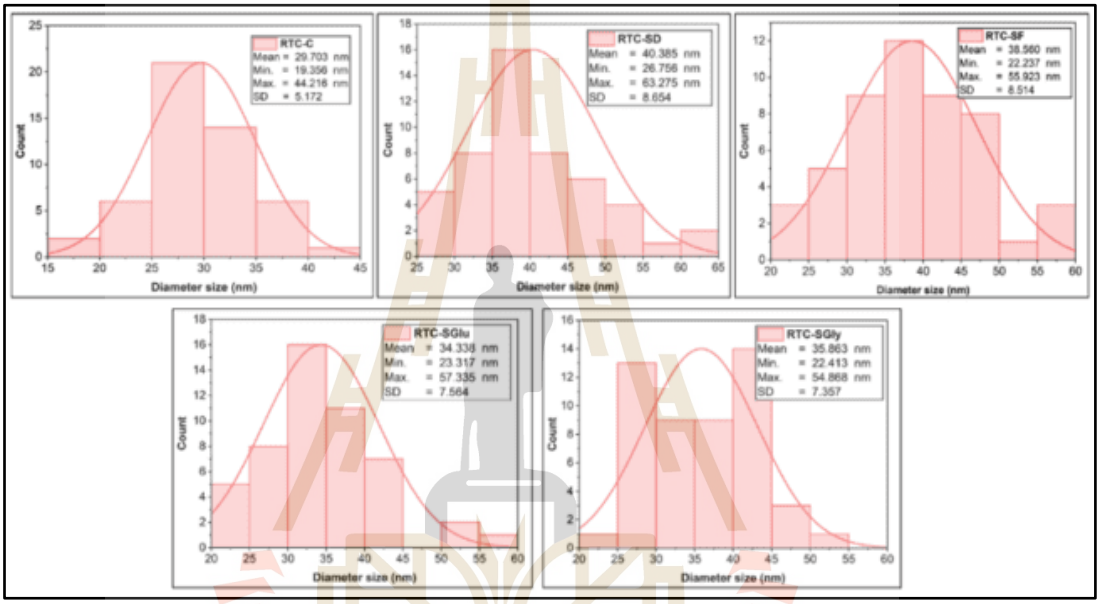

Figure 3.25 Graph of poly distribution size of BC samples diameter from RTC kombucha fermentation with various types of carbon source combinations.

Previous studies support the findings on BC fiber morphology observed in this study. The BC fibers produced by *K. hansenii* 23769 (ATCC) and a cellulose-producing strain isolated from grape juice exhibited diameters ranging from 10 to 60 nm. (Illa et al. 2019). Similarly, BC produced by *K. saccharivorans* MD1 cultivated in HS medium with palm date supplementation exhibited fiber diameters between 10 and 90 nm (Abol-Fotouh et al. 2020). In another study, BC nanofibers synthesized in HS medium had fiber diameters between 18 and 69 nm, with an average diameter of 36 nm, while BC derived from a waste fig medium ranged from 23 to 90 nm, with an average diameter of 44 nm (Yilmaz and Goksungur 2024).

BC fiber produced by *K. rhaeticus* PG2 in HS medium using glucose and glycerol as carbon sources demonstrated a similar diameter range of approximately 30–60 nm (Thorat and Dastager 2018). Additionally, BC synthesized in low-cost media, such as date syrup and cheese whey, by *K. xylinus* exhibited nanofiber diameters averaging 45–55 nm across all samples (Raiszadeh-Jahromi et al. 2020). Wang et al. (2018) reported that BC membranes produced using various carbon sources were composed of nanofibrils with average diameters ranging from 35 to 50 nm (Wang et al. 2018).

In conclusion, the BC fiber diameters obtained from Thai red tea kombucha using different carbon sources align well with the ranges reported in previous studies. This consistency suggests that the BC produced in this study exhibits comparable morphological characteristics to those synthesized using diverse bacterial strains and cultivation conditions in earlier research.

6) Fourier Transform Infrared Spectroscopy Analysis

Figure 3.26 presents the FTIR spectra of BC samples produced from RTC kombucha fermentation with various carbon source combinations (RTC, RTC-SD, RTC-SGlu, RTC-Sgly, and RTC-SF). Overall, all BC samples exhibit similar spectral bands, but the intensity of these bands varies among the samples. The FTIR spectra reveal characteristic absorption bands associated with cellulose, with notable variations in peak intensities and positions such as have been reported in some previous studies (Wang et al. 2018; Adekoya et al. 2022; Razali et al. 2022).

The FTIR spectra of BC samples can be categorized into two primary regions: the feature region and the fingerprint region. The feature region covers the high-frequency range from 4000 to 1330 cm^{-1}, while the fingerprint region extends from 1330 to 500 cm^{-1} (Liu et al. 2023). In the feature region, prominent peaks were identified at approximately 3340 cm^{-1}, 3234 cm^{-1}, and 2895 cm^{-1}. The broad and intense bands around 3340 cm^{-1} and 3234 cm^{-1} are attributed to O-H stretching vibrations, typical of hydroxyl groups. The slight variations in peak intensity indicate differences in the

hydrogen bonding network among the samples. Additionally, the peak near 2895 cm^{-1} is associated with C-H stretching vibrations, which are characteristic of aliphatic groups (CH_2 or CH_3) (Leonarski et al. 2021a; Fatima et al. 2023). The image shows comparable intensities across the spectra, although RTC-SD exhibits slightly reduced absorption, potentially due to altered C-H interactions. Furthermore, a faint peak detected at around 2340 cm^{-1} indicates the possible presence of triple-bond functional groups, such as C≡C or C≡N (Srivastava and Mathur 2022). These functional groups may come from polyphenols and other organic compounds in Thai red tea, fermentation byproducts, or the activity of the kombucha's microbial community, which may contribute to their incorporation into the BC matrix.

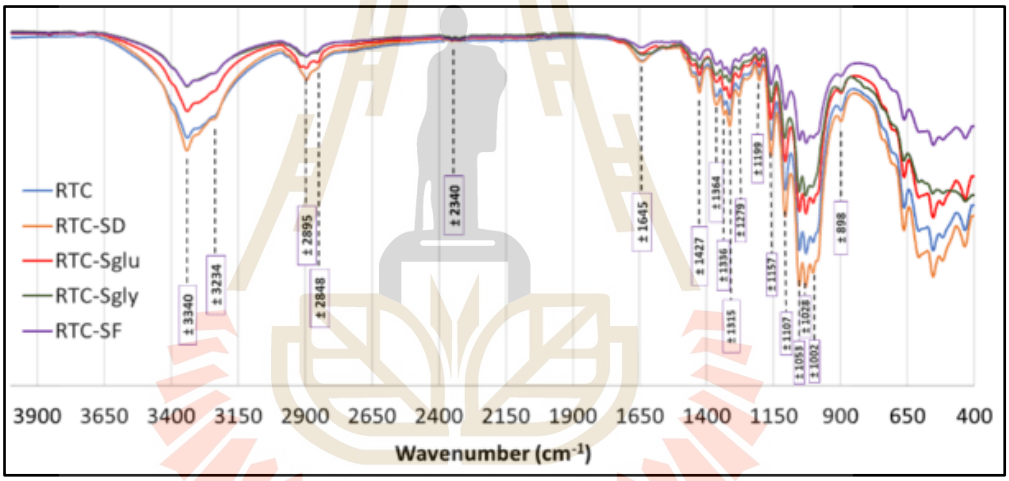

Figure 3.26 FTIR spectra of BCs from RTC kombucha fermentation with various of carbon sources combinations.

A distinct band arose at around between 1350 and 2000 cm^{-1} i.e. 1645, 1427, and 1364 cm^{-1}. The peak at around 1645 cm^{-1} is associated with C=O stretching vibrations from the glucose carbonyl group (Leonarski et al. 2021a; Liu et al. 2023). The peak at 1427 cm^{-1} represents CH_2 symmetric bending, while the peak at 1364 cm^{-1} corresponds to C-H symmetric bending (Fatima et al. 2023; Liu et al. 2023).

In the fingerprint region between 1330 to 500 cm^{-1}, several distinct peaks were detected at 1315 cm^{-1}, 1279 cm^{-1}, 1203 cm^{-1}, 1159 cm^{-1}, 1106 cm^{-1}, 1053 cm^{-1}, 1028 cm^{-1}, 1002 cm^{-1}, and 898 cm^{-1} The peak at 1336 cm^{-1} corresponds to OH in-

plane bending (Liu et al. 2023). The peak at 1315 cm^{-1} is linked to CH_2 wagging at the C-6 position (Liu et al. 2023) or maybe C-OH deformation vibrations (Wu et al. 2014). The peak observed around 1247 cm^{-1} remains unidentified. A similar peak was reported by Wang et al. (2018) in BC samples produced using glucose, fructose, sucrose, and glycerol as carbon sources, appearing at a wavenumber of 1248 cm^{-1}. The band observed at 1159 cm^{-1} is attributed to C-O-C antisymmetric bridge stretching, while the peak at 1106 cm^{-1} represents ring asymmetric stretching. Peaks at 1053 cm^{-1} and 1028 cm^{-1} are associated with C-O-C and C-O-H stretching vibrations within the sugar ring and C-O stretching, respectively (Liu et al. 2023). Additionally, the peak between 898 and 894 cm^{-1} corresponds to C-O-C stretching in β-1,4-glycosidic linkages, signifying the presence of an amorphous absorption band (Ciolacu et al. 2011).

7) X-Ray Diffraction (XRD) Analysis

The X-ray diffraction (XRD) patterns of BC samples obtained from Thai red tea kombucha fermentation using different carbon source combinations are illustrated in **Figure 3.27**. Further analysis result of crystallinity index (CI) and crystallite size are presented in **Table 3.17**. The XRD profiles for all samples consistently display three prominent peaks at 2θ values around 14.74°, 17.03°, and 22.90°, indicative of the crystalline structure characteristic of BC (Said Azmi et al. 2023). These peaks correspond to the 100, 110, and 200 crystallographic planes of monolithic cellulose type I, as reported by Gaspar et al. (2014). Notably, the most intense peak, located near 23°, is associated with cellulose type I (Said Azmi et al. 2023; Hossen et al. 2024), confirming its crystalline nature (Samuel and Adefusika 2019). Despite similarities in peak positions, differences in relative intensities and overall crystallinity among the samples suggest variations in cellulose chain orientation and structural properties (Said Azmi et al. 2023).

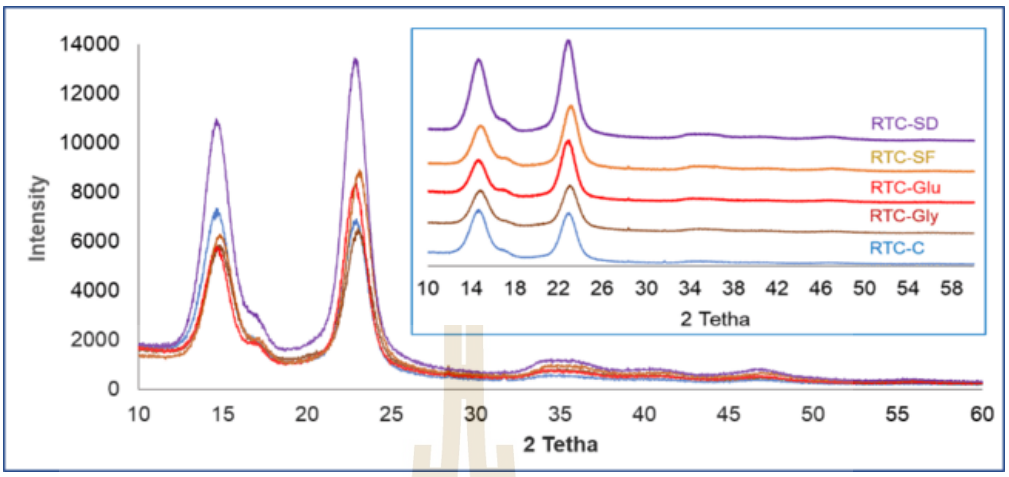

Figure 3.27 XRD spectra of BC from RTC kombucha fermentation with different carbon sources combinations

In the provided XRD spectrum, variations in peak intensities are evident among samples, with RTC-SD exhibiting the highest overall intensities. Such differences likely reflect variations in the degree of crystallinity and cellulose chain orientation, influenced by the type of carbon source used during fermentation (Said Azmi et al. 2023). The peaks at 14.74° and 17.03° exhibit minor shifts in intensity across the samples, further emphasizing these structural differences. Despite these variations, the XRD profiles align closely with previously reported patterns for BC, reinforcing the consistent crystalline structure typical of this material BC (Revin et al. 2018; Jittaut et al. 2023; Said Azmi et al. 2023). The peak at 22.90°, which consistently appears across all samples, highlights the crystalline properties of the cellulose, in agreement with findings by Samuel and Adefusika (2019).

The CI and crystallite size of the BC samples were calculated from the XRD data using the Segal peak height method, which involves subtracting the baseline intensity (**Table 3.17**). The CI values ranged from 84.74% RTC-SGly) to 89.54% (RTC-C). Among the samples, RTC-SD and RTC-SF exhibited relatively similar CI values. Notably, all BC samples produced with carbon source combinations showed relatively lower CI compared to RTC-C, which used sucrose as the sole carbon source. Various factors can affect the crystallinity of BC, including the type of carbon and nitrogen

sources, the addition of specific additives, the bacterial strain used, fermentation conditions (such as temperature and duration), and post-production treatments (Zeng et al. 2011; Thielemans et al. 2023).

Table 3.17 Crystallinity index and average crystallite size of dried BC from RTC kombucha fermentation with different carbon source combinations

Samples	Crystallinity Index (%)	Average Crystallite Size (nm)
RTC-C	89.54	3.194
RTC-SF	88.35	3.112
RTC-SD	88.17	3.181
RTC-SGlu	86.00	3.327
RTC-SGly	84.74	3.069

XRD analysis was performed once; therefore, variance data are not available.

The CI results in this study align with findings from some previous researchs. For instance, the use of glucose, fructose, and sucrose as carbon sources in HS medium for BC production by *K. medellinensis* resulted in CI values of 83%, 90%, and 85%, respectively (Molina-Ramírez et al. 2018b). Similarly, BC produced by *K. hansenii* (ATCC 53582) using glucose and glycerol as carbon sources showed CI values exceeding 80% (Amorim et al. 2024). Furthermore, BC produced by *Komagataeibacter sp.* W1 in HS medium exhibited CI values of 74%, 89%, 86%, and 87% with sucrose, fructose, glucose, and glycerol as carbon sources, respectively (Wang et al. 2018).

The results indicate that while sucrose as the sole carbon source produced BC with the highest crystallinity (89.5%), combinations with glucose or fructose resulted in only slight reductions (86–88%). In contrast, RTC-SGly showed a more noticeable decrease (84.7%), likely due to glycerol's less efficient metabolic conversion. These findings suggest that the choice of carbon source—particularly the inclusion of glycerol—can affect BC's structural properties. Nevertheless, all samples maintained high crystallinity (>84%), highlighting the robust crystalline nature of BC across different carbon sources.

Further analysis is the average of the crystallite size of BC samples as shown in **Table 3.17**. The average crystallite size of BC varies depending on the carbon source and fermentation conditions, as demonstrated in this study and supported by previous research. In this study, BC samples produced using different carbon source combinations exhibited average crystallite sizes ranging from 3.069 to 3.327 nm. Comparatively, BC produced by *G. xylinus* InaCC B404 in HS medium had a crystallite size of 3.06 nm (Agustin et al. 2021). BC derived from *K. xylinus* strains using fructose and glucose as carbon sources showed crystallite sizes between 4.7 and 6.8 nm (Singhsa et al. 2018). BC produced by *Lactobacillus plantarum* in a green tea leaf solution (1% green tea, 10% sucrose) displayed crystallite sizes of 5.36, 5.94, and 5.98 nm after 7, 14, and 30 days of fermentation, respectively (Charoenrak et al. 2023). BC from black tea kombucha exhibited crystallite sizes of 3.29 nm and 4.80 nm after 3 and 5 days of fermentation, respectively (Balistreri et al. 2024). Other average crystallite sizes have been reported in other studies such as with values of 4.9 nm and 4.76 nm (Sardjono et al. 2019), 5.6 nm (Jia et al. 2017), and 8.36 nm (Gayathri and Srinikethan 2019). This comparison highlights the significant influence of carbon source selection on the crystallite size of BC, with variations reflecting differences in substrate composition, microbial activity, and fermentation conditions. The consistent findings reinforce that carbon source plays a crucial role in determining the structural characteristics of BC.

8) Thermogravimetric (TGA/DTG) Analysis

Figure 3.28 illustrates the thermogravimetric (TG) and derivative thermogravimetric (DTG) curves of the BC samples, analyzed through thermogravimetric analysis (TGA). **Table 3.18** summarizes the decomposition data observed during the analysis. The results highlight the thermal stability and decomposition patterns of BC samples, including RTC-C, RTC-SF, RTC-SD, RTC-Glu, and RTC-Gly. TGA and DTG analyses play a vital role in evaluating BC for various applications, as they provide valuable information on the material's purity,

composition, drying behavior, and ignition temperatures. Moreover, these analyses offer insights into the thermal stability of BC, which is crucial for assessing the effectiveness of chemical treatments designed to improve bonding between natural fibers and polymer or synthetic fiber matrices (Nurazzi et al. 2021).

The first-stage weight loss, ranging from 1.34% to 6.03%, corresponds to the dehydration and volatilization of low-molecular-weight components or residual water in the BC matrix (Teixeira et al. 2019; Mohamad et al. 2022a). RTC-SD showed the lowest first-stage weight loss (1.42%), likely due to reduced moisture retention from the sample. This result relatively close result to previous result i.e. 1-2% (Gismatulina and Budaeva 2024) and 5-9% (Mohamad et al. 2022a).

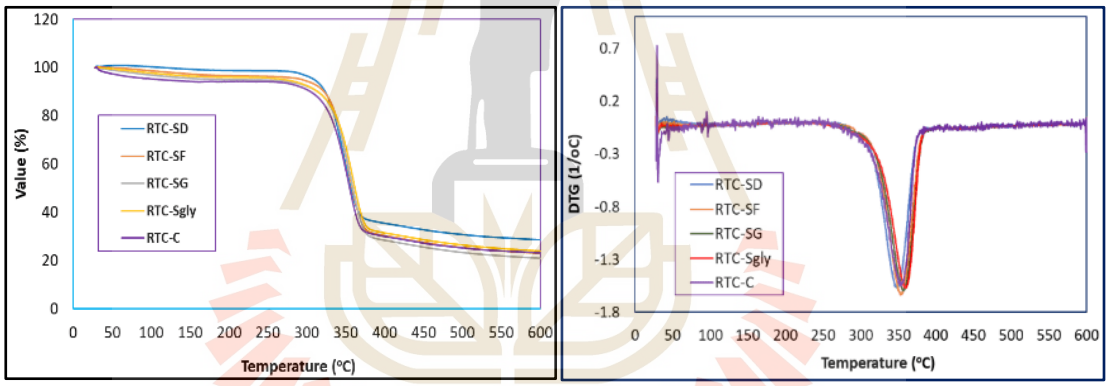

Figure 3.28 TGA (left) and DTG (right) thermographs of BC samples from RTC kombucha fermentation with different combinations of carbon sources.

The second stage of weight loss, attributed to the thermal decomposition of cellulose, ranged from 70.10% in RTC-SD to 73.90% in RTC-SGlu. These values indicate slight variations in thermal stability influenced by the different carbon sources, though the differences are not particularly pronounced. The residual weights at 600°C varied from 20.92% for RTC-SGlu to 28.52% for RTC-SD, reflecting differences in the formation of thermally stable by-products. This stage accounts for the most substantial weight loss, driven primarily by the breakdown of β-glucan chains

and the oxidation of cellulosic materials into carbonaceous residues (Mohammadkazemi et al. 2015; Mohamad et al. 2022a).

Table 3.18 Thermal decomposition of BC produced from RTC kombucha fermentation using different carbon source combinations, as analyzed by thermogravimetric analysis (TGA).

Samples	First stage weight loss (%)	Second stage weight loss (%)	Residue (%)	DTG Peak range (°C)	DTG T_{Max} (°C)
RTC-C	6.03	71.01	23.01	256 – 384	353.67
RTC-SD	1.34	70.10	28.52	260 – 391	349.50
RTC-SF	3.60	73.43	22.94	267 - 390	353.33
RTC-SGlu	5.14	73.90	20.92	268 – 389	356.83
RTC-SGly	4.15	71.92	23.90	258 – 388	359.50

The findings of this study align with previous research. BC from *A. xylinum* AGR 60 showed a first-stage mass loss of about 6%, a second-stage loss of approximately 74%, and a residue weight of around 20% at 700°C, with major thermal decomposition occurring between 300°C and 360°C (Potivara and Phisalaphong 2019). Similarly, BC produced by *G. xylinus* AGR 60 exhibited a first-stage mass loss of 6.2%, a second-stage mass loss of approximately 64.0%, and a residue of around 22.8% at 600°C, with a DTG T_{Max} of 339.6°C (Jenkhongkarn and Phisalaphong 2023). BC produced from different carbon sources, including glucose, fructose, sucrose, and glycerol, showed residual BC at 600°C ranging from 15.2% to 23.1% and exhibited a decomposition pattern similar to that observed in this study (Tureck et al. 2021). Slightly different, BC produced through kombucha fermentation of green tea undergoes three decomposition stages at 152°C, 267°C, and 359°C, with a total weight loss of 74.42% and 25.58% residue remaining, differing from this study, which typically observed only two stages of thermal decomposition (Lima et al. 2023).

The DTG peak temperature range (256–391°C) and maximum degradation temperatures (DTG T_{Max}: 349.50–359.50°C) exhibit slight variations in the thermal degradation profiles, with RTC-SGly showing the highest DTG T_{Max} (359.50°C). These differences underscore the impact of additives on the thermal behavior of BC. BC produced by *G. xylinus* demonstrates a DTG T_{Max} of 328.36°C (Jia et al. 2017). Similarly, BC produced by *G. hansenii* in HS medium shows DTG T_{Max} values of 354.5°C and 355.4°C after freeze-drying and oven-drying, respectively (Vasconcellos and Farinas 2018). The BC produced by *K. medellinensis* from various waste and agricultural by-products exhibits DTG T_{Max} values ranging from 327°C to 368°C (Molina-Ramírez et al. 2018a). Studies report DTG peak ranges of 186–363°C and 199–347°C for BC treated with freeze-drying and hot-press drying methods, yielding DTG T_{Max} values of 343.6°C and 313.4°C, respectively (Mohamad et al. 2022a). Furthermore, BC produced through kombucha fermentation of green tea reaches a DTG T_{Max} of 366°C (Lima et al. 2023). The DTG analysis indicates that different carbon sources have a slight impact on the thermal stability of BC, as evidenced by the small variations in DTG T_{Max} values. While RTC-SGly showed the highest DTG Max, the narrow range of differences suggests that the influence of carbon source on thermal properties is relatively minor.

9) Mechanical Properties Analysis Using Nanoindentation

Nanoindentation analysis was utilized to evaluate the mechanical properties of BC samples at the nanoscale. This precise technique measures localized mechanical responses with high accuracy at micro- and nanoscale resolutions, making it an essential tool for assessing materials designed for applications requiring both strength and flexibility. The analysis focused on BC samples RTC-SD and RTC-SGlu, selected for their higher productivity, with the RTC-C sample included as a control for comparison. The detailed findings are summarized in **Table 3.19.**

The mechanical properties of BC samples, including RTC-SD, RTC-SGlu, and the control (RTC-C), were no significant differences across all parameters, such as maximum depth, plastic indentation depth, hardness, reduced modulus, and

Young's modulus ($P > 0.05$). This indicates that the different carbon sources used, particularly sucrose, combination of sucrose-dextrose (SD), and combinations of sucrose-glucose (SGlu), do not result in distinct variations in the mechanical properties of BC. These findings suggest that the choice of carbon source in these cases has minimal impact on the nanoscale mechanical behavior of BC. Actually, carbon source is one of the factor affect the mechanical properties of BC (Betlej et al. 2020; Chibrikov et al. 2023). However, in this case, the effect is not significantly different.

Various factors can affect the mechanical properties of BC such as bacterial strains, cultivation methods, purification, nutrient composition including carbon and nitrogen sources, and drying techniques. Cultivation methods and bacterial strains significantly affect the structure and crystallinity of BC, which in turn impacts its strength (Krystynowicz et al. 2002; Zeng et al. 2014; Chen et al. 2018a; Betlej et al. 2020; Chibrikov et al. 2023). The NaOH concentration during purification is essential for removing impurities, directly affecting the quality and properties of BC fibers (Suryanto et al. 2019; Chen et al. 2021). Drying methods affect BC's porosity and density, which are crucial for its flexibility, tensile strength, and the organization of intra- and interfibrillar spaces (Zeng et al. 2014; Wang et al. 2023b).

The mechanical properties of BC are closely linked to its crystallinity, which plays a significant role in determining material strength and stiffness. Studies have shown that an increase in the crystallinity index (CI) generally enhances stiffness and hardness while reducing ductility (Dusunceli and Colak 2008). Furthermore, higher crystallinity has been associated with an increase in Young's modulus, reinforcing the connection between CI and mechanical strength (Adekoya et al. 2022).

In this study, the CI values of RTC-C, RTC-SD, and RTC-SGlu samples are relatively similar and show no significant differences in relation to their Young's modulus values. The Young's modulus values of the BC samples vary, with some falling within, below, or above the ranges reported in previous research.

Table 3.19 Mechanical properties of BC from kombucha fermentation of RTC-SD, RTC-SGlu, and RTC-C analyzed using a nano-indenter

Sample	MD (nm)	Pl (nm)	ML (mN)	H (GPa)	RM (GPa)	ERP	CC (nm/mN)	PW (nJ)	EW (nJ)	YM (GPa)
RTC-SD	3402.68 ±388.52	2950.54 ±366.31	50.10 ±0.00	0.23 ±0.07	4.844 ±1.02	0.16 ±0.02	12.03 ±0.82	49.29 ±5.30	21.67 ±1.40	4.43 ±0.94
RTC-SGlu	3206.75 ±250.54	2754.19 ±240.80	50.10 ±0.00	0.26 ±0.05	5.106 ±0.64	0.17 ±0.01	12.04 ±0.65	51.22 ±4.42	21.08 ±1.08	4.67 ±0.59
RTC-C	3412.25 ±259.56	2980.18 ±253.91	50.10 ±0.00	0.22 ±0.05	4.94 ±0.56	0.15 ±0.01	11.50 ±0.22	54.41 ±4.64	20.80 ±0.47	4.51 ±0.51

MD: maximum depth, Pl: plastic, ML: maximum load, H: hardness, RM: reduced modulus, ERP: elastic recovery parameters, CC: contact compliance, PW: plastic work, EW: elastic work, and YM: Young's Modulus. Based on the statistical analysis, there were no significant differences among the samples across all parameters ($P < 0.05$).

For instance, Chen et al. (2018a) reported Young's modulus values ranging from 1.10 to 5.56 GPa for BC produced from various Komagataeibacter strains. Zeng et al. (2014) observed lower values, between 198 and 659 MPa, depending on the bacterial strains and drying methods used. Krystynowicz et al. (2002) found that BC produced by *A. xylinum* E25 under static and rotating conditions exhibited Young's modulus values of 2.7 and 0.3 GPa, respectively. At the higher end, *A. xylinum* AGR60 cultured in coconut water reached 9.14 GPa (Potivara and Phisalaphong 2019), while kombucha-derived BC was reported to have a Young's modulus of 8.0 ± 1.9 GPa (Oliver-Ortega et al. 2021).

3.4.4 Effect of Process Parameters: pH, Harvesting Time, Tea Concentration, and Cultivation Method on Bacterial Cellulose yield and Water Holding Capacity

1) Effect of Initial pH on the Yield and WHC of BC

- **Profile of Fermentation Broth**

The pH and °Brix of the kombucha fermentation broth were measured at the beginning and after 15 days of fermentation. The initial pH of the medium was adjusted to 5, 6, 7, and a control value of 5.20 for the respective treatments. After inoculation with a kombucha starter, the pH dropped significantly to acidic levels of 3.40, 3.55, 3.61, and 3.41, respectively. After 15 days of fermentation, the pH further decreased to 2.48, 2.46, 2.53, and 2.39. These changes, along with the °Brix data, are presented in **Table 3.20.**

A similar pH trend has been observed in previous studies on kombucha fermentation, where the pH typically drops to around 3.5 shortly after inoculation and reaches approximately 2.8 within five days (Petrosian 2021). In black tea kombucha fermentation, the pH was reported to decrease from 4.6 ± 0.1 to 3.6 following the addition of a kombucha starter and further to 2.8 after 30 days (Charoenrak et al. 2023). The continued decline in pH during fermentation is attributed to the production of organic acids, including acetic and gluconic acids, by

microorganisms in the SCOBY acid (Aswini et al. 2020; Lee et al. 2021). These microorganisms thrive in acidic conditions, typically within a pH range of 2–4 (Goh et al. 2012), which protects the fermentation medium from contamination by undesirable microbes (Petrosian 2021; Wang et al. 2023a). Additionally, the presence of polyphenols in the medium supports the growth of the SCOBY while inhibiting the proliferation of other microorganisms (Jayabalan et al. 2014).

Table 3.20 The change of pH and °Brix during RTC kombucha fermentation with different initial pH condition

Sample	The change of the pH		The change of the °Brix	
	initial pH	final pH	initial °Brix	final °Brix
RTC-Control* (pH-5.20)	3.43±0.03^{a}	2.39±0.04^{a}	10.30±0.00^{a}	9.33±0.35^{ab}
RTC-pH-5	3.41±0.01^{a}	2.48±0.01^{b}	10.40±0.00^{b}	9.17±0.13^{a}
RTC-pH-6	3.55±0.02^{b}	2.46±0.03^{b}	10.70±0.00^{d}	9.60±0.17^{b}
RTC-pH-7	3.61±0.03^{c}	2.53±0.03^{c}	10.50±0.00^{c}	9.57±0.22^{ab}

**The control sample was prepared without pH adjustment. Different lowercase letters within a column indicate significant differences among the four treatments, as determined by the LSD test ($P < 0.05$).*

Despite the initial adjustments of pH using HCl (acid) and NaOH (base), the pH of the medium after inoculation dropped to a similar range (3.40–3.61) across all treatments. This suggests a buffering effect likely caused by organic acids in the kombucha starter, as reported in other studies (Hruška et al. 1999; Dartiguenave et al. 2000; Zheng et al. 2023). Kombucha cultures are known to stabilize the pH around this acidic range regardless of initial pH adjustments, driven by microbial metabolic pathways that favor acid production (Teoh et al. 2004; Jayabalan et al. 2007).

The initial pH values recorded in this study align with prior research, which reported ranges such as 3.19–3.27 (Chong et al. 2024), 3.85–4.99 (Phung et al. 2023), and 3.24–3.34 (Leonarski et al. 2021b). However, the final pH values in this study—2.48, 2.46, 2.53, and 2.39—are lower than those in some studies, such as black,

green, and oolong tea fermentations (2.72–2.79) (Chong et al. 2024), black tea fermentation after 30 days (2.8) (Charoenrak et al. 2023), and beverages made from black tea and pineapple (2.95–3.30) (Phung et al. 2023). Similar final pH values have been reported in acerola byproduct-based fermentations (2.49–2.58) (Leonarski et al. 2021b), while others have documented even lower values, such as 1.88 after 21 days of fermentation (Chakravorty et al. 2016).

These findings emphasize the critical role of pH control in BC production. Kombucha fermentation media typically maintain pH levels between 3 and 4, which is conducive to BC synthesis. This observation is consistent with previous studies, such as those by Oliver-Ortega et al. (2021), which identified similar pH conditions as optimal for BC production (Oliver-Ortega et al. 2021).

In addition to pH, we also measured the total soluble solids (TSS) of the broth before and after fermentation (**Table 3.20**). Initially, TSS ranged from 10.30 to 10.70 °Brix, but after fermentation, it dropped to 9.17 to 9.60 °Brix. TSS indicates sugar concentration in the solution (Muzaifa et al. 2022). Similar reductions in TSS during fermentation have been reported in other studies, such as snake fruit kombucha, where TSS decreased from 13.30–14.08 °Brix to 12.43–12.97 °Brix (Zubaidah et al. 2019), and cascara kombucha, which dropped from 10.97 °Brix to 9.97 °Brix over eight days (Muzaifa et al. 2022). This decrease is due to microbial activity, which converts sugar into glucose for microbial growth and development (Sinamo et al. 2022). Although the TSS values remain relatively high, they no longer accurately reflect the original sugar content, as the broth volume has significantly decreased during fermentation, resulting in an actual reduction in total sugar.

- **The Yield and WHC of BC**

This study examined the impact of pH on the yield and water-holding capacity (WHC) of BC by adjusting the medium's initial pH using HCl for pH 5 and NaOH for pH 6 and 7. **Figure 3.29** shows the effect of different pre-inoculation medium pH on the yield and water-holding capacity of BC.

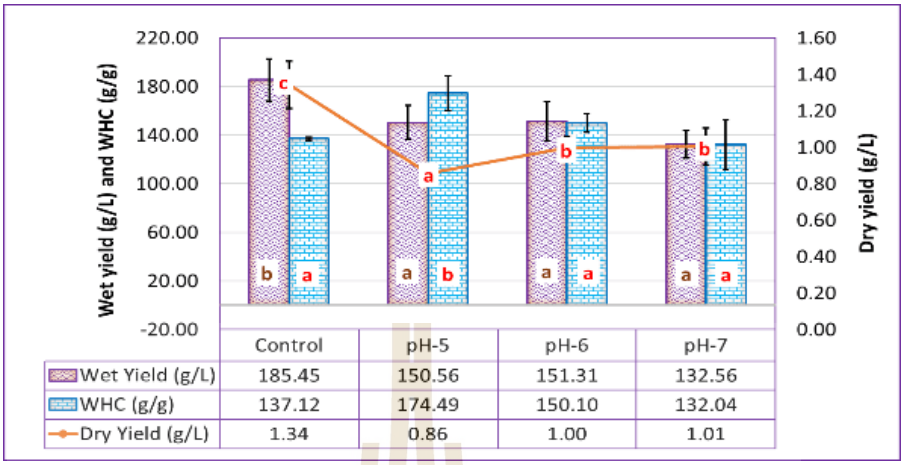

Figure 3.29 Wet yield (g/L), dry yield (g/L), and WHC of BC samples from RTC kombucha fermentation with different pH conditions.

The control sample (pH = 5.20), with the lowest final pH of 2.39, produced the highest wet yield at 185±17.28 g/L and a dry yield of 1.34±0.13 g/L. In contrast, the pH 5, 6, and 7 samples had lower wet yields of 150±13.73, 151±16.17, and 132±11.51 g/L, and dry yields of 0.86±0.01, 1.01±0.06, and 1.01±0.10 g/L, respectively. Despite these variations, the wet yields of the pH 5, 6, and 7 samples were not significantly different from each other ($P > 0.05$), suggesting that adjusting the initial pH with HCl and NaOH had minimal impact on overall yield. The fermentation process caused the pH to drop to similar levels, which normalized microbial activity across all samples (**Table 3.20**). The result of this study show that the pH of around 3.40 is ideal for BC production in kombucha fermentation, as the microorganisms in the SCOBY thrive in pH conditions of 2 to 4 (Goh et al. 2012). This range is typical for BC production using kombucha. However, different bacterial strains and media can require higher pH levels. For example, *K. xylinus* produced BC optimally at a pH of 6.05 using fig waste as the medium (Yilmaz and Goksungur 2024). Other research indicates that a pH range of 4 to 6 is optimal for BC fermentation (Lahiri et al. 2021). Strains like *A. xylinum* thrive at pH levels between 5.5 and 7.5 (Son et al. 2001; Junaidi and Azlan 2012), while *A. senegalensis* MA1 and *K. rhaeticus* K23 require pH levels of 4.5 and 5.5, respectively, for optimal production (Aswini et al. 2020; U˘gurel and Ö˘güt 2024).

The dry yield followed a similar pattern to the wet yield. The control had the highest dry yield (1.34±0.13 g/L), while the pH 5, 6, and 7 samples had lower yields (0.86±0.01, 1.01±0.06, and 1.01±0.10 g/L). There was no significant difference between the pH 6 and 7 samples ($P > 0.05$), but the pH 5 sample had the lowest dry yield ($P < 0.05$). For WHC, the pH 5 sample had the highest value at 174±14.29 g water/g cellulose, while the pH 6, 7, and control samples had lower WHC values (150±7.58, 132±20.42, and 137±1.23 g water/g cellulose) with no significant differences ($P > 0.05$). The low dry yield and high WHC of the pH 5 sample maybe due to the addition of HCl, which could increase WHC by promoting structural changes, enhancing hydrophilic properties, and affecting microbial activity, leading to a BC network better suited for water retention. These findings provide insights into how pH, chemical additions, and fermentation dynamics influence BC production in terms of wet yield, dry yield, and WHC.

2) Effect of Harvesting Period on the Yield and WHC of BC

The objective of this study was to have information about the effect of the harvesting period on the yield of BC from Thai red tea kombucha fermentation. Many previous studies conducted BC fermentation through kombucha fermentation for around one to four weeks (AL-Kalifawi and Hassan 2014; Ramírez Tapias et al. 2022; Charoenrak et al. 2023). After being harvested at a certain time, usually, the fermentation broth is still left over and can be continued to the next fermentation to produce more BC. This study conducted the experiment on various harvesting times during four weeks.

- **Profile of fermentation broth**

Table 3.21 presents the analysis of pH and °Brix changes during the fermentation process. The results indicate a consistent decrease in both pH and °Brix values over time. It is important to note that the final °Brix value does not necessarily reflect the total residual sugar content, as sugars are metabolized by microbial activity and water content may also decrease during fermentation.

The initial pH prior to fermentation was 3.58 ± 0.01, which gradually declined to 2.84 ± 0.06 in the week 1–4 sample, 2.59 ± 0.02 in the week 2–4 sample, 2.45 ± 0.01 in the week 3–4 sample, and 2.33 ± 0.06 in the week 4–4 sample. These reductions were statistically significant across all sampling intervals. After 28 days of fermentation (week 4), all samples exhibited a relatively similar pH range (2.26–2.33), with no statistically significant differences among treatments. Several previous studies have reported comparable trends in pH reduction during kombucha fermentation. Charoenrak et al. (2023) reported a decrease in pH from approximately 3.6 on day 0, to 3.2 on day 7, 3.0 on day 14, and 2.3 after 30 days of fermentation. Ramírez Tapias et al. (2022) observed final pH values ranging from 2.37 to 2.65 after 21 days of herbal infusion fermentation. Similarly, Chakravorty et al. (2016) reported pH values of 2.28, 1.98, and 1.88 after 7, 14, and 21 days of fermentation, respectively.

In addition to pH, TSS evaluation showed that the initial °Brix value for all samples was 10.70 ± 0.00, indicating uniform sugar concentrations at the start of fermentation. Following the first harvest, a decrease in °Brix was observed, likely due to microbial sugar metabolism. However, °Brix values remained relatively stable from the first to the final harvest. No statistically significant differences were detected among the samples after either the first or final harvest. This stabilization may be explained by a balance between ongoing microbial sugar consumption and water loss through evaporation. As the fermentation progressed under static conditions in open vessels, water evaporation likely contributed to a slight concentration of the fermentation broth, partially offsetting further reductions in °Brix. This effect could have masked continued sugar depletion, resulting in relatively unchanged °Brix readings despite ongoing microbial activity.

Table 3.21 The change of pH and °Brix during RTC kombucha fermentation time

Samples	The Change of the pH			The Change of the °Brix		
	Initial	1st harvest	final	initial	1st harvest	final
Week 1-4	3.58±0.01[a]	2.84±0.06[d]	2.26±0.04[a]	10.70±0.17[a]	9.93±0.18[a]	9.73±0.11[a]
Week 2-4	3.58±0.01[a]	2.59±0.02[c]	2.29±0.02[a]	10.70±0.17[a]	9.62±0.10[a]	9.90±0.17[a]
Week 3-4	3.58±0.01[a]	2.45±0.01[b]	2.27±0.01[a]	10.70±0.17[a]	9.82±0.17[a]	9.79±0.24[a]
Week 4-4	3.58±0.01[a]	2.33±0.06[a]	2.33±0.06[a]	10.70±0.17[a]	9.83±0.20[a]	9.83±0.20[a]

- **The Yield and WHC of BC**

Figure 3.30 shows the effect of different harvesting times on the yield and water-holding capacity of BC from Thai red tea kombucha fermentation. Samples W1-4, W2-4, and W3-4 were harvested twice: once at their assigned week (week 1, 2, or 3) and again in the fourth week. W4-4 was harvested only once in the fourth week. The results indicate that harvesting time significantly affects BC yield, with higher yields observed for samples harvested later, especially W4-4. This aligns with studies showing increased BC production with extended fermentation, as *Acetobacter* continues producing cellulose with adequate nutrients and sugar.

For both wet and dry yields, samples harvested after longer fermentation time (W3-4 and W4-4) consistently show higher yields than those harvested earlier (W1-4 and W2-4). The W4-4 sample, which was harvested after four weeks without interruption, achieved the highest wet yield (268.39±35.02 g/L) and dry yield (2.35±2.35 g/L). This trend is expected because BC production typically accelerates after the initial microbial adaptation phase. Previous studies have reported similar increases in yield with extended fermentation time, where wet yields rose from 1,162 ± 28 g (7 days) to 3,931 ± 43 g (30 days), while dry yields increased from 120 ± 10 g to 880 ± 27 g (Charoenrak et al. 2023). Comparable growth trends were also documented over 8, 12, and 20 days of fermentation (Petrosian 2021). This consistent

pattern occurs because bacteria continue synthesizing cellulose until nutrient depletion or the accumulation of inhibitory byproducts limits further production.

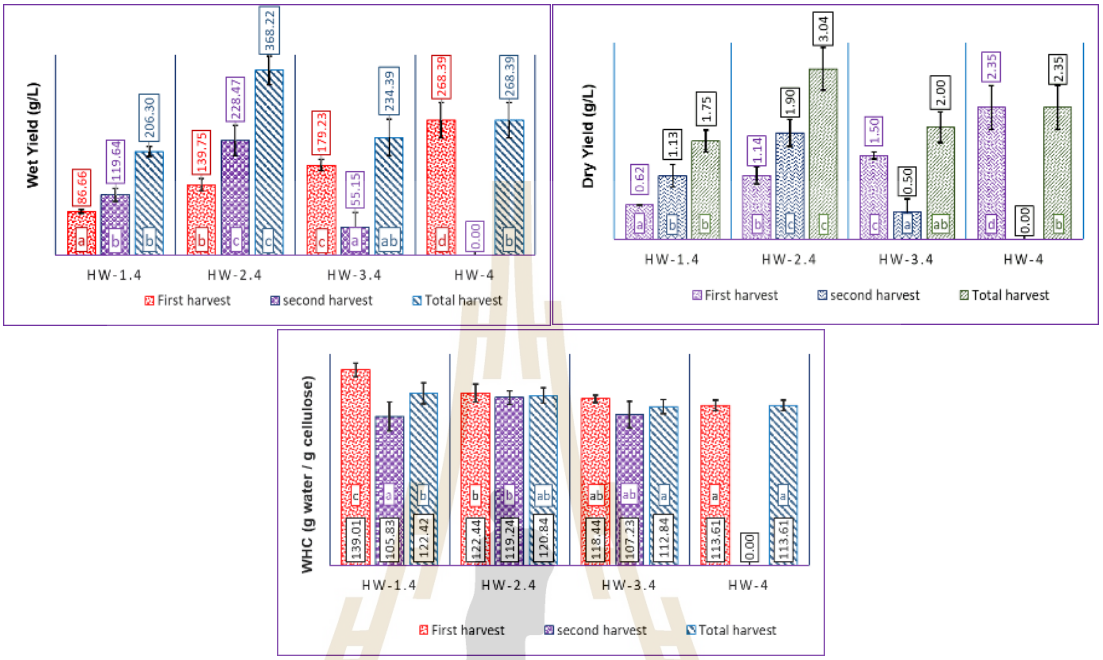

Figure 3.30 Wet yield (g/L), dry yield (g/L), and WHC (g water / g cellulose) of BC samples from RTC kombucha fermentation with different harvesting period

Comparing the total yields across the different samples (W1-4, W2-4, W3-4, and W4-4), W2-4 had the highest overall yield, with a total wet yield of 368.22±28.33 g/L and a total dry yield of 3.04±0.38 g/L. This suggests that harvesting after the second week may strike a balance between maximizing yield and allowing sufficient time for bacterial growth. While W4-4 achieved the highest yields for a single harvest, the cumulative yield from earlier harvesting periods in W2-4 was superior. This finding aligns with some studies where BC production increased until about 15 days of fermentation, and further increases in yield were minor (Yanti et al. 2018; Aswini et al. 2020; Photphisutthiphong and Vatanyoopaisarn 2020).

The WHC trends show a different pattern compared to the yield data (**Figure 3.20**). Initially, the WHC decreases as the fermentation progresses. For example, W1-4 had the highest WHC at the first harvest (139.01±4.77 g water/g

cellulose), while W4-4, which was harvested after the longest period, had the lowest WHC (113.61±3.73 g water/g cellulose). The average WHC values for the samples followed a similar trend, with the earliest sample (W1-4) having the highest average WHC (122.42±7.37) and the later samples (W2-4, W3-4, and W4-4) having lower WHC values (120.84±5.38, 112.84±4.93, and 113.61±3.73 g water/g cellulose, respectively). This finding is align with a previous study (Charoenrak et al. 2023). The reduction in WHC over time could be related to structural changes in the BC matrix. Longer fermentation times allow for more extensive cross-linking of cellulose fibers, leading to a denser structure that holds less water. The reduction of WHC with the age of BC suggests that the nanoribbons arrangement must have significantly varied with incubation time, conditioning the weight of water held per unit weight of cellulose (Corzo Salinas et al. 2021). Previous investigations on sheet BC pellicles have shown that increasing fermentation times, more micro-fibrils were secreted by bacteria, resulted in membranes with a less porous and more compact nanoribbons network structure which in turn affected the water holding capacity (Tang et al. 2010; Cerrutti et al. 2016).

Overall, the results suggest that harvesting time plays a critical role in determining the yield and WHC of BC from kombucha fermentation. Extended fermentation times increase both wet and dry yields but reduce the WHC due to structural changes in the cellulose matrix. Optimal harvesting times depend on whether the goal is to maximize yield or maintain higher WHC properties. Future studies should further investigate the balance between yield and WHC to optimize BC production for specific applications.

3) Effect of Tea Concentration on the Yield and WHC of BC

In kombucha fermentation, tea concentration plays a critical role in BC production. A concentration of 1% (w/v) is most commonly used in previous studies, as it provides essential nutrients—particularly polyphenols—that support the growth of Komagataeibacter species, the primary producers of BC. This level is

generally considered optimal due to its balance between microbial growth support and cost-effectiveness. However, the impact of higher tea concentrations—such as 2% and 3%—on BC production, particularly using Thai red tea, remains largely unexplored. This study aims to investigate the effects of increased tea concentrations on both the yield and WHC of BC. The goal is to determine whether a greater supply of nutrients from higher tea concentrations can enhance BC production or influence its physical characteristics.

- **Profile of Fermentation Broth**

The changes in pH and °Brix before and after fermentation are presented in **Table 3.22**. The observed decrease in °Brix aligns with results reported in previous studies. Regarding pH, the initial values of the tea infusions at 1% (RTC-1%), 2% (RTC-2%), and 3% (RTC-3%) concentrations before inoculation were approximately 5.22, 5.20, and 5.19, respectively. After inoculation, the pH values shifted to 3.72, 3.94, and 4.08, respectively. Notably, higher tea concentrations corresponded with higher pH values after both inoculation and fermentation. This trend may be attributed to the buffering capacity of soluble compounds present in the tea infusions. Previous research has demonstrated that components such as carboxyl and amino groups in green tea extracts contribute to buffering effects—organic acids and carboxylic groups of amino acids buffer around pH 3.7, while catechins, theanine, and amino groups contribute to buffering near pH 9.3 (Yamano and Miyagawa 1997).

In contrast, the °Brix values decreased after fermentation across all samples but remained statistically similar, ranging from approximately 9.8 to 10.0 °Brix. This suggests that sugar consumption during fermentation was relatively consistent despite variations in initial pH and tea concentration.

Table 3.22 The change of pH and °Brix (before and after) RTC kombucha fermentation with different tea concentration

Sample	The Change of the pH		The Change of the Brix	
	Initial pH	final pH	Initial °Brix	°Brix
RTC-1%	3.72±0.00[a]	2.58±0.03[a]	11.00±0.00[a]	9.87±0.13[a]
RTC-2%	3.94±0.01[b]	2.94±0.02[b]	11.10±0.00[b]	9.83±0.10[a]
RTC-3%	4.08±0.00[c]	3.20±0.03[c]	11.40±0.00[c]	10.00±0.07[a]

Overall, these results indicate that while initial pH and tea concentration influence the acidity attained during fermentation, their effect on residual sugar content (as measured by °Brix) is less significant. Microbial activity lowers pH through acid production, but sugar consumption, reflected by the decrease in °Brix, appears to be relatively uniform across treatments.

- **The Yield and WHC of BC**

The effect of varying tea concentrations on the wet yield, dry yield, and WHC of BC from Thai red tea kombucha is presented **in Figure 3.31.** The data reveal distinct trends that align with findings from prior studies on kombucha fermentation and BC production.

The wet yield results indicate that increasing tea concentrations do not necessarily improve BC production. The 2% tea concentration (RTC-2%) yielded the highest wet yield at 195.72±18.53 g/L, although this was not significantly different from the 1% tea sample (177.36±13.72 g/L). Interestingly, the 3% tea concentration (RTC-3%) produced the lowest wet yield (157.60±8.01 g/L), significantly lower than both the 1% and 2% samples ($P < 0.05$). For the dry yield, the RTC-2% sample again showed the highest value at 1.66±0.24 g/L, significantly greater than RTC-1% (1.40±0.03 g/L) and RTC-3% (1.53±0.01 g/L). While RTC-3% had a slightly higher dry yield than RTC-1%, the difference was not statistically significant ($P > 0.05$). These findings suggest

that moderate tea concentrations, between 1% and 2%, provide optimal conditions for cellulose synthesis by balancing nutrient availability and microbial activity.

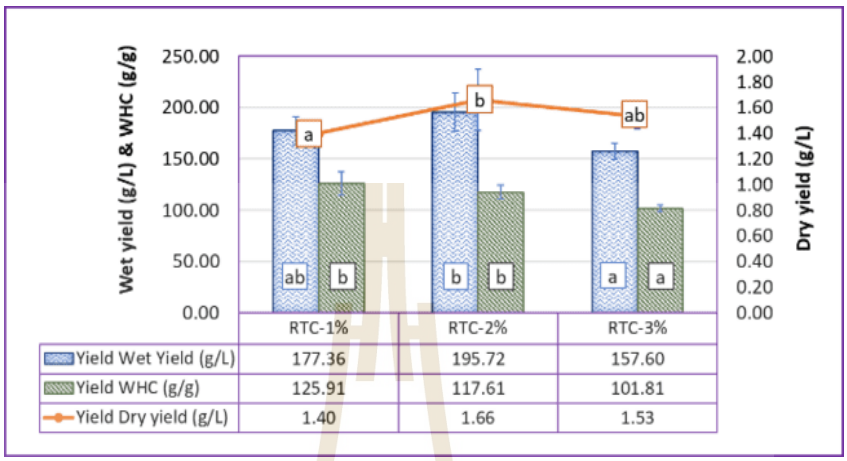

Figure 3.31 Wet yield (g/L), dry yield (g/L), and WHC of BC samples from RTC kombucha fermentation with different tea concentration

This study differs slightly from previous research, where a 1% tea concentration (10 g/L tea infusion) was considered optimal and commonly used for BC production through kombucha fermentation (AL-Kalifawi and Hassan 2014; Kalifawi 2018; Avcioglu et al. 2021; China et al. 2021; Oliver-Ortega et al. 2021). Further investigation is necessary to determine the optimal tea concentration for BC production, particularly using Thai red tea kombucha. Notably, the Thai red tea used in this experiment contains 94% Assam red tea powder, 5% sugar, and 1% other ingredients such as artificial flavoring and coloring agents (as indicated on the packaging). Research findings indicate that higher tea concentrations can reduce the efficiency of cellulose-producing bacteria, possibly due to excess polyphenols and other compounds interfering with fermentation. This inverse relationship between tea concentration and BC yield has been observed in previous studies, where excessive tea inhibited the growth of microbes like *G. xylinus* (Nguyen et al. 2008).

The trend in WHC shows a clear decline with increasing tea concentrations. RTC-1% had the highest WHC (125.91±11.63 g water/g cellulose), though it was not significantly different from RTC-2% (117.6±7.12 g water/g cellulose).

However, the sample from RTC-3% exhibited the lowest WHC (108.81±3.40 g water/g cellulose), with a significant difference from the other samples ($P < 0.05$). The decrease in WHC with higher tea concentrations may be due to the denser and less porous structure of the BC matrix formed in the presence of higher levels of polyphenols. These polyphenols can bind to cellulose, reducing its ability to retain water. Several studies have reported on the interaction between polyphenols and the cellulose matrix, supporting this explanation (Phan et al. 2015; Liu et al. 2017, 2018; Makarewicz et al. 2021). Although NaOH is used to purify BC, some polyphenols may remain bound to the cellulose structure. Stable polyphenols can form strong bonds with cellulose, making them hard to remove completely. Further investigation is necessary to determine whether polyphenols exist in purified BC.

4) Effect of Cultivation Methods on the Yield and WHC Of BC

This study investigated the effects of different cultivation methods—static, agitated, and shaking—on the yield and WHC of BC. The choice of cultivation method is a critical factor in BC production, as it influences not only the yield but also the structural properties and suitability of the material for various applications. Static cultivation is often favored for its simplicity and the high-quality cellulose it produces, though it generally results in lower yields (Wang et al. 2019b; Gao et al. 2020; Lahiri et al. 2021). In contrast, shaking and agitation methods improve oxygen and nutrient availability, which can enhance productivity levels (Lahiri et al. 2021; Akintunde et al. 2022). This study compares the impact of static, agitated, and shaking cultivation methods on the yield and WHC of BC from Thai red tea kombucha fermentations, aiming to understand how different conditions affect production efficiency. The shaking method was performed using an orbital shaker at 150 rpm, while the agitation was carried out with a magnetic stirrer, also set to 150 rpm.

- **Profile of Fermentation Broth**

The changes in pH and °Brix during Thai red tea kombucha fermentation under different cultivation methods (static, shaking, and agitating) are

presented in **Table 3.23**. The results show consistent trends with previous experiments, where the final pH and °Brix values varied depending on the cultivation method. The initial pH for all samples was consistent at 3.43±0.03. After fermentation, the static method resulted in the lowest final pH (2.47±0.03), followed by agitating (2.51±0.15) and shaking (2.53±0.02). However, the differences in pH among the methods were not statistically significant ($P > 0.05$). The slightly lower pH in the static method may be attributed to the accumulation of organic acids produced during fermentation, as static conditions limit oxygen availability, promoting acid production.

Table 3.23 The change of pH and °Brix (before and after) RTC kombucha fermentation with different cultivation methods

Sample	The Change of the pH		The Change of the °Brix	
	Initial pH	final pH	initial °Brix	final °Brix
RTC-static	3.43±0.03[a]	2.47±0.03[a]	10.90±0.00[a]	10.17±0.35[a]
RTC-Shaking	3.43±0.03[a]	2.53±0.02[a]	10.90±0.00[a]	12.37±2.32[b]
RTC-Agitating	3.43±0.03[a]	2.51±0.15[a]	10.90±0.00[a]	12.96±1.33[b]

In terms of °Brix, the initial value for all samples was 10.90±0.00, indicating uniform sugar concentration at the start. However, the final °Brix values varied significantly: static (10.17±0.35), shaking (12.37±2.32), and agitating (12.96±1.33). The static method showed the lowest final °Brix, suggesting greater sugar consumption by microbes due to prolonged fermentation under limited oxygen. In contrast, shaking and agitating methods retained higher °Brix levels, which may be due to water evaporation during fermentation, leading to increased sugar concentration, or improved oxygen and nutrient distribution slowing sugar utilization. These findings align with previous studies, where static conditions promote acid production and sugar consumption, while agitated or shaken methods enhance oxygen availability, potentially altering fermentation dynamics. Further research is needed to fully

understand the impact of cultivation methods on microbial behavior and BC production efficiency.

- **The Yield and WHC of BC**

Figure 3.32 visualized the effect of different cultivation methods on the yields and WHC of BC from Thai red tea kombucha fermentations. In this study, static and shaking cultivations resulted in comparable wet and dry yields, with no significant difference between them ($P > 0.05$). Static cultivation produced a wet yield of 185.45 g/L and a dry yield of 1.34 g/L, while shaking and agitated cultivation yielded of 182.99 g/L and 37.37 g/L for wet yield, respectively and 1.07 g/L and 0.45 g/L for dry yield, respectively. These results contrast with several previous studies, which generally report that shaking provides the highest productivity due to enhanced oxygenation and nutrient dispersion (Ullah et al. 2019; Barja 2021a). However, our findings indicate that under specific conditions, such as optimized inoculum concentration or nutrient availability, static cultivation can match shaking in yield.

Despite the similarity in yields, the WHC results showed significant differences among the cultivation methods. Shaking produced the highest WHC at 171 g/g, which is significantly greater than that of static (137 g/g) and agitated (81.09 g/g) cultivations ($P < 0.05$). This higher WHC under shaking conditions aligns with previous research indicating that shaking promotes a more porous BC structure, enhancing its water holding capacity (Krystynowicz et al. 2002). Conversely, the agitated method, using a magnetic stirrer, had the lowest yield and WHC, likely due to the shear forces and limited oxygenation disrupting BC fibril formation. Many previous studies also emphasize that agitation often leads to lower BC yields compared to both static and shaking methods, due to the excessive shear forces that can inhibit proper cellulose formations (Zhang et al. 2022a). Agitated cultivation presents a challenge in BC production due to the potential for cellulose-producing cells (*Cel+* cells) to mutate into non-producing mutant cells (*Cel-* mutants)) (Moon et al. 2006; Jacek et al. 2019). This genetic instability often results in reduced yields of BC (Martirani-VonAbercron and

Pacheco-Sánchez 2023). Additionally, Furthermore, not all bacterial strains are suitable for cultivation using agitation methods (Barja 2021a), which limits their application in certain cases. Our study supports this trend, with the agitated samples showing significantly lower yields (wet yield of 37.37 g/L and dry yield of 0.45 g/L) and the lowest WHC.

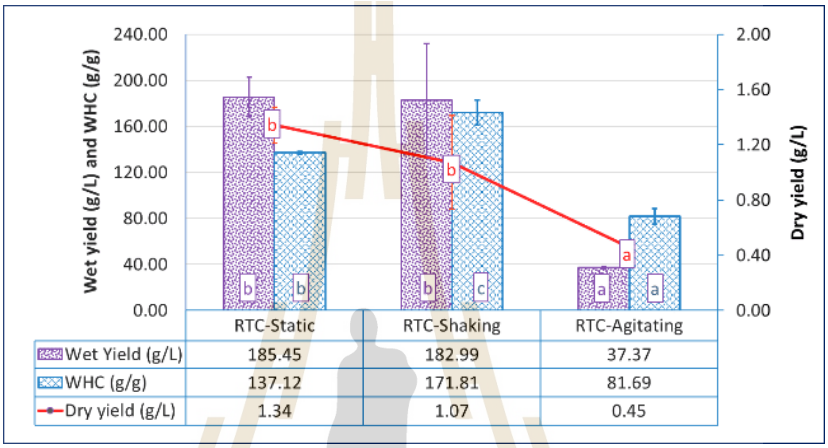

Figure 3.32 Wet yield (g/L), dry yield (g/L), and WHC of BC samples from RTC kombucha fermentation with different cultivation method

3.5 Conclusion

This study has demonstrated that Thai red tea kombucha constitutes a promising and economically viable medium for bacterial cellulose production. Among the four tea varieties evaluated—Chinese Black Tea, *Assamica* Black Tea, Thai Green Tea, and Thai Red Tea—the latter yielded the highest BC production of 168.00 ± 2.93 g/L, which was further enhanced by supplementation with ethanol and specific carbon source combinations, achieving a maximum yield of 259.54 g/L. Optimization of critical fermentation parameters, including maintaining the unadjusted initial pH (~5.20), tea concentrations of 1–2%, cultivation duration, and bi-weekly harvesting over four weeks, significantly increased the cumulative BC yield to 368.22 ± 28.33 g/L under static cultivation at 30 °C. Comprehensive characterization of the produced BC confirmed its favorable physicochemical properties, including a well-defined fiber morphology, high crystallinity, thermal stability, and satisfactory mechanical strength. These results

validate the suitability of Thai red tea kombucha as a culturally relevant and cost-effective substrate for BC biosynthesis. The present study provides essential baseline data to guide subsequent statistical optimization and scale-up efforts aimed at improving BC production efficiency for diverse industrial applications.

3.6 References

Abol-Fotouh D, Hassan MA, Shokry H, et al (2020) Bacterial nanocellulose from agro-industrial wastes: low-cost and enhanced production by Komagataeibacter saccharivorans MD1. Sci Rep 10:1–14. https://doi.org/10.1038/s41598-020-60315-9

Adekoya MA, Liu S, Oluyamo SS, et al (2022) Influence of size classifications on the crystallinity index of Albizia gummifera cellulose. Heliyon 8:. https://doi.org/10.1016/j.heliyon.2022.e12019

Adnan A, Nair GR, Lay MC, et al (2015) Glycerol as a Cheaper Carbon Source in Bacterial Cellulose (BC) Production by Gluconacetobacter Xylinus Dsm46604 in Batch Fermentation System

Agustin S, Wahyuni ET, Suparmo, et al (2021) Production and characterization of bacterial cellulose-alginate biocomposites as food packaging material. Food Res 5:204–210. https://doi.org/10.26656/fr.2017.5(6).733

Agustin YE, Padmawijaya KS (2018) Effect of acetic acid and ethanol as additives on bacterial cellulose production by acetobacter xylinum. IOP Conf Ser Earth Environ Sci 209:. https://doi.org/10.1088/1755-1315/209/1/012045

Agustin YE, Padmawijaya KS, Rixwari HF, Yuniharto VAS (2018) Glycerol as an additional carbon source for bacterial cellulose synthesis. IOP Conf Ser Earth Environ Sci 141:. https://doi.org/10.1088/1755-1315/141/1/012001

Akintunde MO, Adebayo-Tayo BC, Ishola MM, et al (2022) Bacterial Cellulose Production from agricultural Residues by two Komagataeibacter sp. Strains. Bioengineered 13:10010–10025. https://doi.org/10.1080/21655979.2022.2062970

Al-Kalifawi EJ, Hassan IA (2014) Factors Influence on the yield of Bacterial Cellulose of Kombucha (Khubdat Humza). Baghdad Sci J 11:1420–1428. https://doi.org/10.21123/bsj.11.3.1420-1428

AL-Kalifawi EJ, Hassan IA (2014) Factors Influence on the yield of Bacterial Cellulose of Kombucha (Khubdat Humza). Baghdad Sci J 11:1420–1428. https://doi.org/10.21123/bsj.11.3.1420-1428

Al-Kalifawi EJ (2018) Produce bacterial cellulose of kombucha (Khubdat Humza) from honey. J Genet Environ Resour Conserv 2:39–45

Almihyawi RAH, Musazade E, Alhussany N, et al (2024) Production and characterization of bacterial cellulose by Rhizobium sp. isolated from bean root. Sci Rep 14:1–17. https://doi.org/10.1038/s41598-024-61619-w

Amarasekara AS, Wang D, Grady TL (2020) A comparison of kombucha SCOBY bacterial cellulose purification methods. SN Appl Sci 2:1–7. https://doi.org/10.1007/s42452-020-1982-2

Amorim J, Liao K, Mandal A, et al (2024) Impact of Carbon Source on Bacterial Cellulose Network Architecture and Prolonged Lidocaine Release. Polymers (Basel) 16:. https://doi.org/10.3390/polym16213021

Amorim JDP, Costa AFS, Galdino CJS, et al (2019) Bacterial cellulose production using fruit residues as substract to industrial application. Chem Eng Trans 74:1165–1170. https://doi.org/10.3303/CET1974195

Amorim LFA, Fangueiro R, Gouveia IC (2022) Characterization of Bioactive Colored Materials Produced from Bacterial Cellulose and Bacterial Pigments. Materials (Basel) 15:. https://doi.org/10.3390/ma15062069

Amorim LFA, Li L, Gomes AP, et al (2023) Sustainable bacterial cellulose production by low cost feedstock: evaluation of apple and tea by-products as alternative sources of nutrients. Cellulose 30:5589–5606. https://doi.org/10.1007/s10570-023-05238-0

Andritsou V, De Melo EM, Tsouko E, et al (2018) Synthesis and Characterization of

Bacterial Cellulose from Citrus-Based Sustainable Resources. ACS Omega 3:10365–10373. https://doi.org/10.1021/acsomega.8b01315

Aswini K, Gopal NO, Uthandi S (2020) Optimized culture conditions for bacterial cellulose production by Acetobacter senegalensis MA1. BMC Biotechnol 20:1–16. https://doi.org/10.1186/s12896-020-00639-6

Atykyan N, Revin V, Shutova V (2020) Raman and FT-IR Spectroscopy investigation the cellulose structural differences from bacteria Gluconacetobacter sucrofermentans during the different regimes of cultivation on a molasses media. AMB Express 10:. https://doi.org/10.1186/s13568-020-01020-8

Avcioglu NH, Birben M, Seyis Bilkay I (2021) Optimization and physicochemical characterization of enhanced microbial cellulose production with a new Kombucha consortium. Process Biochem 108:60–68. https://doi.org/10.1016/j.procbio.2021.06.005

Azeredo HMC, Barud H, Farinas CS, et al (2019) Bacterial Cellulose as a Raw Material for Food and Food Packaging Applications. Front. Sustain. Food Syst. 3:1–14

Balistreri GN, Campbell IR, Li X, et al (2024) Bacterial cellulose nanoparticles as a sustainable drug delivery platform for protein-based therapeutics. RSC Appl Polym 2:172–183. https://doi.org/10.1039/d3lp00184a

Ball E (1953) Hydrolysis of Sucrose by Autoclaving Media, a Neglected Aspect in the Technique of Culture of Plant Tissues. Bull Torrey Bot Club 80:409–411

Barja F (2021) Bacterial nanocellulose production and biomedical applications. J Biomed Res 35:310–317. https://doi.org/https://doi.org/10.7555/JBR.35.20210036

Betlej I, Salerno-Kochan R, Krajewski KJ, et al (2020) The influence of culture medium components on the physical and mechanical properties of cellulose synthesized by kombucha microorganisms. BioResources 15:3125–3135. https://doi.org/10.15376/biores.15.2.3125-3135

Brandes R, De Souza L, Carminatti C, Recouvreux D (2020) Production with a High Yield of Bacterial Cellulose Nanocrystals by Enzymatic Hydrolysis. Int J Nanosci

19:1–8. https://doi.org/10.1142/S0219581X19500157

Cazón P, Vázquez M (2021) Improving bacterial cellulose films by ex-situ and in-situ modifications: A review. Food Hydrocoll 113:1–9. https://doi.org/10.1016/j.foodhyd.2020.106514

Cerrutti P, Roldán P, García RM, et al (2016) Production of bacterial nanocellulose from wine industry residues: Importance of fermentation time on pellicle characteristics. J Appl Polym Sci 133:1–9. https://doi.org/10.1002/app.43109

Chakravorty S, Bhattacharya S, Chatzinotas A, et al (2016) Kombucha tea fermentation: Microbial and biochemical dynamics. Int J Food Microbiol 220:63–72. https://doi.org/10.1016/j.ijfoodmicro.2015.12.015

Charoenrak S, Charumanee S, Sirisa-ard P, et al (2023) Nanobacterial Cellulose from Kombucha Fermentation as a Potential Protective Carrier of Lactobacillus plantarum under Simulated Gastrointestinal Tract Conditions. Polymers (Basel) 15:. https://doi.org/10.3390/polym15061356

Chen S-Q, Lopez-Sanchez P, Wang D, et al (2018) Mechanical properties of bacterial cellulose synthesised by diverse strains of the genus Komagataeibacter. Food Hydrocoll 1–25. https://doi.org/10.1016/j.foodhyd.2018.02.031.This

Chen SQ, Meldrum OW, Liao Q, et al (2021) The influence of alkaline treatment on the mechanical and structural properties of bacterial cellulose. Carbohydr Polym 271:118431. https://doi.org/10.1016/j.carbpol.2021.118431

Chibrikov V, Pieczywek PM, Cybulska J, Zdunek A (2023) Evaluation of elasto-plastic properties of bacterial cellulose-hemicellulose composite films. Ind Crops Prod 205:117578. https://doi.org/10.1016/j.indcrop.2023.117578

China S La, De Vero L, Anguluri K, et al (2021) Kombucha tea as a reservoir of cellulose producing bacteria: Assessing diversity among komagataeibacter isolates. Appl Sci 11:1–18. https://doi.org/10.3390/app11041595

Chong AQ, Chin NL, Talib RA, Basha RK (2024) Modelling pH Dynamics, SCOBY Biomass Formation, and Acetic Acid Production of Kombucha Fermentation

Using Black, Green, and Oolong Teas. Processes 12:1301. https://doi.org/10.3390/pr12071301

Cielecka I, Ryngajłło M, Maniukiewicz W, Bielecki S (2021a) Highly Stretchable Bacterial Cellulose Produced by. Polymers (Basel) 4455:1–23. https://doi.org/https://doi.org/10.3390/polym13244455

Cielecka I, Ryngajłło M, Maniukiewicz W, Bielecki S (2021b) Response surface methodology-based improvement of the yield and differentiation of properties of bacterial cellulose by metabolic enhancers. Int J Biol Macromol 187:584–593. https://doi.org/10.1016/j.ijbiomac.2021.07.147

Ciolacu D, Ciolacu F, Popa VI (2011) Amorphous cellulose - Structure and characterization. Cellul Chem Technol 45:13–21

Corzo Salinas DR, Sordelli A, Martínez LA, et al (2021) Production of bacterial cellulose tubes for biomedical applications: Analysis of the effect of fermentation time on selected properties. Int J Biol Macromol 189:1–10. https://doi.org/10.1016/j.ijbiomac.2021.08.011

Czernicka M, Zaguła G, Bajcar M, et al (2017) Study of nutritional value of dried tea leaves and infusions of black, green and white teas from Chinese plantations. Rocz Panstw Zakl Hig 68:237–245

Dartiguenave C, Jeandet P, Maujean A (2000) Study of the contribution of the major organic acids of wine to the buffering capacity of wine in model solutions. Am J Enol Vitic 51:352–356. https://doi.org/10.5344/ajev.2000.51.4.352

De Araújo Júnior AM, Braido G, Saska S, et al (2016) Regenerated cellulose scaffolds: Preparation, characterization and toxicological evaluation. Carbohydr Polym 136:892–898. https://doi.org/10.1016/j.carbpol.2015.09.066

de Lange JH (1989) Significance of autoclaving-induced toxicity from and hydrolysis of carbohydrates in in vitro studies of pollen germination and tube growth. South African J Bot 55:1–5. https://doi.org/10.1016/s0254-6299(16)31225-x

De Souza KC, Trindade NM, De Amorim JDP, et al (2021) Kinetic study of a bacterial

cellulose production by komagataeibacter rhaeticus using coffee grounds and sugarcane molasses. Mater Res 24:. https://doi.org/10.1590/1980-5373-MR-2020-0454

Deka H, Sarmah PP, Chowdhury P, et al (2023) Impact of the Season on Total Polyphenol and Antioxidant Properties of Tea Cultivars of Industrial Importance in Northeast India. Foods 12:. https://doi.org/10.3390/foods12173196

Deka H, Sarmah PP, Devi A, et al (2021) Changes in major catechins, caffeine, and antioxidant activity during CTC processing of black tea from North East India. RSC Adv 11:11457–11467. https://doi.org/10.1039/d0ra09529j

Devje S (2022) What Is Thai Tea? Everything You Need to Know About This Sweet, Spiced Delight. https://www.healthline.com/nutrition/thai-tea#basics. Accessed 6 Feb 2023

Dhali K, Ghasemlou M, Daver F, et al (2021) Science of the Total Environment A review of nanocellulose as a new material towards environmental sustainability. Sci Total Environ 775:145871. https://doi.org/10.1016/j.scitotenv.2021.145871

Dusunceli N, Colak OU (2008) Modelling effects of degree of crystallinity on mechanical behavior of semicrystalline polymers. Int J Plast 24:1224–1242. https://doi.org/10.1016/j.ijplas.2007.09.003

El-Gendi H, Taha TH, Ray JB, Saleh AK (2022) Recent advances in bacterial cellulose: a low-cost effective production media, optimization strategies and applications. Cellulose 29:7495–7533

Fahim N, Montazer M (2020) Effect of Althaea officinalis and Green Tea Extracts on the Bacterial Cellulose Production. In: 14 th International Seminar on Polymer Science and Technology (ISPST 2020). Tarbiat Modares University, Tehran - Iran, pp 7–9

Fatima A, Ortiz-Albo P, Neves LA, et al (2023) Biosynthesis and characterization of bacterial cellulose membranes presenting relevant characteristics for air/gas filtration. J Memb Sci 674:. https://doi.org/10.1016/j.memsci.2023.121509

Fei S, Yang X, Xu W, et al (2023) Insights into Proteomics Reveal Mechanisms of Ethanol-Enhanced Bacterial Cellulose Biosynthesis by Komagataeibacter nataicola. Fermentation 9:1–14. https://doi.org/10.3390/fermentation9060575

Feng Y, Ma X, Kong B, et al (2021) Ethanol induced changes in structural, morphological, and functional properties of whey proteins isolates: Influence of ethanol concentration. Food Hydrocoll 111:106379. https://doi.org/10.1016/j.foodhyd.2020.106379

Fontana JD, Franco VC, De Souza SJ, et al (1991) Nature of plant stimulators in the production of Acetobacter xylinum ("tea fungus") biofilm used in skin therapy. Appl Biochem Biotechnol 28–29:341–351. https://doi.org/10.1007/BF02922613

Fornaro T, Burini D, Biczysko M, Barone V (2015) Hydrogen-bonding effects on infrared spectra from anharmonic computations: Uracil-water complexes and uracil dimers. J Phys Chem A 119:4224–4236. https://doi.org/10.1021/acs.jpca.5b01561

Gao H, Sun Q, Han Z, et al (2020) Comparison of bacterial nanocellulose produced by different strains under static and agitated culture conditions. Carbohydr Polym 227:115323. https://doi.org/10.1016/j.carbpol.2019.115323

Gao M, Ploessl D, Shao Z (2019) Enhancing the co-utilization of biomass-derived mixed sugars by yeasts. Front Microbiol 10:1–21. https://doi.org/10.3389/fmicb.2018.03264

Gaspar D, Fernandes SN, De Oliveira AG, et al (2014) Nanocrystalline cellulose applied simultaneously as the gate dielectric and the substrate in flexible field effect transistors. Nanotechnology 25:. https://doi.org/10.1088/0957-4484/25/9/094008

Gayathri G, Srinikethan G (2019) Bacterial Cellulose production by K. saccharivorans BC1 strain using crude distillery effluent as cheap and cost effective nutrient medium. Int J Biol Macromol 138:950–957. https://doi.org/10.1016/j.ijbiomac.2019.07.159

Gayathry G (2015) Production of Nata de Coco - a Natural Dietary Fibre Product from Mature Coconut Water using Gluconacetobacter xylinum (sju-1). Int J Food

Ferment Technol 5:231. https://doi.org/10.5958/2277-9396.2016.00006.4

Gismatulina YA, Budaeva V V. (2024) Cellulose Nitrates-Blended Composites from Bacterial and Plant-Based Celluloses. Polymers (Basel) 16:. https://doi.org/10.3390/polym16091183

Goh WN, Rosma A, Kaur B, et al (2012) Fermentation of black tea broth (kombucha): I. effects of sucrose concentration and fermentation time on the yield of microbial cellulose. Int Food Res J 19:109–117

Gorgieva S, Trček J (2019) Bacterial cellulose: Production, modification and perspectives in biomedical applications. Nanomaterials 9:1–20. https://doi.org/10.3390/nano9101352

Greenwalt CJ, Steinkraus KH, Ledford RA (2000) Kombucha, the fermented tea: microbiology, composition, and claimed health effects. J Food Prot 7:976–981. https://doi.org/doi: 10.4315/0362-028x-63.7.976

Hamed DA, Maghrawy HH, Abdel Kareem H (2023) Biosynthesis of bacterial cellulose nanofibrils in black tea media by a symbiotic culture of bacteria and yeast isolated from commercial kombucha beverage. World J Microbiol Biotechnol 39:1–16. https://doi.org/10.1007/s11274-022-03485-0

Heydorn RL, Lammers D, Gottschling M, Dohnt K (2023) Effect of food industry by-products on bacterial cellulose production and its structural properties. Cellulose 30:4159–4179. https://doi.org/10.1007/s10570-023-05097-9

Ho Jin Y, Lee T, Kim JR, et al (2019) Improved production of bacterial cellulose from waste glycerol through investigation of inhibitory effects of crude glycerol-derived compounds by Gluconacetobacter xylinus. J Ind Eng Chem 75:158–163. https://doi.org/10.1016/j.jiec.2019.03.017

Hossen MT, Kundu CK, Pranto BRR, et al (2024) Synthesis, characterization, and cytotoxicity studies of nanocellulose extracted from okra (Abelmoschus Esculentus) fiber. Heliyon 10:e25270. https://doi.org/10.1016/j.heliyon.2024.e25270

Hruška J, Köhler S, Bishop K (1999) Buffering processes in a boreal dissolved organic carbon-rich stream during experimental acidification. Environ Pollut 106:55–65. https://doi.org/10.1016/S0269-7491(99)00061-5

Illa MP, Khandelwal M, Sharma CS (2019) Modulated Dehydration for Enhanced Anodic Performance of Bacterial Cellulose derived Carbon Nanofibers. ChemistrySelect 4:6642–6650. https://doi.org/10.1002/slct.201901359

Ito A, Yanase E (2022) Study into the chemical changes of tea leaf polyphenols during japanese black tea processing. Food Res Int 160:. https://doi.org/10.1016/j.foodres.2022.111731

Izawa K, Amino Y, Kohmura M, et al (2010) Human-environment interactions - taste. In: Comprehensive Natural Products II: Chemistry and Biology. pp 631–671

Jacek P, Dourado F, Gama M, Bielecki S (2019) Molecular aspects of bacterial nanocellulose biosynthesis. Microb Biotechnol 12:633–649. https://doi.org/10.1111/1751-7915.13386

Jagannath A, Kalaiselvan A, Manjunatha SS, et al (2008) The effect of pH, sucrose and ammonium sulphate concentrations on the production of bacterial cellulose (Nata-de-coco) by Acetobacter xylinum. World J Microbiol Biotechnol 24:2593–2599. https://doi.org/10.1007/s11274-008-9781-8

Jayabalan R, Malbaša R V., Lončar ES, et al (2014) A review on kombucha tea-microbiology, composition, fermentation, beneficial effects, toxicity, and tea fungus. Compr Rev Food Sci Food Saf 13:538–550. https://doi.org/10.1111/1541-4337.12073

Jayabalan R, Marimuthu S, Swaminathan K (2007) Changes in content of organic acids and tea polyphenols during kombucha tea fermentation. Food Chem 102:392–398. https://doi.org/10.1016/j.foodchem.2006.05.032

Jenkhongkarn R, Phisalaphong M (2023) Effect of Reduction Methods on the Properties of Composite Films of Bacterial Cellulose-Silver Nanoparticles. Polymers (Basel) 15:. https://doi.org/10.3390/polym15142996

Jia Y, Wang X, Huo M, et al (2017) Preparation and characterization of a novel bacterial cellulose/chitosan bio-hydrogel. Nanomater Nanotechnol 7:1–8. https://doi.org/10.1177/1847980417707172

Jiménez-Sánchez A, Hernández-Gil L, Jiménez-Sánchez Y, et al (2024) Production of bacterial cellulose from kombucha tea and coffee husk infusion. Nativa 12:567–573. https://doi.org/10.31413/nat.v12i3.17720

Jittaut P, Hongsachart P, Audtarat S, Dasri T (2023) Production and characterization of bacterial cellulose produced by Gluconacetobacter xylinus BNKC 19 using agricultural waste products as nutrient source. Arab J Basic Appl Sci 30:221–230. https://doi.org/10.1080/25765299.2023.2172844

Junaidi Z, Azlan NM (2012) Optimization of Bacterial Cellulose Production from Pineapple Waste: Effect of Temperature, pH and Concentration. In: 5th Engineering Conference, "Engineering Towards Change - Empowering Green Solutions." Kuching Sarawak, pp 1–7

Kamal ASM, Misnon MI, Fadil F (2020) The effect of sodium hydroxide concentration on yield and properties of Bacterial Cellulose membranes. IOP Conf Ser Mater Sci Eng 732:. https://doi.org/10.1088/1757-899X/732/1/012064

Kamal T, Ul-Islam M, Fatima A, et al (2022) Cost-Effective Synthesis of Bacterial Cellulose and Its Applications in the Food and Environmental Sectors. Gels 8:552

Kazemi M, Faranak, Doosthoseini K, Azin M (2015) Effect of Ethanol and Medium on Bacterial Cellulose (Bc) Production By Gluconacetobacter Xylinus (Ptcc 1734). Cellul Chem Technol 49:455–462

Keshk SMAS (2014) Vitamin C enhances bacterial cellulose production in Gluconacetobacter xylinus. Carbohydr Polym 99:98–100. https://doi.org/10.1016/j.carbpol.2013.08.060

Keshk SMAS, Sameshima K (2005) Evaluation of different carbon sources for bacterial cellulose production. African J Biotechnol 4:478–482

Khan A, Wen Y, Huq T, Ni Y (2018) Cellulosic Nanomaterials in Food and Nutraceutical Applications: A Review. J Agric Food Chem 66:8–19. https://doi.org/10.1021/acs.jafc.7b04204

Klepacka J, Tonska E, Rafałowski R, et al (2021) Tea as a Source of Biologically Active Compounds in the Human Diet. Molecules 26:1–14. https://doi.org/https://doi.org/10.3390/molecules26051487

Krystynowicz A, Czaja W, Wiktorowska-Jezierska A, et al (2002) Factors affecting the yield and properties of bacterial cellulose. J Ind Microbiol Biotechnol 29:189–195. https://doi.org/10.1038/sj.jim.7000303

Lahiri D, Nag M, Dutta B, et al (2021) Bacterial cellulose: Production, characterization and application as antimicrobial agent. Int. J. Mol. Sci. 22:1–18

Lee J (2023) Exploring Sucrose Fermentation : Microorganisms , Biochemical Pathways , and Applications. Ferment Technol 12:1000166. https://doi.org/10.4172/2167-7972.23.12.166

Lee KR, Jo K, Ra KS, et al (2021) Kombucha fermentation using commercial kombucha pellicle and culture broth as starter. 2061:1–7

Leonarski E, Cesca K, Zanella E, et al (2021a) Production of kombucha-like beverage and bacterial cellulose by acerola byproduct as raw material. Lwt 135:1–8. https://doi.org/10.1016/j.lwt.2020.110075

Leonarski E, Cesca K, Zanella E, et al (2021b) Production of kombucha-like beverage and bacterial cellulose by acerola byproduct as raw material. Lwt 135:1–8. https://doi.org/10.1016/j.lwt.2020.110075

Li Q, Wu Y, Fang R, et al (2021) Application of Nanocellulose as particle stabilizer in food Pickering emulsion: Scope, Merits and challenges. Trends Food Sci Technol 110:573–583. https://doi.org/10.1016/j.tifs.2021.02.027

Lima NF, Maciel GM, Fernandes I de AA, Haminiuk CWI (2023) Optimising the Production Process of Bacterial Nanocellulose: Impact on Growth and Bioactive Compounds. Food Technol Biotechnol 61:494–504.

https://doi.org/10.17113/ftb.61.04.23.8182

Lin D, Liu Z, Shen R, et al (2020) Bacterial cellulose in food industry: Current research and future prospects. Int J Biol Macromol 158:1007–1019. https://doi.org/10.1016/j.ijbiomac.2020.04.230

Lin SP, Loira Calvar I, Catchmark JM, et al (2013) Biosynthesis, production and applications of bacterial cellulose. Cellulose 20:2191–2219. https://doi.org/10.1007/s10570-013-9994-3

Liu D, Martinez-Sanz M, Lopez-Sanchez P, et al (2017) Adsorption behaviour of polyphenols on cellulose is affected by processing history. Food Hydrocoll 63:496–507. https://doi.org/10.1016/j.foodhyd.2016.09.012

Liu X, Cao L, Wang S, et al (2023) Isolation and characterization of bacterial cellulose produced from soybean whey and soybean hydrolyzate. Sci Rep 13:1–10. https://doi.org/10.1038/s41598-023-42304-w

Liu X, Pan L, Cheng Y, et al (2025) Effect of high hydrostatic pressure on Alcalase-assisted hydrolysis of soy protein isolate and the anti-aging activity of the hydrolysates. Process Biochem 156:191–201. https://doi.org/10.1016/j.procbio.2025.05.020

Liu Y, Ying D, Sanguansri L, et al (2018) Adsorption of catechin onto cellulose and its mechanism study: Kinetic models, characterization and molecular simulation. Food Res Int 112:225–232. https://doi.org/10.1016/j.foodres.2018.06.044

Makarewicz M, Drożdż I, Tarko T, Duda-Chodak A (2021) The interactions between polyphenols and microorganisms, especially gut microbiota. Antioxidants 10:1–70. https://doi.org/10.3390/antiox10020188

Mann FM, Dickmann M, Schneider R, et al (2017) Analysis of the role of acidity and tea substrate on the inhibition of α-amylase by Kombucha. J Nutr Food Res Technol 0:1–5. https://doi.org/10.30881/jnfrt.00001

Martirani-VonAbercron SM, Pacheco-Sánchez D (2023) Bacterial cellulose: A highly

versatile nanomaterial. Microb Biotechnol 16:1174–1178. https://doi.org/10.1111/1751-7915.14243

Mehrotra R, Sharma S, Shree N, Kaur K (2023) Bacterial Cellulose: An Ecological Alternative as A Biotextile. Biosci Biotechnol Res Asia 20:449–463. https://doi.org/10.13005/bbra/3101

Minaker SA, Mason RH, Chow DR (2021) Optimizing Color Performance of the Ngenuity 3-Dimensional Visualization System. Ophthalmol Sci 1:100054. https://doi.org/10.1016/j.xops.2021.100054

Miranda B, Lawton NM, Tachibana SR, et al (2016) Titration and HPLC Characterization of Kombucha Fermentation: A Laboratory Experiment in Food Analysis. J Chem Educ 93:1770–1775. https://doi.org/10.1021/acs.jchemed.6b00329

Mohamad S, Abdullah LC, Jamari SS, et al (2022) Production and Characterization of Bacterial Cellulose Nanofiber by Acetobacter Xylinum 0416 Using Only Oil Palm Frond Juice as Fermentation Medium. J Nat Fibers 19:16005–16016. https://doi.org/10.1080/15440478.2022.2140243

Mohammadkazemi F, Azin M, Ashori A (2015) Production of bacterial cellulose using different carbon sources and culture media. Carbohydr Polym 117:518–523. https://doi.org/10.1016/j.carbpol.2014.10.008

Molina-Ramírez C, Castro C, Zuluaga R, Gañán P (2018a) Physical Characterization of Bacterial Cellulose Produced by Komagataeibacter medellinensis Using Food Supply Chain Waste and Agricultural By-Products as Alternative Low-Cost Feedstocks. J Polym Environ 26:830–837. https://doi.org/10.1007/s10924-017-0993-6

Molina-Ramírez C, Enciso C, Torres-Taborda M, et al (2018b) Effects of alternative energy sources on bacterial cellulose characteristics produced by Komagataeibacter medellinensis. Int J Biol Macromol 117:735–741. https://doi.org/10.1016/j.ijbiomac.2018.05.195

Montenegro-Silva P, Ellis T, Dourado F, et al (2024) Enhanced bacterial cellulose

production in Komagataeibacter sucrofermentans: impact of different PQQ-dependent dehydrogenase knockouts and ethanol supplementation. Biotechnol Biofuels Bioprod 17:1–16. https://doi.org/10.1186/s13068-024-02482-9

Moon S-H, Park J-M, Chun H-Y, Kim S-J (2006) Comparisons of physical properties of bacterial celluloses produced in different culture conditions using saccharified food wastes. Biotechnol Bioprocess Eng 11:

Moura TA, Oliveira L, Rocha MS (2019) Effects of caffeine on the structure and conformation of DNA: A force spectroscopy study. Int J Biol Macromol 130:1018–1024. https://doi.org/10.1016/j.ijbiomac.2019.02.125

Muzaifa M, Rohaya S, Nilda C, Harahap KR (2022) Kombucha Fermentation from Cascara with Addition of Red Dragon Fruit (Hylocereus polyrhizus): Analysis of Alcohol Content and Total Soluble Solid. Proc Int Conf Trop Agrifood, Feed Fuel (ICTAFF 2021) 17:125–129. https://doi.org/10.2991/absr.k.220102.020

Naveed M, BiBi J, Kamboh AA, et al (2018) Pharmacological values and therapeutic properties of black tea (Camellia sinensis): A comprehensive overview. Biomed Pharmacother 100:521–531. https://doi.org/10.1016/j.biopha.2018.02.048

Neffe-Skocińska K, Sionek B, Ścibisz I, Kołożyn-Krajewska D (2017) Acid contents and the effect of fermentation condition of Kombucha tea beverages on physicochemical, microbiological and sensory properties. CYTA - J Food 15:601–607. https://doi.org/10.1080/19476337.2017.1321588

Nguyen TA, Nguyen XC (2022) Bacterial Cellulose-Based Biofilm Forming Agent Extracted from Vietnamese Nata-de-Coco Tree by Ultrasonic Vibration Method: Structure and Properties. J Chem 2022:1–10. https://doi.org/10.1155/2022/7502796

Nguyen VT, Flanagan B, Gidley MJ, Dykes GA (2008) Characterization of cellulose production by a Gluconacetobacter xylinus strain from Kombucha. Curr Microbiol 57:449–453. https://doi.org/10.1007/s00284-008-9228-3

Nie W, Zheng X, Feng W, et al (2022) Characterization of bacterial cellulose produced

by Acetobacter pasteurianus MGC-N8819 utilizing lotus rhizome. Lwt 165:. https://doi.org/10.1016/j.lwt.2022.113763

Nurazzi NM, Asyraf MRM, Rayung M, et al (2021) Thermogravimetric analysis properties of cellulosic natural fiber polymer composites: A review on influence of chemical treatments. Polymers (Basel) 13:. https://doi.org/10.3390/polym13162710

Oliver-Ortega H, Geng S, Espinach FX, et al (2021) Bacterial cellulose network from kombucha fermentation impregnated with emulsion-polymerized poly(Methyl methacrylate) to form nanocomposite. Polymers (Basel) 13:1–17. https://doi.org/10.3390/polym13040664

Perna Manrique O, Lanchero RJ, Garrido LV (2018) Effect of the Source of Carbon and Vitamin C Present in Tropical Fruits, on the Production of Cellulose by Glunconacetobacter Xylinus. Indian J Sci Technol 11:1–8. https://doi.org/10.17485/ijst/2018/v11i22/122280

Petrosian A (2021) Production of bacterial cellulose from kombucha SCOBY: optimization of the bioprocess and industrial application. 77

Pham TT, Tran TTA (2023) Evaluation of the Crystallinity of Bacterial Cellulose Produced from Pineapple Waste Solution by Using Acetobacter Xylinum. ASEAN Eng J 13:81–91. https://doi.org/10.11113/aej.V13.18868

Phan ADT, Netzel G, Wang D, et al (2015) Binding of dietary polyphenols to cellulose: Structural and nutritional aspects. Food Chem 171:388–396. https://doi.org/10.1016/j.foodchem.2014.08.118

Photphisutthiphong Y, Vatanyoopaisarn S (2020) The production of bacterial cellulose from organic low-grade rice. Curr Res Nutr Food Sci 8:206–216. https://doi.org/10.12944/CRNFSJ.8.1.19

Phung LT, Kitwetcharoen H, Chamnipa N, et al (2023) Changes in the chemical compositions and biological properties of kombucha beverages made from black teas and pineapple peels and cores. Sci Rep 13:1–20.

https://doi.org/10.1038/s41598-023-34954-7

Potivara K, Phisalaphong M (2019) Development and characterization of bacterial cellulose reinforced with natural rubber. Materials (Basel) 12:. https://doi.org/10.3390/ma12142323

Rabbani FA, Yasin S, Iqbal T, Farooq U (2022) Experimental Study of Mechanical Properties of Polypropylene Random Copolymer and Rice-Husk-Based Biocomposite by Using Nanoindentation. Materials (Basel) 15:1–14. https://doi.org/10.3390/ma15051956

Rahmayetty, Sulaiman F (2023) Wastewater from the Arenga Starch Industry as a Potential Medium for Bacterial Cellulose and Cellulose Acetate Production. Polymers (Basel) 15:1–15. https://doi.org/10.3390/polym15040870

Raiszadeh-Jahromi Y, Rezazadeh-Bari M, Almasi H, Amiri S (2020) Optimization of bacterial cellulose production by Komagataeibacter xylinus PTCC 1734 in a low-cost medium using optimal combined design. J Food Sci Technol 57:2524–2533. https://doi.org/10.1007/s13197-020-04289-6

Ramírez Tapias YA, Di Monte MV, Peltzer MA, Salvay AG (2022) Bacterial cellulose films production by Kombucha symbiotic community cultured on different herbal infusions. Food Chem 372:. https://doi.org/10.1016/j.foodchem.2021.131346

Razali NAM, Sohaimi RM, Othman RNIR, et al (2022) Comparative Study on Extraction of Cellulose Fiber from Rice Straw Waste from Chemo-Mechanical and Pulping Method. Polymers (Basel) 14:. https://doi.org/10.3390/polym14030387

Reiniati I (2017) Bacterial Cellulose Nanocrystals : Production and Application. The University of Western Ontario

Revin V, Liyaskina E, Nazarkina M, et al (2018) Cost-effective production of bacterial cellulose using acidic food industry by-products. Brazilian J Microbiol 49:151–159. https://doi.org/10.1016/j.bjm.2017.12.012

Roberts RJ, Rowe RC, York P (1994) The Poisson's ratio of microcrystalline cellulose.

Int J Pharm 105:177–180. https://doi.org/10.1016/0378-5173(94)90463-4

Ryngajłło M, Jacek P, Cielecka I, et al (2019) Effect of ethanol supplementation on the transcriptional landscape of bionanocellulose producer Komagataeibacter xylinus E25. Appl Microbiol Biotechnol 103:6673–6688. https://doi.org/10.1007/s00253-019-09904-x

Said Azmi SNN, Samsu Z 'Asyiqin, Mohd Asnawi ASF, et al (2023) The production and characterization of bacterial cellulose pellicles obtained from oil palm frond juice and their conversion to nanofibrillated cellulose. Carbohydr Polym Technol Appl 5:100327. https://doi.org/10.1016/j.carpta.2023.100327

Samuel OS, Adefusika AM (2019) Influence of Size Classifications on the Structural and Solid-State Characterization of Cellulose Materials. In: Pascual R, Martín MEE (eds) Cellulose. IntechOpen

Sardjono SA, Suryanto H, Aminnudin, Muhajir M (2019) Crystallinity and morphology of the bacterial nanocellulose membrane extracted from pineapple peel waste using high-pressure homogenizer. In: AIP Conference Proceedings. AIP Publishing, pp 080015-1-080015–5

Schrecker ST, Gostomski PA (2005) Determining the water holding capacity of microbial cellulose. Biotechnol Lett 27:1435–1438. https://doi.org/10.1007/s10529-005-1465-y

Shahidi F, Dissanayaka CS (2023) Phenolic-protein interactions: insight from in-silico analyses – a review. Food Prod Process Nutr 5:. https://doi.org/10.1186/s43014-022-00121-0

Sharma C, Bhardwaj NK, Pathak P (2021) Static intermittent fed-batch production of bacterial nanocellulose from black tea and its modification using chitosan to develop antibacterial green packaging material. J Clean Prod 279:123608. https://doi.org/10.1016/j.jclepro.2020.123608

Shevchuk A, Megías-Pérez R, Zemedie Y, Kuhnert N (2020) Evaluation of carbohydrates and quality parameters in six types of commercial teas by

targeted statistical analysis. Food Res Int 133:109122. https://doi.org/10.1016/j.foodres.2020.109122

Shim E, Kim HR (2019) Coloration of bacterial cellulose using in situ and ex situ methods. Text Res J 89:1297–1310. https://doi.org/10.1177/0040517518770673

Shu CH (2007) Fungal Fermentation for Medicinal Products. In: Yang S-T (ed) Bioprocessing for Value-Added Products from Renewable Resources: New Technologies and Applications. Elsevier B.V., Amsterdam; Boston, pp 447–463

Sinamo KN, Ginting S, Pratama S (2022) Effect of sugar concentration and fermentation time on secang kombucha drink. IOP Conf Ser Earth Environ Sci 977:. https://doi.org/10.1088/1755-1315/977/1/012080

Singhsa P, Narain R, Manuspiya H (2018) Physical structure variations of bacterial cellulose produced by different Komagataeibacter xylinus strains and carbon sources in static and agitated conditions. Cellulose 25:1571–1581. https://doi.org/10.1007/s10570-018-1699-1

Son H, Heo M, Kim Y, Lee S (2001) Optimization of fermentation conditions for the production of bacterial cellulose by a newly isolated Acetobacter . Biotechnol Appl Biochem 33:1–5. https://doi.org/10.1042/ba20000065

Srivastava S, Mathur G (2022) Komagataeibacter saccharivorans strain BC-G1: an alternative strain for production of bacterial cellulose. Biologia (Bratisl) 77:3657–3668. https://doi.org/10.1007/s11756-022-01222-4

Suryanto H, Muhajir M, Sutrisno TA, et al (2019) The Mechanical Strength and Morphology of Bacterial Cellulose Films: The Effect of NaOH Concentration. IOP Conf Ser Mater Sci Eng 515:. https://doi.org/10.1088/1757-899X/515/1/012053

Tabaii MJ, Emtiazi G (2016) Comparison of bacterial cellulose production among different strains and fermented media. Appl Food Biotechnol 3:35–41. https://doi.org/10.22037/afb.v3i1.10582

Tang W, Jia S, Jia Y, Yang H (2010) The influence of fermentation conditions and post-treatment methods on porosity of bacterial cellulose membrane. World J

Microbiol Biotechnol 26:125–131. https://doi.org/10.1007/s11274-009-0151-y

Teixeira SRZ, Dos Reis EM, Apati GP, et al (2019) Biosynthesis and functionalization of bacterial cellulose membranes with cerium nitrate and silver nanoparticles. Mater Res 22:1–13. https://doi.org/10.1590/1980-5373-MR-2019-0054

Teoh AL, Heard G, Cox J (2004) Yeast ecology of Kombucha fermentation. Int J Food Microbiol 95:119–126. https://doi.org/10.1016/j.ijfoodmicro.2003.12.020

Thegreencreator.com (2022) Thai Tea: made from scratch. https://thegreencreator.com/thai-tea/. Accessed 8 Aug 2024

Theppakorn T, Luthfiyyah A, Ploysri K (2014) Comparison of the Composition and Antioxidant Capacities of Green Teas Produced From the Assam and the Chinese Varieties Cultivated in Thailand. J Microbiol Biotechnol food Sci 3:364–370

Thielemans K, De Bondt Y, Comer L, et al (2023) Decreasing the Crystallinity and Degree of Polymerization of Cellulose Increases Its Susceptibility to Enzymatic Hydrolysis and Fermentation by Colon Microbiota. Foods 12:1100. https://doi.org/10.3390/foods12051100

Thorat MN, Dastager SG (2018) High yield production of cellulose by a: Komagataeibacter rhaeticus PG2 strain isolated from pomegranate as a new host. RSC Adv 8:29797–29805. https://doi.org/10.1039/c8ra05295f

Trevino-Garza MZ, Guerrero-Medina AS, González-Sánchez RA, et al (2020) Production of Microbial Cellulose Films from Green Tea (Camellia Sinensis) Kombucha with Various Carbon Sources. MDPI Coat 10:1–14. https://doi.org/doi:10.3390/coatings10111132

Treviño-Garza MZ, Guerrero-Medina AS, González-Sánchez RA, et al (2020) Production of microbial cellulose films from green tea (Camellia sinensis) kombucha with various carbon sources. Coatings 10:1–14. https://doi.org/10.3390/coatings10111132

Tsouko E, Kourmentza C, Ladakis D, et al (2015) Bacterial cellulose production from industrial waste and by-product streams. Int J Mol Sci 16:14832–14849.

https://doi.org/10.3390/ijms160714832

Tureck BC, Hackbarth HG, Neves EZ, et al (2021) Obtaining and characterization of bacterial cellulose synthesized by Komagataeibacter hansenii from alternative sources of nitrogen and carbon. Rev Mater 26:. https://doi.org/10.1590/S1517-707620210004.1392

U˘gurel C, Ö˘güt H (2024) Optimization of Bacterial Cellulose Production by Komagataeibacter rhaeticus K23. fibers 12:1–16. https://doi.org/https://doi.org/10.3390/fib12030029

Ul-Islam M, Khan T, Park JK (2012) Water holding and release properties of bacterial cellulose obtained by in situ and ex situ modification. Carbohydr Polym 88:596–603. https://doi.org/10.1016/j.carbpol.2012.01.006

Ullah MW, Manan S, Kiprono S, Islam MU (2019) Synthesis , Structure , and Properties of Bacterial Cellulose. In: Huang J, Dufresne A, Lin N (eds) Nanocellulose: From Fundamentals to AdvancedMaterials, first. Wiley-VCHVerlag GmbH& Co. KGaA, pp 81–114

Vasconcellos VM, Farinas CS (2018) The effect of the drying process on the properties of bacterial cellulose films from gluconacetobacter hansenii. Chem Eng Trans 64:145–150. https://doi.org/10.3303/CET1864025

Villarreal-Soto SA, Beaufort S, Bouajila J, et al (2018) Understanding Kombucha Tea Fermentation: A Review. J Food Sci 83:580–588. https://doi.org/10.1111/1750-3841.14068

Vohra B, Fazry S, Sairi F, Othman BA (2019) Effects of medium variation and fermentation time towards the pH level and ethanol content of Kombucha. In: AIP Conference Proceedings

Volova TG, Prudnikova S V., Kiselev EG, et al (2022) Bacterial Cellulose (BC) and BC Composites: Production and Properties. Nanomaterials 12:. https://doi.org/10.3390/nano12020192

Waghmare PR, Patil SM, Jadhav SL, et al (2018) Utilization of agricultural waste

biomass by cellulolytic isolate Enterobacter sp. SUK-Bio. Agric Nat Resour 52:399–406. https://doi.org/10.1016/j.anres.2018.10.019

Wang B, Rutherfurd-Markwick K, Naren N, et al (2023a) Microbiological and Physico-Chemical Characteristics of Black Tea Kombucha Fermented with a New Zealand Starter Culture. Foods 12:. https://doi.org/10.3390/foods12122314

Wang B, Rutherfurd-Markwick K, Zhang XX, Mutukumira AN (2022a) Kombucha: Production and Microbiological Research †. Foods 11:1–18. https://doi.org/10.3390/foods11213456

Wang C, Han J, Pu Y, Wang X (2022b) Tea (Camellia sinensis): A Review of Nutritional Composition, Potential Applications, and Omics Research. Appl Sci 12:1–20. https://doi.org/10.3390/app12125874

Wang G, Liu J, Liu X, et al (2023b) Oxidation-resistant vitamin C/MXene foam via surface hydrogen bonding for stable electromagnetic interference shielding in air ambient. Appl Surf Sci 610:155396. https://doi.org/10.1016/j.apsusc.2022.155396

Wang J, Tavakoli J, Tang Y (2019) Bacterial cellulose production , properties and applications with di ff erent culture methods – A review. Carbohydr Polym 219:63–76. https://doi.org/10.1016/j.carbpol.2019.05.008

Wang SS, Han YH, Chen JL, et al (2018) Insights into bacterial cellulose biosynthesis from different carbon sources and the associated biochemical transformation pathways in Komagataeibacter sp. W1. Polymers (Basel) 10:. https://doi.org/10.3390/polym10090963

Wang T, Wang J, Han D, et al (2024) Elucidating the adsorption mechanisms of yeast extract on trimethylamine and dimethylamine based on multi-spectroscopic techniques and molecular docking. J Mol Liq 405:125087. https://doi.org/10.1016/j.molliq.2024.125087

Wang W, Khabazian S, Roig-Sanchez S, et al (2021) Carbons derived from alcohol-treated bacterial cellulose with optimal porosity for Li–O2 batteries. Renew Energy 177:209–215. https://doi.org/10.1016/j.renene.2021.05.059

Wang YY, Zhao XQ, Li DM, et al (2023c) Review on the strategies for enhancing mechanical properties of bacterial cellulose. J Mater Sci 58:15265–15293. https://doi.org/10.1007/s10853-023-08803-x

Wen W, Hu M, Gao Y, et al (2024) Effect of Soy Protein Products on Growth and Metabolism of Bacillus subtilis, Streptococcus lactis, and Streptomyces clavuligerus. Foods 13:. https://doi.org/10.3390/foods13101525

Wu JM, Liu RH (2013) Cost-effective production of bacterial cellulose in static cultures using distillery wastewater. J Biosci Bioeng 115:284–290. https://doi.org/10.1016/j.jbiosc.2012.09.014

Wu LM, Tong DS, Zhao LZ, et al (2014) Fourier transform infrared spectroscopy analysis for hydrothermal transformation of microcrystalline cellulose on montmorillonite. Appl Clay Sci 95:74–82. https://doi.org/10.1016/j.clay.2014.03.014

Yamano H, Miyagawa K (1997) Buffer Capacity Curves of Green Tea Extracts Using a Personal Computer with Numerically Treated Online Software. Food Sci Technol Int Tokyo 3:69–73. https://doi.org/10.3136/fsti9596t9798.3.69

Yanti NA, Ahmad SW, Muhiddin NH (2018) Evaluation of inoculum size and fermentation period for bacterial cellulose production from sago liquid waste. J Phys Conf Ser 1116:. https://doi.org/10.1088/1742-6596/1116/5/052076

Yao H, Dai Q, You Z (2015) Fourier Transform Infrared Spectroscopy characterization of aging-related properties of original and nano-modified asphalt binders. Constr Build Mater 101:1078–1087. https://doi.org/10.1016/j.conbuildmat.2015.10.085

Yilmaz M, Goksungur Y (2024) Optimization of Bacterial Cellulose Production from Waste Figs by Komagataeibacter xylinus. Fibers 12:1–18. https://doi.org/10.3390/fib12030029

Zeng M, Laromaine A, Roig A (2014) Bacterial cellulose films: influence of bacterial strain and drying route on film properties. Cellulose 21:4455–4469. https://doi.org/10.1007/s10570-014-0408-y

Zeng X, Liu J, Chen J, et al (2011) Screening of the common culture conditions affecting crystallinity of bacterial cellulose. J Ind Microbiol Biotechnol 38:1993–1999. https://doi.org/10.1007/s10295-011-0989-5

Zhang H, Chen C, Yang J, et al (2022) Effect of Culture Conditions on Cellulose Production by a Komagataeibacter xylinus Strain. Macromol Biosci 22:. https://doi.org/10.1002/mabi.202100476

Zhang K, Huang J, Wang D, et al (2024) Covalent polyphenols-proteins interactions in food processing: formation mechanisms, quantification methods, bioactive effects, and applications. Front Nutr 11:1–15. https://doi.org/10.3389/fnut.2024.1371401

Zhao ZJ, Sui YC, Wu HW, et al (2018) Flavour chemical dynamics during fermentation of kombucha tea. Emirates J Food Agric 30:732–741. https://doi.org/10.9755/ejfa.2018.v30.i9.1794

Zheng D, Zhang Y, Guo Y, Yue J (2019) Isolation and characterization of nanocellulose with a novel shape from walnut (Juglans Regia L.) shell agricultural waste. Polymers (Basel) 11:. https://doi.org/10.3390/polym11071130

Zheng G, Su H, Cheng Y (2023) Role of Carbon Dioxide, Ammonia, and Organic Acids in Buffering Atmospheric Acidity: The Distinct Contribution in Clouds and Aerosols. Environ Sci Technol 57:12571–12582. https://doi.org/10.1021/acs.est.2c09851

Zubaidah E, Ifadah RA, Afgani CA (2019) Changes in chemichal characteristics of kombucha from various cultivars of snake fruit during fermentation. IOP Conf Ser Earth Environ Sci 230:. https://doi.org/10.1088/1755-1315/230/1/012098

Zywicka A, Peitler D, Rakoczy R, et al (2015) The Effect of Different Agitation Modes on Bacterial Cellulose Synthesis. Acta Sci Pol Zootech 14:137–150

CHAPTER 4

OPTIMIZATION OF BACTERIAL CELLULOSE PRODUCTION FROM THAI RED TEA KOMBUCHA USING CENTRAL COMPOSITE DESIGN IN RESPONSE SURFACE METHODOLOGY

4.1 Abstract

This study optimized bacterial cellulose (BC) production from Thai red tea kombucha using response surface methodology (RSM) with a central composite design (CCD), based on previous data. Thirty-four runs evaluated the effects of sucrose–glucose ratio, tea concentration, and ethanol concentration on BC wet yield, dry yield, and water-holding capacity (WHC), with emphasis on wet yield. Despite some limitations, the model showed acceptable predictive accuracy. During optimization, the software generated 53 formulations, from which three—RTC-V1 (recommended), RTC-V46 (highest predicted yield), and RTC-V53 (lowest predicted yield)—were selected for validation. Observed yields and WHC values closely matched predictions, confirming model reliability. RTC-V1 (7.97% (w/v) sucrose, 2.03% (w/v) glucose, 1.41% (w/v) tea, 1.56% (v/v) ethanol) achieved a wet BC yield of 621.71 ± 24.06 g/L, a 238% increase over the RTC-SGlu formulation. The optimized BC was characterized by SEM, FTIR, XRD, TGA, and nanoindentation, confirming a uniform nanofiber network, cellulose I structure with high crystallinity (83.23–85.97%), thermal stability, and strong mechanical properties. These findings support the effectiveness of CCD-based RSM for scalable, high-quality BC production.

Keywords: Bacterial cellulose optimization, Thai red tea kombucha, Composite central design (CCD), Fermentation process, BC production.

4.2 Introduction

Bacterial cellulose (BC) is a microbial exopolysaccharide produced predominantly by *Komagataeibacter* sp. Compared to plant-derived cellulose, BC is free from lignin and hemicellulose and possesses superior characteristics, including high purity, crystallinity, tensile strength, water-holding capacity (WHC), and biocompatibility. These properties make BC a promising material in various sectors, such as food, biomedical, and packaging industries (Azeredo et al. 2019b; Barja 2021b; Bizeau and Mertz 2021; Padmanabhan et al. 2023).

Among sustainable production methods, kombucha fermentation has attracted growing interest for BC production. Kombucha, a fermented tea beverage, is produced by a SCOBY in a sugar-enriched tea medium. During fermentation, the microbial community metabolizes the carbon source and forms a cellulose pellicle on the surface of the liquid. This process presents a natural, cost-effective, and scalable approach to BC production, utilizing readily available substrates such as tea and sugar (Cavicchia and de Almeida 2022; Ramírez Tapias et al. 2022; Charoenrak et al. 2023).

BC production during fermentation is influenced by several factors, including the type and concentration of tea, the ratio of carbon sources (glucose and sucrose), ethanol supplementation, and fermentation parameters such as time, pH, and temperature. Glucose serves as the primary carbon source for BC biosynthesis, whereas sucrose must first be hydrolyzed, potentially affecting the fermentation rate. Tea provides essential nutrients—including nitrogen, polyphenols, and micronutrients—that support microbial growth and activity. Low concentrations of ethanol have been shown to enhance BC yield, though higher levels may have inhibitory effects (Kazemi et al. 2015; Molina-Ramírez et al. 2018b; Fei et al. 2023).

To maximize BC productivity and reduce production costs, statistical optimization approaches like Response Surface Methodology (RSM) have been widely employed. RSM is an effective tool to evaluate the effects and interactions of multiple variables on a given response. Specifically, Central Composite Design (CCD) within the

RSM framework offers an efficient experimental layout for identifying optimal conditions with a reduced number of runs. For example, the Box-Behnken design has been used to optimize temperature, pH, and agitation speed, resulting in a threefold increase in BC yield (Pandey et al. 2024). Likewise, Plackett–Burman and RSM were used to optimize BC production by *K. rhaeticus* N1 MW32270, increasing the yield from 4.3 g/L to 9.2 g/L (Mohammad et al. 2021). In another study, CCD was applied using low-cost nutrient sources like molasses, ethanol, corn steep liquor (CSL), and ammonium sulfate, leading to a 6.3-fold increase in productivity compared to the standard Hestrin–Schramm (HS) medium (Rodrigues et al. 2019). Optimization of the growth medium for *A. senegalensis* MA1 using CCD-RSM increased BC production up to 20 times relative to unoptimized HS medium (Aswini et al. 2020). These findings highlight the effectiveness of RSM in elucidating complex parameter interactions and improving BC production outcomes.

Despite the promising use of alternative substrates for BC production, limited studies have explored Thai red tea kombucha as a fermentation medium. Thai red tea is commercially popular and contains both natural polyphenols and artificial colorants such as FD&C Yellow No. 6 (INS 110), which may influence microbial growth and cellulose biosynthesis. Furthermore, flavored teas used in this context may introduce additional bioactive compounds or fermentation modulators.

This study aims to optimize BC production from Thai red tea kombucha through CCD-RSM. The key variables examined include tea concentration, sucrose-to-glucose ratio, and ethanol content. Based on previous work, the fermentation was conducted at a tea concentration of 2%, ethanol 1%, and a carbon source mixture totaling 10% under static conditions for 15 days at pH ~5.20. The objectives are to (i) maximize wet and dry BC yield and WHC, (ii) verify the fit between predicted and actual results, and (iii) characterize the optimized BC using SEM, FTIR, XRD, TGA, and nanoindentation to assess its structural, thermal, and mechanical properties. These

findings aim to support the development of a cost-effective, reproducible, and industrially scalable BC production method for functional and packaging applications.

4.3 Materials and Methods

The materials and equipment used in this stage include commercial kombucha starter (SCOBY) bought from Neo Cold Brew Shop (online market, Thailand), sucrose, Thai red tea-vanilla flavor (*ChaTraMue* brand), sucrose, glucose, ethanol, sodium hydroxide (NaOH), Hydrochloric acid (HCl), Reverse osmosis (RO) water, Deionized (DI) water, cheese cloth, coffee filter, glass jar, funnel, autoclave, laminar air flow, laboratory glassware, analytical balance, incubator, pH-meter (Oakton, pH 700), refractometer, oven dryer (XUE058, FRANCE ETUVES), FT-IR (Bruker VERTEX 70), XRD (Bruker D8 Advance), SEM (FESEM) (Zeiss, AURIGA, Germany), HPLC (Hitachi Chromaster), and, nano-indenter (NanoTest Vantage system, Micro Materials Limited in Wrexham, UK).

4.3.1 Experimental Design Using CCD of RSM

The optimization of BC (BC) production was carried out using Response Surface Methodology (RSM) with a Central Composite Design (CCD), developed using Design-Expert 11 software. The selection of independent variables and their ranges was based on findings from previous experiments (**Chapter 3**). The optimization aimed to maximize BC yield (g/L, wet and dry basis) and water holding capacity (WHC).

Three independent variables were selected: Thai red tea concentration (1–3%, with 2% as the center point), ethanol concentration (0–2%, with 1% as the center point), and the ratio of sucrose to glucose as the carbon source, with a fixed total sugar concentration of 10%. The goal was to determine the optimal sucrose-to-glucose ratio within this fixed concentration. These ranges were chosen based on previous results showing that a 1:1 ratio (5% sucrose + 5% glucose) yielded favorable outcomes.

The cultivation conditions were kept constant throughout the optimization: unadjusted initial pH (~5.20), static fermentation, room temperature, and a 15-day fermentation time. Although a 14-day fermentation had previously been found optimal, a 15-day duration was used in this study to maintain consistency with earlier experimental protocols and to allow slight flexibility in timing without affecting BC quality. The variables and their levels used in the experimental design are summarized in **Table 4.1**, and the full design matrix generated by the software is presented in **Table 4.2.**

The following is further information on the optimization methods:

Study Type : Response Surface
Subtype : Randomized
Design Type : Central Composite
Runs : 34
Design Model : Quadratic
Blocks : No Blocks

Table 4.1 The factors used in the design of experiment for BC production from RTC kombucha fermentation and its value

F	Name	Units	Type	Min.	Max.	CL	CH	Mean	SD
A	[Sucrose]	%	Numeric	0.00	10.00	-1 ↔ 2.03	+1 ↔ 7.97	5.00	2.70
B	[Tea]	%	Numeric	1.00	3.00	-1 ↔ 1.41	+1 ↔ 2.59	2.00	0.54
C	[Ethanol]	%	Numeric	0.00	2.00	-1 ↔ 0.41	+1 ↔ 1.59	1.00	0.54

F = Factors, Min. = Minimum, Max. = Maximum, Cl = Coded Low, CH = Coded high, SD = Standard Deviation.

Table 4.2 Design of experiment for the optimization of BC production from RTC kombucha fermentation

		Factors			Responses		
Std	Run	[Sucrose]*	[Tea]	[Ethanol]	Wet yield	Dry yield	WHC
		%	%	%	g/L	g/L	g/g
2	1	2.0270	1.4054	0.4054			
17	2	0	2	1			
11	3	7.9730	1.4054	1.5946			
13	4	2.0270	2.5946	1.5946			
32	5	5	2	1			
1	6	2.0270	1.4054	0.4054			
34	7	5	2	1			
21	8	5	1	1			
20	9	10	2	1			
16	10	7.9730	2.5946	1.5946			
22	11	5	1	1			
27	12	5	2	2			
7	13	7.9730	2.5946	0.4054			
24	14	5	3	1			
30	15	5	2	1			
12	16	7.9730	1.4054	1.5946			
3	17	7.9730	1.4054	0.4054			
29	18	5	2	1			
25	19	5	2	0			
26	20	5	2	0			
8	21	7.9730	2.5946	0.4054			
23	22	5	3	1			
15	23	7.9730	2.5946	1.5946			

Table 4.2 Design of experiment for the optimization of BC production (Continued)

Std	Run	Factors			Responses		
		[Sucrose]*	[Tea]	[Ethanol]	Wet yield	Dry yield	WHC
		%	%	%	g/L	g/L	g/g
28	24	5	2	2			
19	25	10	2	1			
9	26	2.0270	1.4054	1.5946			
18	27	0	2	1			
6	28	2.0270	2.5946	0.4054			
10	29	2.0270	1.4054	1.5946			
33	30	5	2	1			
31	31	5	2	1			
14	32	2.0270	2.5946	1.5946			
4	33	7.9730	1.4054	0.4054			
5	34	2.0270	2.5946	0.4054			

*) *Total carbon source is 10%, the glucose was added until total carbon source is 10%. Std (standard order)*

4.3.2 Laboratory Experimentation

For each experimental run, Thai red tea kombucha fermentation was prepared according to the designed formula. The fermentation process was conducted under controlled conditions, and the BC produced was harvested after a predetermined incubation period. The harvested BC samples were washed, purified, and analyzed for wet yield (g), dry yield (g), and water holding capacity (WHC, g water/g cellulose).

1) Regeneration of Kombucha Starter

A 480-ml jar was filled with 40g of sucrose and RTC tea extract, prepared by brewing 4g of tea with 360 ml of hot water (T = ±90°C). The tea was filtered using coffee filter paper, placed in a jar filled with sucrose, stirred, and sterilized

by autoclaving (P=1.2 psi, T = 121oC, t = 20 minutes). The mixture was then cooled to near room temperature (30–35°C), inoculated with 40 ml of the previous starter, and fermented for 14 days.

2) Preparation of Medium and Fermentation

A total of 34 jars were prepared, each containing 10 g of a sucrose and glucose mixture, as specified in **Table 4.2**. To each jar, 90 ml of Thai red tea extract was added according to the treatments outlined in **Table 4.2**, and the mixture was stirred until the sugar completely dissolved. The tea extract was prepared by brewing the specified amount of tea in hot water at approximately 90 °C for about 15 minutes, followed by filtration using coffee filter papers. The jars were covered with two layers of cheesecloth and sterilized in an autoclave at 1.2 psi and 121 °C for 20 minutes. After sterilization, the mixture was allowed to cool to 30–35 °C. Once cooled, the appropriate amount of ethanol was added (as shown in **Table 4.2**), and each jar was inoculated with 10 ml of the culture starter. The mixtures were thoroughly mixed and allowed to ferment for 15 days at a temperature of 30 °C under static cultivation conditions.

3) Harvesting and Purification of BC

After around 15 days of fermentation, the BC was separated by lifting it using tweezers and drained for about 10 minutes. The BC was then weighed to determine the wet gross weight, heated in boiling water (± 90–95°C) for about 30 minutes, and drained for about 10 minutes. The BC was then heated at ± 90°C in the alkaline solution (NaOH, 2%) for 120 minutes, drained, rinsed with RO water until the pH was neutral, and washed with DI water (Yanti et al. 2018; Aswini et al. 2020). After that, the BC was then drained for about 10 minutes and weighed to determine the net wet weight. Further, for making the dry samples, the BC sample was then dried using an oven at a temperature of 40°C until it reached a constant weight (Aswini et al. 2020).

4.3.3 Data Analysis and Model Fitting

The response data (wet yield, dry yield, and WHC) were input into the software. Statistical models were developed for each response variable, and their adequacy was evaluated using analysis of variance (ANOVA). Response surfaces and contour plots were generated to visualize the effect of factors and their interactions on BC production.

4.3.4 Optimization and Solution Validation

The optimization module of the software was used to determine the best formula solution for maximizing the desired responses. The predicted optimal conditions were validated by conducting laboratory experiments using the solution formula. The experimental data were compared with the predicted values to validate the optimization model.

4.3.5 Bacterial cellulose characterization

The BC produced using the optimized formula was characterized to confirm its quality and properties. The characterization included yield and WHC, as well as analyses using scanning electron microscopy (SEM), Fourier-transform infrared spectroscopy (FTIR), X-ray diffraction (XRD), thermogravimetric analysis (TGA), and nano-indentation. The detailed methods and procedures for these analyses, including statistical analysis, have been described in Chapter 3 of this thesis.

4.3.6 Statistical Analysis

Analysis of variance was carried out using Ms. Excel software. The differences between the mean values were analyzed using least significant difference (LSD) test and the significance level was set at $P < 0.05$.

4.4 Results and Discussion

4.4.1 Data Analysis of Experimental Design

A total of 34 experimental runs were generated using a CCD as part of the RSM approach. Following a 15-day fermentation, BC samples were purified, and

their wet yield, dry yield, and WHC were determined. The resulting response data were entered into the software for model development and statistical analysis. A summary of the experimental results is presented in **Table 4.3.**

In this study, three response variables—wet yield, dry yield, and WHC—were selected to provide a comprehensive assessment of both BC productivity and quality. Wet yield was considered the primary response, as it represents the total amount of BC produced under each fermentation condition and is directly relevant for industrial and process-scale evaluations. Dry yield and WHC were included as secondary responses to offer additional insight into the structural and functional characteristics of the produced BC. Dry yield reflects the actual amount of cellulose synthesized, independent of water content, and is critical for evaluating true BC productivity. WHC, on the other hand, indicates the material's capacity to retain water, an important functional property for applications in food, cosmetics, biomedical materials, and other moisture-sensitive products. The combination of these three responses allows for a more holistic evaluation of the process, enabling the identification of optimal conditions that not only maximize yield but also ensure desirable material properties suitable for practical applications.

Table 4.3 The data of wet yield, dry yield, and WHC from the laboratory experiment

		Factors			Responses		
STD	Run	Sucrose* (%)	Tea (%)	Ethanol (%)	Wet Yield (g/L)	Dry Yield (g/L)	WHC (g/g)
2	1	2.0270	1.4054	0.4054	512.36	3.54	143.65
17	2	0	2	1	466.90	3.78	122.42
11	3	7.9730	1.4054	1.5946	632.24	5.54	113.18
13	4	2.0270	2.5946	1.5946	550.64	4.77	114.41
32	5	5	2	1	570.60	4.32	131.08
1	6	2.0270	1.4054	0.4054	500.34	3.68	135.15

Table 4.3 The data of wet yield, dry yield, and water holding capacity from the laboratory experiment (Continued)

STD	Run	Factors			Responses		
		Sucrose* (%)	Tea (%)	Ethanol (%)	Wet Yield (g/L)	Dry Yield (g/L)	WHC (g/g)
34	7	5	2	1	597.70	4.63	128.06
21	8	5	1	1	619.05	4.58	134.05
20	9	10	2	1	350.63	3.33	104.29
16	10	7.9730	2.5946	1.5946	594.61	5.37	109.79
22	11	5	1	1	636.29	4.75	133.04
27	12	5	2	2	675.54	5.52	121.45
7	13	7.9730	2.5946	0.4054	612.56	5.94	102.07
24	14	5	3	1	552.14	4.51	121.45
30	15	5	2	1	589.35	4.67	125.17
12	16	7.9730	1.4054	1.5946	679.74	5.87	114.84
3	17	7.9730	1.4054	0.4054	667.51	3.54	143.65
29	18	5	2	1	586.55	4.61	126.23
25	19	5	2	0	372.12	3.38	109.03
26	20	5	2	0	417.43	4.43	93.25
8	21	7.9730	2.5946	0.4054	576.29	5.72	99.84
23	22	5	3	1	529.82	4.36	120.46
15	23	7.9730	2.5946	1.5946	561.57	5.32	104.62
28	24	5	2	2	627.10	5.75	107.99
19	25	10	2	1	426.18	3.74	112.92
9	26	2.0270	1.4054	1.5946	609.09	5.22	115.66
18	27	0	2	1	476.86	3.69	128.23
6	28	2.0270	2.5946	0.4054	551.06	3.94	138.83
10	29	2.0270	1.4054	1.5946	588.62	5.23	111.46

Table 4.3 The data of wet yield, dry yield, and water holding capacity from the laboratory experiment (Continued)

STD	Run	Factors			Responses		
		Sucrose* (%)	Tea (%)	Ethanol (%)	Wet Yield (g/L)	Dry Yield (g/L)	WHC (g/g)
33	30	5	2	1	642.82	5.03	126.85
31	31	5	2	1	561.20	4.36	127.69
14	32	2.0270	2.5946	1.5946	587.45	4.84	120.30
4	33	7.9730	1.4054	0.4054	668.37	4.92	134.82
5	34	2.0270	2.5946	0.4054	478.60	3.70	128.53

** Glucose was added to the sucrose until total weight of carbon source is 10%*

In this study, predicted values are not presented in the initial results table to maintain clarity and emphasize the actual experimental data used for model development. Predicted values are instead reported during the model validation stage, where they are compared with experimental results to assess the accuracy and reliability of the optimized conditions.

After inputting and analyzing the data, the software generated a summary of the response data, which is presented in **Table 4.4.**

Table 4.4 Summary of data analysis from the laboratory experiment

Res.	Obs.	Analysis	Min.	Max.	Mean	Sd	Ratio	Trans	Model
Wet yield (g/L)	34	Polynomial	350.63	679.74	560.86	84.33	1.94	None	Quadratic
Dry yield (g/L)	34	Polynomial	3.33	5.943	4.64	0.754	1.78	None	Quadratic
WHC (g/g)	34	Polynomial	93.25	143.65	120.64	12.56	1.54	None	Quadratic

Res. = Response, Obs. (Observation), Min. (Minimum), Max. (maximum), Sd (Standard deviation), Trans. (transformation), unit of WHC g/g (g water/g cellulose).

Table 4.4 provides detailed information about the response values, including minimum, maximum, mean, standard deviation (SD), transformation (Trans), ratio, and model. The wet yield from the experiments ranged from 350.63 g/L to 679.74 g/L, with a mean of 560.86 g/L and a SD of 84.33. The dry yield varied between 3.33 g/L and 5.943 g/L, with a mean of 4.64 g/L and a standard deviation of 0.754. The ratio of wet yield to dry yield was 1.94, reflecting the water content in the BC, which is critical for assessing its water retention capabilities. For WHC, the values ranged from 93.25 g/g to 143.65 g/g, with a mean of 120.64 g/g and a standard deviation of 12.56. The ratio for WHC was 1.54. The models developed in this study were quadratic polynomial models for all responses, as indicated in the table.

The 'Transform column in **Table 4.4** indicates whether a data transformation was applied during the analysis. For all responses (wet yield, dry yield, and WHC), the entry 'None' signifies that no transformations were needed. This suggests that the raw data met the assumptions required for statistical analysis and model development without the need for adjustments such as logarithmic or square root transformations. The quadratic polynomial models developed in this study establish a mathematical relationship between the independent variables and the responses, providing insights into how variations in the medium composition influence BC production. These models were found to be statistically significant and were validated through ANOVA.

4.4.2 Response Surface Analysis

The next phase of this study involved analyzing the data based on response parameters obtained from laboratory experiments. A software program was used to generate a comprehensive data analysis report, including transformations, fit summaries, model evaluations, ANOVA diagnostics, and graphical representations of the model.

1) Wet Yield Analysis

The Fit Summary for the quadratic model in the wet yield response demonstrates its suitability for predicting outcomes (**Table 4.5**). The model was chosen based on prior research suggesting a nonlinear relationship between the variables, where effects may change direction at a certain point, such as reaching an optimal threshold before decreasing. The model explains 54.76% of the variance (R^2), with an adjusted R^2 of 37.79%, indicating a moderate fit after accounting for the number of predictors. However, the predicted R^2 of 4.17% suggests that the model may not generalize well to new, unseen data, indicating potential overfitting. Additionally, the lack of fit value of < 0.0001 suggests that the model does not perfectly capture the underlying data patterns, with residuals significantly deviating from the observed values. This indicates that the quadratic model might not fully account for all the variability in the data. Despite these challenges, the quadratic model remains relevant due to its alignment with theoretical expectations of nonlinear effects and the possibility of an optimal threshold. The relatively low R^2, adjusted R^2, and predicted R^2 values are common in RSM studies involving biological systems like fermentation, where inherent variability and unmeasured factors contribute to response fluctuations.

The ANOVA results (**Table 4.6**) show that the overall model is significant for wet yield analysis (F-value = 3.23, p-value = 0.0105), meaning it explains a meaningful amount of variation in the response. Ethanol (C) has a significant effect on the response (p-value = 0.0042), while sucrose (A) and tea (B) do not (p-values of 0.3463 and 0.0793, respectively). The interactions between the factors and the quadratic effects of tea and ethanol are not significant. However, the quadratic effect of sucrose (A^2) is significant (p-value = 0.0092), suggesting a nonlinear relationship. The lack of fit is significant (F-value = 22.27, p-value < 0.0001), meaning the model does not fully capture the data, and there are differences between observed and predicted values. The addition information from the program is about the adequate precision (Adeq Precision). The adequate precision value of 5.9319 indicates the model has an

adequate signal for making predictions, although it may need refinement to better fit the data.

Table 4.5 The resume of fit summary report of wet yield analysis

Source	Sequential p-value	Lack of Fit p-value	R^2	Adjusted R^2	Predicted R^2	
Linear	0.0226	< 0.0001	0.2694	0.1963	0.035	
2FI	0.5614	< 0.0001	0.322	0.1713	-0.0307	
Quadratic	0.0194	< 0.0001	0.5476	0.378	0.0417	**Suggested**
Cubic	0.0071	< 0.0001	0.7689	0.6188	0.2399	**Aliased**

Table 4.6 ANOVA for Quadratic Model of wet yield analysis

Source	Sum of Squares	df	Mean Square	F-value	p-value	
Model	1.285E+05	9	14281.44	3.23	0.0105	significant
A-[Sucrose]	4082.45	1	4082.45	0.9228	0.3463	
B-[Tea]	14859.54	1	14859.54	3.36	0.0793	
C-[Ethanol]	44281.66	1	44281.66	10.01	0.0042	
AB	4230.79	1	4230.79	0.9563	0.3379	
AC	7656.69	1	7656.69	1.73	0.2007	
BC	455.33	1	455.33	0.1029	0.7511	
A^2	35524.13	1	35524.13	8.03	0.0092	
B^2	4951.52	1	4951.52	1.12	0.3006	
C^2	1056.54	1	1056.54	0.2388	0.6295	
Residual	1.062E+05	24	4423.97			
Lack of Fit	90701.46	5	18140.29	22.27	< 0.0001	significant
Pure Error	15473.81	19	814.41			
Cor Total	2.347E+05	33				

To predict the wet yield, the program generated a table displaying the final actual equation, which is presented as the Equation **(Eq.4.1)**. In this equation, S represents sucrose, T represents tea, and E represents ethanol. It is important to note that glucose must be added to ensure the total carbon source combination reaches 10% (w/v) of the total formulation. The effects of the interactions among sucrose, tea, and ethanol on the wet yield are illustrated in **Figure 4.1**, highlighting the influence of nutritional and additive compositions on the results of the wet yield.

$$Wet\ yield = 428.512 + 79.792[S] - 145.806[T] + 198.491[E] - 9.199[S][T] - 12.375[S][E] - 15.087[T][E] - 4.491[S]^2 + 41.915[T]^2 - 19.362[E]^2 \quad \textbf{(Eq. 4.1)}$$

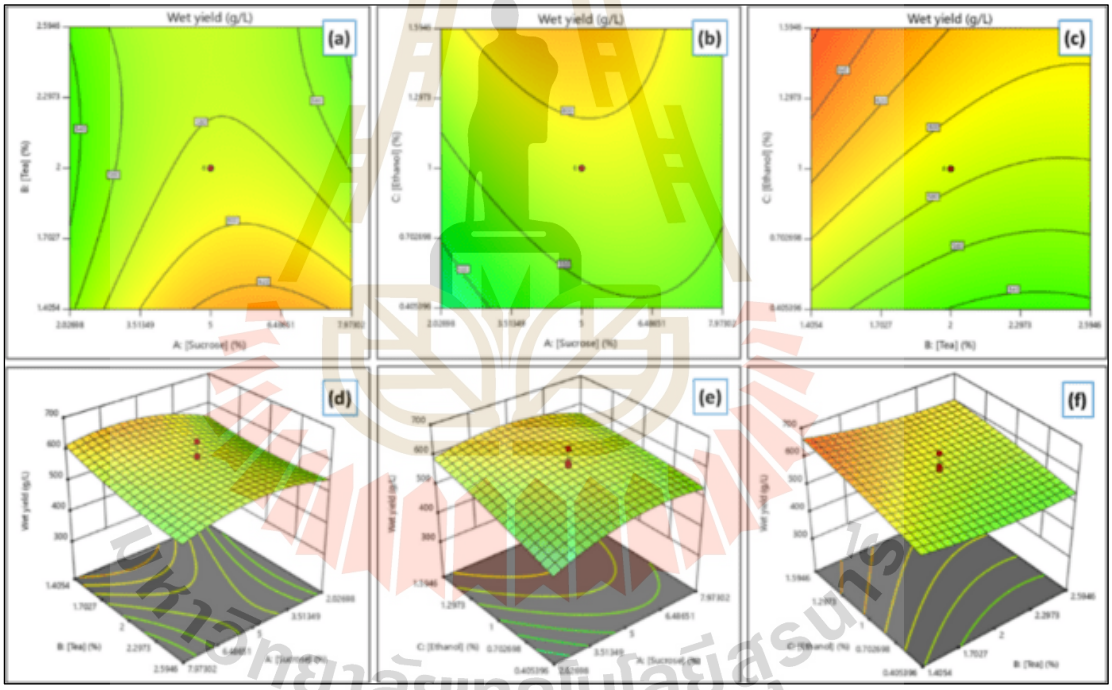

Figure 4.1 Graph model of the effect of formula composition interaction to the wet yield of BC.

The figure illustrates that the wet yield of BC increased due to specific interactions between the variables. An interaction between sucrose and tea concentrations showed an increase in BC yield, reaching its peak at a sucrose concentration of approximately 6.49% and a tea concentration of 1.41%. However, at

higher sucrose concentrations, around 7.97%, the yield began to decline (**Figure 4.1(a) and 4.1(d)**). Similarly, the interaction between sucrose and ethanol concentrations (**Figure 4.1(b) and 4.1(e)**) resulted in the highest BC productivity at a sucrose concentration of approximately 5% and an ethanol concentration of 1.59%. Additionally, the interaction between tea and ethanol concentrations (**Figure 4.1(c) and 4.1(f)**) contributed to an increase in BC yield, with the maximum productivity observed at a tea concentration of 1.41% and an ethanol concentration of 1.59%.

2) Dry Yield Analysis

The Fit Summary for the quadratic model in the dry yield response underscores its potential suitability for predicting outcomes (**Table 4.7**). This model was chosen based on evidence suggesting that the relationship between variables may be nonlinear, with effects reaching a maximum point before declining. The model explains 67.71% of the variance (R^2) and the adjusted R^2 of 55.61% indicates a moderate level of explanatory power after accounting for the number of predictors. The predicted R^2 of 0.3217 suggests the model has reasonable predictive ability for new data, though it may still have limitations in generalization. However, the significant lack of fit ($p < 0.0001$) indicates that the model does not fully capture the complexity of the data, as the residuals deviate considerably from the observed values. Despite these shortcomings, the quadratic model remains relevant, as it aligns with the theoretical expectations of nonlinear relationships and provides valuable insights into the interactions between variables affecting dry yield.

Table 4.7 The resume of fit summary report of dry yield analysis

Source	Sequential p-value	Lack of Fit p-value	R^2	Adjusted R^2	Predicted R^2	
Linear	0.0017	< 0.0001	0.3919	0.3311	0.1909	
2FI	0.0885	< 0.0001	0.5205	0.4139	0.2565	
Quadratic	0.0215	< 0.0001	0.6771	0.5561	0.3217	**Suggested**
Cubic	0.0166	< 0.0001	0.819	0.7013	0.4166	**Aliased**

The ANOVA results (**Table 4.8**) demonstrate that the overall quadratic model is significant for dry yield analysis, with an F-value of 5.59 and a p-value of 0.0003. This indicates that the model explains a substantial portion of the variation in the response. Among the individual factors, sucrose (A) and ethanol (C) significantly impact the dry yield, with p-values of 0.0068 and 0.0001, respectively. However, tea (B) does not have a significant effect, as indicated by its p-value of 0.9656. For interaction effects, none of the interactions between factors (AB, AC, BC) show a significant influence on dry yield, as their p-values exceed the 0.05 threshold. Additionally, the quadratic terms (A^2), (B^2), and (C^2) show varying levels of influence but do not meet the criteria for statistical significance, with p-values of 0.0578, 0.2974, and 0.0844, respectively.

Table 4.8 ANOVA for Quadratic Model of dry yield analysis

Source	Sum of Squares	df	Mean Square	F-value	p-value	
Model	12.69	9	1.41	5.59	0.0003	significant
A-[Sucrose]	2.21	1	2.21	8.78	0.0068	
B-[Tea]	0.0005	1	0.0005	0.0019	0.9656	
C-[Ethanol]	5.13	1	5.13	20.35	0.0001	
AB	0.1875	1	0.1875	0.7435	0.3971	
AC	1.22	1	1.22	4.82	0.0380	
BC	1.01	1	1.01	3.99	0.0572	
A^2	1.00	1	1.00	3.97	0.0578	
B^2	0.2860	1	0.2860	1.13	0.2974	
C^2	0.8175	1	0.8175	3.24	0.0844	
Residual	6.05	24	0.2522			
Lack of Fit	4.89	5	0.9782	16.01	< 0.0001	significant
Pure Error	1.16	19	0.0611			
Cor Total	18.74	33				

The lack of fit is significant, with an F-value of 16.01 and a p-value of less than 0.0001, suggesting that the model does not fully capture the complexity of the data. This indicates discrepancies between observed and predicted values, pointing to areas where the model could be refined for improved accuracy. Additionally, the model's adequate precision value of 8.6008 exceeds the recommended minimum threshold of 4.0, indicating that the model has a sufficient signal-to-noise ratio for making reliable predictions. While adequate precision suggests the model's predictions are reasonable, the significant lack of fit highlights the need for further refinement to better align the model with the observed data.

To estimate the dry yield, the program provided a table with the final actual equation, which is reformulated and shown as Equation 4.2 (**Eq. 4.2**). In this equation, S, T, and E represent sucrose, tea, and ethanol, respectively. Additionally, glucose must be incorporated to ensure the total carbon source combination equals 10% (w/v) of the overall formulation. **Figure 4.9** illustrates the impact of interactions between sucrose, tea, and ethanol on the dry yield, emphasizing the role of nutritional and additive compositions in influencing the results.

$$Dry\ yield = 2.975 + 0.368[S] - 0.864[T] + 1.850[E] + 0.061[S][T] - 0.156[S][E] - 0.709[T][E] - 0.024[S]^2 + 0.319[T]^2 + 0.539[E]^2$$

.....(**Eq. 4.2**)

The figure demonstrates that the dry yield of BC is influenced by interactions between the variables. The interaction between sucrose and tea concentrations led to an increase in BC dry yield, peaking at a sucrose concentration of approximately 7.97% and a tea concentration of about 2.59% (**Figure 4.2(a) and 4.2(d)**). The interaction between sucrose and ethanol concentrations resulted in the highest dry yield at a sucrose concentration of approximately 5.00% and an ethanol concentration of 1.59% (**Figure 4.2(b) and 4.2(e)**). Furthermore, the interaction between tea and ethanol concentrations contributed to an enhanced BC yield, with

maximum productivity observed at a tea concentration of 1.41% and an ethanol concentration of 1.59% (**Figure 4.2(c) and 4.2(f)**).

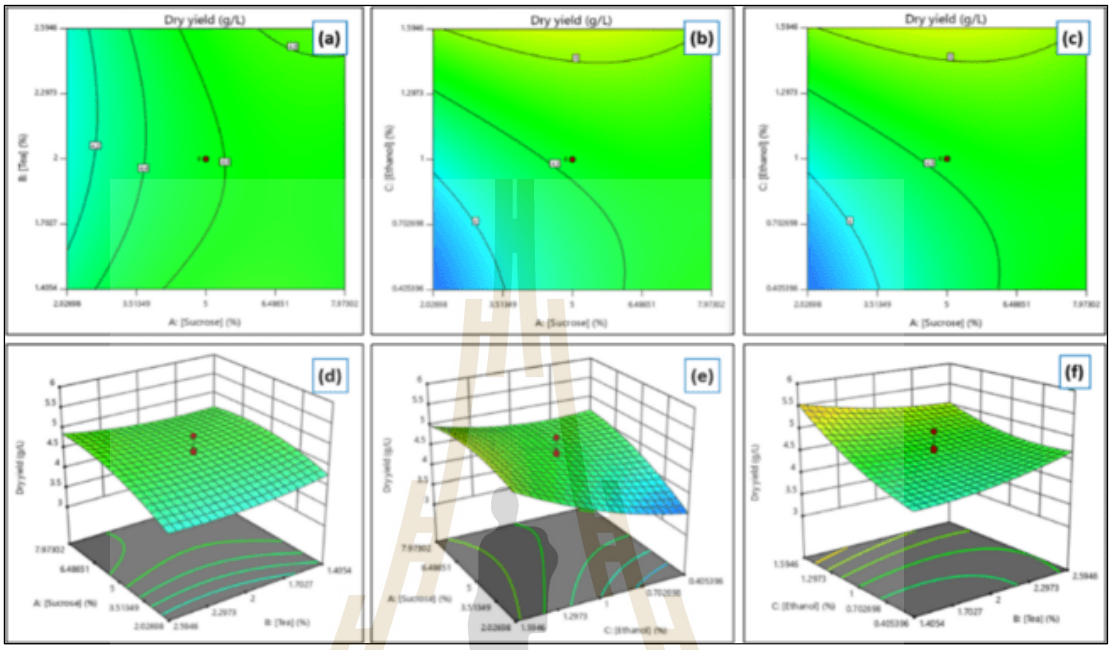

Figure 4.2 Graph model of the effect of formula composition interaction to the dry yield of BC.

3) Water Holding Capacity (WHC) Analysis

The Fit Summary for the quadratic model in the WHC response highlights its potential suitability for understanding the interactions among variables (**Table 4.9**). This model was selected as it aligns with theoretical expectations of nonlinear relationships, where effects may increase to a maximum point before declining. The model explains 70.4% of the variance (R^2), while the adjusted R^2 of 59.3% reflects a moderate explanatory power after accounting for the number of predictors. The predicted R^2 of 0.3665 suggests the model has reasonable predictive ability for new data, though its generalization may still be limited. However, the significant lack of fit ($p = 0.0001$) indicates that the model does not fully capture the complexity of the data, as residuals deviate substantially from observed values. Despite these limitations, the quadratic model provides valuable insights into the

nonlinear interactions influencing WHC and remains a relevant tool for exploring variable relationships.

Table 4.9 The resume of fit summary report of dry yield analysis

Source	Sequential p-value	Lack of Fit p-value	R^2	Adjusted R^2	Predicted R^2	
Linear	0.0101	< 0.0001	0.3102	0.2412	0.0921	
2FI	0.0328	< 0.0001	0.4983	0.3868	0.2421	
Quadratic	0.0048	0.0001	0.704	0.593	0.3665	Suggested
Cubic	0.0002	0.0655	0.8981	0.8318	0.6588	Aliased

The ANOVA results (**Table 4.10**) confirm that the quadratic model is significant for the analysis of WHC, with an F-value of 6.34 and a p-value of 0.0001. These results indicate that the model accounts for a substantial portion of the variability in WHC. Among the individual factors, sucrose (A) and tea (B) have significant effects on WHC, with p-values of 0.0021 and 0.0039, respectively. In contrast, ethanol (C) does not exhibit a statistically significant effect, as indicated by its p-value of 0.0907.

Significant interactions are also observed. The interaction between sucrose and tea (AB) is notable, with a p-value of 0.0155, as is the interaction between tea and ethanol, with a p-value of 0.0210. Additionally, the quadratic effect of ethanol (C^2) is significant, with a p-value of 0.0014, suggesting the presence of a nonlinear relationship between ethanol concentration and WHC. These findings underscore the importance of considering both individual factors and their interactions when evaluating WHC.

The lack of fit is significant (F-value = 9.45, p-value = 0.0001), indicating that the model does not fully capture the complexity of the data and that discrepancies exist between the observed and predicted values. However, the adequate precision value of 9.040 exceeds the recommended threshold of 4.0,

indicating that the model has a sufficient signal-to-noise ratio and is reliable for predictive purposes. While the significant lack of fit suggests room for improvement, the model's overall performance justifies its continued use. The model provides valuable insights into the factors influencing WHC and offers a reliable foundation for further refinement and optimization.

Table 4.10 ANOVA for Quadratic Model of WHC

Source	Sum of Squares	df	Mean Square	F-value	p-value	
Model	3662.98	9	407.00	6.34	0.0001	significant
A-[Sucrose]	761.53	1	761.53	11.87	0.0021	
B-[Tea]	653.03	1	653.03	10.18	0.0039	
C-[Ethanol]	199.39	1	199.39	3.11	0.0907	
AB	435.91	1	435.91	6.79	0.0155	
AC	151.15	1	151.15	2.36	0.1379	
BC	391.75	1	391.75	6.10	0.0210	
A^2	189.73	1	189.73	2.96	0.0984	
B^2	12.19	1	12.19	0.1900	0.6669	
C^2	837.94	1	837.94	13.06	0.0014	
Residual	1540.18	24	64.17			
Lack of Fit	1098.58	5	219.72	9.45	0.0001	significant
Pure Error	441.60	19	23.24			
Cor Total	5203.16	33				

The program generated a table with the final actual equation for estimating WHC, which has been reformulated and presented as Equation 7.3. (**Eq. 4.3**) In this equation, S, T, and E correspond to sucrose, tea, and ethanol, respectively. Furthermore, glucose is included to ensure that the total carbon source combination reaches 10% (w/v) in the overall formulation. **Figure 4.3** highlights the interactions

between sucrose, tea, and ethanol on WHC, showcasing the influence of both nutritional and additive compositions on the observed outcomes.

$$WHC = 147.174 + 5.673[S] - 15.775[T] - 6.743[E] - 2.953[S][T] + 1.739[S][E] + 13.996[T][E] - 0.328[S]^2 + 2.080[T]^2 - 17.243[E]^2 \quad \text{.....(Eq. 7.3)}$$

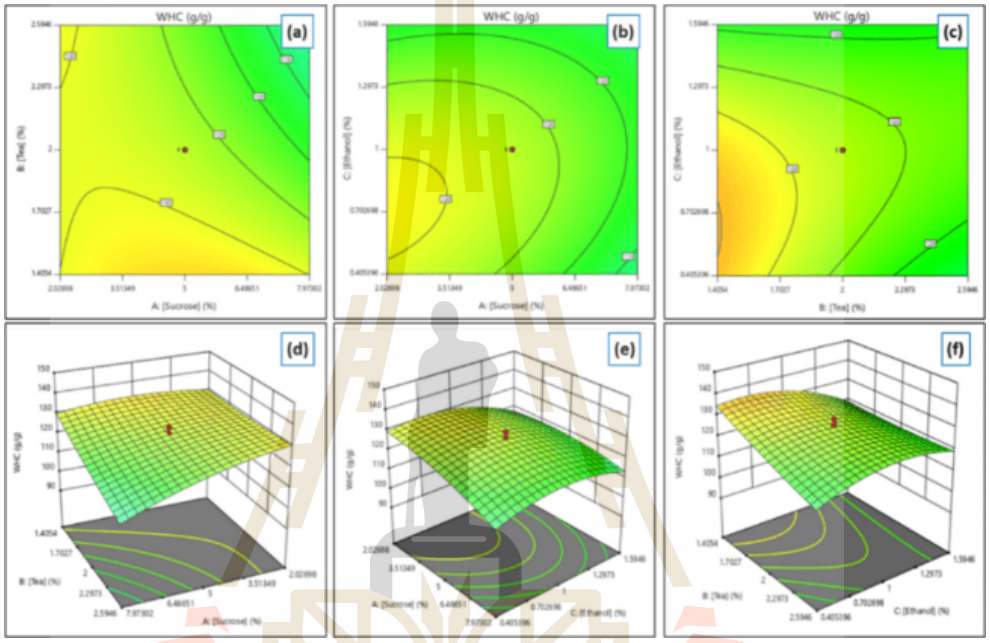

Figure 4.3 Graph model of the effect of formula composition interaction to WHC of BC.

The **Figure 4.3** demonstrates that the WHC of BC is influenced by interactions between the variables or factors. The interaction between sucrose and tea concentrations led to an increase in WHC, peaking at a sucrose concentration of approximately 5.00% and a tea concentration of about 1.41% (**Figure 4.3(a) and 4.3(d)**). Similarly, the interaction between sucrose and ethanol concentrations resulted in the highest WHC at a sucrose concentration of approximately 5.00% and an ethanol concentration of 1.59% (**Figure 4.3(b) and 4.3(e)**). Furthermore, the interaction between tea and ethanol concentrations contributed to an enhanced BC yield, with maximum productivity observed at a tea concentration of 1.41% and an ethanol concentration of 1.59% (**Figure 4.3(c) and 4.3(f)**).

4.4.3 Optimization of Formula, Validation, and Data Confirmation

The formula optimization was performed using the software by establishing specific criteria for the process. The primary objective was to maximize the wet yield of BC production, with the assumption that the dry yield would correlate closely with the wet yield due to the WHC values remaining within the specified range. The goal is to achieve the highest yield while utilizing raw materials economically and efficiently. The summary of the criteria setting and its constraints are presented in **Table 4.11**. The optimization process results (generated by the software) were presented in a Table containing multiple alternative medium formulations (**See Appendix C, Table 6.).** Among these, one formula was highlighted as the most optimal, featuring the highest desirability value (close to 1). The software generated approximately 53 formulations. From these, three sample formulas were selected for experimental testing: the most frequently recommended by the program (RTC-V1), the formulation with the highest predicted yield (RTC-V46), and the one with the lowest predicted yield (RTC-V53). These codes (RTC-V1, RTC-V46, RTC-V53) serve as identifiers for the experiments to facilitate easier reference. The letter "V" denotes the validation step, and the number following it indicates the solution or formula order. Details of the selected formulations and their predicted responses are presented in **Table 4.12**.

The selected formula was validated through laboratory experiments, and the experimental results were used to confirm the predictions provided by the software. The confirmation data is presented in **Table 4.13**, demonstrating that the experimental outcomes align well with the predicted values. These findings validate the accuracy of the equation and the selected formula for BC production. Notably, the most recommended formula achieved a wet yield of 621.71 g/L, representing a 238.54% increase compared to the highest yield obtained in the preliminary study (RTC-SGlu), discussed in an earlier chapter of this thesis. Similarly, the dry yield increased by 214.67%, while the WHC results were comparable to the previous findings.

Table 4.11 Summary of the criteria and constraints for optimizing the medium formulation.

Name	Goal	Lower Limit	Upper Limit	Lower Weight	Upper Weight	Importance
A: [Sucrose]	maximize	2.027	7.973	1	1	5
B: [Tea]	minimize	1.405	2.594	1	1	3
C: [Ethanol]	is in range	0.405	1.594	1	1	3
Wet yield	maximize	350.62	679.74	1	1	5
Dry yield	is in range	3.33	5.94	1	1	3
WHC	is in range	93.25	143.65	1	1	3

Glucose was added to the sucrose solution to reach a final concentration of 10%. The lower and upper limits for the optimization variables were automatically determined by the software based on prior experimental data from laboratory experiment.

Table 4.12 Software-Generated Optimal Formula and Predicted BC Production

No/Code	Sucrose	Tea	Ethanol	Wet yield	Dry yield	WHC	Desira-bility
RTC-V1	7.973	1.405	1.595	630.159	5.238	119.265	0.939
RTC-V46	7.260	1.407	1.595	645.117	5.35	119.754	0.912
RTC-V53	7.973	1.405	0.580	593.081	4.446	130.125	0.889

Codes (RTC-V1, RTC-V46, RTC-V53) identify experiments; "V" indicates the validation step, and the number represents the solution order of the selected formula

RSM has been widely recognized as an effective tool for optimizing BC production. This study successfully increased BC productivity, aligning with previous research that demonstrated the efficacy of RSM in enhancing BC yields. Approaches such as CCD and Rotatable CCD have consistently resulted in significant improvements in BC productivity under optimized conditions (Hegde et al. 2013; Singh et al. 2017; Rodrigues et al. 2019; Aswini et al. 2020; Yilmaz and Goksungur 2024).

Table 4.13 Software-Generated Data Confirmation Output

Sample Code	Response	Predicted Mean	n	95% PI low	Actual Mean	95% PI high
	Wet yield	630.16±54.37	3	517.94	621.71±24.06	742.37
RTC-V1	Dry yield	5.24±0.41	3	4.39	5.56±0.50	6.09
	WHC	119.27±6.55	3	105.75	107.32±8.01	132.78
	Wet yield	645.12±51.31	3	539.22	658.66±34.91	751.02
RTC-V46	Dry yield	5.35±0.39	3	4.55	5.56±0.33	6.15
	WHC	119.77±6.18	3	107.02	115.08±8.81	132.53
	Wet yield	593.19±50.85	3	488.16	593.88±39.27	698.06
RTC-V53	Dry yield	4.45±0.38	3	3.65	5.09±0.92	5.24
	WHC	130.13±6.12	3	117.49	115.60±17.24	142.77

Two-sided Confidence = 95%, n = the number of replications. Unit for yield (g/L) and unit for WHC (g water/ g cellulose)

4.4.4 Characterization of BC Product Resulted from Selected Formula

1) BC productivity and water holding capacity

BC produced from kombucha fermentation with different composition of the medium formulation on the wet yields, dry yields, and WHC, as shown in **Figure 4.4**. The results showed that different formulation that was suggested by the program i.e. RTC-V1, RTC-V46, and RTC-V53 are not significantly different ($P > 0.05$) in the wet yield ($P = 0.135$), dry yield ($P = 0.377$), and water holding capacity ($P = 0.544$).

RSM has been used to optimize BC production. In earlier studies, the CCD, a form of RSM, was applied to optimize BC production, resulting in a sixfold increase (0.318% to 1.72% (w/v)) in BC productivity (Hegde et al. 2013). Using the Rotatable Central Composite Design (RCCD), RSM successfully increased BC production by optimizing five independent variables—temperature, pH, incubation time, molasses concentration, and corn steep liquor concentration—each at five levels, achieving a

maximum yield of 4.34 g/L (dry weight), compared to a regular yield of approximately 3.85 g/L after 172 hours of fermentation (Singh et al. 2017). CCD has also been reported to significantly enhance BC productivity (Rodrigues et al. 2019). Optimization using RSM under optimal conditions yielded the highest BC productivity of approximately 469.83 g/L (wet weight) (Aswini et al. 2020). An RSM-based study further enhanced BC productivity, achieving a fivefold increase compared to the regular medium, reaching 8.45 g/L (dry weight) (Yilmaz and Goksungur 2024). The WHC of BC observed in this study is comparable to or within the range of results reported in the previous chapter.

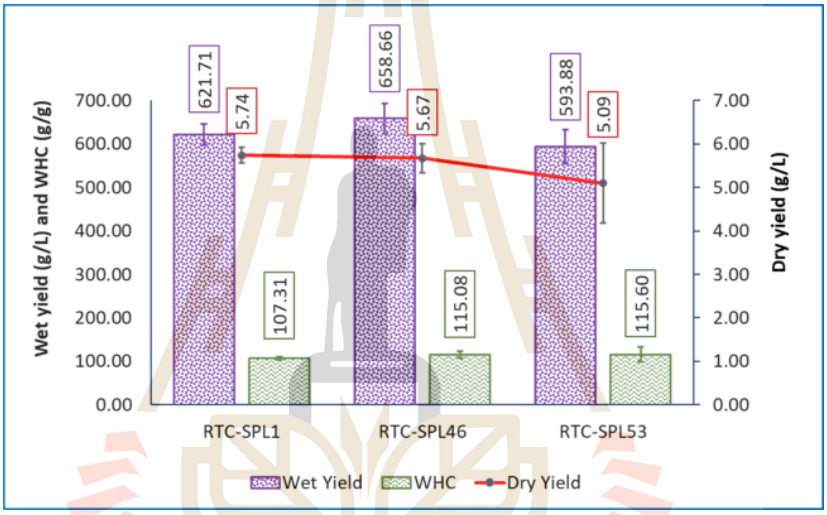

Figure 4.4 Wet yield (g/L), Dry yield (g/L), and WHC (g water/g cellulose) of purified BC from kombucha fermentation with different type of tea.

2) Morphology Analysis (SEM)

The morphology of BC samples produced from kombucha fermentation using various medium formulations—RTC-V1, RTC-V46, and RTC-V53—was examined through scanning electron microscopy (SEM). Each sample was observed at magnifications of 10,000x, 30,000x, and 50,000x (**Figure 4.5**). The fiber diameter distribution of dried BC was analyzed using the ImageJ software, and the results are presented in **Figure 4.6**. For comparison, RTC-C was included in this analysis. Overall, the SEM images revealed similar morphologies among the samples, displaying a uniform fiber pattern consistent with findings from previous studies.(Illa et al. 2019;

Brandes et al. 2020; Nguyen and Nguyen 2022). However, the BC fiber size appeared larger after optimization compared to the RTC control, likely due to differences in medium composition. This observation is supported by the fiber diameter analysis, which showed that the fiber diameters of RTC-V1, RTC-V46, and RTC-V53 were 37.85 ± 6.46 nm, 38.42 ± 7.52 nm, and 38.87 ± 6.91 nm, respectively, significantly larger than the RTC-C control, which had a fiber diameter of 30.65 ± 6.46 nm. In a previous chapter, BC produced using a medium containing a combination of sucrose and glucose (RTC-SGlu) had a fiber diameter of 34.33 ± 7.56 nm, while BC produced with ethanol as an additive (RTC-EtOH) exhibited a fiber diameter of 45.98 ± 9.38 nm.

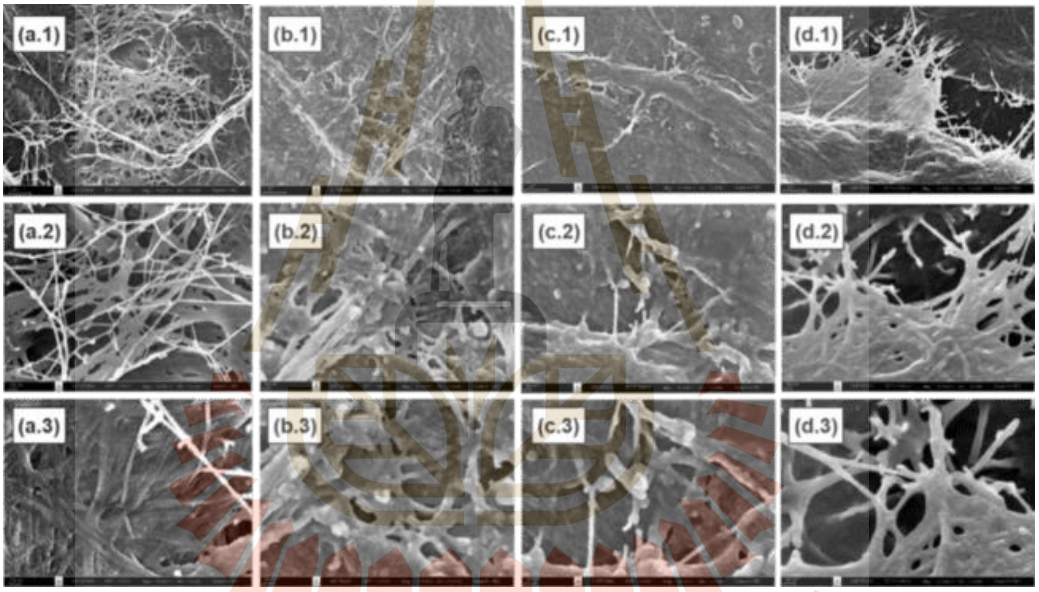

Figure 4.5 SEM image of BC from (a) RTC-C, (b) RTC-V1, (c) RTC-V46, and (d) RTC-V53. (1) 10k, (2) 30k, and (3) 50k magnifications.

The results of this study align with previous findings on BC fiber diameters. *K. hansenii* 23769 (ATCC) and a strain isolated from grape juice (GBHS) produced BC fibers with average diameters of 28.9 ± 5.6 nm and 28.6 ± 6.7 nm, respectively (Illa et al. 2019). Similarly, *K. rhaeticus* PG2 cultivated in HS medium using glucose and glycerol as carbon sources produced BC fibers with diameters of 30–60 nm (Thorat and Dastager 2018). BC nanofibers derived from HS medium and waste fig medium had average diameters of 36 nm and 44 nm, respectively (Yilmaz and

Goksungur 2024). In low-cost media like date syrup and cheese whey, *K. xylinus* produced fibers averaging 45–55 nm (Raiszadeh-Jahromi et al. 2020). Wang et al. (2018) also reported BCNFs with diameters of 35–50 nm using various carbon sources (Wang et al. 2018).. In contrast, glucose supplemented with 1.5% ethanol resulted in larger fiber diameters of 64.1 ± 5.11 nm to 82.3 ± 3.28 nm, which increased further with 3% ethanol (Fatima et al. 2023). These findings highlight the influence of carbon source composition and ethanol supplementation in the optimized formulation on BC fiber morphology.

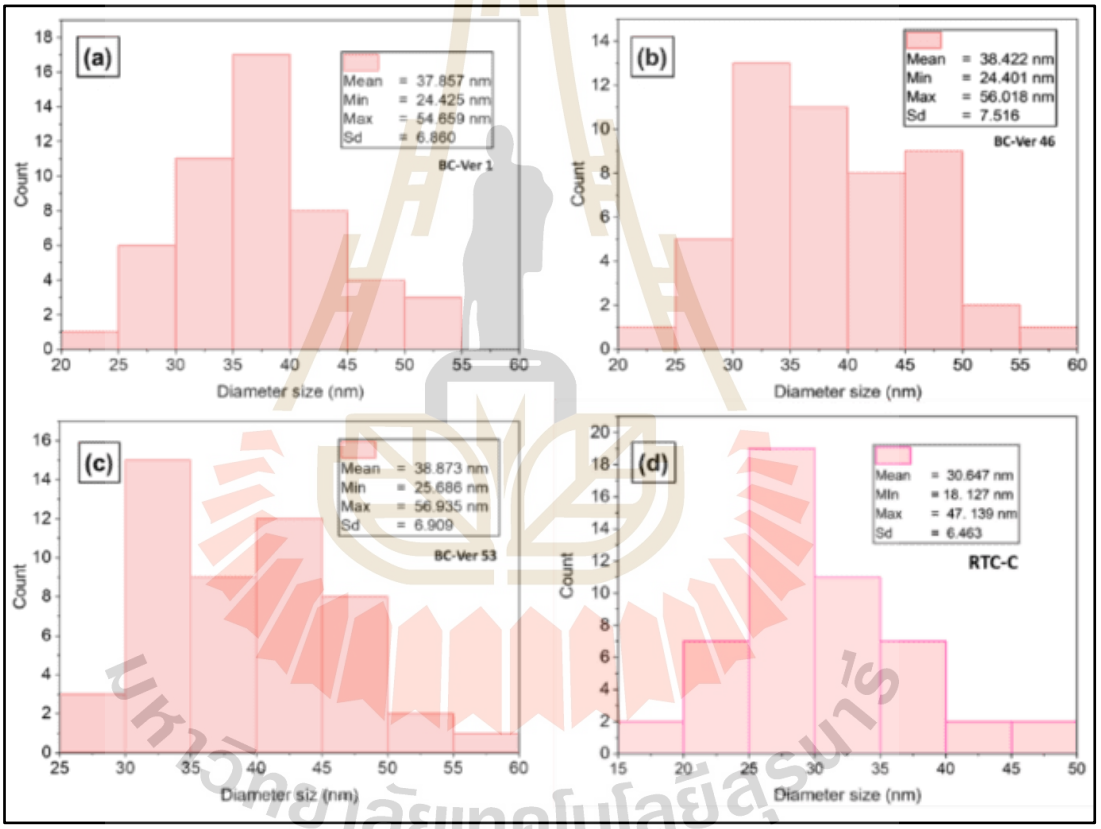

Figure 4.6 Graph of the polydispersity in fiber diameter for BC samples: (a) RTC-V1, (b) RTC-V46, (c) RTC-V53, and (d) RTC-C.

3) Fourier Transform Infrared Spectroscopy Analysis

Figure 4.7 shows the FTIR spectra of BC samples produced from various optimized medium kombucha fermentation with i.e. RTC-V1, RTC-V46, and RTC-V53. RTC-C is used for comparison. The FTIR spectra of the BC samples reveal distinct

differences, particularly in the optimized samples compared to RTC-C. These differences highlight the impact of adding glucose and ethanol to the medium, in addition to sucrose and Thai red tea solution used in the control sample (RTC-C).

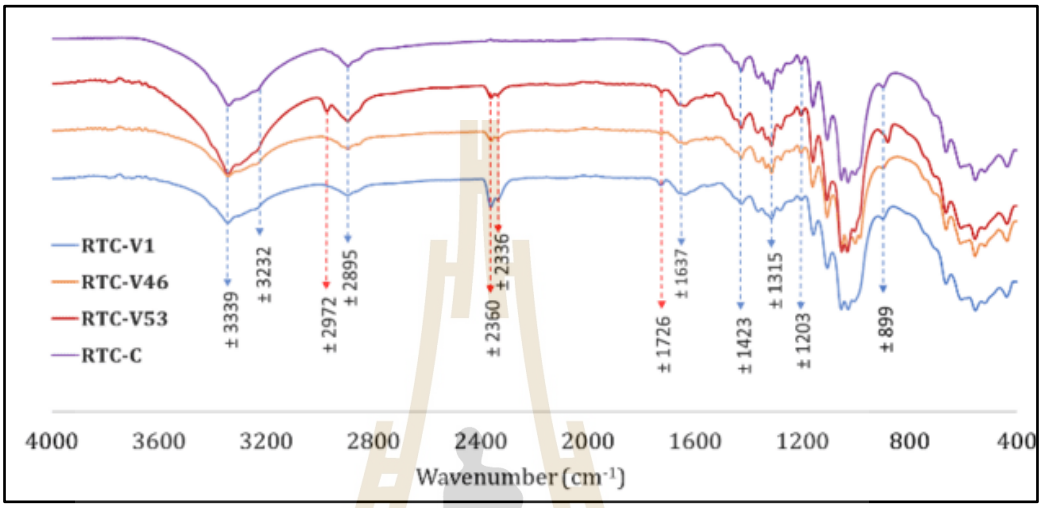

Figure 4.7 FTIR spectra of BCs from various of medium formulations i.e. RTC-V1, RTC-V46, RTC-V53, and RTC-C.

Some keys observation is the appearance of a band at 2972 cm^{-1} (particularly in RTC-V53) and then peak at around 2360 cm^{-1}, 2336 cm^{-1}, and 1726 cm^{-1}. The peaks observed at approximately 3339 cm^{-1} and 3232 cm^{-1} correspond to O-H stretching vibrations, which are characteristic of hydroxyl groups. The subtle differences in peak intensity suggest variations in the hydrogen bonding network among the samples. Additionally, the peak around 2895 cm^{-1} is attributed to C-H stretching vibrations, which are typically associated with aliphatic groups such as CH2 or CH3 (Leonarski et al. 2021a; Fatima et al. 2023).

The peak observed at 2972 cm^{-1} (in RTC-V53) is likely due to the stretching vibrations of C-H bonds in methyl and methylene groups, which may result from the addition of ethanol to the fermentation medium. However, this band is absent or less pronounced in the control sample (RTC-C) and the other optimized samples (RTC-V1, RTC-V46). The faint peaks observed around 2360 cm^{-1} and 2336 cm^{-1} in optimized BCs suggests the presence of triple-bond functional groups, such as C≡C

or C≡N (Srivastava and Mathur 2022). These groups could originate from polyphenols and other organic compounds, protein, yeast cell, and bacteria (Amarasekara et al. 2020). The same observation was reported in previous studies, such as BC derived from *nata de coco* (Fuller et al. 2018; Rachtanapun et al. 2021). Fuller et al. (2018) noted that this peak was present in samples contaminated with residual proteins, nucleic acids, and whole cells (Fuller et al. 2018). The incorporation of these impurities into the BC matrix may be attributed to the thick and dense structure of the pellicle, which can hinder complete removal during the purification process. Evidence of such impurities can also be seen in the SEM images (**Figure 4.5**).

The peak around 1726 cm^{-1} in purified BC is likely attributed to the C=O stretching vibration of carbonyl groups, which are commonly found in aldehyde groups (1720–1740 cm^{-1}), ketones (1705–1725 cm^{-1}), and carboxylic acids (1700–1725 cm^{-1}) (Yao et al. 2015). These groups may originate from polyphenols and other organic compounds, as well as proteins, yeast cells, and bacterial components (Amarasekara et al. 2020). Fuller et al. (2018) reported that the presence of impurities contributes to the emergence of bands between 1800 cm^{-1} and 1500 cm^{-1}, which are attributed to functional groups such as NH_2, C–N, and C=O, originating from lipids, proteins, and nucleic acids (Fuller et al. 2018).

4) X-Ray Diffraction (XRD) Analysis

The XRD analysis of BC samples, including optimized (RTC-V1, RTC-V46, RTC-V53) and control (RTC-C) formulations are demonstrated **Figure 4.8**. The Crystallinity index and the crystallite size of BC the optimized BC samples and control of BC from Thai red tea kombucha are presented in **Table 4.14**. The XRD spectra visualized the characteristics diffraction peaks at around 14.54°, subtle peak at around 17.11°, and 23.03° (2θ).

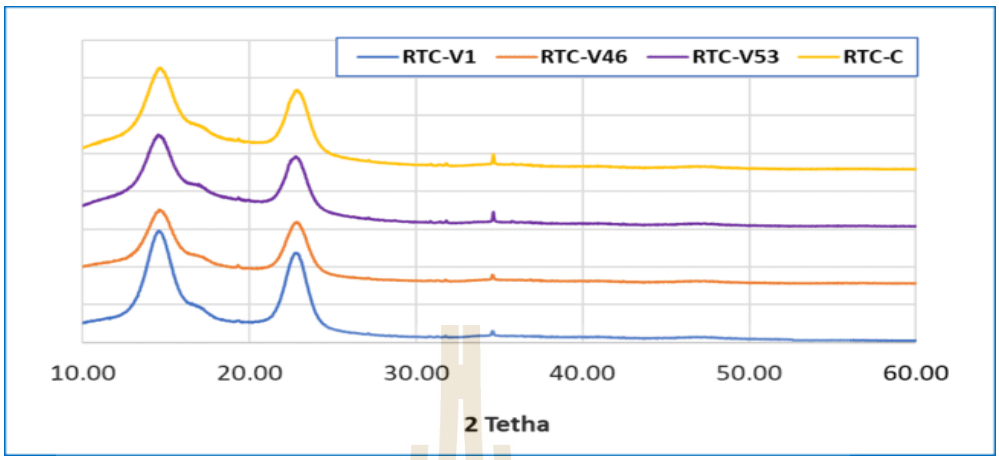

Figure 4.8 XRD spectra of BCs from various of medium formulations i.e. RTC-V1, RTC-V46, and RTC-V53.

The observed peaks confirm the crystalline structure characteristic of BC, consistent with previous findings reported by Said Azmi et al. (Said Azmi et al. 2023). The XRD profiles closely match those described in earlier studies on BC (Revin et al. 2018; Jittaut et al. 2023; Said Azmi et al. 2023), as well as the results presented in the previous chapter of this study. While the XRD patterns confirm the uniform chemical structure across the samples, variations in diffraction peak intensities are noticeable, suggesting subtle differences in the cellulose chain orientation (Said Azmi et al. 2023). The most prominent peak observed near 23° corresponds to the characteristic cellulose type I (Said Azmi et al. 2023; Hossen et al. 2024). According to Gaspar et al. peaks at 2θ values of 14.7°, 16.8°, and 22.7° can be attributed to the 100, 110, and 200 crystallographic planes, which are typical of native cellulose type I (Gaspar et al. 2014). Similarly, the peak appearing at approximately 22.90° (2θ) further confirms the crystalline nature of the cellulose samples (Samuel and Adefusika 2019). These results align with previous observations, reinforcing the consistency of BC's structural properties across various studies.

The CI and crystallite size of BC samples were calculated from the XRD data using the Segal method, which involves assessing the peak height and subtracting baseline intensity. As shown in **Table 4.14**, the results reveal slight

variations in peak intensities, indicating changes in crystallinity. The control sample (RTC-C) exhibits the highest crystallinity index (86.74%) with the most intense peaks, suggesting a more ordered cellulose structure. In comparison, the optimized samples display slightly reduced crystallinity, with RTC-V1, RTC-V46, and RTC-V53 showing values of 83.23%, 84.46%, and 85.97%, respectively. This reduction is likely due to the inclusion of ethanol and glucose in the fermentation medium, which may disrupt the alignment of cellulose chains during synthesis. This observation is consistent with findings from the previous chapter, where the use of a combination of sucrose and glucose as carbon sources, as well as ethanol as an additive, resulted in BC samples with lower crystallinity (around 86.00% and 80.22%, respectively).

Table 4.14 CI and crystallite size of BC samples from various of medium formulations i.e. RTC-V1, RTC-V46, and RTC-V53.

Parameter	RTC-C	RTC-V1	RTC-V46	RTC-V53
Crystallinity index (%)	89.54	83.23	84.46	85.97
Crystallite size (nm)	3.34	3.19	3.33	3.30

The CI results of this study are consistent with those reported in previous research. For instance, BC produced from pineapple peel waste fermentation achieved a CI of 87% (Sardjono et al. 2019), while BC derived from pineapple waste solution had a CI of 82.2% (Pham and Tran 2023). Similarly, BC obtained from citrus processing waste exhibited a CI of 86.9% (Andritsou et al. 2018). Heydorn et al. reported a CI range of 57% to 85% for BC produced in HS medium using various carbon sources (Heydorn et al. 2023). In addition, BC without interfering components demonstrated a CI of 84%–90%, as observed by (Cazón and Vázquez 2021). Slightly lower CI values were noted in BC produced from crude distillery effluent (80.2%) (Gayathri and Srinikethan 2019), and wastewater from Arenga starch production (79.6%) (Rahmayetty and Sulaiman 2023). These findings further validate the results presented in the previous chapter of this study.

Further analysis of the average crystallite size of BC (**Table 4.14**), which reflects the dimension of ordered crystalline regions, reveals minor variations among the samples. The control sample has the largest crystallite size (3.34 nm), while the optimized samples exhibit slightly smaller sizes: 3.19 nm for RTC-V1, 3.33 nm for RTC-V46, and 3.30 nm for RTC-V53. This reduction can be attributed to the altered fermentation medium, where ethanol and glucose may have influenced the biosynthetic process of cellulose, leading to finer crystalline structures.

Several of the previous studies reported the average of BC diameter size from the lower to the higher results. BC produced by *G. xylinus* InaCC B404 in HS medium has average crystallite size of 3.06 nm for BC produced by (Agustin et al. 2021). Average crystallite sizes of BC range from 3.29 nm and 4.80 nm were observed in BC produced from black tea kombucha after 3 and 5 days of fermentation, respectively (Balistreri et al. 2024). More results of the studies reported the higher average crystallite size such as BC derived from *K. xylinus* strains using fructose and glucose as carbon sources exhibited crystallite sizes ranging from 4.7 to 6.8 nm (Singhsa et al. 2018). BC produced by *Lactobacillus plantarum* in a green tea leaf solution (1% green tea, 10% sucrose) had crystallite sizes of 5.36, 5.94, and 5.98 nm after 7, 14, and 30 days of fermentation, respectively (Charoenrak et al. 2023). BC produced under different conditions also exhibited crystallite sizes of 5.6 nm (Jia et al. 2017) and 8.36 nm (Gayathri and Srinikethan 2019). These results highlight the impact of fermentation medium composition on the structural characteristics of BC. The crystallinity of BC can be influenced by several factors, including carbon and nitrogen sources, type of additives, bacterial strains, fermentation conditions such as temperature and duration, and the methods used in post-production processing (Zeng et al. 2011; Thielemans et al. 2023).

5) Thermogravimetric (TGA/DTG) Analysis

Figure 4.9 depicts the thermogravimetric (TG) and differential thermal degradation (DTG) curves for BC samples. The results were gathered using

thermogravimetric analysis (TGA). From the spectra graph, it is observed that overall optimized BC has similar spectra pattern. However, a slightly distinction is observed in the graph, particularly in DTG graph, optimized BC has lower DTG T_{Max} temperature compare to control (RTC-C). The analysis detail of TGA and TG analysis result is summarized in **Table 4.15**.

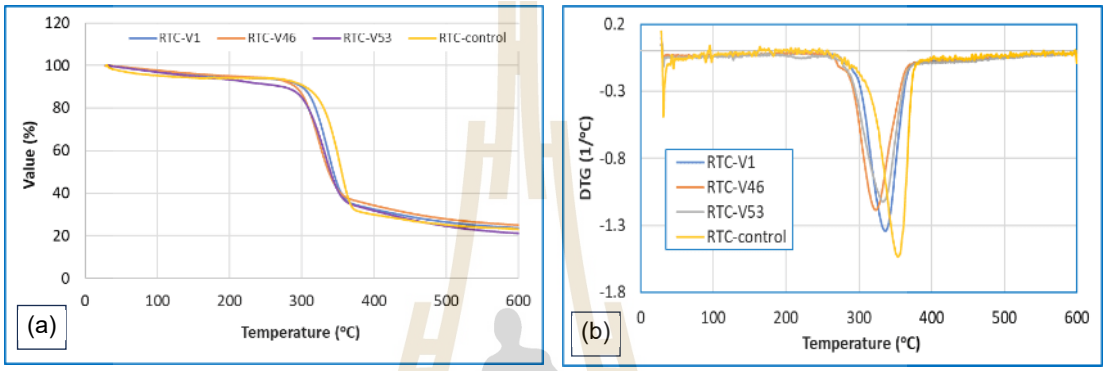

Figure 4.9 TGA (a) and DTG (b) thermograph of optimized and control BC samples

In the TGA analysis, the first-stage weight loss, ranging from 5.25% to 7.47%, is attributed to the dehydration and volatilization of low-molecular-weight components or residual water within the BC matrix (Teixeira et al. 2019; Mohamad et al. 2022a). RTC-V1 and RTC-V46 exhibited first-stage weight losses of 5.25% and 5.62%, respectively, which were slightly lower than that of RTC-C (6.03%). In contrast, RTC-V53 demonstrated a higher weight loss of 7.74%. This value exceeds the range reported by Gismatulina and Budaeva (1 – 2%) (Gismatulina and Budaeva 2024) but aligns closely with findings from Mohamad et al., who observed a weight loss of 5 – 9% (Mohamad et al. 2022a).

The second-stage weight loss, occurring between 240°C and 600°C across the samples, exhibited relatively consistent values ranging from 69.70% to 71.35%. The remaining material (residue) after decomposition at 600°C ranged from 21.14% to 25.02%. Compared to previous experiments, BC produced using RTC-SGlu and RTC-EtOH showed second-stage weight losses of 73.90% and 68.13% and residues of 20.92% and 28.52%, respectively. In earlier results, RTC-C demonstrated a higher

second-stage weight loss and lower residue, whereas RTC-EtOH exhibited the opposite trend, with lower weight loss and higher residue. These findings suggest that using a combination of sucrose and glucose as carbon sources tends to increase the second-stage weight loss while reducing the residual content. In contrast, the addition of ethanol appears to reduce the weight loss and increase the residue in BC samples.

This study's findings comparable to previous research. BC from *A. xylinum* AGR 60 exhibited a first-stage mass loss of 6%, a second-stage loss of 74%, and a residue of 20% at 700°C, with major decomposition between 300°C and 360°C (Potivara and Phisalaphong 2019). BC produced by *G. xylinus* AGR 60 showed a first-stage loss of 6.2%, a second-stage loss of 64.0%, and a residue of 22.8% at 600°C (Jenkhongkarn and Phisalaphong 2023). BC produced from various carbon sources, including glucose, fructose, sucrose, and glycerol, had residuals at 600°C ranging from 15.2% to 23.1% and a similar decomposition pattern (Tureck et al. 2021). In contrast, BC from kombucha fermentation of green tea showed three decomposition stages at 152°C, 267°C, and 359°C, with a total weight loss of 74.42% and 25.58% residue (Lima et al. 2023), differing from the two-stage decomposition observed in this study.

Table 4.15 Detail parameter of TGA/DTG analysis of BC samples from optimized kombucha

Samples	First stage weight loss (%)	Second stage weight loss (%)	Residue (%)	DTG Peak range (°C)	DTG T_{Max} (°C)
RTC-V1	5.62	70.69	23.66	272 – 378	336.50
RTC-V46	5.25	69.70	25.02	266 – 378	323.50
RTC-V53	7.47	71.35	21.14	260 – 378	333.33
RTC-C	6.03	71.01	23.01	265 – 380	353.67

The DTG T_{Max} results demonstrate the impact of carbon sources on the thermal stability of BC. In this study, optimized BC samples (RTC-V1, RTC-V46, RTC-V53) showed lower DTG T_{Max} values (336.50°C, 323.50°C, and 333.33°C, respectively)

compared to RTC-C (353.67°C). In previous experiments reported in the earlier chapter, RTC-SGlu exhibited a higher DTG T_{Max} (356.83°C) than RTC-C, while RTC-EtOH showed a lower value (347.50°C), suggesting that sucrose-glucose combinations improve thermal stability, whereas ethanol reduces it. For comparison, prior studies reported DTG T_{Max} values of 328.36°C for BC produced by *G. xylinus* (Jia et al. 2017), 354.5°C–355.4°C for BC from *G. hansenii* in HS medium (Vasconcellos and Farinas 2018), BC produced by *K. medellinensis* from various waste and agricultural by-products exhibits DTG T_{Max} values ranging from 327°C to 368°C (Molina-Ramírez et al. 2018a), and 366°C for kombucha-fermented green tea BC (Lima et al. 2023). These findings indicate that both carbon source combinations and fermentation conditions influence BC's thermal properties.

6) Mechanical Properties Analysis Using Nanoindentation

In this study, the sample of BC from RTC-V1 as the most suggested formulation is selected as representative of the optimized BC sample. RTC-C sample is included as a control for comparison. The detailed findings are summarized in **Table 4.16**. This table shows that the optimized BC sample (RTC-V1) exhibits no significant differences in mechanical properties compared to the control sample (RTC-C) across all parameters. Similarly, in the previous chapter, BC produced using a sucrose-glucose combination as the carbon source (RTC-SGlu) also showed no significant differences from RTC-C, while BC produced with ethanol as an additive (RTC-EtOH) displayed the highest number of parameters that were not significantly different from RTC-C. These findings suggest that using sucrose-glucose or ethanol as additives does not significantly impact the mechanical properties of BC produced from Thai red tea kombucha fermentation.

The Young's modulus values observed in this study fall within a wide range, similar to those reported in previous research, with some values being lower or higher than others. For example, BC produced from various *Komagataeibacter* strains showed a range of 1.10 to 5.56 GPa (Chen et al. 2018a), while BC from different

strains and drying methods exhibited values between 198 and 659 MPa (Zeng et al. 2014). BC produced by *A. xylinum* E25 under static and rotating cultivation conditions showed Young's modulus values of 2.7 GPa and 0.3 GPa, respectively (Krystynowicz et al. 2002). Some studies report even higher values, such as *A. xylinum* AGR60 in coconut water, which achieved a Young's modulus of 9.14 GPa (Potivara and Phisalaphong 2019), and BC from kombucha fermentation, which reached 8.0 ± 1.9 GPa (Oliver-Ortega et al. 2021).

Table 4.16 Mechanical properties data analysis using nano-indenter of BC from kombucha fermentation of RTC-V1 and RTC-C.

Sample	MD (nm)	Pl (nm)	ML (mN)	H (GPa)	RM (GPa)	ERP	CC (nm/mN)	PW (nJ)	EW (nJ)	YM (GPa)
RTC-V1	3534.23 ±565.98	3124.20 ±567.15	50.10 ±0.00	0.22 ±0.09	5.10 ±1.08	0.14 ±0.03	10.91 ±0.85	54.78 ±7.74	19.64 ±1.29	4.66 ±0.99
RTC-C	3412.25 ±259.56	2980.18 ±253.91	50.10 ±0.00	0.22 ±0.05	4.94 ±0.56	0.15 ±0.01	11.50 ±0.22	54.41 ±4.64	20.80 ±0.47	4.51 ±0.51

MD: maximum depth, Pl: plastic, ML: maximum load, H: hardness, RM: reduced modulus, ERP: elastic recovery parameters, CC: contact compliance, PW: plastic work, EW: elastic work, and YM: Young's Modulus. Based on the statistical analysis, there were no significant differences among the samples across all parameters (P < 0.05).

4.5 Conclusion

This study employed Central Composite Design–Response Surface Methodology (CCD-RSM) to optimize BC (BC) production from Thai red tea kombucha. The effects and interactions of sucrose–glucose, tea, and ethanol concentrations were evaluated in relation to wet yield, dry yield, and WHC.

Although the model exhibited some limitations—such as relatively low R^2, adjusted R^2, predicted R^2 values, and a significant lack of fit—the quadratic model was still considered relevant. This is due to its theoretical suitability for capturing nonlinear effects and identifying potential optimal thresholds. Furthermore, the adequate precision value indicated that the model possessed an acceptable signal-to-noise ratio for predictive purposes.

Three formulations were selected from the optimization results for validation: RTC-V1 (the most recommended by the model), RTC-V46 (predicted to produce the highest yield), and RTC-V53 (predicted to produce the lowest yield). The validation results showed wet yields of 593.88 ± 39.27 to 658.66 ± 34.91 g/L, dry yields of 5.09 ± 0.92 to 5.56 ± 0.50 g/L, and WHC of 107.32 ± 8.01 to 115.60 ± 17.24 g water/g cellulose. No significant differences were observed among the three formulations, and all results fell within the predicted ranges, confirming the model's validity.

Characterization of the optimized BC further confirmed its quality. SEM analysis revealed uniform nanofiber networks with larger diameters (37.85–38.87 nm) compared to the control (30.65 nm). FTIR and XRD analyses indicated high crystallinity indices (83.23%–85.97%) and crystallite sizes ranging from 3.19 to 3.33 nm. Thermal analysis (TGA) showed lower DTG T_{max} values, while mechanical properties remained comparable across samples.

In conclusion, CCD-RSM proved to be an effective strategy for optimizing BC production from Thai red tea kombucha fermentation. Despite certain model

limitations, the approach yielded robust, reproducible, and scalable results, highlighting its strong potential for future industrial applications.

4.6 References

Agustin S, Wahyuni ET, Suparmo, et al (2021) Production and characterization of bacterial cellulose-alginate biocomposites as food packaging material. Food Res 5:204–210. https://doi.org/10.26656/fr.2017.5(6).733

Amarasekara AS, Wang D, Grady TL (2020) A comparison of kombucha SCOBY bacterial cellulose purification methods. SN Appl Sci 2:1–7. https://doi.org/10.1007/s42452-020-1982-2

Andritsou V, De Melo EM, Tsouko E, et al (2018) Synthesis and Characterization of Bacterial Cellulose from Citrus-Based Sustainable Resources. ACS Omega 3:10365–10373. https://doi.org/10.1021/acsomega.8b01315

Aswini K, Gopal NO, Uthandi S (2020) Optimized culture conditions for bacterial cellulose production by Acetobacter senegalensis MA1. BMC Biotechnol 20:1–16. https://doi.org/10.1186/s12896-020-00639-6

Azeredo HMC, Barud H, Farinas CS, et al (2019) Bacterial Cellulose as a Raw Material for Food and Food Packaging Applications. Front Sustain Food Syst 3:. https://doi.org/10.3389/fsufs.2019.00007

Balistreri GN, Campbell IR, Li X, et al (2024) Bacterial cellulose nanoparticles as a sustainable drug delivery platform for protein-based therapeutics. RSC Appl Polym 2:172–183. https://doi.org/10.1039/d3lp00184a

Barja F (2021) Bacterial nanocellulose production and biomedical applications. J Biomed Res 35:310–317. https://doi.org/10.7555/JBR.35.20210036

Bizeau J, Mertz D (2021) Design and applications of protein delivery systems in nanomedicine and tissue engineering. Adv Colloid Interface Sci 287:. https://doi.org/10.1016/j.cis.2020.102334

Brandes R, De Souza L, Carminatti C, Recouvreux D (2020) Production with a High

Yield of Bacterial Cellulose Nanocrystals by Enzymatic Hydrolysis. Int J Nanosci 19:1–8. https://doi.org/10.1142/S0219581X19500157

Cavicchia LOA, de Almeida MEF (2022) Health benefits of Kombucha: drink and its biocellulose production. Brazilian J Pharm Sci 58:1–13. https://doi.org/10.1590/s2175-97902022e20766

Cazón P, Vázquez M (2021) Improving bacterial cellulose films by ex-situ and in-situ modifications: A review. Food Hydrocoll 113:1–9. https://doi.org/10.1016/j.foodhyd.2020.106514

Charoenrak S, Charumanee S, Sirisa-ard P, et al (2023) Nanobacterial Cellulose from Kombucha Fermentation as a Potential Protective Carrier of Lactobacillus plantarum under Simulated Gastrointestinal Tract Conditions. Polymers (Basel) 15:. https://doi.org/10.3390/polym15061356

Chen S-Q, Lopez-Sanchez P, Wang D, et al (2018) Mechanical properties of bacterial cellulose synthesised by diverse strains of the genus Komagataeibacter. Food Hydrocoll 1–25. https://doi.org/10.1016/j.foodhyd.2018.02.031.This

Fatima A, Ortiz-Albo P, Neves LA, et al (2023) Biosynthesis and characterization of bacterial cellulose membranes presenting relevant characteristics for air/gas filtration. J Memb Sci 674:. https://doi.org/10.1016/j.memsci.2023.121509

Fei S, Yang X, Xu W, et al (2023) Insights into Proteomics Reveal Mechanisms of Ethanol-Enhanced Bacterial Cellulose Biosynthesis by Komagataeibacter nataicola. Fermentation 9:1–14. https://doi.org/10.3390/fermentation9060575

Fuller ME, Andaya C, McClay K (2018) Evaluation of ATR-FTIR for analysis of bacterial cellulose impurities. J Microbiol Methods 144:145–151. https://doi.org/10.1016/j.mimet.2017.10.017

Gaspar D, Fernandes SN, De Oliveira AG, et al (2014) Nanocrystalline cellulose applied simultaneously as the gate dielectric and the substrate in flexible field effect transistors. Nanotechnology 25:. https://doi.org/10.1088/0957-4484/25/9/094008

Gayathri G, Srinikethan G (2019) Bacterial Cellulose production by K. saccharivorans

BC1 strain using crude distillery effluent as cheap and cost effective nutrient medium. Int J Biol Macromol 138:950–957. https://doi.org/10.1016/j.ijbiomac.2019.07.159

Gismatulina YA, Budaeva V V. (2024) Cellulose Nitrates-Blended Composites from Bacterial and Plant-Based Celluloses. Polymers (Basel) 16:. https://doi.org/10.3390/polym16091183

Hegde S, Bhadri G, Narsapur K, et al (2013) Statistical Optimization of Medium Components by Response Surface Methodology for Enhanced Production of Bacterial Cellulose by Gluconacetobacter persimmonis. J Bioprocess Biotech 04:1–5. https://doi.org/10.4172/2155-9821.1000142

Heydorn RL, Lammers D, Gottschling M, Dohnt K (2023) Effect of food industry by-products on bacterial cellulose production and its structural properties. Cellulose 30:4159–4179. https://doi.org/10.1007/s10570-023-05097-9

Hossen MT, Kundu CK, Pranto BRR, et al (2024) Synthesis, characterization, and cytotoxicity studies of nanocellulose extracted from okra (Abelmoschus Esculentus) fiber. Heliyon 10:e25270. https://doi.org/10.1016/j.heliyon.2024.e25270

Illa MP, Khandelwal M, Sharma CS (2019) Modulated Dehydration for Enhanced Anodic Performance of Bacterial Cellulose derived Carbon Nanofibers. ChemistrySelect 4:6642–6650. https://doi.org/10.1002/slct.201901359

Jenkhongkarn R, Phisalaphong M (2023) Effect of Reduction Methods on the Properties of Composite Films of Bacterial Cellulose-Silver Nanoparticles. Polymers (Basel) 15:. https://doi.org/10.3390/polym15142996

Jia Y, Wang X, Huo M, et al (2017) Preparation and characterization of a novel bacterial cellulose/chitosan bio-hydrogel. Nanomater Nanotechnol 7:1–8. https://doi.org/10.1177/1847980417707172

Jittaut P, Hongsachart P, Audtarat S, Dasri T (2023) Production and characterization of bacterial cellulose produced by Gluconacetobacter xylinus BNKC 19 using

agricultural waste products as nutrient source. Arab J Basic Appl Sci 30:221–230. https://doi.org/10.1080/25765299.2023.2172844

Kazemi M, Faranak, Doosthoseini K, Azin M (2015) Effect of Ethanol and Medium on Bacterial Cellulose (Bc) Production By Gluconacetobacter Xylinus (Ptcc 1734). Cellul Chem Technol 49:455–462

Krystynowicz A, Czaja W, Wiktorowska-Jezierska A, et al (2002) Factors affecting the yield and properties of bacterial cellulose. J Ind Microbiol Biotechnol 29:189–195. https://doi.org/10.1038/sj.jim.7000303

Leonarski E, Cesca K, Zanella E, et al (2021) Production of kombucha-like beverage and bacterial cellulose by acerola byproduct as raw material. Lwt 135:1–8. https://doi.org/10.1016/j.lwt.2020.110075

Lima NF, Maciel GM, Fernandes I de AA, Haminiuk CWI (2023) Optimising the Production Process of Bacterial Nanocellulose: Impact on Growth and Bioactive Compounds. Food Technol Biotechnol 61:494–504. https://doi.org/10.17113/ftb.61.04.23.8182

Mohamad S, Abdullah LC, Jamari SS, et al (2022) Production and Characterization of Bacterial Cellulose Nanofiber by Acetobacter Xylinum 0416 Using Only Oil Palm Frond Juice as Fermentation Medium. J Nat Fibers 19:16005–16016. https://doi.org/10.1080/15440478.2022.2140243

Mohammad NH, El-Sherbiny GM, Hammad AA, et al (2021) Optimization of bacterial cellulose production using Plackett-Burman and response surface methodology. Egypt J Med Microbiol 30:93–101. https://doi.org/10.21608/EJMM.2021.197467

Molina-Ramírez C, Castro C, Zuluaga R, Gañán P (2018a) Physical Characterization of Bacterial Cellulose Produced by Komagataeibacter medellinensis Using Food Supply Chain Waste and Agricultural By-Products as Alternative Low-Cost Feedstocks. J Polym Environ 26:830–837. https://doi.org/10.1007/s10924-017-0993-6

Molina-Ramírez C, Enciso C, Torres-Taborda M, et al (2018b) Effects of alternative

energy sources on bacterial cellulose characteristics produced by Komagataeibacter medellinensis. Int J Biol Macromol 117:735–741. https://doi.org/10.1016/j.ijbiomac.2018.05.195

Nguyen TA, Nguyen XC (2022) Bacterial Cellulose-Based Biofilm Forming Agent Extracted from Vietnamese Nata-de-Coco Tree by Ultrasonic Vibration Method: Structure and Properties. J Chem 2022:1–10. https://doi.org/10.1155/2022/7502796

Oliver-Ortega H, Geng S, Espinach FX, et al (2021) Bacterial cellulose network from kombucha fermentation impregnated with emulsion-polymerized poly(Methyl methacrylate) to form nanocomposite. Polymers (Basel) 13:1–17. https://doi.org/10.3390/polym13040664

Padmanabhan SK, Lamanna L, Friuli M, Licciulli A (2023) Carboxymethylcellulose-Based Hydrogel Obtained from Bacterial Cellulose. Molecules 28:1–10. https://doi.org/https://doi.org/10.3390/molecules28020829

Pandey A, Singh A, Singh MK (2024) Novel low-cost green method for production bacterial cellulose. Polym Bull 81:6721–6741. https://doi.org/10.1007/s00289-023-05023-w

Pham TT, Tran TTA (2023) Evaluation of the Crystallinity of Bacterial Cellulose Produced from Pineapple Waste Solution by Using Acetobacter Xylinum. ASEAN Eng J 13:81–91. https://doi.org/10.11113/aej.V13.18868

Potivara K, Phisalaphong M (2019) Development and characterization of bacterial cellulose reinforced with natural rubber. Materials (Basel) 12:. https://doi.org/10.3390/ma12142323

Rachtanapun P, Jantrawut P, Klunklin W, et al (2021) Carboxymethyl bacterial cellulose from nata de coco: Effects of NaOH. Polymers (Basel) 13:1–17. https://doi.org/10.3390/polym13030348

Rahmayetty, Sulaiman F (2023) Wastewater from the Arenga Starch Industry as a Potential Medium for Bacterial Cellulose and Cellulose Acetate Production.

Polymers (Basel) 15:1–15. https://doi.org/10.3390/polym15040870

Raiszadeh-Jahromi Y, Rezazadeh-Bari M, Almasi H, Amiri S (2020) Optimization of bacterial cellulose production by Komagataeibacter xylinus PTCC 1734 in a low-cost medium using optimal combined design. J Food Sci Technol 57:2524–2533. https://doi.org/10.1007/s13197-020-04289-6

Ramírez Tapias YA, Di Monte MV, Peltzer MA, Salvay AG (2022) Bacterial cellulose films production by Kombucha symbiotic community cultured on different herbal infusions. Food Chem 372:. https://doi.org/10.1016/j.foodchem.2021.131346

Revin V, Liyaskina E, Nazarkina M, et al (2018) Cost-effective production of bacterial cellulose using acidic food industry by-products. Brazilian J Microbiol 49:151–159. https://doi.org/10.1016/j.bjm.2017.12.012

Rodrigues AC, Fontão AI, Coelho A, et al (2019) Response surface statistical optimization of bacterial nanocellulose fermentation in static culture using a low-cost medium. N Biotechnol 49:19–27. https://doi.org/10.1016/j.nbt.2018.12.002

Said Azmi SNN, Samsu Z 'Asyiqin, Mohd Asnawi ASF, et al (2023) The production and characterization of bacterial cellulose pellicles obtained from oil palm frond juice and their conversion to nanofibrillated cellulose. Carbohydr Polym Technol Appl 5:100327. https://doi.org/10.1016/j.carpta.2023.100327

Samuel OS, Adefusika AM (2019) Influence of Size Classifications on the Structural and Solid-State Characterization of Cellulose Materials. In: Pascual R, Martín MEE (eds) Cellulose. IntechOpen

Sardjono SA, Suryanto H, Aminnudin, Muhajir M (2019) Crystallinity and morphology of the bacterial nanocellulose membrane extracted from pineapple peel waste using high-pressure homogenizer. In: AIP Conference Proceedings. AIP Publishing, pp 080015-1-080015–5

Singh O, Panesar PS, Chopra HK (2017) Response surface optimization for cellulose

production from agro industrial waste by using new bacterial isolate Gluconacetobacter xylinus C18. Food Sci Biotechnol 26:1019–1028. https://doi.org/10.1007/s10068-017-0143-x

Singhsa P, Narain R, Manuspiya H (2018) Physical structure variations of bacterial cellulose produced by different Komagataeibacter xylinus strains and carbon sources in static and agitated conditions. Cellulose 25:1571–1581. https://doi.org/10.1007/s10570-018-1699-1

Srivastava S, Mathur G (2022) Komagataeibacter saccharivorans strain BC-G1: an alternative strain for production of bacterial cellulose. Biologia (Bratisl) 77:3657–3668. https://doi.org/10.1007/s11756-022-01222-4

Teixeira SRZ, Dos Reis EM, Apati GP, et al (2019) Biosynthesis and functionalization of bacterial cellulose membranes with cerium nitrate and silver nanoparticles. Mater Res 22:1–13. https://doi.org/10.1590/1980-5373-MR-2019-0054

Thielemans K, De Bondt Y, Comer L, et al (2023) Decreasing the Crystallinity and Degree of Polymerization of Cellulose Increases Its Susceptibility to Enzymatic Hydrolysis and Fermentation by Colon Microbiota. Foods 12:1100. https://doi.org/10.3390/foods12051100

Thorat MN, Dastager SG (2018) High yield production of cellulose by a: Komagataeibacter rhaeticus PG2 strain isolated from pomegranate as a new host. RSC Adv 8:29797–29805. https://doi.org/10.1039/c8ra05295f

Tureck BC, Hackbarth HG, Neves EZ, et al (2021) Obtaining and characterization of bacterial cellulose synthesized by Komagataeibacter hansenii from alternative sources of nitrogen and carbon. Rev Mater 26:. https://doi.org/10.1590/S1517-707620210004.1392

Vasconcellos VM, Farinas CS (2018) The effect of the drying process on the properties of bacterial cellulose films from gluconacetobacter hansenii. Chem Eng Trans 64:145–150. https://doi.org/10.3303/CET1864025

Wang SS, Han YH, Chen JL, et al (2018) Insights into bacterial cellulose biosynthesis

from different carbon sources and the associated biochemical transformation pathways in Komagataeibacter sp. W1. Polymers (Basel) 10:. https://doi.org/10.3390/polym10090963

Yanti NA, Ahmad SW, Muhiddin NH (2018) Evaluation of inoculum size and fermentation period for bacterial cellulose production from sago liquid waste. J Phys Conf Ser 1116:. https://doi.org/10.1088/1742-6596/1116/5/052076

Yao H, Dai Q, You Z (2015) Fourier Transform Infrared Spectroscopy characterization of aging-related properties of original and nano-modified asphalt binders. Constr Build Mater 101:1078–1087. https://doi.org/10.1016/j.conbuildmat.2015.10.085

Yilmaz M, Goksungur Y (2024) Optimization of Bacterial Cellulose Production from Waste Figs by Komagataeibacter xylinus. Fibers 12:1–18. https://doi.org/10.3390/fib12030029

Zeng M, Laromaine A, Roig A (2014) Bacterial cellulose films: influence of bacterial strain and drying route on film properties. Cellulose 21:4455–4469. https://doi.org/10.1007/s10570-014-0408-y

Zeng X, Liu J, Chen J, et al (2011) Screening of the common culture conditions affecting crystallinity of bacterial cellulose. J Ind Microbiol Biotechnol 38:1993–1999. https://doi.org/10.1007/s10295-011-0989-5

CHAPTER 5

IMPACT OF HIGH-PRESSURE MICROFLUIDIZATION TREATMENT ON THE PROPERTIES OF BACTERIAL CELLULOSE DERIVED FROM THAI RED TEA KOMBUCHA

5.1 Abstract

This study investigates the effect of high-pressure microfluidization (HPM) on the characteristics of bacterial cellulose (BC) produced from optimized Thai red tea formulations. BC was purified, blended, and subjected to HPM at 10,000 Psi for 10, 15, and 20 cycles. The treatment significantly altered BC properties, reducing moisture content (96.85%–98.96%) and water-holding capacity (WHC), with untreated BC (96.58 ± 13.91 g/g) exhibiting higher WHC than HPM-treated samples (30.93 ± 3.05–31.04 ± 3.18 g/g). Fiber diameter decreased with increased HPM cycles, from 37 nm (untreated) to 24.99 nm (BCH-20-FD), especially in freeze-dried samples. Particle size analysis showed smaller, more uniform particles post-HPM, though polydispersity index and zeta potential indicated partial re-aggregation. Scanning electron microscopy (SEM) and X-ray diffraction (XRD) confirmed morphological and crystallinity changes, with freeze-drying enhancing fibril refinement and porosity, while oven-drying yielded denser structures. Thermogravimetric analysis (TGA) indicated reduced thermal stability in freeze-dried BC. These findings highlight HPM and drying as key factors influencing BC's physical, structural, and thermal properties, offering adaptable strategies for optimizing BC in various applications.

Keywords: Thai red tea, bacterial cellulose, high-pressure microfluidic, BC properties, freeze drying

5.2 Introduction

BC is a unique biopolymer distinguished by its high purity, biocompatibility, flexibility, nano-porosity, and biodegradability, setting it apart from plant-derived cellulose (Hussain et al. 2019; Yilmaz and Goksungur 2024). These attributes have led to its wide application across various industries, including food, packaging, cosmetics, biomedical, pharmaceutical, textiles, and electronics (Hussain et al. 2019; Zhong 2020; Choi et al. 2022). Its nanofibrillar network provides an excellent platform for developing advanced functional materials, particularly when modified through post-production treatments.

Although BC exhibits impressive native properties, its structure often requires further modification to meet the demands of specific industrial applications. High-pressure techniques such as high-pressure homogenization (HPH) and high-pressure microfluidization (HPM) have emerged as effective physical treatments for altering cellulose morphology. These methods apply intense shear forces under high pressure to reduce particle and fiber sizes, improving functionality (Wang et al. 2015; Mert 2020). Notably, HPM differs from HPH in its use of a specialized interaction chamber with microchannels, allowing for finer and more uniform particle breakdown through combined shear, impact, and cavitation forces (Guo et al. 2020).

Several studies have investigated the use of HPH and HPM to alter the structure and properties of cellulose, including BC. These treatments can modify critical characteristics such as fiber diameter, crystallinity index, and thermogravimetric properties, demonstrating significant potential for diverse applications (Wang et al. 2015, 2019a; Li et al. 2020; Suryanto et al. 2021; Muhajir et al. 2022). Specifically, HPH has been shown to reduce the crystallinity index and porosity of BC, especially at higher pressures (Muhajir et al. 2022). The number of HPH cycles is a critical factor influencing BC properties, affecting film tensile strength, surface roughness, porosity, crystallinity index, and crystallite size (Suryanto et al. 2021). Adjusting processing parameters such as pressure levels, number of cycles, and initial BC characteristics can

further refine BC properties. Increasing the number of HPH cycles progressively decreases fiber size, modifies crystallinity, and increases surface area, thereby influencing properties like water-holding capacity, mechanical strength, and rheological behavior (Suryanto et al. 2021; Muhajir et al. 2022). While HPH has been extensively studied, particularly for plant-based cellulose, research on the effects of HPM on BC properties remains limited.

This study aims to address this gap by investigating the impact of high-pressure microfluidization on BC produced from Thai red tea kombucha. Building on a previously optimized fermentation formula, the research evaluates structural and functional changes in BC under varying HPM conditions. The findings aim to contribute to the development of post-processing strategies that enhance BC's applicability across multiple sectors.

5.3 Materials and Methods

The materials and equipment used in this study include commercial kombucha starter (SCOBY) bought from Neo Cold Brew Shop (online market, Thailand), Thai red tea-vanila flavor *ChaTraMue* brand (RTC), commercial white sugar (sucrose), glucose, ethanol, sodium hydroxide (NaOH, Merck), Reverse osmosis (RO) water, Deionized (DI) water, cheesecloth, coffee filter, glass jar, funnel, autoclave, laboratory glassware, laminar air flow, analytical balance (Mettler Toledo), incubator, pH-meter (Oakton, pH 700), refractometer, Electric-Hydraulic Microfluidizer Processor Homogenizer (M-110EH-30, Microfluidics, USA), centrifugal machine (Avanti JXN-26, Beckman Coulter, USA), Oven dryer (XUE058, FRANCE ETUVES), freeze dryer (SJ-10N-60A Vacuum Freeze Dryer), FT-IR (Bruker VERTEX 70), XRD (Bruker D8 Advance), SEM/FESEM (Zeiss, AURIGA, Germany), TGA-instrument, and nano particle size and zeta potential analyzer (Malvern/Zetasizer-ZS).

5.3.1 Bacterial Cellulose Production

1) Medium Preparation and Fermentation

BC production was carried out based on the procedure outlined in the previous chapter (Chapter 3), using the optimized medium formula (RTC-V1) identified as the most suitable. The medium for Thai red tea kombucha fermentation consists of 7.97% (w/v) sucrose, 2.03% (w/v) glucose, 1.41% (w/v) Thai red tea, and 1.60% (v/v) ethanol, with a final volume of 2 to 4 liters per batch. The fermentation vessel was a plastic box measuring 44 x 31 x 12 cm (length x width x height).

Prior to BC production, an inoculum was prepared, comprising 10% (v/v) of the total fermentation medium. The inoculum was prepared using the RTC-C formula, which included 10% (w/v) sucrose and 1% (w/v) Thai red tea, inoculated with 10% of the culture from the previous fermentation, and incubated for 14 days. For medium preparation, sucrose and glucose were added to a 5L Duran bottle. Thai red tea was brewed with hot deionized water (approximately 90°C) to around 60% of the final volume for 15 minutes. The tea was then filtered using coffee filter paper, and the volume was recorded. The residue was further rinsed with a small amount of hot deionized water (approximately 90°C) and shaken for about 1 minute to complete the extraction, achieving a final volume of tea extract equal to 80% of the total volume. The tea extract was then poured into the Duran bottle with sucrose and glucose and mixed well. The solution was sterilized by autoclaving at 121°C and 1 psi for 15 minutes. After sterilization, the medium was allowed to cool to room temperature (35–40°C) before being inoculated with the prepared inoculum. The medium was carefully shaken, transferred from a 5 L Duran bottle to a plastic box, and fermented for 15 days at 30°C.

2) BC Harvesting and Purification

After 15 days of fermentation, the BC was carefully removed from the fermentation batch. The BC was then cut into small pieces, approximately 2 x 2 x 2 cm, depending on its thickness. The sample was boiled in water for 30 minutes,

drained for 10 minutes, and treated with a 2% NaOH solution at approximately 90°C for 120 minutes to remove impurities. Following this, the BC was thoroughly rinsed with reverse osmosis (RO) water and soaked in RO water with frequent changes until the pH became neutral (Yanti et al. 2018; Aswini et al. 2020). The purified BC was then stored for further processing and analysis.

5.3.2 Bacterial cellulose nanofibrilation

The purified BC slice was crushed using a blender. Approximately 250 grams of BC (wet weight) were placed in a blender, mixed with RO water at a ratio of 1:2, and ground for about 10 minutes. BC suspension was then separated using a stainless-steel strainer with a mesh size of approximately 2 x 2 mm. The resulting filtrate suspension was used for high-pressure micro-fluidization (HPM) treatment.

To investigate the effects of HPM, approximately 3000 ml of the BC suspension was processed using a high-pressure microfluidizer (M-110EH-30, Microfluidics, USA) at 10,000 psi for varying cycles: 10 cycles (BCH-10), 15 cycles (BCH-15), and 20 cycles (BCH-20). The resulting BC nanofibers (BCNFs)/BCH were separated by centrifugation at 6000 rpm for 30 minutes at 25°C using a centrifuge (Avanti JXN-26, Beckman Coulter, USA). A sample of the BC suspension without HPM treatment was also centrifuged under the same conditions and labeled as BCP (BC-pulp). The sample of BCP and BCH were stored in jars at a temperature of 4–6°C. For analysis, some of the BCNFs samples were dried using two different methods: oven drying at 40°C and freeze-drying.

5.3.3 Characterization of BC and BCNFs

1) Moisture Content and WHC

The WHC of the samples was determined by drying the purified BC and BCNFs samples. For BC, approximately one slice of purified samples weighing about 10 grams per slice was used, while for BC pulp and BC-HPM, around 5.00 grams (wet weight) of samples were prepared. All samples were dried in an oven at 40°C until a constant dry weight was achieved. The measurements were performed in triplicate,

and the moisture content and WHC were calculated using Equations below (**Eq. 5.1 and Eq. 5.2**).

$$Moisture\ content = \frac{wet\ wight - dry\ weight}{wet\ weight}\ x\ 100\% \quad \text{.....(Eq. 5.1)}$$

$$WHC = \frac{wet\ wight - dry\ weight}{dry\ weight} \quad \text{.....(Eq. 5.2)}$$

2) Characterization of BC Particles

BC-pulp and BC-HPM samples were prepared for particle size analysis by dispersing them 50 times. Specifically, 1 gram of each sample was diluted in a 50 ml volumetric flask with deionized (DI) water. The sample was stirred at 300 rpm for 15 minutes, sonicated for 10 minutes, and then stirred again for 10 minutes. The size distribution of nanoparticles was measured using a Malvern Zetasizer Nano ZS (Malvern Instruments Ltd., UK) employing the dynamic light scattering (DLS) technique. The parameters for the BC sample were set to an absorption of 0.0000 and a refractive index of 1.618, while the dispersant (water) parameters were set to a refractive index of 1.330 and a viscosity of 0.8882 cP. The analysis was performed at a temperature of 25°C, using a disposable sizing cuvette, with a measurement duration of 60 seconds and a measurement position of 4.65 mm. The size distribution graphs were recorded.

The samples were diluted 100 times for zeta potential analysis and prepared using the same procedure as for particle size analysis. The dispersant (water) parameters were set to a refractive index of 1.330, a viscosity of 0.8872 mPa.s, and a dielectric constant of 78.5. The analysis was conducted at a temperature of 25°C using a zeta dip cell, with 12 zeta runs and a measurement position of 4.5 mm.

3) Other Characterization of BC

Additional characterization of BC was performed using SEM, FTIR, XRD, and TGA. The detailed methods and procedures for these analyses are provided in **Chapter 3** of this thesis.

5.3.4 Statistical Analysis

Analysis of variance was carried out using Ms. Excel software. The differences between the mean values were analyzed using least significant difference (LSD) test and the significance level was set at $P < 0.05$.

5.4 Results and Discussion

5.4.1 Moisture Content and Water Holding Capacity

The moisture content and water-holding capacity (WHC) of the BC samples, including purified BC sheets (BCC), centrifuged blended BC suspensions (BCP), and centrifuged microfluidized BC suspensions (BCH-10, BCH-15, and BCH-20), are summarized in **Table 5.1.**

Table 5.1 Moisture content and WHC of BC pulp and microfluidized BC

Samples	Moisture content (%)	WHC (g water/g cellulose)
BCC	98.96±0.15	96.58±13.91
BCP	97.60±0.11	40.70±1.93
BCH-10	96.85±0.32	30.93±3.05
BCH-15	96.86±0.24	31.01±2.53
BCH-20	96.87±0.21	31.04±2.21

The moisture content of the samples ranged from 96.85% to 98.96%. BCC exhibited the highest moisture content (98.96±0.15%), indicating its high capacity to retain water in its purified sheet form. In contrast, BCP, a centrifuged BC suspension, had slightly lower moisture content (97.60±0.11%), likely due to partial dehydration during the centrifugation process. The microfluidized BC samples (BCH-10, BCH-15, BCH-20) showed the lowest moisture content, ranging from 96.85% to 96.87%.

The reduction in moisture content in BCP and microfluidized samples can be attributed to mechanical processes such as blending and HPM. The blending process applies mechanical shear forces that partially disrupt the cellulose network,

reducing its ability to retain water. HPM further intensifies this structural disruption, leading to enhanced water release. Additionally, the centrifugation process expels loosely bound water through centrifugal force. Similar effects of mechanical processing on cellulose structure and water retention have been reported (Betlej et al. 2021). Despite these reductions, the high overall moisture content in all samples reflects the inherently hydrophilic nature of BC, attributed to its porous, three-dimensional network structure (Fang and Catchmark 2014; Gayathry and Gopalaswamy 2014; R. Rebelo et al. 2018; Widyastuti and Kartika Fitri 2023). Variations in moisture content among the samples underscore the significant role of processing techniques in modulating BC's water retention properties.

WHC values showed significant variation among the samples, ranging from 96.58±13.91 g water/g cellulose in BCC to 30.93±3.05 g water/g cellulose in BCH-10. BCC demonstrated the highest WHC, reflecting its intact, undisturbed network structure in sheet form, which can trap and retain a large amount of water. On the other hand, BCP, with a WHC of 40.70±1.93 g water/g cellulose, exhibited a lower capacity due to partial disruption of the network due to the centrifugation, which reduced the size of BC, its porosity, and water retention ability. The microfluidized BC samples (BCH-10, BCH-15, BCH-20) showed the lowest WHC, approximately 30.93–31.04 g water/g cellulose. This significant reduction in WHC can be attributed to the microfluidization process, which breaks down the cellulose fibers into smaller fragments and disrupts the interconnected network. The mechanical forces during homogenization reduce porosity and the surface area available for water entrapment (Suryanto et al. 2021; Muhajir et al. 2022; Tomkowiak et al. 2024). The similarity in WHC values among the microfluidized samples suggests that the degree of microfluidization (10, 15, or 20 passes) had minimal additional impact on WHC beyond the initial disruption caused by the process.

5.4.2 Particle Analysis

The particles of BCP and microfluidized BC samples were analyzed for particle size distribution, polydispersity index, and zeta potential. The results of the particle analysis are summarized in **Table 5.2**, with the particle size distribution also visualized in graphical form (**Figure 5.1**).

Table 5.2 Results of polydispersity index analysis of BC from different mechanical treatments

Samples	diameter average (nm)			% intensity			PDI	ZP (mV)
	peak 1	peak 2	peak 3	peak 1	peak 2	peak 3		
BCP	4968.33	132.23	1.39	69.53	27.67	2.80	0.997	-14.133
	±208.80	±52.11	±2.41	±6.71	±3.21	±4.85	±0.01	±1.60
BCH-10	4570.67	253.80	25.63	51.83	37.23	8.87	0.813	-5.830
	±177.39	±16.60	±11.95	±4.20	±1.84	±2.15	±0.09	±0.43
BCH-15	5501.67	248.90	19.62	28.07	62.37	9.77	0.993	-6.773
	±101.04	±20.87	±10.10	±1.77	±15.79	±1.46	±0.01	±0.167
BCH-20	247.43	34.81	10.07	58.53	33.90	7.57	0.935	-5.357
	±72.61	±26.59	±8.86	±0.64	±40.41	±1.74	±0.07	±0.94

BC suspensions showed significant differences in particle size distribution between non-microfluidized (BCP) and microfluidized (BCH) samples. BCP exhibited a broad size distribution with large aggregates (4968.33 ± 208.80 nm) and smaller peaks (132.23 ± 52.11 nm and 1.39 ± 2.41 nm), indicating high polydispersity. Micro-fluidized samples showed progressive size reductions: BCH-10 had peaks at 4570.67 ± 177.39 nm, 253.80 ± 16.60 nm, and 25.63 ± 11.95 nm; BCH-15 had peaks at 5501.67 ± 101.04 nm, 248.90 ± 20.87 nm, and 19.62 ± 10.10 nm; BCH-20 showed the most significant reduction with peaks at 247.43 ± 72.61 nm and smaller peaks dominating the distribution. These results confirm that high-pressure, especially HPM, effectively reduces BC aggregates, producing smaller, more uniform particles,

consistent with previous studies on biopolymer suspensions (Suryanto et al. 2021; Muhajir et al. 2022).

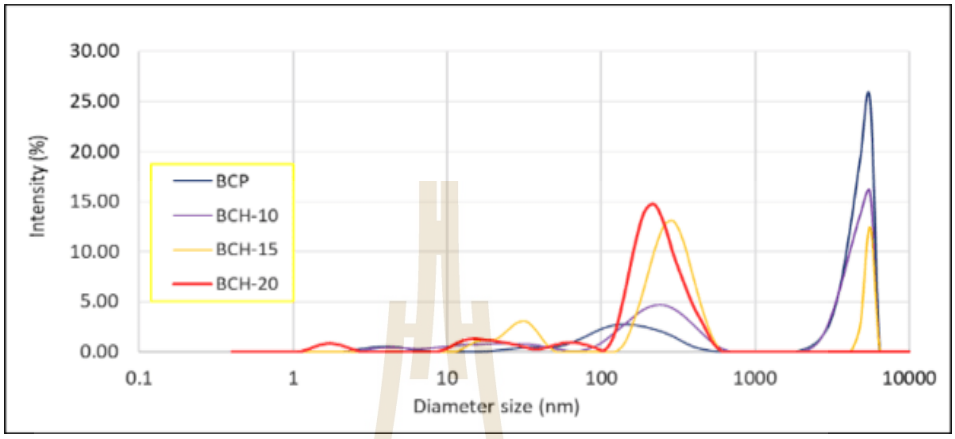

Figure 5.1 Graph of poly distribution particle size from BC-Pulp and microfluidized BC suspension

The polydispersity index (PDI) further supports these observations. The BCP sample exhibited a PDI of 0.997 ± 0.01, confirming its highly polydisperse nature. With microfluidization, the PDI values decreased, indicating improved uniformity in particle size distribution. BCH-10 had a PDI of 0.813 ± 0.09, reflecting the reduction in size variability. However, BCH-15 showed a slight increase in PDI to 0.993 ± 0.07, likely due to the dominance of a large primary peak alongside smaller peaks, suggesting partial re-aggregation during processing. BCH-20 exhibited a PDI of 0.935 ± 0.07, indicating a relatively uniform size distribution compared to BCP but still reflecting a polydisperse system. The PDI value ranges from 0.0, indicating a perfectly uniform sample in terms of particle size, to 1.0, representing a highly polydisperse sample with a wide range of particle size populations (Danaei et al. 2018). A similar trend of the result was also reported in a study. Microfluidized BC with HPM in 1, 10, and 25 cycles has a PDI value of 1.000, 0.154, and 0.551 (Dima et al. 2017).

The ZP values provide insights into the stability of BC suspensions. The BCP sample exhibited a ZP of -14.133 ± 1.60 mV, indicating moderate stability due to limited electrostatic repulsion between particles. After microfluidization, BCH-10

showed a slight improvement to -5.830 ± 0.43 mV, while BCH-15 and BCH-20 had the ZP values of -6.773 ± 0.167 mV and -5.357 ± 0.94 mV, respectively. Despite significant size reduction, the relatively low ZP values across all samples indicate that microfluidization does not enhance suspension stability. A ZP of at least ±30 mV is typically required for high colloidal stability (Yan et al. 2016). For comparison, previous studies reported ZP values of -10.4, -10.2, and -13.1 mV for microfluidized BC after 1, 10, and 20 passes, respectively (Dima et al. 2017).

Information on the specific effects of HPM on the size, PDI, and zeta potential of BC remains limited in previous studies. However, some research has explored nanoparticle synthesis from BC using alternative methods. For instance, nanocellulose produced through a wet milling process followed by chemical and filtration treatments exhibited average particle sizes of 44.06 nm (peak 1), 132.1 nm (peak 2), and 637.4 nm (peak 3), with PDIs of 10.4%, 16.9%, and 12.8%, respectively (Nurfadila et al. 2019). Similarly, BC aqueous suspensions treated with HCl hydrolysis yielded BC nanoparticles (BCNPs) with average sizes of 590.9 nm and 221.4 nm for untreated and treated samples, respectively, PDIs of 0.37 and 0.18, and zeta potentials of −21.36 ± 3.32 mV and −39.50 ± 4.01 mV, respectively (Zhai et al. 2020). Additionally, BCNPs produced via shaking methods followed by alkaline treatment, dialysis, sonication with polysorbate 80 surfactant, and filtration through a 200 nm syringe filter showed a particle size of 478.9 ± 129.6 nm and a zeta potential of −14.1 ± 4.2 mV, closely matching values reported in this study (Balistreri et al. 2024).

In summary, HPM had variable effects on BC suspensions. BCH-20 demonstrated a significant reduction in particle size, indicating the effectiveness of HPM in breaking down aggregates. However, the PDI of BCH-15 and BCH-20 remained comparable to that of BCP, suggesting inconsistent improvements in size uniformity across the samples. Additionally, the low ZP values observed for all samples indicate limited electrostatic stabilization, pointing to poor suspension stability. These findings emphasize the need for further optimization, such as incorporating stabilizing agents,

surfactants, or pH adjustments, to enhance both the stability and functionality of BC suspensions, which are critical for their application in industrial and biomedical fields.

5.4.3 BC Morphology

The SEM images show the structural differences in BC sheets after various treatments (Figure 6.2). These include HPM at 10, 15, and 20 passes and two drying methods: oven-dried and freeze-dried. The non-microfluidized BC (BCP-O and BCP-FD) displays dense and compact fibril networks, with the freeze-dried sample showing slightly more porosity than the oven-dried sample. After microfluidization, BCH-10-O shows disrupted fibril arrangements, while BCH-10-FD has a more open and porous structure. In BCH-15 and BCH-20, higher microfluidization intensity causes finer and more fragmented fibril networks. Freeze-dried samples are consistently more porous and less compact than oven-dried ones, showing the drying method strongly affects the microstructure. The BCC samples, used as a control, demonstrate a well-preserved fibril network in the oven-dried state. These results highlight the significant influence of microfluidization intensity and drying methods on the BC microstructure. Higher microfluidization intensities lead to finer and more fragmented fibril networks, while freeze-drying, observed in other samples, promotes a more porous morphology. The result of this study is in accordance with the previous study on the effect of HPM (Suryanto et al. 2021; Muhajir et al. 2022) and on the effect of different drying method (Zhang et al. 2011; Andree et al. 2021; Mohamad et al. 2022b).

The SEM image analysis was further utilized to determine the fiber diameter of BC. The results are summarized in **Table 5.3**, while the graphs illustrating the fiber size distribution of BC are presented in **Figure 5.2.**

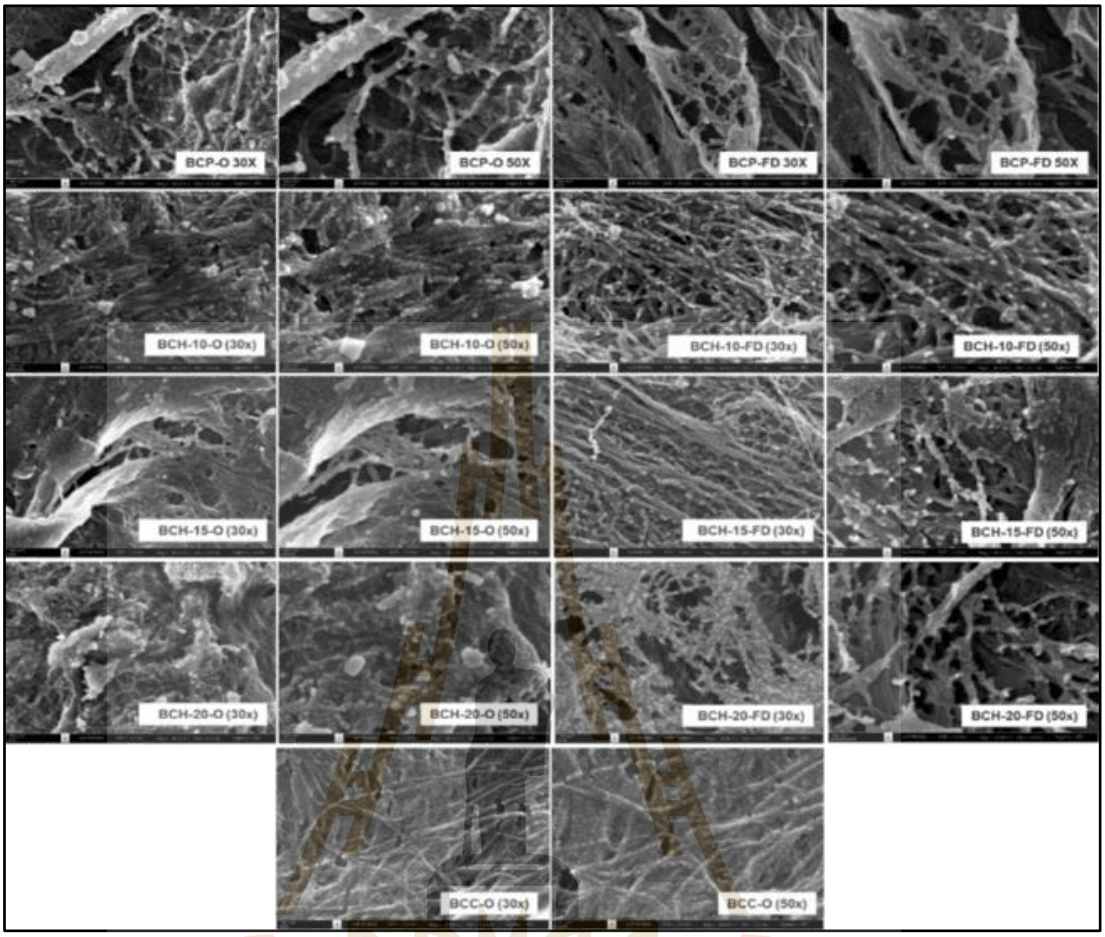

Figure 5.2 SEM image of BC sample BC sheet (BCC), BCP, HPM1, HPM2, dan HPM3. The symbol of O (oven drying), and FD (freeze dried)

Table 5.3 Resume of the diameter size of the dried BC samples with different mechanical treatment and drying methods.

	Diameter (nm)								
	Oven Dried (O)					Freez Dried (FD)			
	BC-C	BCP	BCH-10	BCH-15	BCH-20	BCP	BCH-10	BCH-15	BCH-20
Mean	37.00	37.15	31.61	30.57	26.72	33.26	31.33	26.71	24.99
Min.	26.65	23.80	18.87	23.32	19.24	24.67	22.28	18.78	16.49
Max.	51.24	53.76	46.75	45.24	35.06	46.30	39.68	39.78	39.24
Sd	4.77	7.18	6.38	4.55	3.92	5.17	4.46	4.06	3.98

Min = minimum, Max = maximum, Sd = standard deviation

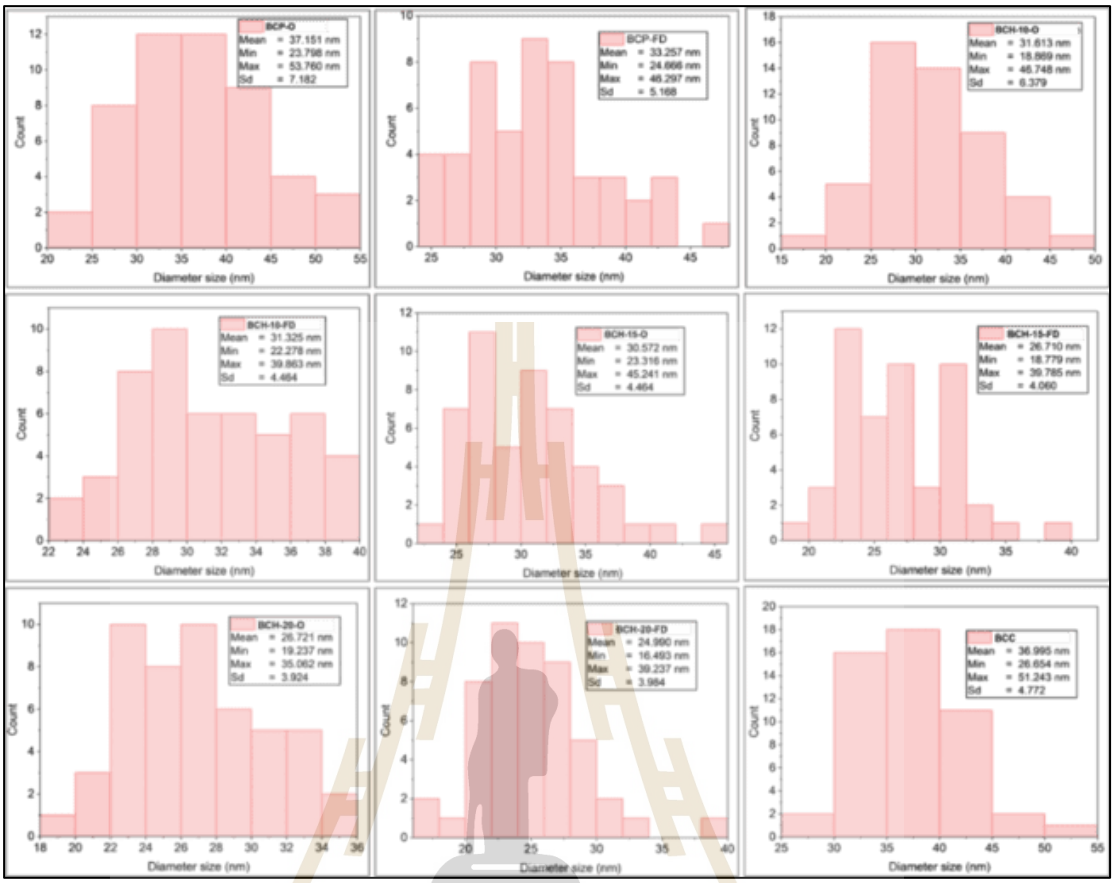

Figure 5.3 Fiber size distribution of BC-C, BCP, and microfluidized BC samples (BCH-10, BCH-15, and BCH-20), with "O" indicating oven-dried and "FD" indicating freeze-dried samples.

The BCC-O (control) and BCP-O samples have similar average fiber diameters of around 37 nm, while the BCP-FD sample is slightly smaller at 33.26 nm. As microfluidization intensity increases, the average fiber diameter decreases. The BCH-10-O and BCH-10-FD samples have average diameters of 31.61 nm and 31.33 nm, respectively. With stronger microfluidization, the diameters shrink further, with BCH-15-O and BCH-15-FD averaging 30.57 nm and 26.71 nm, respectively. The smallest diameters are in BCH-20-O and BCH-20-FD samples, with averages of 26.72 nm and 24.99 nm. Freeze-dried samples consistently have smaller fibers than oven-dried ones, indicating that the drying method affects fiber size. Standard deviations show less variation in fiber size with higher microfluidization, suggesting more uniform fiber sizes. The narrowing size range supports this trend.

The finding of this study is comparable with some of the previous studies. The HPH of 150 bar and 5 cycles effectively reduced the diameter of BC fiber size from a range of 75 to 100 nm into the range size of 30 to 35 nm (Sardjono et al. 2019). The HPH in 150 bar pressure decrease diameter of fiber size from 61.7±36.98 nm (control) to 53.24±27.05, 49.82±19.32, 47.2±15.34, and 46.38±17.18 nm for 5, 10, 15, and 20 cycles, respectively (Suryanto et al. 2021). This study indicates that microfluidization can effectively reduce the fiber size of BC, with freeze-drying resulting in more porous and smaller fibers compared to oven drying.

5.4.4 Fourier Transform Infrared Spectroscopy (FT-IR) Analysis

The FTIR spectra reveal slight differences among BC samples, including BCC, BCP, and microfluidized samples (BCH-10, BCH-15, BCH-20), with oven-dried (O) and freeze-dried (FD) treatments (**Figure 5.4(a, b, and c)**. A prominent band around 3430 and 3234 cm cm^{-1} corresponds to O–H stretching vibrations, indicating hydrogen bonding in the cellulose structure. The signal at approximately 2890 cm^{-1} arises from C–H stretching in CH_2 groups (Suryanto et al. 2021). Two distinct bands at 2360 and 2324 cm cm^{-1} suggest the presence of triple-bond functional groups, such as C≡C or C≡N, which may originate from polyphenols, organic compounds, proteins, yeast cells, or bacteria (Amarasekara et al. 2020; Srivastava and Mathur 2022). These bands were previously observed in BC produced with ethanol or sucrose-glucose combinations in the fermentation medium (reported in previous chapter). Similar findings have been reported in studies on nata de coco-derived BC, where residual proteins, nucleic acids, and microbial cells contributed to these signals (Fuller et al. 2018; Rachtanapun et al. 2021). The presence of these impurities in the BC matrix may be due to the thick and dense structure of the pellicle, which can impede their complete removal during the purification process.

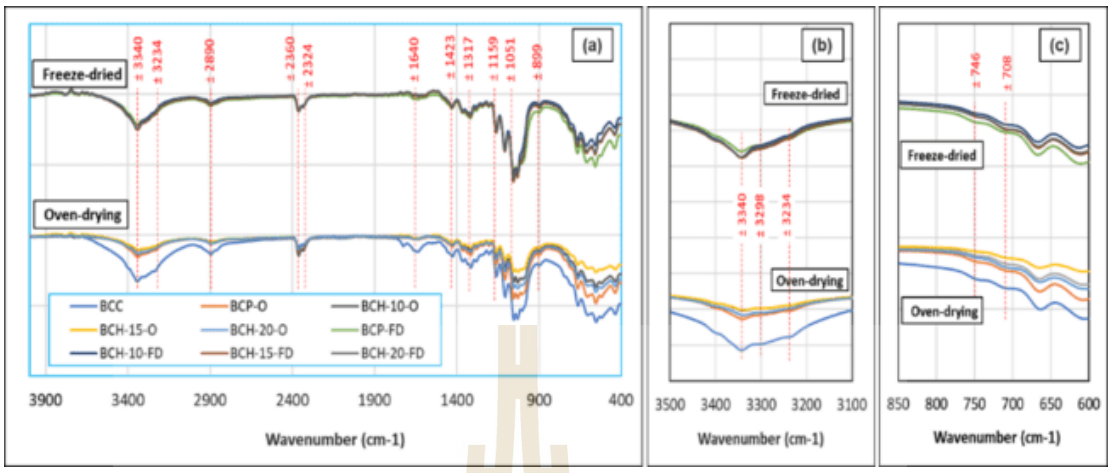

Figure 5.4 FTIR spectra of BC-C, BCP, and microfluidized BC samples (BCH-10, BCH-15, and BCH-20), with "O" indicating oven-dried and "FD" indicating freeze-dried samples

The band observed around 1640 cm^{-1} expressed the O-H signal of absorbed water (Suryanto et al. 2021). The band observed at 1427 cm^{-1} represents CH_2 symmetric bending, while the band at 1364 cm^{-1} corresponds to C-H symmetric bending (Fatima et al. 2023; Liu et al. 2023). In the fingerprint region between 1330 and 500 cm^{-1}, several distinct bands were observed, including those at approximately 1317, 1169, 1051, and 898 cm^{-1}. The band near 1317 cm^{-1} is associated with CH_2 wagging at the C-6 position (Liu et al. 2023) or could correspond to C–OH deformation vibrations (Wu et al. 2014). The band observed at 1051 cm^{-1} and 1028 cm^{-1} is associated with C-O-C stretching vibrations within the sugar ring (Liu et al. 2023). Additionally, the band at around 899cm^{-1} corresponds to C-O-C stretching in β-1,4-glycosidic linkages, signifying the presence of an amorphous absorption band (Ciolacu et al. 2011). The characteristic signals observed at 899 cm^{-1} and approximately 1423 cm^{-1} confirm that the samples are of cellulose type I (Kawee et al. 2018).

Mechanical treatment significantly impacts the FTIR spectral intensity of BC samples. The BCP and the BCH, processed using HPM, display a progressive reduction in peak sharpness and intensity compared to the untreated control sample (BCC). Prominent changes are observed in peaks around 3340 cm^{-1} (O–H stretching),

2890 cm^{-1} (C–H stretching), and 1159–1051 cm^{-1} (C–O–C and C–O stretching). Despite these intensity differences, the spectra retain the characteristic features of cellulose type I. The FTIR results indicate that although there is a slight reduction in transmittance peak intensity, the HPM process does not impact the chemical group of the BC sample. This result align with the previous finding (Kawee et al. 2018; Suryanto et al. 2021; Mohamad et al. 2022b).

The reduced intensity of the peaks at 3340 cm^{-1} and 3234 cm^{-1}, corresponding to hydroxyl group stretching vibrations, may result from the high pressure during HPM, which disrupts the cellulose network and induces defibrillation into nanofibrils (Kawee et al. 2018). The decrease in O–H bonding intensity is likely associated with the smaller fiber size, which limits the formation of extensive hydrogen bonding networks. The increased surface area exposes more hydroxyl groups that are not strongly bound within the network, further contributing to the observed reduction. These structural changes may lower the density of the crystalline structure, decreasing the number of O–H bonds. Additionally, smaller fibers are less capable of retaining bound water, which may also explain the reduced O–H stretching intensity observed in the spectra (Kawee et al. 2018).

The drying method significantly influences the intensity of the FTIR spectra of BC. In the 3000–3500 cm^{-1} region, corresponding to O–H stretching vibrations associated with hydrogen bonding in cellulose, freeze-dried samples exhibit sharper and more defined peaks compared to oven-dried ones. This suggests that freeze-drying affects the hydrogen bonding network differently, potentially preserving more hydroxyl groups in a less disrupted state. A similar phenomenon is observed in the 900–1200 cm^{-1} region, associated with C–O–C stretching and C–H deformation vibrations of the cellulose backbone. The more pronounced peaks in freeze-dried samples may indicate a looser, less compact structure with greater distances between cellulose macromolecules, leading to weaker hydrogen bonds (Zhang et al. 2011). These findings are consistent with previous studies (Zhang et al. 2011; Mohamad et al. 2022b).

5.4.5 X-Ray Diffraction (XRD) Analysis

The XRD patterns, (**Figure 5.5**), illustrate the effects of mechanical treatment, particularly HPM, and drying methods (oven-drying and freeze-drying) on the crystalline structure of BC. All the BC samples exhibit crystalline peaks characteristic of cellulose type I, with prominent reflections at 2θ values of ~14.56°, 16.72°, and 22.80°, corresponding to the (100), (010), and (110) crystallographic planes, respectively (Gaspar et al. 2014). The most intense peak, near 23°, is a defining feature of cellulose type I (Said Azmi et al. 2023; Hossen et al. 2024), confirming its crystalline structure (Samuel and Adefusika 2019). While the peak positions are consistent across samples, variations in their relative intensities and overall crystallinity indicate differences in cellulose chain orientation and structural properties (Said Azmi et al. 2023).

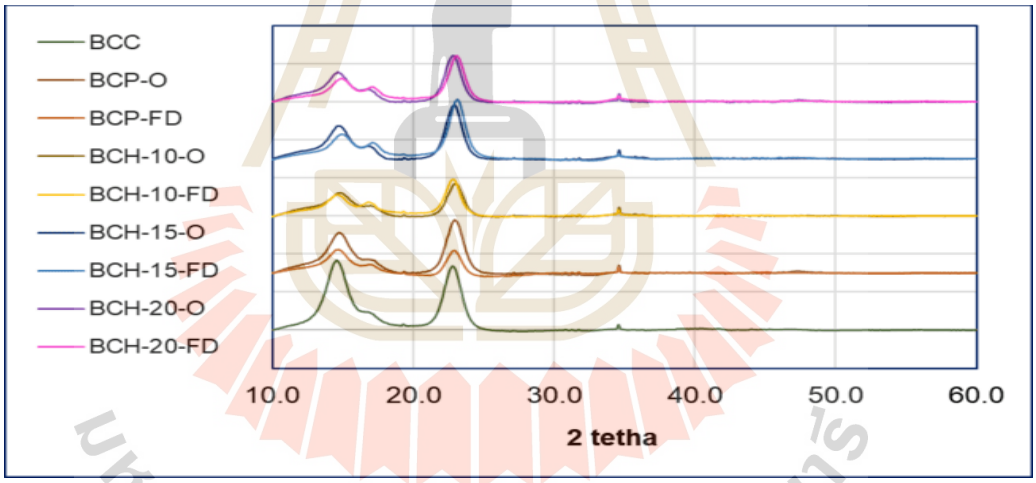

Figure 5.5 XRD spectra from the BC samples with different mechanical treatments and drying methods.

After mechanical treatments (BCP and BCH), a noticeable reduction in peak intensity and sharpness is observed, especially in BCH samples, indicating partial disruption of the crystalline structure. This disruption is attributed to defibrillation and fiber size reduction caused by HPM, which alters the ordered hydrogen bonding network in cellulose and lowers crystallinity (Kawee et al. 2018; Suryanto et al. 2021; Muhajir et al. 2022). Supporting data show that BCP and BCH samples have lower

crystallinity indices (CI) compared to the control (BCC), with BCH samples exhibiting progressively lower CI as the number of HPM cycles increases (Table 4). Previous studies align with these findings: the CI of BC and BCNFs after 10, 20, and 30 HPH cycles decreased from 85.65% to 76.99% (Kawee et al. 2018), while HPM pressures of 0–600 bar reduced CI from 87% to 70% (Muhajir et al. 2022). Similarly, BCNFs subjected to 5–20 HPH cycles at 150bar showed a CI decrease from 83% to 74% (Suryanto et al. 2021). These results confirm that increasing HPM intensity reduces the crystallinity of BC fibers.

Comparing the drying methods, freeze-dried samples (denoted by "-FD") exhibit broader and less intense peaks compared to oven-dried samples ("-O"). Freeze-drying appears to create a looser structure, possibly due to the sublimation of water, which minimizes compression and retains a more disordered arrangement of cellulose molecules. This aligns with the crystallinity index results, where freeze-dried samples generally have lower crystallinity compared to oven-dried counterparts (Zhang et al. 2011). Oven-drying, in contrast, may promote tighter packing of cellulose chains due to water removal under thermal conditions, preserving or even enhancing crystalline regions.

Further analysis of the XRD data reveals the average crystallite size of BC under various processing conditions, as summarized in **Table 5.4**. The data highlight the influence of HPM and drying methods on the crystalline structure of BC. Among the oven-dried samples, BCC (control) exhibits the largest crystallite size at 3.46 nm, indicating the crystalline domains remain largely undisturbed. In the case of BCP-O, the crystallite size decreases slightly to 3.41 nm, likely due to the blending processes. These treatments introduce mild mechanical forces, which may cause minor disruption to the crystalline regions without significant structural alteration. A more pronounced reduction in crystallite size is observed in BCH-10-O (3.08 nm), the lowest among oven-dried samples. This reduction is attributed to the mechanical shear forces exerted during 10 cycles of HPM, which fragment the cellulose fibrils and disrupt the crystalline

structure. Interestingly, additional HPM cycles (15 and 20) lead to an increase in crystallite size to 3.45 nm and 3.46 nm, respectively, nearly returning to the control value. This phenomenon suggests that extended mechanical treatment may promote reorganization or partial aggregation of cellulose chains during oven drying.

Table 5.4 Crystallinity index and average crystallite size of dried BC with various mechanical treatment and drying methods

Samples	Average Crystallite Size (nm)	Crystallinity Index (%)
BCC	3.46	86.33
BCP-O	3.41	82.73
BCP-FD	2.01	80.48
BCH-10-O	3.08	81.82
BCH-10-FD	2.16	74.69
BCH-15-O	3.45	78.75
BCH-15-FD	2.17	73.35
BCH-20-O	3.46	78.28
BCH-20-FD	2.14	71.82

For freeze-dried samples, the crystallite sizes are consistently smaller than oven-dried sample, highlighting the significant impact of the freeze-drying process on BC's crystalline structure. BCP-FD shows the smallest crystallite size (2.01 nm), indicating that the sublimation process during freeze drying disrupts hydrogen bonding and crystalline domains more effectively. BCH-10-FD, BCH-15-FD, and BCH-20-FD exhibit a slightly larger crystallite size (2.16 nm, 2.17 nm, and 2.14 nm, respectively) compared to BCP-FD, but it is still significantly smaller than oven-dried samples with little variation among them. This suggests that freeze drying limits the potential for chain reorganization regardless of the number of HPM cycles.

In summary, HPM reduces crystallite size by fragmenting fibrils, with the greatest reduction at 10 cycles (BCH-10). Beyond 10 cycles (15 and 20), some recovery

occurs during oven drying, likely due to chain reorganization. Freeze drying consistently produces smaller crystallites, as the sublimation process limits chain reorganization. The smallest crystallite size is in BCP-FD (2.01 nm), while BCH-10-O has the lowest crystallite size (3.08 nm) among oven-dried samples.

5.4.6 Thermogravimetric (TGA/DTG) Analysis

The TGA and DTG results in **Figure 5.6** and **Table 5.5** show how mechanical treatments and drying methods affect the thermal stability and decomposition of BC from Thai red tea kombucha. The control sample (BC-C), which was oven-dried without mechanical treatment, is used as a baseline for comparison. These results highlight the impact of different processes on the thermal behavior of BC.

Thermogravimetric analysis reveals that the thermal decomposition of BC occurs in two main stages. The first stage, occurring below 150°C, corresponds to the evaporation of moisture physically bound to the BC (Teixeira et al. 2019; Mohamad et al. 2022a). The second stage, spanning from 250°C to 600°C, involves the thermal degradation of cellulose, including the breakdown of glycosidic bonds, depolymerization, and the release of volatile compounds, followed by the oxidation of residual cellulose and β-glucan chains into carbonaceous char (Mohammadkazemi et al. 2015; Teixeira et al. 2019; Mohamad et al. 2022a). The effect of mechanical treatment, including HPM, appears minimal in samples subjected to oven drying (**Figure 5.6(a)**). Within these oven-dried samples, HPM cycles show only a subtle impact on peak degradation temperatures, with higher cycles causing slight shifts in the degradation profiles (**Figure 5.6(b)**). The first weight loss ranged from 4.68% to 5.69%, while the second weight loss ranged from 71.63% to 73.89%, leaving a residual weight between 21.23% and 22.82%. These findings are corroborated by the DTG analysis **(Figure 5.6(d)** and **(e)**), which shows that the maximum degradation temperatures (DTG max) for all oven-dried samples are within a comparable range of approximately 275–385°C. The DTG T_{Max} values are closely clustered, spanning from

341.67°C to 343.67°C. Compared to freeze-dried samples (e.g., BC-P-FD and BC-HPM10-FD), which exhibit higher DTG T_{Max} values (ranging from 356°C to 371.17°C), oven-dried samples (e.g., BC-P-O and BC-HPM10-O) demonstrate slightly lower peak thermal stability. However, oven-dried samples exhibit higher onset degradation temperatures, likely due to their denser structure, which may provide greater resistance to initial decomposition.

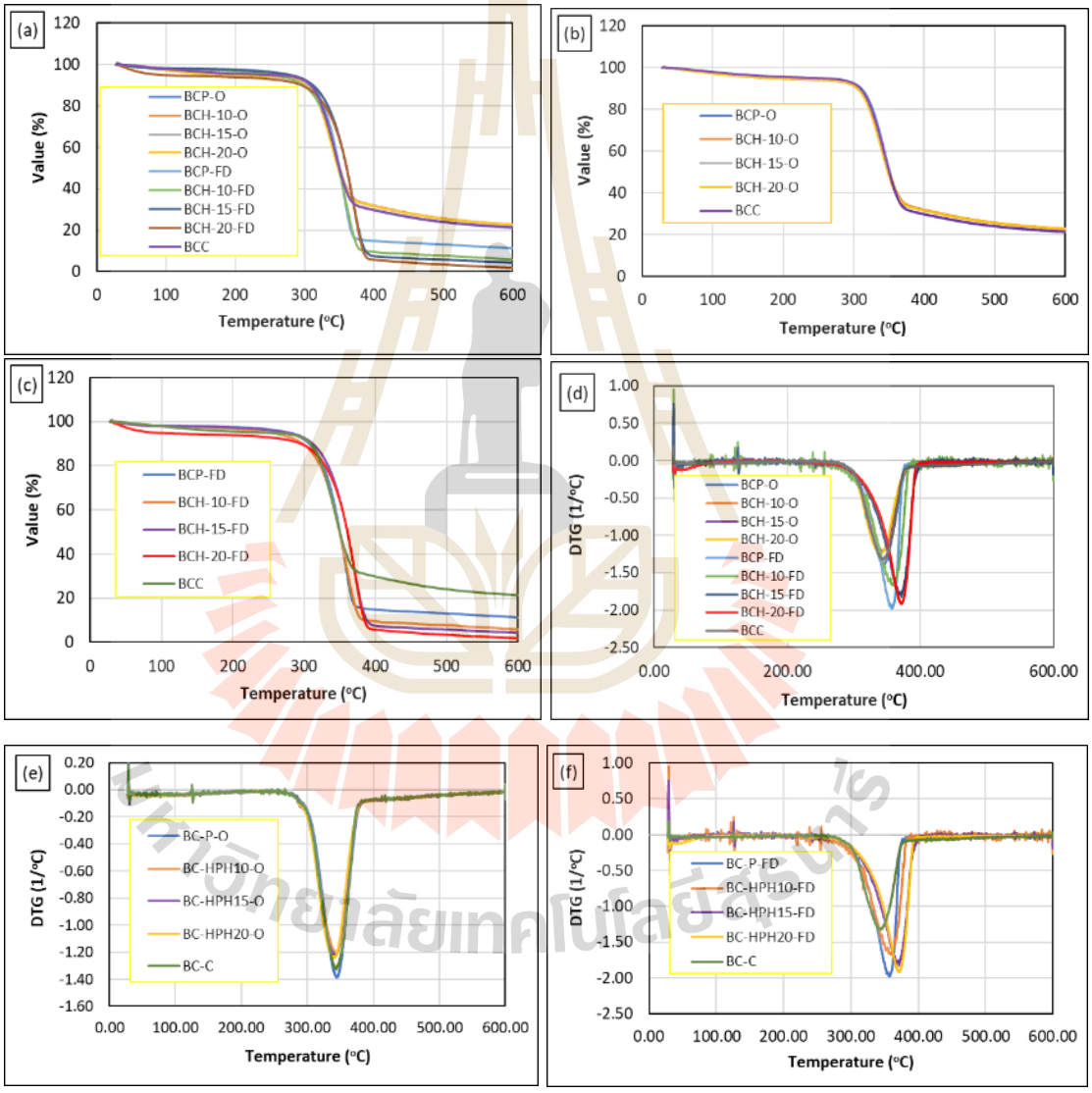

Figure 5.6 TGA (a) and DSC (b) results of dried BC from optimized RTC kombucha with various treatments and drying methods.

Table 5.5 Detail parameter of TGA/DTG analysis of BC samples with different mechanical treatments and drying methods

Samples	First stage weight loss (%)	Second stage weight loss (%)	Residue (%)	DTG Peak range (°C)	DTG T_{Max} (°C)
BCC	4.68	73.86	21.43	275 – 385	342.67
BCP-O	4.86	73.89	21.23	275 – 385	343.67
BCP-FD	2.80	85.80	11.31	285 - 382	356.67
BCH-10-O	5.52	71.63	22.82	275 – 385	343.17
BCH-10-FD	3.55	90.46	5.85	265 - 385	359.17
BCH-15-O	5.69	71.76	22.53	275 – 385	342.17
BCH-15-FD	3.09	92.55	4.25	266 - 403	371.17
BCH-20-O	5.59	71.77	22.73	275 – 385	341.67
BCH-20-FD	6.53	91.50	1.93	265 - 399	371.17

In contrast, samples prepared using freeze-drying methods show more varied TGA and DTG results across all samples. Mechanical treatments significantly influence these analysis results. Microfluidized BC samples (BCH-10-FD, BCH-15-FD, BCH-20-FD) exhibit higher weight loss during the second stage of decomposition and leave less residual material after cellulose decomposition at 600°C (Figure 6(a)). As the number of HPM cycles increases, the weight loss becomes greater, and the residual values decrease (Figure 6(c)). The DTG profiles of freeze-dried samples vary considerably, with peak temperatures ranging from approximately 265°C to 403°C. The DTG T_{Max} values for these samples fall between 356°C and 371.17°C, which are relatively higher than those of oven-dried samples. While freeze-dried samples are more porous, their DTG T_{Max} values indicate that they can exhibit higher peak degradation temperatures than oven-dried samples. This suggests that while porosity might accelerate degradation under direct flame exposure, the intrinsic stability of the material in controlled thermal analysis may be slightly better due to structural

modifications. Freeze-dried samples also display sharper DTG peaks compared to oven-dried samples, suggesting a faster degradation rate due to their porous structure resulting in a lower effect of flame retardant (Dai et al. 2018; Mohamad et al. 2022b). The porous structure is a result of sublimation during the freeze-drying process. Overall, freeze-drying combined with mechanical treatments reduces the thermal stability of BC compared to oven drying.

5.5 Conclusion

This study demonstrates that mechanical treatment, particularly high-pressure microfluidization (HPM), plays a critical role in modifying the physicochemical, structural, and thermal properties of bacterial cellulose (BC). HPM treatment led to a significant decrease in moisture content and water holding capacity (WHC), likely due to the disruption of the cellulose fiber network. Notably, the highest WHC was observed in the untreated BC (96.58 ± 13.91 g water/g cellulose), whereas microfluidized samples exhibited markedly lower capacities.

Increasing HPM cycles resulted in reduced fiber diameters, from 37 nm in the control to 24.99 nm in the most treated samples. The method of drying also influenced BC morphology: freeze-drying produced finer fibrils and enhanced porosity, while oven drying led to denser structures. Particle size analysis confirmed that HPM generated smaller and more uniform particles, although PDI and zeta potential values indicated moderate stability due to partial re-aggregation.

Structural modifications were supported by SEM and XRD analyses, revealing distinct morphological and crystallinity shifts depending on treatment intensity and drying method. Thermal analysis further confirmed that freeze-dried BC, despite being more porous, demonstrated higher degradation temperatures (DTG T_{max} 341.67°C–371.17°C) than oven-dried counterparts.

In conclusion, the combination of HPM and appropriate drying techniques offers a versatile approach to tailoring BC characteristics. These modifications are

crucial for expanding BC's potential in various industrial applications, particularly where specific structural and thermal attributes are required.

5.6 References

Amarasekara AS, Wang D, Grady TL (2020) A comparison of kombucha SCOBY bacterial cellulose purification methods. SN Appl Sci 2:1–7. https://doi.org/10.1007/s42452-020-1982-2

Andree V, Niopek D, Müller C, et al (2021) Influence of drying methods on the physical properties of bacterial nanocellulose. Mater Res Express 8:. https://doi.org/10.1088/2053-1591/abe016

Aswini K, Gopal NO, Uthandi S (2020) Optimized culture conditions for bacterial cellulose production by Acetobacter senegalensis MA1. BMC Biotechnol 20:1–16. https://doi.org/10.1186/s12896-020-00639-6

Balistreri GN, Campbell IR, Li X, et al (2024) Bacterial cellulose nanoparticles as a sustainable drug delivery platform for protein-based therapeutics. RSC Appl Polym 2:172–183. https://doi.org/10.1039/d3lp00184a

Betlej I, Salerno-Kochan R, Jankowska A, et al (2021) The impact of the mechanical modification of bacterial cellulose films on selected quality parameters. Coatings 11:1–12. https://doi.org/10.3390/coatings11111275

Choi SM, Rao KM, Zo SM, Shin EJ (2022) Bacterial Cellulose and Its Applications. Polymers (Basel) 14:1–44. https://doi.org/https://doi.org/10.3390/polym14061080

Ciolacu D, Ciolacu F, Popa VI (2011) Amorphous cellulose - Structure and characterization. Cellul Chem Technol 45:13–21

Dai H, Ou S, Huang Y, Huang H (2018) Utilization of pineapple peel for production of nanocellulose and film application. Cellulose 25:1743–1756. https://doi.org/10.1007/s10570-018-1671-0

Danaei M, Dehghankhold M, Ataei S, et al (2018) Impact of particle size and

polydispersity index on the clinical applications of lipidic nanocarrier systems. Pharmaceutics 10:1–17. https://doi.org/10.3390/pharmaceutics10020057

Dima SO, Panaitescu DM, Orban C, et al (2017) Bacterial nanocellulose from side-streams of kombucha beverages production: Preparation and physical-chemical properties. Polymers (Basel) 9:. https://doi.org/10.3390/polym9080374

Fang L, Catchmark JM (2014) Structure characterization of native cellulose during dehydration and rehydration. Cellulose 21:3951–3963. https://doi.org/10.1007/s10570-014-0435-8

Fatima A, Ortiz-Albo P, Neves LA, et al (2023) Biosynthesis and characterization of bacterial cellulose membranes presenting relevant characteristics for air/gas filtration. J Memb Sci 674:. https://doi.org/10.1016/j.memsci.2023.121509

Fuller ME, Andaya C, McClay K (2018) Evaluation of ATR-FTIR for analysis of bacterial cellulose impurities. J Microbiol Methods 144:145–151. https://doi.org/10.1016/j.mimet.2017.10.017

Gaspar D, Fernandes SN, De Oliveira AG, et al (2014) Nanocrystalline cellulose applied simultaneously as the gate dielectric and the substrate in flexible field effect transistors. Nanotechnology 25:. https://doi.org/10.1088/0957-4484/25/9/094008

Gayathry G, Gopalaswamy G (2014) Production and characterisation of microbial cellulosic fibre from Acetobacter xylinum. Indian J Fibre Text Res 39:93–96

Guo X, Chen M, Li Y, et al (2020) Modification of food macromolecules using dynamic high pressure microfluidization: A review. Trends Food Sci Technol 100:223–234. https://doi.org/10.1016/j.tifs.2020.04.004

Hossen MT, Kundu CK, Pranto BRR, et al (2024) Synthesis, characterization, and cytotoxicity studies of nanocellulose extracted from okra (Abelmoschus Esculentus) fiber. Heliyon 10:e25270. https://doi.org/10.1016/j.heliyon.2024.e25270

Hussain Z, Sajjad W, Khan T, Wahid F (2019) Production of bacterial cellulose from industrial wastes: a review. Cellulose 26:2895–2911

Kawee N, Lam NT, Sukyai P (2018) Homogenous isolation of individualized bacterial nanofibrillated cellulose by high pressure homogenization. Carbohydr Polym 179:394–401. https://doi.org/10.1016/j.carbpol.2017.09.101

Li P, Wang Y, Hou Q, et al (2020) Preparation of cellulose nanofibrils from okara by high pressure homogenization method using deep eutectic solvents. Cellulose 27:2511–2520. https://doi.org/10.1007/s10570-019-02929-5

Liu X, Cao L, Wang S, et al (2023) Isolation and characterization of bacterial cellulose produced from soybean whey and soybean hydrolyzate. Sci Rep 13:1–10. https://doi.org/10.1038/s41598-023-42304-w

Mert ID (2020) The applications of microfluidization in cereals and cereal-based products: An overview. Crit Rev Food Sci Nutr 60:1007–1024. https://doi.org/10.1080/10408398.2018.1555134

Mohamad S, Abdullah LC, Jamari SS, et al (2022a) Influence of drying method on the crystal structure and thermal property of oil palm frond juice-based bacterial cellulose. J Mater Sci 57:1462–1473. https://doi.org/10.1007/s10853-021-06685-5

Mohamad S, Abdullah LC, Jamari SS, et al (2022b) Production and Characterization of Bacterial Cellulose Nanofiber by Acetobacter Xylinum 0416 Using Only Oil Palm Frond Juice as Fermentation Medium. J Nat Fibers 19:16005–16016. https://doi.org/10.1080/15440478.2022.2140243

Mohammadkazemi F, Azin M, Ashori A (2015) Production of bacterial cellulose using different carbon sources and culture media. Carbohydr Polym 117:518–523. https://doi.org/10.1016/j.carbpol.2014.10.008

Muhajir M, Suryanto H, Pradana YRA, Yanuhar U (2022) Effect of Homogenization Pressure on Bacterial Cellulose Membrane Characteristic Made from Pineapple Peel Waste. J Mech Eng Sci Technol 6:34. https://doi.org/10.17977/um016v6i12022p034

Nurfadila N, Maddu A, Winarti C, Kurniati M (2019) Cellulose-based nano hydrogel from corncob by gamma irradiation. IOP Conf Ser Earth Environ Sci 299:.

https://doi.org/10.1088/1755-1315/299/1/012003

R. Rebelo A, Archer AJ, Chen X, et al (2018) Dehydration of bacterial cellulose and the water content effects on its viscoelastic and electrochemical properties. Sci Technol Adv Mater 19:203–211. https://doi.org/10.1080/14686996.2018.1430981

Rachtanapun P, Jantrawut P, Klunklin W, et al (2021) Carboxymethyl bacterial cellulose from nata de coco: Effects of NaOH. Polymers (Basel) 13:1–17. https://doi.org/10.3390/polym13030348

Said Azmi SNN, Samsu Z 'Asyiqin, Mohd Asnawi ASF, et al (2023) The production and characterization of bacterial cellulose pellicles obtained from oil palm frond juice and their conversion to nanofibrillated cellulose. Carbohydr Polym Technol Appl 5:100327. https://doi.org/10.1016/j.carpta.2023.100327

Samuel OS, Adefusika AM (2019) Influence of Size Classifications on the Structural and Solid-State Characterization of Cellulose Materials. In: Pascual R, Martín MEE (eds) Cellulose. IntechOpen

Sardjono SA, Suryanto H, Aminnudin, Muhajir M (2019) Crystallinity and morphology of the bacterial nanocellulose membrane extracted from pineapple peel waste using high-pressure homogenizer. In: AIP Conference Proceedings. AIP Publishing, pp 080015-1-080015–5

Srivastava S, Mathur G (2022) Komagataeibacter saccharivorans strain BC-G1: an alternative strain for production of bacterial cellulose. Biologia (Bratisl) 77:3657–3668. https://doi.org/10.1007/s11756-022-01222-4

Suryanto H, Muhajir M, Susilo BD, et al (2021) Nanofibrillation of bacterial cellulose using high-pressure homogenization and its films characteristics. J Renew Mater 9:1717–1728. https://doi.org/10.32604/jrm.2021.015312

Teixeira SRZ, Dos Reis EM, Apati GP, et al (2019) Biosynthesis and functionalization of bacterial cellulose membranes with cerium nitrate and silver nanoparticles. Mater Res 22:1–13. https://doi.org/10.1590/1980-5373-MR-2019-0054

Tomkowiak K, Mazela B, Szubert Z, Perdoch W (2024) Hydrophobic Cellulose-Based

Sorbents for Oil/Water Separation. Molecules 29:. https://doi.org/10.3390/molecules29194661

Wang H, Zuo M, Ding N, et al (2019) Preparation of Nanocellulose with High-Pressure Homogenization from Pretreated Biomass with Cooking with Active Oxygen and Solid Alkali. ACS Sustain Chem Eng 7:9378–9386. https://doi.org/10.1021/acssuschemeng.9b00582

Wang Y, Wei X, Li J, et al (2015) Study on nanocellulose by high pressure homogenization in homogeneous isolation. Fibers Polym 16:572–578. https://doi.org/10.1007/s12221-015-0572-1

Widyastuti FK, Kartika Fitri AC (2023) Optimization Production and Characterization of Bacterial Cellulose from Cornhusk. CHEESA Chem Eng Res Artic 6:49. https://doi.org/10.25273/cheesa.v6i1.11781.49-55

Wu LM, Tong DS, Zhao LZ, et al (2014) Fourier transform infrared spectroscopy analysis for hydrothermal transformation of microcrystalline cellulose on montmorillonite. Appl Clay Sci 95:74–82. https://doi.org/10.1016/j.clay.2014.03.014

Yan H, Chen X, Li J, et al (2016) Synthesis of alginate derivative via the Ugi reaction and its characterization. Carbohydr Polym 136:757–763. https://doi.org/10.1016/j.carbpol.2015.09.104

Yanti NA, Ahmad SW, Muhiddin NH (2018) Evaluation of inoculum size and fermentation period for bacterial cellulose production from sago liquid waste. J Phys Conf Ser 1116:. https://doi.org/10.1088/1742-6596/1116/5/052076

Yilmaz M, Goksungur Y (2024) Optimization of Bacterial Cellulose Production from Waste Figs by Komagataeibacter xylinus. Fibers 12:1–18. https://doi.org/10.3390/fib12030029

Zhai X, Lin D, Li W, Yang X (2020) Improved characterization of nanofibers from bacterial cellulose and its potential application in fresh-cut apples. Int J Biol Macromol 149:178–186. https://doi.org/10.1016/j.ijbiomac.2020.01.230

Zhang CJ, Wang L, Zhao JC, Zhu P (2011) Effect of drying methods on structure and mechanical properties of bacterial cellulose films. Adv Mater Res 239–242:2667–2670. https://doi.org/10.4028/www.scientific.net/AMR.239-242.2667

Zhong C (2020) Industrial-Scale Production and Applications of Bacterial Cellulose. Front. Bioeng. Biotechnol. 8:1–19

CHAPTER 6

EFFECTS OF BACTERIAL CELLULOSE NANOFIBRILS ON JELLY CANDY PROPERTIES AND BIOACTIVE COMPOUND PROFILES DURING SIMULATED DIGESTION

6.1 Abstract

This study developed jelly candy (JC) enriched with bacterial cellulose nanofibrils (BCNF) and bioactive ingredients, evaluating their effects on texture, color, and compound bioaccessibility during simulated digestion. BCNF, produced via microfluidic homogenization, was added at 5–20 g concentrations. Although it minimally affected appearance, higher homogenization and concentration reduced a* and b* values. Texture analysis showed BCH10 improved firmness and chewiness, with JC-BCH20-5 closely matching the control. Four bioactive ingredients—vitamin C (VC), vitamin E (VE), butterfly pea flower powder (BF), and tomato extract powder (TOM)—were added to assess their impact on texture and bioaccessibility; BF and TOM served as natural bioactive sources. VE produced the firmest texture, while VC and TOM led to softer gels. In vitro digestion revealed JC-VENBC retained the highest total phenolic content (TPC) and antioxidant activity, while others showed reduced TPC, especially during the gastric phase. Total flavonoid content (TFC) remained low across samples, possibly due to low flavonoid levels or assay limitations; more sensitive methods like HPLC may be needed. BCNF improved antioxidant retention in VC formulations, suggesting a protective effect, but its influence was limited in BF and TOM compared to non-BC counterparts. These findings highlight BCNF's potential to modulate texture and bioaccessibility, supporting its use as a functional ingredient in healthy jelly candy.

Keywords: bacterial cellulose nanofibrils, jelly candy, gastrointestinal, bioaccessibility, s profile, bioactivity

6.2 Introduction

Bacterial cellulose, a dietary fiber, has gained significant attention for its versatility and broad applications in the food, nutraceutical, and pharmaceutical industries. Derived from sources such as coconut water (e.g., nata de coco), BC is prized for its high purity, ability to retain natural flavor and color, and its contribution to enhancing firmness, water retention, and texture—making it ideal for functional food development (Shi et al. 2014; Choi et al. 2022). In the food sectors, BC is commonly featured in products like nata de coco, incorporated into instant beverages, and utilized in ice cream formulations, showcasing its potential to enhance product quality and consumer appeal (Tangkanakul 2022; Xavier and Ramana 2022).

Structurally, BC offers unique properties that enable it to function as a carrier for active compounds, an immobilization matrix, an emulsifier, and a stabilizer in Pickering emulsions. For example, curcumin-loaded emulsions stabilized with BC and soy protein particles have shown high encapsulation efficiency and significantly improved curcumin bioaccessibility, increasing it to 30.54% (Shen et al. 2021). Moreover, lysozyme immobilized in BC nanofibers (BCNF) exhibited antimicrobial activity against *Staphylococcus aureus*, *Escherichia coli*, and *Aspergillus niger* (Bayazidi et al. 2021). These findings illustrate BC's potential in delivering bioactive compounds within food and pharmaceutical products.

Recent advancements in BC research have also explored its applications in drug delivery systems. BC-based materials have been used for controlled-release applications, improving drug bioavailability and stability. For instance, cellulose nanofibril aerogels achieved a 69.2% drug release rate within 24 hours, with a 3.25-fold increase in drug bioavailability (Bhandari et al. 2017). Similarly, nanocomplexes of BC nanocrystals (BCNC) and bioactive compounds have shown promising results in enhancing therapeutic efficacy while reducing toxicity (Soeiro et al. 2021). Such findings underscore BC's multifunctionality across different industries.

Furthermore, BC's nano- and micro-scaled forms enhance its functional performance. Milling BC increases its surface area and swelling capacity, improving water retention, bile acid and sugar binding, and the production of short-chain fatty acids. These features contribute to health benefits such as improved laxation, cholesterol reduction, and glucose regulation (Dubey et al. 2018). Smaller BC particles also improve texture and rheological properties, making them especially well-suited for use in confectionery products like jelly candy (Blok et al. 2023). Variations in high-pressure microfluidization (HPM) treatments can produce BCNFs with different sizes and characteristics, which may further influence JC properties. Additionally, differences in BCNF concentration could also impact JC quality attributes.

This study aims to develop JC enriched with BCNF and bioactive ingredients. Initially, various homogenization treatments and BCNF concentrations were evaluated for their effects on JC properties, including color and texture. The formulation exhibiting texture closest to the control was selected for further analysis. Subsequently, the study investigated the impact of BCNF-enriched JC containing bioactive ingredients (vitamins and plant extracts) on texture and the bioaccessibility of the bioactive compounds during in vitro simulated gastrointestinal digestion. This research underscores the potential of BCNF as a functional ingredient in innovative confectionery products with enhanced health benefits.

6.3 Materials and Methods

The materials used in this study are BC pulp as a control (BCP) and BCNF (BC pulp with different HPM treatment (BCH)), gelatin, sucrose, glucose, sorbitol, extra virgin olive oil, citric acid, vitamin C (VC) spray-dried Butterfly pea flower (*Clitoria ternatea*) extract (BF), freeze-dried Tomato extract (TOM), vitamin E (VE), alfa-amylase from porcine pancrease 10 U/mg soilid (Sigma, A3176-1MU), pepsin porcine gastric mucosa 424 U/mg solid (Sigma Aldrich, P7000), pancreatin from porcine pancreas (Sigma, P1750), methanol (RCI-Labscan, AR1115-P2.5L), ethanol (RCI-Labscan, AR1069-P4L), alumunium chloride hexa-hydrate (Al.Cl3.6H_2O, Univar), sodium nitrite ($NaNO_2$,

Carlo Erba), sodium carbonate (Na_2CO_3, Carlo Erba), sodium hydroxide pellet (NaOH, Carlo Erba), sodium phosphate monobasic (NaH_2PO_4, Carlo Erba), sodium phosphate dibasic (Na_2HPO_4, Carlo Erba), gallic acid (Acros-Organic, 410860050), catechin powder (Sigma-Aldrich, C1251), 2,2-diphenyl-1-picrylhydrazyl (DPPH) ($C_{18}H_{12}N_5O_6$, Alfa Aesar), trolox (C14H18O4, Acros-Organics), RO water, and DI water.

The instruments used in this study include a water bath (Julabo), silicon mold, texture analyzer (TA.XT Plus), colorimeter (HunterLab ColorQuest XE), digital balance (Mettler Toledo, New Classics MS), sonicator (Ultrason-P Selecta), centrifuge (Thermo Scientific, Sorvall Legend Mach 1.6R), mini centrifuge (MIULAB, MU-E23-91357), water bath shaker (Julabo, SW22), spectrophotometer (Thermo Scientific, Genesys 150), and pH meter (SevenCompact Duo, Mettler Toledo)

6.3.1 Experimental Design

1) Effect of Different BCNF Treatments and Concentrations on Jelly Candy Properties

This study aimed to determine the optimal formulation of JC based on different BC treatments (BCNF) and their concentrations. The BC samples used in the study consist of four types: BC-Pulp and BC samples after homogenization using high-pressure microfluidization for 10, 15, and 20 cycles at a pressure of 10,000 Psi, coded as BCH-10, BCH-15, and BCH-20. The JC formulations are shown in **Table 6.1**. The resulting jelly candies were primarily evaluated for texture characteristics, including hardness, chewiness, adhesiveness, cohesiveness, gumminess, springiness, and resilience, as well as for color. The best formulation identified from this study will be used for subsequent experiments.

2) Profiling of Bioactive Compounds During In Vitro Gastrointestinal Simulation

This study aimed to evaluate the effects of in vitro gastrointestinal digestion on the profile and bioaccessibility of bioactive compounds in JC. The

bioactive ingredients included a water-soluble vitamin (vitamin C, VC), a fat-soluble vitamin (vitamin E, VE), and plant extracts from spray-dried butterfly pea flower (BF) and freeze-dried tomato (TOM). JC samples were analyzed for color, texture, and bioactive compound profiles, including antioxidant activity (AA), total phenolic content (TPC), and total flavonoid content (TFC), both in the final product and throughout digestion. Each formulation was designed to provide the recommended daily intake, containing 1350 mg of VC, 450 mg of VE, 3000 mg of BF, or 3000 mg of TOM. A control sample (JC-C) was prepared using the same base formula as a previous study but without BC or bioactive ingredients.

6.3.2 Jelly Candy Production

The JC preparation process followed the method described by (Teixeira-Lemos et al. 2021) with modifications(Teixeira-Lemos et al. 2021). Gelatin was placed in a 200 mL beaker, while the other ingredients—BC, sucrose, glucose, sorbitol, citric acid, essential oils, and 200 mL of water—were mixed in separate beakers. The mixture was heated and stirred at approximately 80°C for 10 minutes. Meanwhile, the gelatin was soaked in deionized water for 10 minutes and then heated at the same temperature until fully melted (approximately 3 minutes). The melted gelatin was combined with the other ingredients and heated together for an additional 5 minutes. The final mixture was poured into silicone molds (120 x 120 x 100 mm per cavity) and cooled to room temperature. The samples were then refrigerated at 4°C overnight. Once set, the jelly candies were removed from the molds, sealed in airtight PET plastic, and stored in the refrigerator at 4°C for further analysis. For samples containing bioactive ingredients, each bioactive ingredient was pre-mixed with BC and gently stirred for 10 minutes before incorporating the remaining ingredients.

Table 6.1 JC formulation based on different BC treatment and its concentration

Sample code		Ingredients (%)										
		Gelatin (g)	Sucrose (g)	Sorbitol (g)	Glucose (g)	Citric acid (g)	Essential oil (g)	Total (dry weight) (g)	BC (g)	%BC	Water 1 (ml)	Water 2 (ml)
JC-Ctrl	0	9.00	30.00	3.00	24.00	2.00	2.00	70.00	0.00	0.00	20.00	10.00
JC-BCP	5	9.00	30.00	3.00	24.00	2.00	2.00	70.00	5.00	7.14	20.00	10.00
	10	9.00	30.00	3.00	24.00	2.00	2.00	70.00	10.00	14.29	20.00	10.00
	15	9.00	30.00	3.00	24.00	2.00	2.00	70.00	15.00	21.43	20.00	10.00
	20	9.00	30.00	3.00	24.00	2.00	2.00	70.00	20.00	28.57	20.00	10.00
JC-BCH10	5	9.00	30.00	3.00	24.00	2.00	2.00	70.00	5.00	7.14	20.00	10.00
	10	9.00	30.00	3.00	24.00	2.00	2.00	70.00	10.00	14.29	20.00	10.00
	15	9.00	30.00	3.00	24.00	2.00	2.00	70.00	15.00	21.43	20.00	10.00
	20	9.00	30.00	3.00	24.00	2.00	2.00	70.00	20.00	28.57	20.00	10.00
JC-BCH15	5	9.00	30.00	3.00	24.00	2.00	2.00	70.00	5.00	7.14	20.00	10.00
	10	9.00	30.00	3.00	24.00	2.00	2.00	70.00	10.00	14.29	20.00	10.00
	15	9.00	30.00	3.00	24.00	2.00	2.00	70.00	15.00	21.43	20.00	10.00
	20	9.00	30.00	3.00	24.00	2.00	2.00	70.00	20.00	28.57	20.00	10.00

Table 6.1 JC formulation based on different BC treatment and its concentration (Continued)

Sample code		Ingredients (%)										
		Gelatin (g)	Sucrose (g)	Sorbitol (g)	Glucose (g)	Citric acid (g)	Essential oil (g)	Total (dry weight) (g)	BC (g)	%BC	Water 1 (ml)	Water 2 (ml)
JC-BCH20	5	9.00	30.00	3.00	24.00	2.00	2.00	70.00	5.00	7.14	20.00	10.00
	10	9.00	30.00	3.00	24.00	2.00	2.00	70.00	10.00	14.29	20.00	10.00
	15	9.00	30.00	3.00	24.00	2.00	2.00	70.00	15.00	21.43	20.00	10.00
	20	9.00	30.00	3.00	24.00	2.00	2.00	70.00	20.00	28.57	20.00	10.00

BC = Bacterial cellulose, Water 1 was used for soaking gelatin and water 2 was added to sugar. Source of JC formulation (Jiamjariyatam 2018; Lorenz 2021) with modification.

6.3.3 Selection of the Optimal Jelly Candy Formulation Incorporating BC

The selection of the JC formula was based on the Euclidean Distance Method (EDM), which was applied to the texture properties data of the JC samples. The texture properties of the JC-C sample were used as the control, with each parameter set to 100%. The values of the other samples were then converted into percentages by comparing them to the control. The sample selection was determined by calculating the total value (i.e., the minimum distance, *D*) of all parameters that most closely matched the control sample. The Euclidean distance equation (**Eq. 6.1**) used for this calculation is as follows (Koshti et al. 2022):

$$D(x,y) = \sqrt{\sum_i^n (y_i - x_i)^2} \quad \text{.....(Eq. 6.1)}$$

Where: *D* is the Euclidean distance, x_i is the value of the control for each parameter, y_i is the value of the sample for each parameter, *n* represents the total number of texture property parameters.

6.3.4 In Vitro Gastrointestinal Digestion Simulation

The JC sample underwent simulated digestion based on the methods described by Sopade and Gidley (2009) and Na-Nakorn (2019), with modifications. In the gastric step simulation, 0.5 g of the JC sample was mixed with 1 mL of **α**-amylase solution (250 U/mL in phosphate buffer, pH ~7) and incubated for 15 to 30 seconds. Next, 5 mL of pepsin solution (7.37 mg of pepsin (424 U/mg) per mL of 0.02 M HCl, pH 2) was added, and the mixture was shaken with glass balls at 170 rpm and 37°C for 30 minutes. The phosphate buffer used was prepared from 0.02 M phosphate buffer and 0.76 mM sodium chloride. After incubation, the sample was neutralized with 5 mL of 0.02 M NaOH and centrifuged at 2000 g for 10 minutes.

For the intestinal step, a new sample was prepared following the same procedure as the gastric step until it was neutralized with NaOH. Then, 20 mL of 0.1 M phosphate buffer (pH ~7) and 5 mL of pancreatin solution (2 mg/mL pancreatin in 0.1 M phosphate buffer) were added. The mixture was then shaken at 170 rpm and 37°C

for 240 minutes. Samples were collected at each digestion stage for subsequent analysis (Sopade and Gidley 2009; Na-Nakorn et al. 2019).

Phosphate buffer (0.02 M, pH ~7) was prepared by dissolving 3.82 g of sodium phosphate dibasic ($Na_2HPO_4 \cdot 12H_2O$), 1.29 g of sodium phosphate monobasic ($NaH_2PO_4 \cdot H_2O$), and 0.39 g of sodium chloride in 800 mL of DI water. The solution was mixed thoroughly and then adjusted to a final volume of 1000 mL with DI water. Hydrochloric acid (0.02 M) was prepared by diluting 0.417 mL of 37% HCl in a 250 mL volumetric flask, then filling it to the final volume with DI water. For the 0.1 M phosphate buffer (pH ~7), 5.15 g of $Na_2HPO_4 \cdot 2H_2O$ and 2.91 g of $NaH_2PO_4 \cdot H_2O$ were dissolved in 400 mL of DI water, and the solution was then diluted to a final volume of 500 mL with DI water. Enzyme solutions for α-amylase and pancreatin were prepared by dissolving the enzymes in a suitable solution. Pepsin enzyme was prepared by dissolving it in the HCl solution. To separate any undissolved components, the enzyme solutions were centrifuged at 2000 g for 10 minutes.

6.3.5 Analysis of Jelly Candy Product

1) Texture Characterization

Texture Profile Analysis (TPA), was performed using the "*TA.XT Plus*" Texture Analyzer. Before analysis, samples were removed from refrigeration and allowed to equilibrate at room temperature (±23°C) for approximately 4 hours. The TPA was conducted using a two-cycle test to determine the hardness, adhesiveness, springiness, cohesiveness, gumminess, chewiness, and resilience. The procedure began by powering on the UPS and the texture analyzer. Once the machine's "busy" light turned off, the computer was started. A folder was created to save the data, followed by launching the "Texture Experiment 32" software. The probe (P/50 aluminum cylinder) was then attached. Calibration was performed by selecting the "TA" button, setting the return distance to 15 mm, return speed to 10 mm/sec, and contact force to 1 g. Next, test parameters were configured by navigating to "TA Setting" and selecting the "TPA" option (Sample TPA PRJ). The test parameters were set as follows:

pretest speed = 1 mm/sec, test speed = 1 mm/sec, post-test speed = 1 mm/sec, strain = 50%, time = 5 sec, trigger type = auto with a trigger force of 5 g, tare mode = auto, and advance option = on. The test was initiated by selecting “Test Configuration,” followed by “Probe Selection” (P/50), and then “Archive Information” to define the file ID and path. Autosave was enabled, and the test was run. This process was repeated for 10 samples per treatment. The texture profile data was automatically calculated by the software. For statistical analysis, data was processed using Microsoft Excel and SPSS to calculate averages and Sd and perform ANOVA and Duncan’s multiple range test.

2) Color Analysis

Color Analysis of the JC was conducted using a *HunterLab ColorQuest* XE colorimeter. The device, along with the associated computer, was connected to a power outlet and allowed a warm-up period of approximately 10 minutes to stabilize the light source. After the connection between the instrument and computer was established, the software was launched to control the device and record data, ensuring that a flash drive was inserted before starting the software.

Calibration was performed by selecting the appropriate mode within the software (Sensor; Set Mode; RSEX_SAV; Sensor; Standardize) and following the on-screen instructions. Once calibration was successfully completed, the samples were prepared for measurement. The measurement mode was configured via the software interface (Right-click; Configure; Select “CIELAB (A, B, C); Illuminant Observers “D65/10”; OK). Each sample was placed at the reflectance port, and the measurement was initiated by either pressing the measurement button or using F3.

Color values were displayed on the computer screen and saved or exported as needed. This process was repeated for 10 samples per treatment, with recalibration performed as required throughout the analysis. Once all measurements were completed, the device was powered off and unplugged, and the sample holder and calibration standards were cleaned. The equipment and data were stored in a

clean, dry location. The collected data were analyzed using Microsoft Excel and SPSS for calculating averages, SD, conducting ANOVA, and performing Duncan's multiple range test.

3) Sample Preparation for Analysis of Bioactive Compound Profiles

A 400 mg sample was weighed and diluted with 10 mL of methanol-water solution (80:20) in a 15 mL Falcon tube. Then, 0.1 mL of 37% HCl was added. The sample was sonicated for 15 minutes at approximately 20–25°C, followed by storage at ~4°C for 24 hours. After the incubation, the sample was re-sonicated for an additional 15 minutes at the same temperature and centrifuged at 2580 g at 4°C for 10 minutes. The supernatant was collected, stored at –20°C, and used for further analysis. This method was adapted from Aiello et al et al. (2024) with modifications (Aiello et al. 2024).

During the in vitro gastrointestinal simulation, samples were collected at each digestion stage—gastric and small intestinal phases—for the analysis of total phenolic content (TPC), total flavonoid content (TFC), and antioxidant activity. The analytical procedures are detailed in the following sections. All measurements were performed in triplicate to ensure data accuracy and reliability.

4) Total Phenolic Content (TPC) Analysis

The TPC was determined using a modified version of the Folin–Ciocalteu (F-C) method. In a 10-mL reaction tube, 2.5 mL of distilled water, 120 µL of sample extract, and 400 µL of F-C reagent were combined. After 8 minutes, 0.6 mL of sodium carbonate solution (1:5 w/v) was added, and the mixture was incubated at room temperature (~25°C) for 2 hours. The absorbance was measured at 760 nm using a UV-VIS spectrophotometer. Gallic acid served as the standard, and a calibration curve (R^2 = 0.999) was constructed. Results were expressed as milligrams of Gallic Acid Equivalent (GAE) per 100 grams of candy (mg GAE/100g). This method was adapted from Cedeño-Pinos et al. (2020) with modifications (Cedeño-Pinos et al. 2020).

5) Total Flavonoid Content (TFC) Analysis

The flavonoid content was determined using a spectrophotometric method, with modifications based on the procedure described by Aiello (2024). In a 10-mL reaction tube, 0.25 mL of each sample solution was mixed with 75 µL of $NaNO_2$ aqueous solution (15% w/v) and 1.0 mL of deionized (DI) water. After 6 minutes, 75 µL of $AlCl_3$ solution (10% w/v) was added. Following another 6 minutes, 1.5 mL of NaOH solution (4% w/v) was added. The mixture was left in the dark for 15 minutes, and the absorbance was then measured at 510 nm using a spectrophotometer. The results were expressed in milligrams of catechin equivalent per gram of JC (mg CE/100g), based on a calibration curve (Aiello et al. 2024).

6) Antioxidant Activity (AA) Analysis

Antioxidant activity was assessed using the 2,2-Diphenyl-1-Picrylhydrazyl (DPPH) Radical-Scavenging Activity assay, adapted from the method described by Cedeño-Pinos et al. (2020). A DPPH solution was prepared by dissolving 3.9 mg of DPPH in 100 mL of methanol-water (80:20) and allowing it to stand in the dark for 30 minutes. For the assay, 0.30 mL of the sample extract was mixed with 1.97 mL of the DPPH solution and incubated in the dark for 10 minutes. Absorbance was measured at 517 nm using a spectrophotometer. Antioxidant activity was quantified using a calibration curve (R^2 = 0.999), with results expressed as milligrams of Trolox Equivalent (TE) per 100 grams of JC (mg TE/100 g).

6.3.6 Statistical Analysis

Statistical analyses were performed using Microsoft Excel and IBM SPSS Statistics software, depending on the type and complexity of the data. For datasets with a limited number of treatments, such as bioactive compound profiles, one-way analysis of variance (ANOVA) was conducted using Microsoft Excel. Differences among treatment means were further evaluated using the least significant difference (LSD) test at a significance level of $P < 0.05$.

For more complex datasets involving a larger number of treatments—such as texture profile and color measurements—analysis was conducted using IBM SPSS Statistics. One-way univariate ANOVA was used to assess treatment effects. When significant differences were observed (α = 0.05), Duncan's multiple range test was applied as a post hoc analysis to determine statistical differences between treatment means.

6.4 Results and Discussion

In this study, gelatin-based jelly candies were formulated using various types and concentrations of BCNFs produced from Thai red tea kombucha fermentation. The BC types included BC pulp and BC pulp subjected to high-pressure homogenization for 10 (BCH-10), 15 (BCH-15), and 20 (BCH-20) cycles at a pressure of 10,000 psi. The characteristics of BCNF were detailed in the previous chapter, highlighting properties such as particle size, water content, and water-holding capacity, which may influence the quality of the JC. Wet BC was incorporated into the basic formula (total dry weight of 70 g) at concentrations of 5 g (BC5), 10 g (BC10), 15 g (BC15), and 20 g (BC20), based on preliminary experiments.

6.4.1 The effect of different BC treatment and its concentration on the characteristics of JC

1) Visual Appearance of the Jelly Candy

Both the JC made from the basic formula (BC0) and those with added cellulose, visually, exhibited relatively similar colors, as shown in **Figure 6.1.** Visual observation revealed that the color of the JC was translucent white with a slight yellowish tint, likely due to the presence of gelatin and virgin olive oil. This color is consistent with gelatin-based JCs made from the basic formula, as reported in previous studies (Čižauskaite et al. 2019; Vojvodić Cebin et al. 2024).

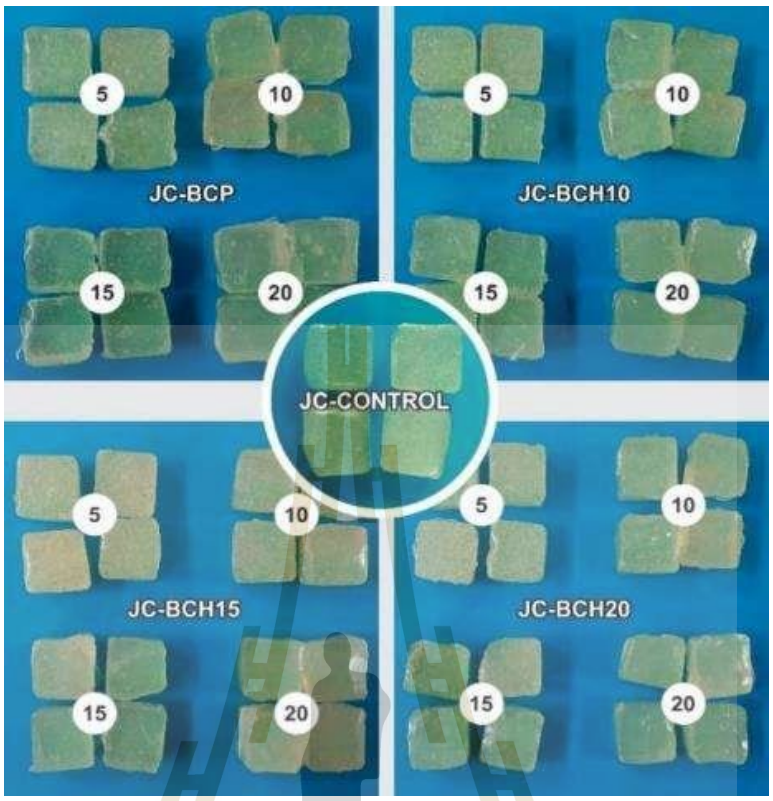

Figure 6.1 Image of JC products with the addition of BC (JCBC) and without the addition of BC (JC-Control). The numbers 5, 10, 15, and 20 indicate the concentration of wet BC (g) added to the formula.

2) Color Characteristics of Jelly Candy

To distinguish the color clearly, color analysis was conducted with the scale of CIELAB / L*, a*, b*. The mean color analysis data, along with the results of statistical analyses, including standard deviation, the result of ANOVA/Univariate analysis, and Duncan post-hoc tests, are summarized in **Table 6.2**. For visual representation, the mean L*, a*, and b* values are also shown in **Figures 6.2, 6.3**, and **6.4**, respectively.

Table 6.2 Summary of L, a, b* Values from JC with different type and concentration of BC addition

Sampel	Mean of L* Value					
	BC0	BC5	BC10	BC15	BC20	R
JC-BCP	34.68±3.53	28.65±1.88	27.34±1.48	27.72±0.98	28.83±1.31	A
JC-BCH10		26.99±1.63	27.15±1.37	28.34±1.56	30.79±2.10	A
JC-BCH15		27.09±1.33	27.86±1.64	28.22±1.83	29.13±1.77	A
JC-BCH20		27.77±1.54	27.92±1.26	28.31±1.95	28.60±1.51	A
R	a	c	c	c	b	

Sampel	Mean of a* Value					
	BC0	BC5	BC10	BC15	BC20	R
JC-BCP	-	-0.52 ± 0.09^{de}	-0.62 ± 0.09^{ef}	-0.93 ± 0.11^{h}	-1.11 ± 0.19^{jk}	B
JC-BCH10		-0.22 ± 0.12^{a}	-0.56 ± 0.10^{de}	-0.98 ± 0.14^{hi}	-1.17 ± 0.12^{jkl}	A
JC-BCH15	0.29 ± 0.12^{ab}	-0.37 ± 0.08^{bc}	-0.69 ± 0.08^{fg}	-1.05 ± 0.18^{ij}	-1.24 ± 0.17^{l}	BC
JC-BCH20		-0.45 ± 0.09^{bc}	-0.74 ± 0.09^{g}	-1.10 ± 0.11^{jk}	-1.20 ± 0.10^{jk}	C
R	a	b	c	d	e	

Sampel	Mean of b* Value					
	BC0	BC5	BC10	BC15	BC20	R
JC-BCP	3.81 ± 0.60^{a}	3.84 ± 0.40^{a}	3.15 ± 0.40^{b}	1.63 ± 0.19^{e}	0.94 ± 0.21^{f}	A
JC-BCH10		3.69 ± 0.60^{a}	2.32 ± 0.39^{c}	1.01 ± 0.18^{f}	0.21 ± 0.10^{i}	B
JC-BCH15		4.06 ± 0.51^{a}	2.09 ± 0.51^{cd}	0.67 ± 0.20^{f}	0.26 ± 0.10^{i}	B
JC-BCH20		4.03 ± 0.62^{a}	1.83 ± 0.62^{de}	0.75 ± 0.17^{fg}	0.36 ± 0.17^{gh}	B
R	a	a	b	c	d	

The lowercase letters in the bottom row indicate significant differences between different BC concentrations. The capital letters in the right column denote significant differences between different types of BC. Additionally, the lowercase letters within each column indicate significant differences between samples. R = remark.

For JC samples with varying types and concentrations of BC, the L* values range from 26.99±1.63 to 30.79±2.10, a* values from -1.24 to -0.22, and b* values from 0.21 to 4.06. These values have not been reported in previous studies, as no prior research has explored the incorporation of BC into JC formulations. Univariate analysis using SPSS showed that the type of BCNF does not significantly affect the L* value ($P > 0.05$). However, BCNF concentration has a significant impact: the control JC exhibits the highest L* value, differing significantly from all other samples ($P < 0.05$). Among the BC samples, BC5, BC10, and BC15 are not significantly different from each other but differ from BC20, which has a higher L* value, likely due to its greater BC content. Since there was no significant interaction between BC type and concentration, Duncan's post-hoc analysis was not performed. **Figure 6.2** visually represents the effects of BC type and concentration on L* values in this study.

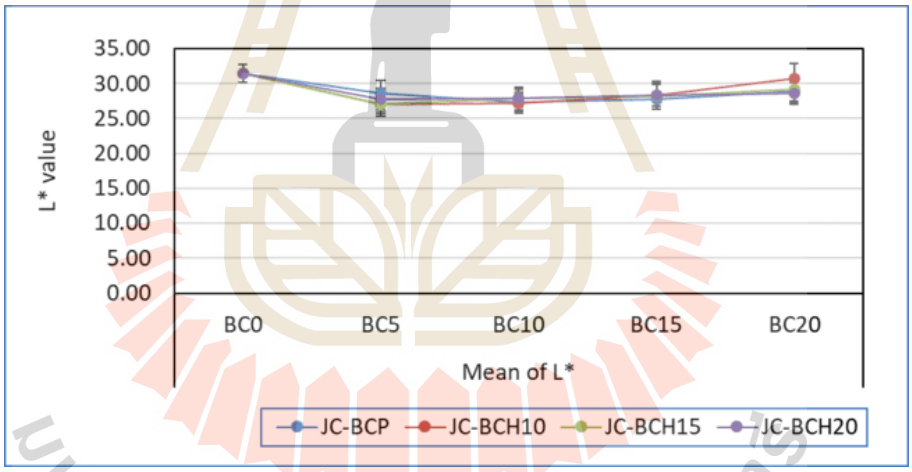

Figure 6.2 The effect of different type and concentration of BC to the L* value characteristics of JC. Data are presented as mean ± SD (n = 10).

Univariate analysis of the a* value revealed that the type and concentration of BC, as well as their interaction, significantly affect the a* value ($P < 0.05$) (**Table 6.2**). Among the BC types, BCH-10 has the highest a* value and significantly differs from all other types. BCP and BCH-15 do not differ significantly from each other, and BCH-15 and BCH-20 also show no significant difference. However, BCP and BCH-20 differ significantly. Concerning BC concentrations, all samples exhibit significant

differences, with higher concentration of BC leading to lower a* values. Duncan's post-hoc analysis, detailed in **Table 6.2** (mean of a* value), further clarifies these differences. **Figure 6.3** provides a visual representation of the impact of BC type and concentration on a* values in this study.

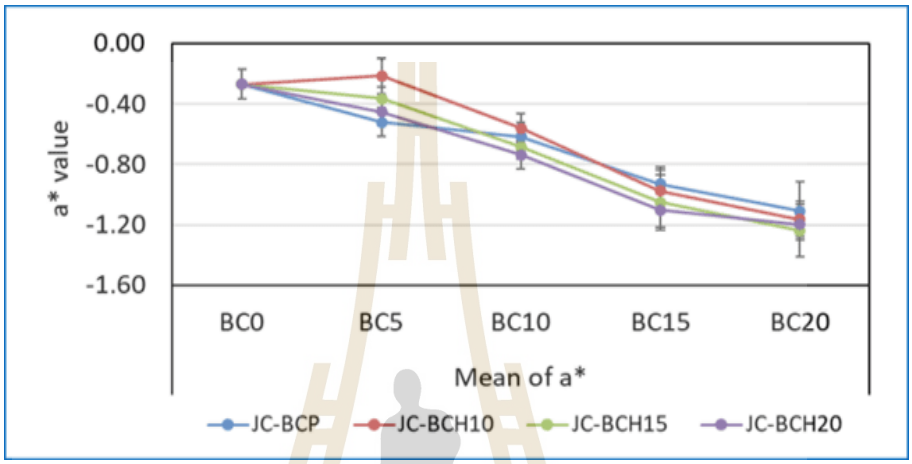

Figure 6.3 The effect of different type and concentration of BC to the a* value characteristics of JC. Data are presented as mean ± SD (n = 10).

The subsequent univariate analysis focused on the b* value. The results indicated that the type and concentration of BC, as well as their interaction, significantly affect the b* value ($P < 0.05$) (**Table 6.2**). Generally, BCP exhibits the highest b* value and significantly differs from all other samples. In contrast, BCH10, BCH15, and BCH20 do not show significant differences among themselves. This suggests that BC treated with micro-fluidic homogenization results in a lower b* value for JC. The effect of BC concentration on the b* value follows a similar trend to that observed for a*, with higher BC concentrations leading to lower b* values. Duncan's post-hoc analysis, presented in **Table 6.2**, provides additional details on these differences. **Figure 6.4** visually depicts the impact of different BC types and concentrations on the b* values observed in this study.

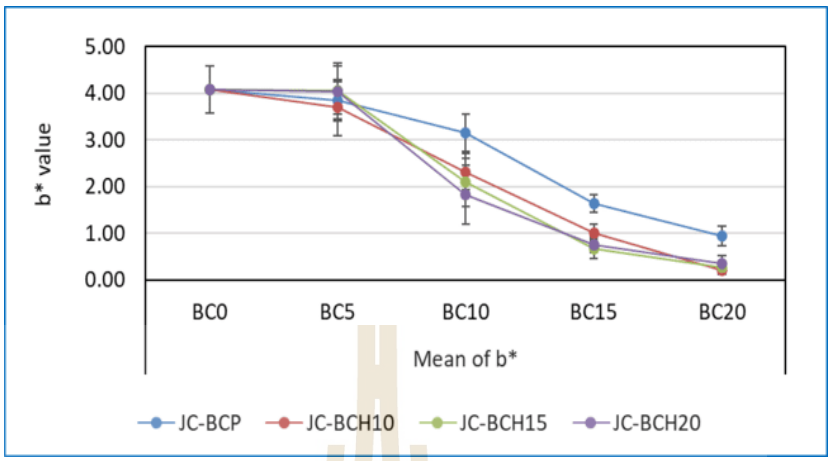

Figure 6.4 The effect of different type and concentration of BC to the b* value characteristics of JC. Data are presented as mean ± SD (n = 10).

The reduction in L*, a*, and b* values in JC with added wet BCNF is due to increased light scattering and higher moisture content. The fibrous structure of BCNF scatters light more effectively than the smooth jelly matrix, reducing transparency and lowering the lightness (L*) value. Additionally, BCNF's high water-holding capacity increases moisture content, further diffusing light and muting colors, leading to lower a* (red-green) and b* (yellow-blue) values. Similar effects have been observed in nanocellulose-containing films, where added fibers decrease transmittance and make colors appear less vivid (Snyder et al. 2013; Jaiswal et al. 2021; Kaschuk et al. 2024).

3) Textures Profile of Jelly Candy

Texture is a critical quality attribute in both the fresh and processed food industry, playing a significant role in determining consumer acceptability (Alemu 2023). Textural analysis is primarily conducted in the food and pharmaceutical industries to assess digestibility and to identify the sensory characteristics of products (Srilakshmi 2020). The graph result from the texture analysis is presented in **Figure 6.5**. The general result of the texture profile analysis from the JC of this study are demonstrated in **Figure 6.6.**

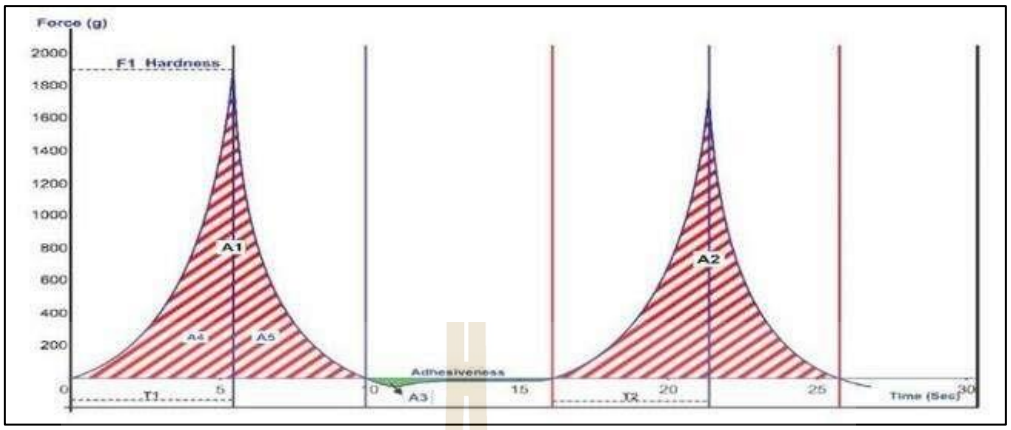

Figure 6.5 Illustration of the graph obtained from the texture analysis of JC using a texture analyzer.

Hardness: Hardness measures the force needed to compress food, experienced during biting and chewing (Szczesniak, 2002). In JC, it reflects firmness between the teeth or tongue and the mouth's roof (Cruz et al., 2015). In this study, hardness ranged from 1699.71±107.81 to 4208.09±231.22 g, with the control at 1761.53±94.26 g. ANOVA showed that both BC type and concentration, and their interaction of them significantly affected hardness ($P < 0.05$). JC-BCP exhibited the highest hardness, significantly differing from other JC-BCH types. JC-BCH10 had lower hardness than JC-BCP but was higher than both BCH15 and BCH20, which did not show significant differences ($P > 0.05$). In terms of BC concentration, BC0 had the lowest hardness, which was significantly different from all other samples. BC10 exhibited the highest hardness, showing significant differences compared to all other concentrations ($P < 0.05$). **Figure 6.6(a)** shows how BCNF types and concentrations affect JC hardness, while **Table 6.3** outlines the interaction effects between BCNF types and concentrations.

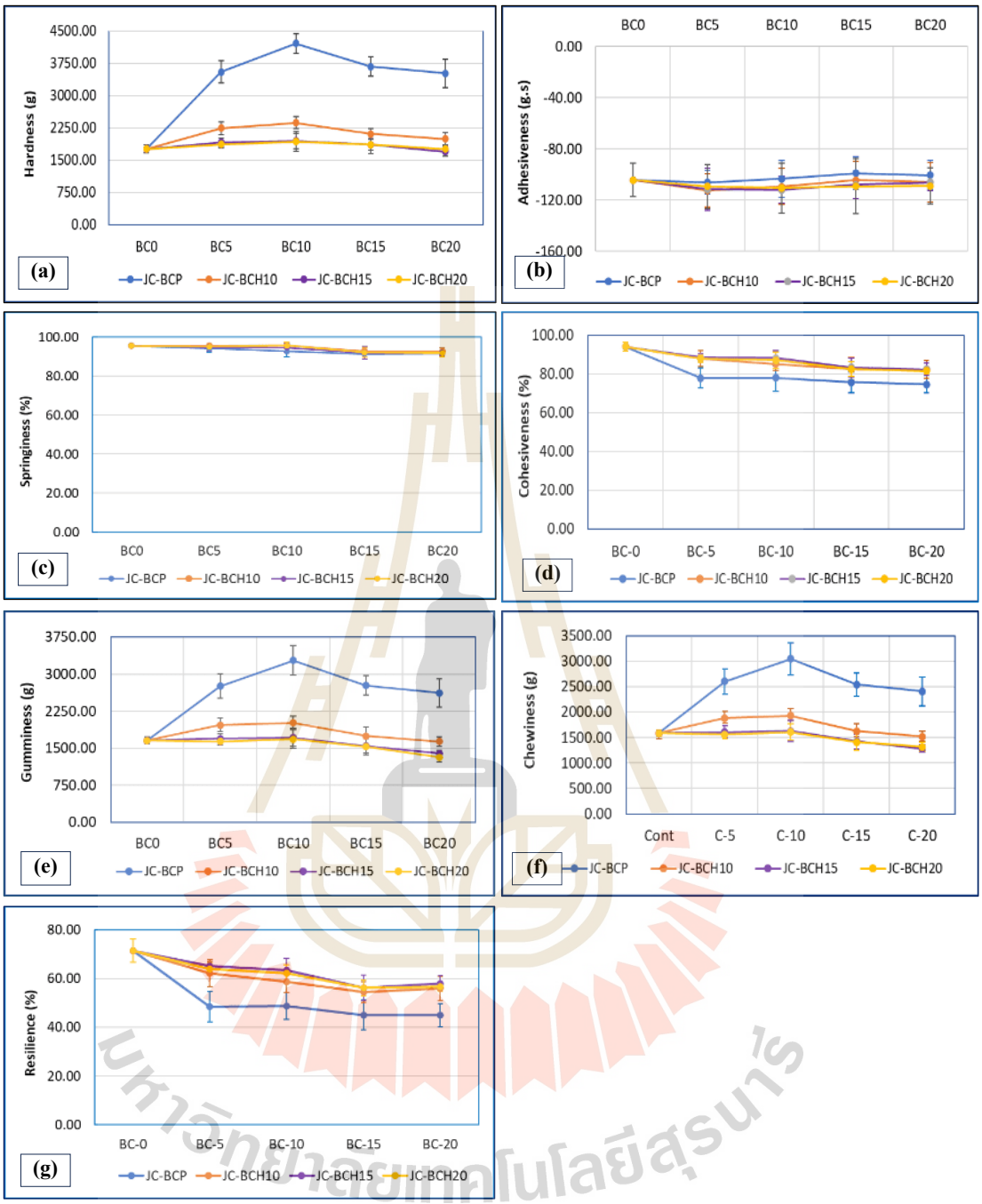

Figure 6.6 Texture profile analysis result of JC with various BCNF and its concentration (a) hardness, (b) adhesiveness, (c) springiness, (d) cohesiveness, (e) gumminess, (f) chewiness, (g) resilience. Data are presented as mean ± SD (n = 10).

Table 6.3 The data of JC hardness as the effect of the type of BC, concentration of BC, and their interaction.

Samples	Hardness (g)					
	BC0	BC5	BC10	BC15	BC20	R
JC-BCP	1761.53 ±94.26^{hij}	3545.97 ±258.1^{bc}	4208.09 ±231.22^{a}	3675.52 ±223.07^{b}	3512.91 ±332.02^{c}	A
JC-BCH10		2242.73 ±151.19^{de}	2369.84 ±136.81^{d}	2114.74 ±114.26^{ef}	1991.38 ±142.15^{fg}	B
JC-BCH15		1918.01 ±100.44^{ghi}	1944.69 ±173.86^{g}	1858.12 ±123.63^{ghij}	1699.71 ±107.81^{j}	C
JC-BCH20		1866.83 ±80.42^{ghij}	1935.94 ±234.43^{gh}	1860.18 ±207.93^{ghij}	1759.02 ±99.34^{ij}	C
R	d	b	a	b	c	

Lowercase letters in the bottom row show significant differences between BC concentrations. Capital letters in the right column highlight significant differences between BC types. Within each column, lowercase letters indicate significant differences between samples. R = remark.

The addition of BCP to the formulation significantly increased the hardness of the JC, with BCH10 also showing a notable rise in hardness. The increased hardness observed with BCP and BCH10 can be attributed to their ability to effectively reinforce the gel network structure. The larger fiber size of BCP and BCH-10 contribute to forming a stronger and more cohesive gel matrix, resulting in a substantial increase in hardness. In contrast, the addition of BCH-15 and BCH-20 did not result in significant changes compared to the sample without BC. Undergoing more homogenization cycles may have led to excessive fiber breakdown, thereby reducing their reinforcing effect on the gel structure. This aligns with the findings of Avelar and Efraim (2020), who reported that hydrocolloids can enhance the hardness of JC (de Avelar and Efraim 2020). Although the hardness values for BCH15 and BCH20 were higher than the control, they were not statistically significant. These results are comparable to previous studies: gelatin-based jelly candies incorporating berries and aromatic plants exhibited

hardness values ranging from 22.8 to 30.3 N (2324.95 to 3089.74 g) (Guiné et al. 2020), those containing grape pomace extract ranged from 6.3 to 17.1 N (642.42 to 1743.71 g) (Spinei and Oroian 2024), and those with varying concentrations of pomegranate juice, sugar, and citric acid had hardness values ranging from 743 to 3664 g (Cano-La Madrid et al. 2020).

Adhesiveness: adhesiveness reflects the effort needed to detach JC from surfaces like teeth or the tongue, indicating stickiness (Bourne 2002). In this study, JC adhesiveness ranged from -114.00±16.31 to -98.82±13.02 g, with no significant differences between samples ($P > 0.05$). The addition of BC in varying sizes and concentrations likely did not alter the adhesiveness of the JC, as adhesiveness is more influenced by the gel's moisture content and surface properties. BC primarily strengthens the gel structure but does not significantly affect its stickiness. Additionally, because BC retains water well, it helps stabilize the gel without altering its adhesive properties. For comparison, gelatin-based JC with pomegranate juice showed adhesiveness from -3.3 to -2.9 N (-336.50 to -295.72 $g.s^{-1}$) (Spinei and Oroian 2024), while other pomegranate-based JCs ranged from -2,138 to -9,898 $g.s^{-1}$(Cano-La Madrid et al. 2020). Lower values were found in JC with berries and aromatic plants, between -0.03 to -0.16 N (-3.05 to -16.31 $g.s^{-1}$) (Guiné et al. 2020). **Figure 6.6(b)** illustrates the effects of BCNF types and concentration on JC adhesiveness. Details on the effects of BCNF types and concentrations to the adhesiveness are presented in **Table 6.4**.

Table 6.4 The data of JC adhesiveness as the effect of the type of BC, concentration of BC, and their interaction.

Sample	Adhesiveness ($g.s^{-1}$)					
	BC0	BC5	BC10	BC15	BC20	R
JC-BCP	-104.29 ±13.02	-106.07 ±9.23	-103.26 ±14.32	-98.82 ±13.02	-100.36 ±11.18	A
JC-BCH10		-112.45 ±13.22	-109.39 ±14.08	-104.21 ±14.69	-105.87 ±15.55	A
JC-BCH15		-111.51 ±16.33	-111.85 ±10.62	-108.00 ±10.79	-106.09 ±11.80	A
JC-BCH20		-114.00 ±16.31	-110.56 ±19.25	-109.08 ±21.50	-108.90 ±14.05	A
R	a	a	a	a	a	

Lowercase letters in the bottom row show significant differences between BC concentrations. Capital letters in the right column highlight significant differences between BC types. Within each column, lowercase letters indicate significant differences between samples. R = remark.

Springiness: springiness refers to the candy's ability to return to its original shape after compression, indicating its elasticity (Cruz et al. 2015). While **Figure 6.6(c)** shows similar springiness values across all samples, statistical analysis reveals significant differences. The type and concentration of BCNF significantly affect springiness ($P < 0.05$), though their interaction is not significant ($P = 0.49$). Springiness values range from 91.48±1.55% to 95.75±1.73%, with the highest values observed in the control sample (JC-BC0) and homogenized BC samples (JC-BCH10, JC-BCH15).

Compared to BCP, BCH samples exhibit higher springiness, suggesting that the homogenization process positively influences elasticity. The addition of BC at a concentration of 5 g does not significantly alter springiness. However, increasing the BC concentration (especially at 10 g or more) results in a reduction in springiness. This decline is likely due to the increased water content in BC, which makes the matrix denser and less flexible. For example, JC-BC15

(92.71±1.81%) and JC-BC20 (91.48±1.55%) exhibit significantly lower springiness than JC-BC5 (94.28±2.71%) and JC-BC10 (94.28±2.71%). In comparison with other studies, gelatin-based JC with pomegranate juice reported springiness values ranging from 83% to 89% (Spinei and Oroian 2024), while other pomegranate-based jelly candies ranged from 55% to 108% (Cano-La Madrid et al. 2020). Lower springiness values were observed in jelly candies with berries and aromatic plants, ranging from 88.4% to 91.8% (Guiné et al. 2020). The results of this study show relatively higher and more consistent springiness values than those reported in the literature.

Overall, the findings indicate that BC incorporation does not enhance JC springiness. Instead, higher BC concentrations (≥10 g) negatively impact elasticity due to increased water content. However, homogenization of BC appears to mitigate some of this effect, leading to slightly higher springiness values in BCH samples. These results highlight the importance of optimizing BC concentration and processing methods to balance texture and elasticity in JC formulations. Detailed effects of BCNF types and concentrations on springiness are shown in **Table 6.5.**

Table 6.5 The data of JC springiness as the effect of the type of BC, concentration of BC, and their interaction.

Sample	Springiness (%)					
	BC0	BC5	BC10	BC15	BC20	R
JC-BCP	95.59±0.87	95.59±1.79	94.28±2.71	92.71±1.81	91.48±1.55	B
JC-BCH10		95.61±0.70	95.70±1.15	92.97±2.12	92.80±1.76	A
JC-BCH15		94.82±1.69	94.60±2.64	92.02±3.27	92.01±1.70	A
JC-BCH20		95.09±1.62	95.75±1.73	92.15±2.48	91.84±1.71	AB
R	a	ab	b	c	c	

Lowercase letters in the bottom row show significant differences between BC concentrations. Capital letters in the right column highlight significant differences between BC types. R = remark.

Cohesiveness: cohesiveness measures how well the candy withstands breaking under compression, reflecting its structural integrity (Cruz et al., 2015). **Figure 6.6(d)** illustrates the cohesiveness of the JC samples in this study, with values ranging from 74.67±4.57% to 94.12±2.33%. The JC control had the highest cohesiveness at 94.12±2.33%. Statistical analysis revealed that adding cellulose decreased cohesiveness. JC-BCP consistently showed lower cohesiveness, which was significantly different ($P < 0.05$) from all JC-BCH samples. The cohesiveness of JC-BCP samples did not differ significantly from each other ($P > 0.05$) at different concentrations. The results in JC-BCH sample, these suggests that water content plays an important role in reducing cohesiveness. Higher water content weakens the gel structure, making it less cohesive. Overall, higher BCNF concentrations led to lower cohesiveness, likely because the increased water content disrupts the gel network and reduces its cohesion. **Table 6.6** presents a detailed statistical analysis of JC cohesiveness with various BCNF types and concentrations.

Table 6.6 The data of JC cohesiveness as the effect of the type of BC, concentration of BC, and their interaction

Sample	Cohesiveness (%)					
	BC0	BC5	BC10	BC15	BC20	R
JC-BCP	94.12±2.33^{a}	77.90±5.10^{de}	78.06±6.95^{de}	75.60±5.43^{e}	74.67±4.57^{e}	B
JC-BCH10		87.99±4.01^{b}	85.21±3.51^{bc}	82.65±5.87^{c}	82.28±4.60^{c}	A
JC-BCH15		88.49±1.97^{b}	88.27±3.93^{b}	83.36±4.86^{c}	82.34±3.09^{c}	A
JC-BCH20		87.92±1.99^{b}	87.10±4.26^{b}	82.53±3.85^{c}	81.53±1.71^{cd}	A
R	a	b	b	c	c	

Lowercase letters in the bottom row show significant differences between BC concentrations. Capital letters in the right column highlight significant differences between BC types. Within each column, lowercase letters indicate significant differences between samples. R = remark.

Compared to other studies, gelatin-based JC with pomegranate juice showed cohesiveness values between 0.23 and 0.25 (23–25%) (Spinei and Oroian 2024). Other pomegranate-based JCs had a wider range of 0.26 to 0.71 (26–71%) (Cano-

La Madrid et al. 2020). In contrast, JCs made with berries and aromatic plants exhibited higher cohesiveness, ranging from 76.4% to 76.7% (Guiné et al. 2020). The cohesiveness of JC observed in this study is relatively higher than that reported in previous research.

Gumminess: gumminess is a combination of hardness and cohesiveness, representing the energy needed to break down a semi-solid food until it is ready for swallowing (Bourne 2002). **Figure 6.6(e)** shows the gumminess measurements of JC in this study, with detailed statistical analysis provided in **Table 6.7.** The gumminess pattern closely mirrors those of hardness and chewiness. Among the BCNF types, JC-BCP exhibited the highest gumminess, followed by JC-BCH10, with significant differences between them ($P < 0.05$). JC-BCH15 and JC-BCH20 showed lower gumminess, with no significant difference between them. The addition of 10 g BCNF had the greatest impact on gumminess, followed by the 5 g addition, while 15 g and 20 g additions resulted in lower gumminess values.

Table 6.7 The data of JC gumminess as the effect of the type of BC, concentration of BC, and their interaction

Sample	Gumminess (g)					
	BC0	BC5	BC10	BC15	BC20	R
JC-BCP		2760.41 ±249.75^{bc}	3280.47 ±297.42^{a}	2774.12 ±201.46^{b}	2622.66 ±290.03^{c}	A
JC-BCH10	1657.02 ±70.41^{efg}	1971.45 ±132.92^{d}	2018.86 ±134.98^{d}	1749.46 ±177.54^{e}	1635.13 ±94.60^{efg}	B
JC-BCH15		1697.29 ±96.09^{efg}	1718.00 ±184.55^{ef}	1549.28 ±139.41^{fgh}	1397.89 ±70.58^{h}	C
JC-BCH20		1641.03 ±74.29^{efg}	1682.08 ±189.94^{efg}	1535.60 ±191.46^{gh}	1434.12 ±89.63^{h}	C
R	e	b	a	c	d	

Lowercase letters in the bottom row show significant differences between BC concentrations. Capital letters in the right column highlight significant differences between BC types. Within each column, lowercase letters indicate significant differences between samples. R = remark.

In comparison to other studies, gelatin-based JC with pomegranate juice had cohesiveness values between 48.9 N and 55.2 N (equivalent to 4986.41 to 5628.83 N) (Spinei and Oroian 2024). Cohesiveness in other pomegranate-based JCs ranged from 203.4 to 847.8 g (Cano-La Madrid et al. 2020). Additionally, JCs prepared using various mixing techniques, gelatin concentrations, and fruit juices exhibited gumminess values ranging from 830.69±111 to 1425±102 g (Mutlu et al. 2018).

Chewiness: chewiness builds on gumminess and springiness, representing the overall effort required to chew the food (Bourne 2002). In general, the form of graph from chewiness in this study has the same pattern to those of hardness and gumminess. So, thus with the statistical analysis result. **Figure 6.6(f)** present the value of the chewiness of JC with various of BCNF types and concentration. The details of statistical analysis are presented in **Table 6.8**.

Table 6.8 The data of JC chewiness as the effect of the type of BC, concentration of BC, and their interaction

Sample	Chewiness					
	BC0	BC5	BC10	BC15	BC20	R
JC-BCP	1583.83 ±70.05^{ef}	2603.15 ±248.39^{b}	3044.98 ±322.19^{a}	2540.21 ±222.97^{bc}	2406.75 ±286.09^{c}	A
JC-BCH10		1884.95 ±129.28^{d}	1932.12 ±132.11^{d}	1624.55 ±143.84^{e}	1517.98 ±102.00^{efg}	B
JC-BCH15		1610.52 ±114.85^{e}	1628.41 ±210.16^{e}	1426.19 ±145.90^{fgh}	1286.00 ±64.67^{h}	C
JC-BCH20		1560.65 ±79.67^{efg}	1608.72 ±165.89^{e}	1413.86 ±168.67^{gh}	1317.41 ±89.62^{h}	C
R	d	b	a	c	d	

Lowercase letters in the bottom row show significant differences between BC concentrations. Capital letters in the right column highlight significant differences between BC types. Within each column, lowercase letters indicate significant differences between samples. R = remark.

The chewiness of JC was significantly influenced by both BC concentration and the extent of BC homogenization. The chewiness of the JC with various of BCNF types and concentration ranged from 1286.00±64.67 to 3044.98±322.19 g. JC-BCP exhibited the highest chewiness across all concentrations, likely due to its larger, less processed BC fibers, which reinforced the gel structure more effectively. In contrast, JC-BCH samples showed lower chewiness, particularly at higher homogenization cycles (15 and 20), as increased processing reduced BCNF fiber size, weakening the gel network. Higher BC concentrations also resulted in increased water content due to BC's high water-holding capacity. While moderate BC addition (up to 10 g) enhanced chewiness by strengthening the gel matrix, excessive BC (15–20 g) disrupted the structure, leading to a softer texture.

Previous studies about gelatin-based JC production reported the chewiness value such as JC with pomegranate juice exhibited chewiness ranged from 209.5 to 900.8 g.mm^{-1} (Cano-Lamadrid, 2020) and JC with berries and aromatic plants, ranging from 1764.11 to 2141.40 g (Guiné et al. 2020). The various of JC made with different mixing techniques, gelatine doses and fruit juices have the gumminess ranged from 809.27±115.37 to 1485±91 g (Mutlu et al. 2018). These findings highlight the importance of balancing BC concentration and fiber size to optimize JC's texture.

Resilience: resilience is how quickly the candy recovers its shape after deformation, indicating its ability to return to its original form (Bourne 2002). The resilience of JC with the addition of various BCNF types and concentrations ranging from 45.00±4.81 to 65.08±1.74 %. The control sample JC has a resilience of 71.50±4.77% and is significantly different from all of the other samples ($P < 0.05$). The addition of JC in various types and concentrations decreased resilience, in general. The bigger the size and the more concentration of BCNF, the lower the resilience value of JC. **Figure 6.6(g)** visualizes the value of resilience from JC with the addition of various BCNF types and concentration. The detail of the statistical analysis is demonstrated in **Table 6.9**. A study reported a lower resilience value of JC that was made with the

addition of berries and aromatic plants, ranging from 37.9 to 43.8% (Guiné et al. 2020). Healthy JC containing orange juice with honey and containing red fruit puree without honey has a resilience of about 63.95±7.73% and 48.51±5.42%, respectively (Teixeira-Lemos et al. 2021). Higher Resilience indicates that the JC recovers more quickly and completely after being deformed (compressed), giving it a more elastic, bouncy texture. This is often desirable in jelly candies, as it makes the product feel firmer and more elastic when chewed, which is generally associated with freshness and quality in gel-based confections.

Table 6.9 The data of JC resilience as the effect of the type of BC, concentration of BC, and their interaction.

Sample	Resilience					
	BC0	BC5	BC10	BC15	BC20	R
JC-BCP	71.50±4.77[a]	48.46±6.25[e]	48.71±5.54[e]	45.11±6.02[e]	45.00±4.81[e]	C
JC-BCH10		62.22±5.47[bc]	58.77±4.45[cd]	54.54±4.22[d]	55.90±4.92[d]	B
JC-BCH15		65.08±1.74[b]	63.36±4.84[b]	56.21±5.20[d]	57.95±3.23[cd]	AB
JC-BCH20		64.06±2.65[b]	62.13±3.65[bc]	56.21±3.35[d]	56.63±1.98[d]	A
R	a	b	b	c	c	

Lowercase letters in the bottom row show significant differences between BC concentrations. Capital letters in the right column highlight significant differences between BC types. Within each column, lowercase letters indicate significant differences between samples. R = remark.

Texture profile of JC can be affected by several factors such as gelatin concentration, type and sugar compositions, water content, additive materials, and processing conditions. In this study the discussion mainly focused on the effect of addition of various BCNF size and concentration. The higher size of BCNF, the higher value of hardness, gumminess, and chewiness and the higher size of BCNF the lower cohesiveness and resilience. Different size (types) of BCNFs not significantly affect the adhesiveness and springiness. Related to the BCNF concentration, the addition of 5 and 10 g of BCNF to the basic formula tends to produce higher JC hardness,

gumminess, and chewiness. In the higher concentration of BCNF (15 g and 20 g), the hardness, gumminess, and chewiness of JC tends to decrease.

6.4.2 Selection of the best JC formulation

JC formula selection was conducted using Euclidean Distance Method (EDM). The EDM is a mathematical approach used to measure the similarity or difference between multiple data points (Koshti et al. 2022). In the context of JC formula selection, this method quantifies how close or far a given formulation is from an ideal or reference formulation based on multiple texture parameters. The result of analysis is presented in **Table 6.10.**

The EDM results show that JC-BCP has a very high ED value, ranging from 133.5 to 196.8, indicating significantly different texture properties compared to the control sample. JC-BCH10 closely resembles the control in terms of adhesiveness (JC-BCH10-15) and springiness (JC-BCH10-5). JC-BCH15 most closely matches the control for cohesiveness and resilience (JC-BCH15-5). JC-BCH20 is most similar to the control for hardness (JC-BCH20-20), chewiness, and gumminess (JC-BCH20-5). Overall, the JC-BCH20-5 formula, with the lowest D value of 14.6, exhibits the closest texture properties to the control sample. These results suggest that smaller BC particle sizes have less impact on JC texture properties. Therefore, the selected formula for the next experiment is JC-BCH20-5. The EDM is a good choice for selecting the best JC formula based on texture properties because it compares the differences between different formulations and the ideal texture profile. It looks at all texture factors at once and helps identify the formulation that is closest to the desired result. This method is commonly used in food science for making decisions when multiple factors need to be considered.

Table 6.10 Analysis result for selected formula determination using EDM

Samples		H	A	Ch	G	S	Co	R	ED
Control		100.0	100.0	100.0	100.0	100.0	100.0	100.0	0.0
JC-BCP	5	201.3	101.7	164.4	166.6	98.6	82.8	67.7	142.1
	10	238.9	99.0	192.3	198.0	97.0	82.9	68.1	196.8
	15	208.7	94.7	160.4	167.4	95.7	80.3	63.1	147.6
	20	199.4	96.2	152.0	158.3	95.9	79.3	62.9	133.5
JC-BCH10-	5	127.3	107.8	119.0	119.0	100.0	93.5	87.0	41.7
	10	134.5	104.9	122.0	121.8	100.1	90.5	82.2	50.8
	15	120.1	99.9	102.6	105.6	97.3	87.8	76.3	34.0
	20	113.0	101.5	95.8	98.7	97.1	87.4	78.2	28.9
JC-BCH-15-	5	108.9	106.9	101.7	102.4	99.2	94.0	91.0	15.9
	10	110.4	107.2	102.8	103.7	99.0	93.8	88.6	18.7
	15	105.5	103.6	90.0	93.5	96.3	88.6	78.6	28.0
	20	96.5	101.7	81.2	84.4	96.3	87.5	81.0	33.8
JC-BCH-20-	5	106.0	104.7	98.5	99.0	99.5	93.4	89.6	**14.6**
	10	109.9	106.0	101.6	101.5	100.2	92.5	86.9	19.1
	15	105.6	104.6	89.3	92.7	96.4	87.7	78.6	29.0
	20	99.9	104.4	83.2	79.5	96.1	86.6	79.2	36.7

Remark: *H = hardness, A = adhesiveness, Ch = chewiness, G = gumminess, S = springiness, Co = cohesiveness, R = resilience, and ED = Euclidean distance value. The bolded number in each parameter represents the ED value most similar to the control sample.*

6.4.3 Investigation of Bioactive Compound Profiles During In Vitro Gastrointestinal Simulation

1) Production of Jelly Candy Containing BC and Bioactive Ingredients

In the gastrointestinal digestion effect simulation study, JC samples with the addition of bioactive ingredients were used, based on the selected formula. JC-BCH20-5, a selected formula from a previous study, is the basic formula for JC with

BC, which includes the addition of 5 g of BCH-20 to the total formula. For the JC without BC, JC-control (JC-C) was used as the basic formula. The bioactive ingredients used in this study include vitamin C (VC), vitamin E (VE), freeze-dried tomato extract powder (TOM), and spray-dried Butterfly Pea flower extract powder (BF).

2) Appearance and Color Profile of Jelly Candy with Various Bioactive Ingredients

The appearance of JC is visualized in **Figure 6.7**. JC with the addition of VC (JCVC) and VE (JCVE) has a similar color to JC control (JC-C). In JC with the addition of TOM and BF (JCTOM and JCBF) shows relatively similar color with the color of their powder. JC-C, JCVC, and JCVE have a translucent white color with a slight yellow. JCTOM has an orange color and JCBF has a blue-purple color. For each group of the sample, the treatment was distinguished by the addition of BC (JC-BC) and without BC (JC-NBC).

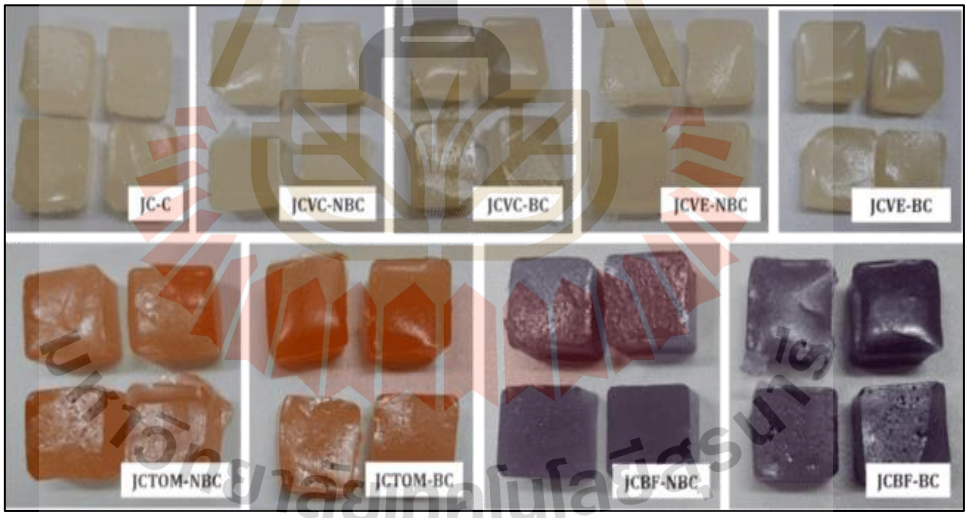

Figure 6.7 Appearance of JC products (JC-BC and JC-NBC) with the addition of different bioactive ingredients

The sample's color was analyzed using the CIELAB system, and the results, along with the statistical analysis, are presented in **Figure 6.8**. This analysis evaluated the color characteristics of each sample, comparing those with BCNF (JCBC) to those without BCNF (JCNBC) on both the top and bottom surfaces. For the control

sample (JC-C), the L*, a*, and b* values on the top surface were 37.53 ± 5.83, -0.30 ± 0.09, and 3.87 ± 0.55, respectively, while the bottom surface exhibited values of 31.84 ± 2.13, -0.27 ± 0.07, and 7.32 ± 1.68.

Across all samples, noticeable differences were observed between JCNBC and JCBC. For the JCNBC group, the top surfaces had significantly higher L* values (indicating a lighter color) than the bottom surfaces ($P < 0.05$). In contrast, JCBC samples displayed lower and more uniform L* values across both surfaces, with no significant differences ($P > 0.05$). This uniformity is likely due to the bubbles formed from gelatin during heating, which accumulated on the JC surface during the molding process in the JCNBC samples. The addition of BCNF appeared to prevent bubble formation during heating, resulting in a more uniform appearance. Regarding the a* values, the JCVC and JCVE samples (both with and without BCNF) showed no significant differences between the top and bottom surfaces ($P > 0.05$). However, in the JCTOM and JCBF samples without BCNF, the bottom surfaces exhibited significantly higher a* values compared to the top surfaces ($P < 0.05$). In contrast, samples with BCNF showed no significant differences in a* values between the top and bottom surfaces. For the b* values, in the JCVC and JCVE samples without BCNF, the bottom surfaces exhibited significantly higher b* values compared to the top surfaces. However, in samples with BCNF, no significant differences were observed between the top and bottom surfaces. For the JCTOM and JCBF samples, both with and without BCNF, no significant differences in b* values were observed across all samples. These findings indicate that the addition of BCNF to the JC formulation led to a more uniform color distribution across both surfaces. The BCNF likely facilitated a more even dispersion of particles, reducing color variability and preventing the accumulation of bubbles during the heating and molding process. This resulted in a more consistent appearance throughout the JC.

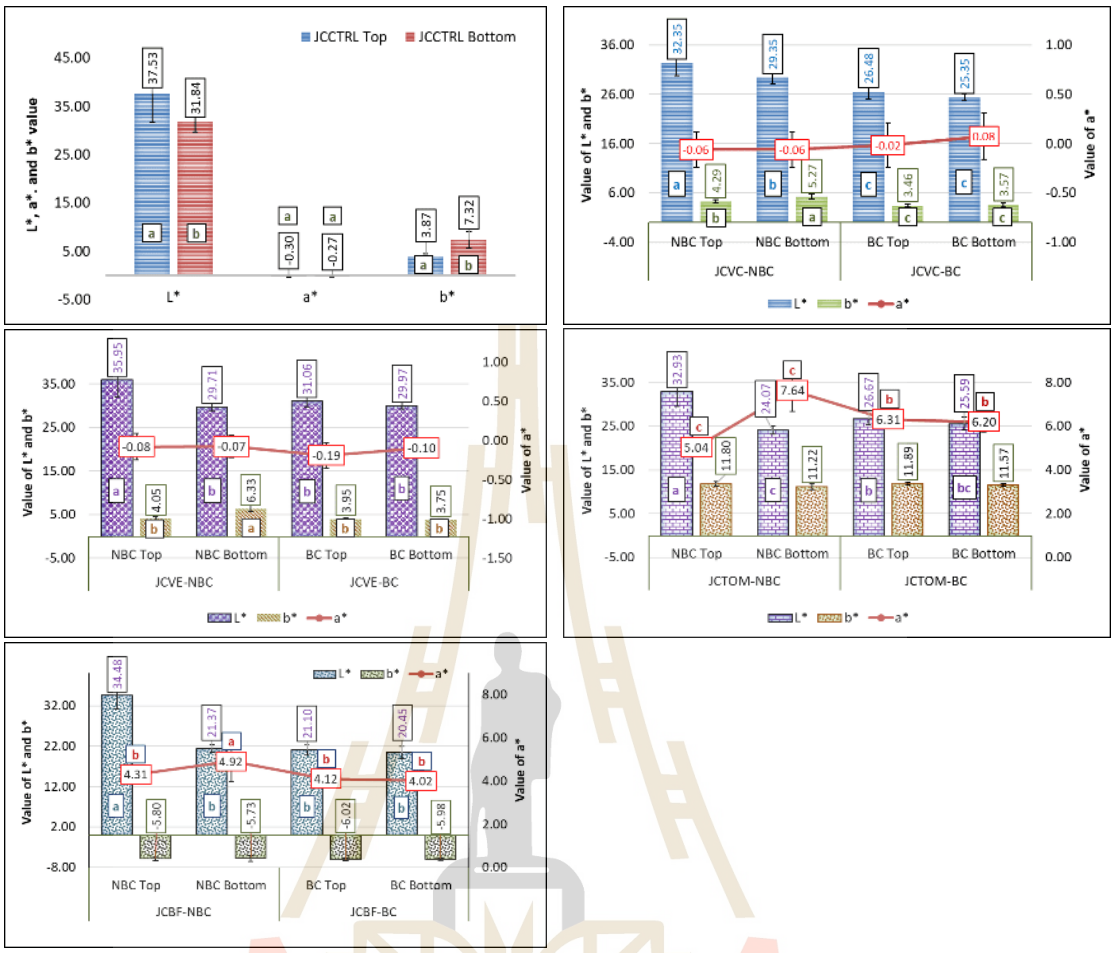

Figure 6.8 Color analysis results of JC-BC and JC-NBC with the addition of different bioactive ingredients. Data are presented as mean ± SD (n = 10)

3) Texture Properties of JC Containing Various Bioactive Ingredients

Texture profile analysis (TPA) was performed to evaluate the texture characteristics of JC samples (JCBC and JCNBC), each containing various bioactive ingredient. The results, along with the statistical analysis, are presented in **Figure 6.9.** Consistent with previous studies, the texture profile parameters measured include hardness, adhesiveness, springiness, cohesiveness, gumminess, chewiness, and resilience. A concise description of the texture analysis is provided for reference.

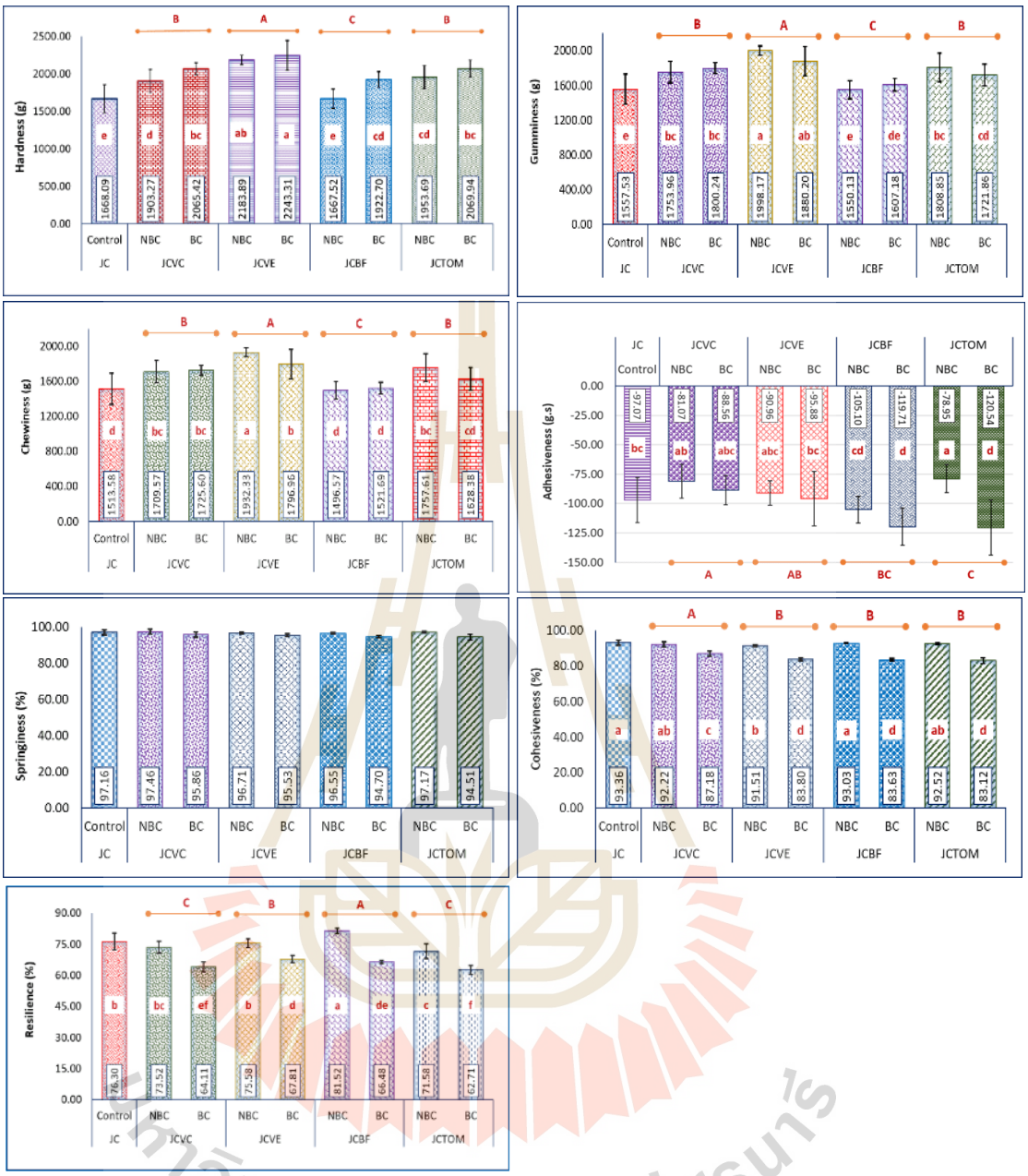

Figure 6.9 Texture properties analysis results of JC-BC and JC-NBC with the addition of different bioactive ingredient. Data are presented as mean ± SD (n = 10).

The texture of the JC in this study, in general, was significantly influenced by the addition of BC and bioactive ingredients materials. The control sample (JC-C) had the lowest hardness (1668.09 g), indicating the softest texture. The addition of VC or TOM moderately increased hardness, with BC further enhancing the

firmness of these samples. BF had minimal impact, resulting in hardness levels similar to the control in NBC samples but slightly higher with the inclusion of BC. VE had the most pronounced effect, yielding the highest hardness, particularly in BC-containing samples. Overall, BC consistently increased the hardness of all formulations, highlighting its potential as a reinforcing agent to enhance the structural integrity of JC, with the combination of BC and VE producing the firmest texture.

The increase in hardness can be attributed to the specific interactions between BC and bioactive ingredients within the gel matrix. The addition of VC to gelatin-based jelly candies enhances hardness by promoting hydrogen bonding and cross-linking within the gelatin structure (Guerrero et al. 2020). VC interacts with gelatin molecules, facilitating the formation of covalent cross-links, which may strengthen the gel network, resulting in a more compact, rigid structure and increased hardness. Similarly, the hydrophobic interaction between VE and gelatin reduces water activity within the gelatin matrix, enhancing hardness. VE's hydrophobic nature interacts with gelatin, decreasing free water and promoting a denser, more compact gel network, which may also encourage additional cross-linking, further enhancing rigidity and firmness (Chen et al. 2018b; Takei et al. 2020). The TOM contributes to increased hardness in JC. It contains water-soluble compounds such as sugars, organic acids, vitamins (including VC), lycopene, lycopene, minerals, amino acids, and insoluble fibers like pectin and cellulose. These compounds may interact with the gelatin matrix, improving gel strength and stability (Lavelli et al. 2001; Farooq et al. 2020; Fei et al. 2021). In contrast, BF has a minimal effect on JC hardness. While BF can reduce water content by binding free water, its high carbohydrate content (98.5%) does not effectively interact with the gelatin matrix, resulting in only a slight increase in hardness when combined with BC (Darroca et al. 2024).

Gumminess and chewiness are important textural properties that are closely related to hardness but influenced by additional factors such as cohesiveness and elasticity. While hardness refers to the force required to compress a

material, gumminess represents the energy needed to break down a semi-solid food, and chewiness describes the effort required to chew a solid food until it is ready for swallowing (Bourne 2002). In gelatin-based systems, BC generally enhances hardness by reinforcing the gel network through hydrogen bonding and cross-linking interactions, increasing structural rigidity (Chen et al. 2018b; Takei et al. 2020). However, in the JCVE and JCTOM samples, the addition of BC resulted in decreased gumminess and chewiness despite an increase in hardness. This can be attributed to BC's strong water-holding capacity, which competes with gelatin for water, thereby reducing cohesiveness and leading to a weaker gel matrix. Additionally, the hydrophobic nature of Vitamin E and the presence of polyphenols in tomato extract may interfere with gelatin cross-linking, causing phase separation and reducing the elasticity of the gel. As a result, while BC strengthens the gel structure and increases resistance to deformation (hardness), it simultaneously disrupts gel uniformity and elasticity, leading to lower gumminess and chewiness in certain formulations. These findings highlight the complex interactions between BC, gelatin, and bioactive ingredients in determining the final texture of food products.

The adhesiveness of the JC formulations varies depending on the presence of BC and plant extracts. The JC-C sample, which does not contain BC, shows no significant difference in adhesiveness compared to other samples without BC, such as JCVC-NBC, JCVC-BC, JCVE-NBC, JCVE-BC, and JCBF-NBC, indicating that these additives have minimal impact on adhesiveness. However, JC-C demonstrates significantly higher adhesiveness than JCTOM-NBC, which exhibits the lowest adhesiveness among all non-BC samples. In contrast, JC-C is significantly less adhesive than both JCBF-BC and JCTOM-BC, highlighting the notable increase in adhesiveness when plant extract samples are combined with BC. The minimal differences in adhesiveness observed between JC-C, JCVC, JCVC-NBC, JCVE-NBC, and JCBF-NBC suggest that the additives alone have limited interactions with the gelatin-sugar matrix. VC and VE, being hydrophilic and hydrophobic, respectively, may influence water

distribution and matrix interactions differently, but these effects seem insufficient to significantly alter adhesiveness in the absence of BC. The lower adhesiveness of the JCTOM-NBC sample may be attributed to the organic acids, polyphenols, and fibers in tomato extract (Darroca et al. 2024), which could disrupt the gelatin-sugar matrix by binding water molecules and reducing the availability of free water, ultimately decreasing stickiness. On the other hand, the significant increase in adhesiveness in samples containing both plant extracts and BC (JCBF-BC and JCTOM-BC) suggests a synergistic effect. BC, known for its high WHC, likely forms strong hydrogen bonds with the matrix, enhancing the gel network's integrity when combined with plant extracts rich in polyphenols and fibers. Although direct studies on these interactions in JC are limited, food chemistry principles suggest that BC plays a crucial role in reinforcing the product's structure. By improving the matrix structure and enhancing water retention, BC stabilizes the gel and contributes to increased adhesiveness. Additionally, polyphenols in plant extracts may interact with the matrix, further enhancing its cohesiveness and adhesiveness (Phan et al. 2015; Liu et al. 2017; Fernandes et al. 2021).

The figure of cohesiveness illustrates the cohesiveness of various JC samples, including the control (JC-C), samples without BC (NBC), and samples with BC, combined with different bioactive ingredients (VC, VE, BF, and TOM). The control sample (93.36%) exhibited the highest cohesiveness, while NBC samples showed similar values, indicating that the addition of VC, VE, and plant extracts alone did not significantly impact cohesiveness.

However, incorporating BC led to a reduction in cohesiveness across all samples. For JCVC, NBC-JCVC (92.22%) remained close to the control, whereas BC-JCVC (87.18%) showed a noticeable decrease. A similar trend was observed in JCVE, where NBC-JCVE (91.51%) maintained high cohesiveness, but BC-JCVE (83.80%) experienced a significant drop. This pattern was consistent in JCBF and JCTOM, where NBC samples (93.03% and 92.52%, respectively) retained high cohesiveness, while BC

samples (83.63% and 83.12%) demonstrated a marked reduction. This reduction can be attributed to BC's ability to stabilize the gel and retain water while increasing firmness. The increased firmness strengthens the gel but reduces flexibility, limiting the smooth interaction of gel components and leading to lower cohesiveness. Additionally, BC's high water-holding capacity tightly binds water molecules, reducing free water availability and restricting gel component mobility, further decreasing cohesiveness.

Interactions between BC and bioactive ingredients may also contribute to this effect. Hydrophilic additives like VC and hydrophobic additives like VE influence water distribution, while polyphenols and organic acids in plant extracts modify the gel network. These interactions alter the cohesive properties of the gel. Overall, BC incorporation consistently reduces cohesiveness in JC, likely due to its high water-holding capacity affecting gel flexibility and structure. The effect was most pronounced in samples containing VE, BF, and TOM, whereas VC had a comparatively milder impact. This suggests that BC interacts with both the gel matrix and bioactive ingredients, modifying the cohesive properties of the product.

For the springiness, observations show that all the samples are consistently high, ranging between approximately 94% and 97%. The control sample (97.16%) exhibited springiness similar to all other samples, regardless of the type of additive or the presence of BC. The addition of BC did not significantly alter the springiness, and minor differences in springiness percentages (e.g., JCTOM-BC at 94.51%) were not statistically significant. In conclusion, the results indicate that the addition of BC and various additives does not significantly affect the springiness of JC, suggesting that the gel matrix retains its elastic properties across all formulations. This underscores the structural integrity of the JC, regardless of the type of additive or the presence of BC.

The resilience of JC samples is influenced by the type of additive and the presence of BC. The results indicate that NBC samples generally exhibit higher resilience compared to their BC-containing counterparts, with JCBF-NBC (81.52%)

showing the highest resilience among all samples. This suggests that the powder of BF extract enhances the gel network's elastic recovery properties, aligning with studies highlighting the structural reinforcement potential of plant-based additives in a gel or hydrocolloid systems (Sharma et al. 2022; Chang et al. 2024). In contrast, the addition of BC consistently reduces resilience across all formulations, with BC-containing samples showing significantly lower resilience values compared to JC-C (76.30%) and their NBC counterparts. This reduction may be attributed to the disruptive interactions between BC fibers and the gel matrix, which contains a high-water content (Figiel and Tajner-Czopek 2006). Notably, JCVC-BC (64.11%) and JCTOM-BC (62.71%) exhibited the lowest resilience, highlighting that both the type of additive and the inclusion of BC affect the gel's structural properties.

The texture of JC was significantly influenced by the addition of BC and bioactive ingredients. BC consistently increased hardness across all formulations, enhancing the structural integrity of the gel, with VE having the most pronounced effect. However, BC reduced gumminess, chewiness, and cohesiveness due to its high water-holding capacity, which interfered with gel flexibility and cohesion. On the other hand, BC combined with plant extracts like BF and TOM increased adhesiveness, likely due to improved water retention and the reinforcing effect of BC on the gel network. Springiness remained stable across all samples, and resilience was lower in BC-containing formulations, suggesting that BC disrupts the gel's elastic recovery. Overall, BC enhanced the gel's firmness but impacted its elasticity and cohesiveness, while VE contributed to a firmer texture.

4) Bioactive Compound Profiles in Jelly Candy Product and During In Vitro Gastrointestinal Digestion Simulation

This study investigated the TPC, TFC, and AA in the JC samples both before (as the JC product) and after digestion simulation in the gastric and intestinal steps. For JCVC, only AA was analyzed, as vitamin C does not contain phenolic or flavonoid compounds. For JCVE, the characterization included AA and TPC, as vitamin

E does not contain flavonoid compounds. Meanwhile, for JCBF and JCTOM, all parameters— TPC, TFC, and AA —were evaluated.

Total Phenolic Content Profile: Total Phenolic Content (TPC) analysis was conducted using the F-C method on samples containing VE, BF, and TOM. The sample with VC was excluded from the analysis because ascorbic acid does not inherently contain phenolic compounds and its reaction with the F-C reagent could lead to inaccurate results. The F-C assay measures total phenolic content based on electron transfer. Phenolic compounds reduce the F–C reagent, causing a color change from yellow to blue, proportional to phenolic concentration. The reaction occurs under alkaline conditions and is measured at 760 nm, with results expressed as gallic acid equivalents (GAE) (Pérez et al. 2023). The TPC analysis outcomes are presented in **Figure 6.10**.

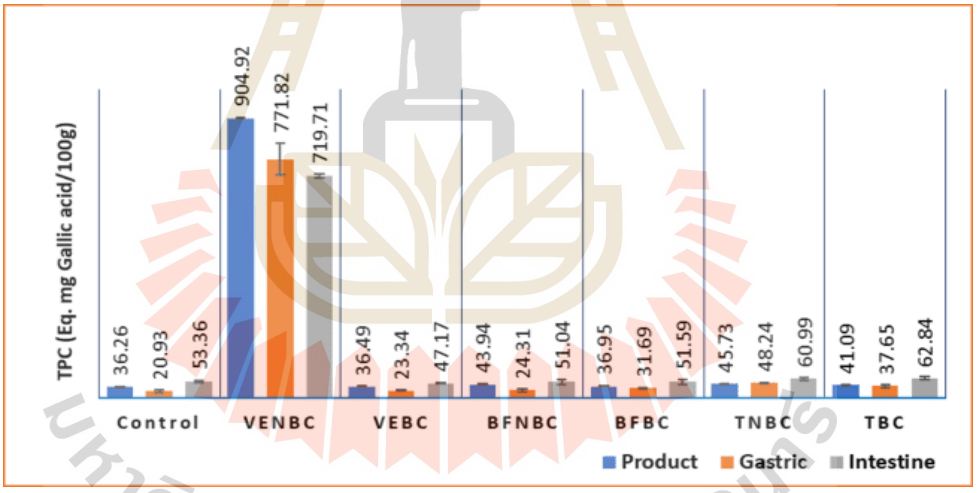

Figure 6.10 TPC of JC with and without BC, incorporating various additives (control, VE, BF, and TOM), across the product, gastric, and intestinal phases. Data are presented as mean ± standard deviation (n = 3).

The bar chart presents the TPC of various JC samples across three phases: product, gastric, and intestinal. JC-VENBC exhibited the highest TPC in the product phase (904.92 mg/100g), which decreased during the gastric phase (771.82mg/100g) and remained relatively stable in the intestinal phase (719.71 mg/100 g). In contrast, all other samples exhibited lower total TPC values across all phases.

Most samples exhibited a decrease in TPC during the gastric phase, followed by an increase during the intestinal phase, with the exception of JC-VENBC. The reduction in TPC during the gastric phase is primarily attributed to the low pH, which can lead to the degradation or reduced solubility of certain phenolic compounds. The acidic environment facilitates the cleavage of phenolics bound to proteins and carbohydrate polymers (İlbay et al. 2014). While gastric enzymes like pepsin do not directly degrade polyphenols, the conditions of the gastric phase may still influence their overall availability (Oteiza et al. 2018).

The increasing of TPC during the intestinal phase is likely due to interactions between free amino acids and peptides from gelatin with the F-C reagent, potentially inflating TPC values artificially (Diep et al. 2022). A similar phenomenon was reported in a study examining the gastrointestinal effects on TPC in cinnamon extract, where TPC increased after digestion simulation, particularly in samples combined with yogurt (Helal and Tagliazucchi 2018). Amino acids such as tyrosine and tryptophan have been confirmed to interfere with TPC analysis using the F-C reagent, producing a blue coloration in the solution (Sánchez-Rangel et al. 2013; Bastola et al. 2017). The consistently lower TPC observed in JC-VEBC, despite containing the same amount of vitamin E, suggests that BC may encapsulate phenolic compounds, preventing their release. Furthermore, the absence of cellulase in the digestion simulation limits the breakdown of the BC matrix, further restricting phenolic availability. These findings suggest that BC inhibits the release of phenolic compounds in the JC-VEBC sample.

Total Flavonoid Content Profile: the study of TFC content from the JC shows a very low result as depicted in **Figure 6.11**. As VC and VE were considered to have no flavonoid content, these samples were excluded. It was known that butterfly pea flower (*C. ternatea* sp) and tomato have a flavonoid content (Lakshmi et al. 2014; Silva-Beltrán et al. 2015). The availability of flavonoids in the extract depends on the extraction method. The analysis of TFC relies on the reaction between flavonoids and sodium nitrite ($NaNO_2$), followed by complexation with

aluminum ions (Al^{3+}) under acidic conditions. Initially, flavonoids react with $NaNO_2$, forming nitroso derivatives that generate an orange color. Upon the addition of Al^{3+}, a stable complex is formed, which, in the presence of sodium hydroxide (NaOH), shifts to a pink hue. The intensity of this color is measured spectrophotometrically, enabling flavonoid quantification using a standard curve, typically based on catechin (Shraim et al. 2021).

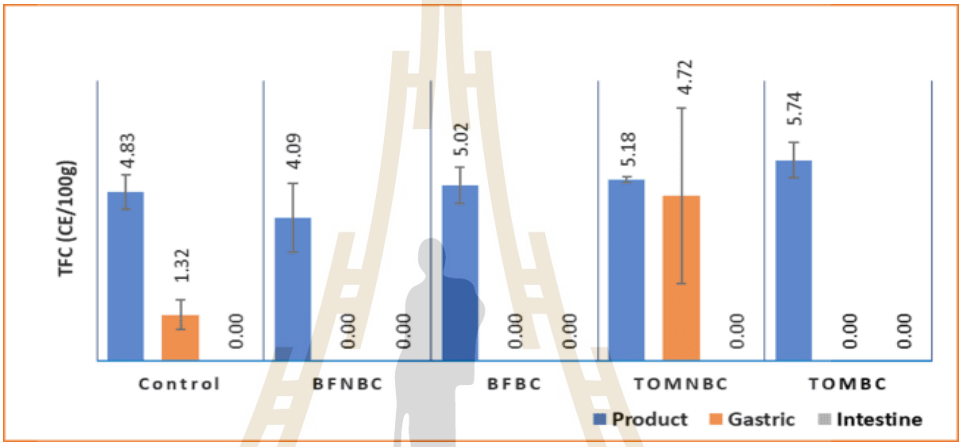

Figure 6.11 TFC of JC with and without BC, incorporating various additives (control, BF and TOM), across the product, gastric, and intestinal phases. Data are presented as mean ± standard deviation (n = 3).

Figure 6.11 shows the TFC values in the product and gastric phases for JC-C and JC-TOMNBC samples. TFC levels were higher in the product phase but significantly decreased after digestion. No detectable TFC was found in the gastric phase for most samples, except JC-C and JC-TOMNBC, and none was detected in the intestinal phase. This decline in TFC after gastric digestion follows a similar pattern observed in TPC analysis, likely due to comparable degradation mechanisms.

Flavonoids, such as flavonols, are inherently unstable and prone to degradation during digestion. Bioactive compounds like anthocyanins, typically present in glycosylated forms (e.g., cyanidin-3-xylo-rutin, delphinidin-3-xylo-rutin), are particularly susceptible to hydrolysis. During the intestinal phase, the alkaline environment and enzymatic activity, such as trypsin-mediated hydrolysis, lead to the

breakdown of ester bonds linking glycosides. This process results in significantly lower TFC levels in the intestinal phase (Luo et al. 2022). Furthermore, the presence of BCNFs did not appear to affect the loss of TFC, as no notable differences were observed.

The extremely low TFC values observed in this study are attributed to minimal absorbance at 510 nm, with most samples exhibiting absorbance below 0.003. These findings suggest that flavonoid concentrations in the samples were minimal, likely near or below the detection limit of the aluminum chloride assay, raising concerns about the reliability of these measurements (Sultana et al. 2024). Consequently, the results should be interpreted with caution. While the assay offers a preliminary indication of flavonoid presence, the consistently low absorbance values highlight the need for more sensitive analytical techniques, such as high-performance liquid chromatography (HPLC), to confirm the findings and more accurately quantify flavonoid content.

Antioxidant Activity profile: AA analysis was conducted using DPPH assay. The DPPH assay checks how well antioxidants can neutralize free radicals. DPPH is a purple-colored free radical that absorbs light at 517 nm. When an antioxidant donates a hydrogen atom or electron, DPPH turns into a stable form, changing color from purple to pale yellow. This color change is measured using a spectrophotometer, and a bigger color change means stronger antioxidant activity (Sadeer et al. 2020). Analysis result is presented in **Figure 6.12**. From this figure it is known that the addition of VC, VE, BF, and TOM can increase the profile of AA in the JC products. In the JC-C, VEBC, BFNBC, BFBC, TOMNBC, and TOMBC there are significant AA reduction during digestion simulations. A unique thing occurred in the VCNBC, VCBC, and VENBC sample. In these sample, AA increased significantly in the gastric simulation step and decrease significantly after intestine simulation steps.

To assess the impact of BC on the bioacessibility of AA, the percentage change was calculated across the digestion simulation: from the product to the gastric phase, from the gastric phase to the intestinal phase, and the total

change during digestion. In the JC-C sample, AA decreased by 88.34±3.38% during the gastric phase compared to the product, followed by an additional reduction of 84.82±8.08% in the intestinal phase, resulting in a total AA loss of 98.01±1.21%. The AA in JC-C was primarily attributed to olive oil, a key ingredient in the formulation that may contain vitamin E. The reduction in AA during digestion was likely due to the degradation of vitamin E under digestive conditions and potential lipid oxidation, which diminished its bioaccessibility and antioxidant activity (Jiménez-Monreal et al. 2025).

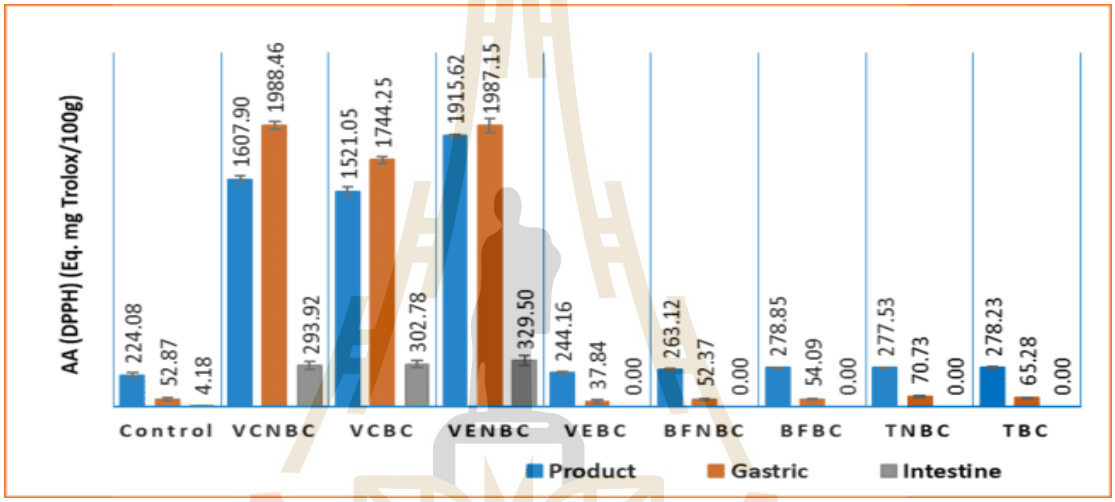

Figure 6.12 AA of JC with and without BC, incorporating various additives (VC, VE, BF, and TOM), across the product, gastric, and intestinal phases. Data are presented as mean ± standard deviation (n = 3).

In JCVC samples, AA increased during the gastric phase by 23.69±1.94% (JC-VCNBC) and 14.70±2.19% (JC-VCBC) compared to the product phase, with BC moderating the increase. This is likely due to the low pH of the stomach, which helps stabilize and release antioxidants, enhancing their bioaccessibility. However, during the intestinal phase, AA decreased significantly by 85.21±1.33% (JCVC-NBC) and 82.65±1.79% (JCVC-BC) relative to the gastric phase, leading to total reductions of 81.70±1.80% and 80.07±1.47%, respectively. BC reduced both the AA increase in the gastric phase and the AA loss in the intestine, suggesting it may protect antioxidants during digestion by slowing their degradation or maintaining their stability. The increase in AA during the gastric phase is consistent with findings from studies on phenolic

compounds in *Kadsura coccinea* fruits (Luo et al. 2022) and from Sorghum (*Sorghum bicolor* (L.) Moench) (Ziółkiewicz et al. 2023). Despite these changes, the final AA bioaccessibility in the intestine was not significantly different between JCVC-NBC (18.30±1.80%) and JCVC-BC (19.93±1.47%), indicating that BC influenced AA dynamics but did not alter overall antioxidant bioaccessibility. This decline in AA during the intestinal phase is likely due to the more neutral or alkaline pH, which reduces antioxidant activity as some compounds degrade or become less active in the higher pH environment.

The antioxidant activity (AA) of JCVE-NBC and JCVE-BC differs significantly across all phases, despite containing the same amount of vitamin E. In the product phase, JCVE-NBC shows higher AA, suggesting that BC in JCVE-BC may interfere with vitamin E's accessibility or activity, possibly through interactions with the BC matrix. In the gastric phase, JCVE-NBC experiences a larger increase in AA (3.74±2.50%) compared to the product phase, indicating that the absence of BC allows for better release and stabilization of vitamin E in the acidic environment. In contrast, BC in JCVE-BC may restrict vitamin E's release or reduce its activity. In the intestinal phase, AA decreases for both (by 83.43% for JCVE-NBC and 100% for JCVE-BC) compared to the gastric phase, but remains higher in JCVE-NBC (by 17.20±1.60%), further supporting the idea that BC limits vitamin E's bioaccessibility. The reduction in antioxidant activity (AA) observed in JCVE samples may be attributed to the decreased efficacy of vitamin E, influenced by factors such as pancreatic lipase activity and pH variations, which are key determinants of vitamin E bioaccessibility (Catelli Rocha Torres et al. 2022; Jiménez-Monreal et al. 2025). Overall, these findings suggest that BC interferes with the antioxidant performance of vitamin E, whereas its absence in JCVE-NBC enhances vitamin E's effectiveness during digestion. The increase in AA during the gastric phase is consistent with the results observed in the JC-VC sample in this study, as well as findings from studies on phenolic compounds in *K. coccinea* fruits (Luo et al. 2022).

An intriguing observation in this experiment was that when VE and BC were combined and incorporated into the gelatin-based JC, the antioxidant activity of VE was absent at every stage of the experiment. This absence of activity in the product phase is likely due to the inability of VE to be released from the BC matrix. Potential interactions between BC and VE, such as encapsulation or complex formation, may hinder VE's release and chemical availability. BC's porous and hydrophilic structure can encapsulate VE, limiting its solubility and accessibility in the extraction solvent (methanol: water: HCl). Under specific conditions, VE and cellulose can form a complex that is significantly different from a simple physical mixture. For analytical purposes, the release of VE from this complex requires enzymatic hydrolysis to break down the cellulose structure (Li et al. 2024). Furthermore, during the digestion simulation (gastric and intestinal phases), the absence of enzymes that degrade the BC matrix, particularly cellulase, prevents the release of VE from the complex. Without cellulases or similar enzymes, the VE-BC complex remains intact, restricting VE's release into the digestive environment. These combined factors help explain the undetectable antioxidant activity, as well as TPC of vitamin E in the product phase and throughout the digestion simulation.

In the JC samples with added plant extracts, both BF and TOM extracts significantly increased the antioxidant activity (AA) in the product phase compared to JC-C. This increase can be attributed to the higher levels of bioactive compounds, such as polyphenols and flavonoids, present in BF and TOM extracts, which are known for their antioxidant properties (Ahmad et al. 2019; Farooq et al. 2020; Darroca et al. 2024). During the gastric phase, the AA in JC-BFNBC and JC-BFBC decreased by 84.07±2.90% and 86.26±0.75%, respectively, compared to the product phase, with no significant difference between the two samples ($P > 0.05$). Similarly, the AA in JC-TOMNBC and JC-TOMBC decreased by 79.74±1.95% and 82.43±0.48%, respectively, compared to the product phase, again showing no significant difference between the samples. This reduction in AA during the gastric phase may be due to the

degradation of antioxidant compounds under acidic conditions and the presence of pepsin, which can impact the stability of polyphenols (Wanyo et al. 2024). In the intestinal phase, none of the samples exhibited any detectable AA, likely due to the further breakdown or transformation of antioxidant compounds under the alkaline conditions of the intestinal environment (Luo et al. 2022). These results suggest that the addition of BC to the JC (JC) did not significantly affect the bioaccessibility of antioxidant compounds from the plant extracts during digestion, as the observed changes in antioxidant activity (AA) were consistent regardless of the presence of BC.

6.5 Conclusion

This study highlights the impact of microfluidic-treated bacterial cellulose (BC) on jelly candy (JC) formulations, particularly in terms of texture, color, and the bioaccessibility of incorporated bioactive ingredients. Although BC did not visibly alter the overall appearance, color analysis revealed that increasing treatment cycles and concentrations led to decreased a* and b* values.

Texture analysis showed that both BCP and BCH10 enhanced hardness, gumminess, and chewiness, while reducing adhesiveness, cohesiveness, and resilience. The optimal formulation—BCH20 containing 5 g of bacterial cellulose nanofiber (BCNF)—exhibited texture characteristics most similar to the control. When combined with bioactive ingredients, BC further increased hardness, with vitamin E (VE) resulting in the firmest texture. In contrast, vitamin C (VC) and tomato extract (TOM) had milder effects. BC also consistently reduced gumminess, chewiness, cohesiveness, and resilience, while having minimal influence on springiness.

During in vitro digestion, JC-VENBC maintained a high total phenolic content (TPC), whereas JC-VEBC showed significantly lower levels, suggesting that BC limited phenolic compound release and reduced bioaccessibility. JC-C, JC-BF, and JC-TOM had low initial TPC, which declined in the gastric phase but slightly increased during the intestinal phase.

Total flavonoid content (TFC) remained consistently low across all JC samples, indicating the need for more sensitive detection techniques such as HPLC. Regarding

antioxidant activity, BC in JC-VC helped minimize antioxidant loss, suggesting a protective effect. However, JC-VEBC exhibited significantly lower antioxidant activity compared to JC-VENBC. In JC-BF and JC-TOM, the protective role of BC was minimal compared to the non-BC (NBC) formulations.

In summary, microfluidic-treated BC influenced JC formulations by altering textural properties and modulating the bioaccessibility of bioactive compounds, with its effects varying depending on the type of bioactive ingredient used.

6.6 References

Ahmad NA, Heng LY, Salam F, et al (2019) A colorimetric pH sensor based on Clitoria sp and Brassica sp for monitoring of food spoilage using chromametry. Sensors (Switzerland) 19:1–19. https://doi.org/10.3390/s19214813

Aiello F, Caputo P, Oliviero Rossi C, et al (2024) Formulation of Antioxidant Gummies Based on Gelatin Enriched with Citrus Fruit Peels Extract. Foods 13:. https://doi.org/10.3390/foods13020320

Alemu T (2023) Texture Profile and Design of Food Product. J Agric Hortic Res 6:272–281

Bastola KP, Guragain YN, Bhadriraju V, Vadlani PV (2017) Evaluation of Standards and Interfering Compounds in the Determination of Phenolics by Folin-Ciocalteu Assay Method for Effective Bioprocessing of Biomass. Am J Anal Chem 08:416–431. https://doi.org/10.4236/ajac.2017.86032

Bayazidi P, Almasi H, Pourfathi B (2021) Immobilized lysozyme onto bacterial cellulose nanofibers as active and reinforcing agent of sodium caseinate based films: physical characteristics and antimicrobial activity. J Food Bioprocess Eng J 4:11–18

Bhandari J, Mishra H, Mishra PK, et al (2017) Cellulose nanofiber aerogel as a promising biomaterial for customized oral drug delivery. Int J Nanomedicine 12:2021–2031. https://doi.org/10.2147/IJN.S124318

Blok AE, Bolhuis DP, Arnaudov LN, et al (2023) Influence of thickeners

(microfibrillated cellulose, starch, xanthan gum) on rheological, tribological and sensory properties of low-fat mayonnaises. Food Hydrocoll 136:108242. https://doi.org/10.1016/j.foodhyd.2022.108242

Bourne MC (2002) Food Texture and Viscosity: Concept and Measurement, second. Academic Press

Cano-La Madrid M, Calin-Sanchez Á, Clemente-Villalba J, et al (2020) Quality Parameters and Consumer Acceptance. Foods 9:1–17. https://doi.org/10.3390/foods9040516

Catelli Rocha Torres L, Giovanini de Oliveira Sartori A, de Souza Silva AP, Matias de Alencar S (2022) Bioaccessibility and uptake/epithelial transport of vitamin E: Discoveries and challenges of in vitro and ex vivo assays. Food Res Int 162:112143. https://doi.org/10.1016/j.foodres.2022.112143

Cedeño-Pinos C, Martínez-Tomé M, Murcia MA, et al (2020) Assessment of rosemary (Rosmarinus officinalis L.) extract as antioxidant in jelly candies made with fructan fibres and Stevia. Antioxidants 9:1–16

Chang H, Hu Y, Shi Y, et al (2024) Effects of Gnaphalium affine Extract on the Gel Properties of •OH-Induced Oxidation of Myofibrillar Proteins. Foods 13:. https://doi.org/10.3390/foods13101447

Chen Y, Lu W, Guo Y, et al (2018) Superhydrophobic coatings on gelatin-based films: Fabrication, characterization and cytotoxicity studies. RSC Adv 8:23712–23719. https://doi.org/10.1039/c8ra04066d

Choi SM, Rao KM, Zo SM, Shin EJ (2022) Bacterial Cellulose and Its Applications. Polymers (Basel) 14:1–44. https://doi.org/https://doi.org/10.3390/polym14061080

Čižauskaite U, Jakubaityte G, Žitkevičius V, Kasparavičiene G (2019) Natural ingredients-based gummy bear composition designed according to texture analysis and sensory evaluation in vivo. Molecules 24:. https://doi.org/10.3390/molecules24071442

Cruz AC, Guiné RPF, Gonçalves JC (2015) Drying Kinetics and Product Quality for Convective Drying of Apples (cvs. Golden Delicious and Granny Smith). Int J Fruit Sci 15:54–78. https://doi.org/10.1080/15538362.2014.931166

Darroca RMF, Lopez MJA, Thuy NM, et al (2024) Development and characterization of butterfly pea (Clitoria ternatea L.) flower juice from spray dried powder. Int J Chem Biochem Sci 25:357–365. https://doi.org/10.62877/41-ijcbs-24-25-19-41

de Avelar MHM, Efraim P (2020) Alginate/pectin cold-set gelation as a potential sustainable method for jelly candy production. Lwt 123:109119. https://doi.org/10.1016/j.lwt.2020.109119

Diep TT, Yoo MJY, Rush E (2022) Effect of In Vitro Gastrointestinal Digestion on Amino Acids, Polyphenols and Antioxidant Capacity of Tamarillo Yoghurts. Int J Mol Sci 23:. https://doi.org/10.3390/ijms23052526

Dubey R, Toh YR, Yeh AI (2018) Enhancing cellulose functionalities by size reduction using media-mill. Sci Rep 8:1–11. https://doi.org/10.1038/s41598-018-29777-w

Farooq S, A. Rather S, Gull A, et al (2020) Physicochemical and nutraceutical properties of tomato powder as affected by pretreatments, drying methods, and storage period. Int J Food Prop 23:797–808. https://doi.org/10.1080/10942912.2020.1758716

Fei X, Jones OG, Reuhs BL, Campanella OH (2021) Soluble pectin acts as a particle stabilizer of tomato suspensions: The impact on tomato products rheological characterization. Lwt 139:110508. https://doi.org/10.1016/j.lwt.2020.110508

Fernandes I de AA, Maciel GM, Ribeiro VR, et al (2021) The role of bacterial cellulose loaded with plant phenolics in prevention of UV-induced skin damage. Carbohydr Polym Technol Appl 2:. https://doi.org/10.1016/j.carpta.2021.100122

Figiel A, Tajner-Czopek A (2006) The effect of candy moisture content on texture. J Foodserv 17:189–195. https://doi.org/10.1111/j.1745-4506.2006.00037.x

Guerrero P, Zugasti I, Etxabide A, et al (2020) Effect of fructose and ascorbic acid on the performance of cross-linked fish gelatin films. Polymers (Basel) 12:1–11.

https://doi.org/10.3390/polym12030570

Guiné RPF, Correia PMR, Reis C, Florença SG (2020) Evaluation of texture in jelly gums incorporating berries and aromatic plants. Open Agric 5:450–461. https://doi.org/10.1515/opag-2020-0043

Helal A, Tagliazucchi D (2018) Impact of in-vitro gastro-pancreatic digestion on polyphenols and cinnamaldehyde bioaccessibility and antioxidant activity in stirred cinnamon-fortified yogurt. Lwt 89:164–170. https://doi.org/10.1016/j.lwt.2017.10.047

İlbay Z, Şahin S, Büyükkabasakal K (2014) A novel approach for olive leaf extraction through ultrasound technology : Response surface methodology versus artificial neural networks. Korean J Chem Eng 31:1661–1667. https://doi.org/10.1007/s11814-014-0106-3

Jaiswal AK, Hokkanen A, Kumar V, et al (2021) Thermoresponsive Nanocellulose Films as an Optical Modulation Device: Proof-of-Concept. ACS Appl Mater Interfaces 13:25346–25356. https://doi.org/10.1021/acsami.1c03541

Jiamjariyatam R (2018) Influence of gelatin and isomaltulose on gummy jelly properties. Int Food Res J 25:776–783

Jiménez-Monreal AM, Cedeño-Pinos C, Bañón S, et al (2025) Effect of in vitro gastrointestinal digestion on the antioxidant properties of fruit and vegetable powdered smoothies reinforced with WPC80. Lwt 215:. https://doi.org/10.1016/j.lwt.2024.117301

Kaschuk JJ, Al Haj Y, Valdez Garcia J, et al (2024) Processing factors affecting roughness, optical and mechanical properties of nanocellulose films for optoelectronics. Carbohydr Polym 332:121877. https://doi.org/10.1016/j.carbpol.2024.121877

Koshti P, Paryani A, Talreja J, Zope V (2022) AttenQ- Attention Span Detection Tool for Online Learning. SSRN Electron J. https://doi.org/10.2139/ssrn.4096416

Lavelli V, Hippeli S, Dornisch K, et al (2001) Properties of tomato powders as

additives for food fortification and stabilization. J Agric Food Chem 49:2037–2042. https://doi.org/10.1021/jf000490e

Li Y, Dong X, Yao L, et al (2024) Preparation of regenerated cellulose-vitamin E complex. Cellulose 31:7153–7162. https://doi.org/10.1007/s10570-024-06042-0

Liu D, Martinez-Sanz M, Lopez-Sanchez P, et al (2017) Adsorption behaviour of polyphenols on cellulose is affected by processing history. Food Hydrocoll 63:496–507. https://doi.org/10.1016/j.foodhyd.2016.09.012

Lorenz M (2021) How to Make Gummy Bears. https://www.wikihow.com/Make-Gummy-Bears. Accessed 28 Aug 2024

Luo X, Tian M, Cheng Y, et al (2022) Effects of simulated in vitro gastrointestinal digestion on antioxidant activities and potential bioaccessibility of phenolic compounds from K. coccinea fruits. Front Nutr 9:1–12. https://doi.org/10.3389/fnut.2022.1024651

Mutlu C, Tontul SA, Erbaş M (2018) Production of a minimally processed jelly candy for children using honey instead of sugar. LWT - Food Sci Technol 93:499–505. https://doi.org/10.1016/j.lwt.2018.03.064

Na-Nakorn K, Kulrattanarak T, Hamaker BR, Tongta S (2019) Starch digestion kinetics of extruded reformed rice is changed in different ways with added protein or fiber. Food Funct 10:4577–4583. https://doi.org/10.1039/c9fo00521h

Oteiza PI, Fraga CG, Mills DA, Taft DH (2018) Flavonoids and the gastrointestinal tract: Local and systemic effects. Mol Aspects Med 61:41–49. https://doi.org/10.1016/j.mam.2018.01.001

Pérez M, Dominguez-López I, Lamuela-Raventós RM (2023) The Chemistry Behind the Folin-Ciocalteu Method for the Estimation of (Poly)phenol Content in Food: Total Phenolic Intake in a Mediterranean Dietary Pattern. J Agric Food Chem 71:17543–17553. https://doi.org/10.1021/acs.jafc.3c04022

Phan ADT, Netzel G, Wang D, et al (2015) Binding of dietary polyphenols to cellulose: Structural and nutritional aspects. Food Chem 171:388–396.

https://doi.org/10.1016/j.foodchem.2014.08.118

Sadeer NB, Montesano D, Albrizio S, et al (2020) The versatility of antioxidant assays in food science and safety—chemistry, applications, strengths, and limitations. Antioxidants 9:1–39. https://doi.org/10.3390/antiox9080709

Sánchez-Rangel JC, Benavides J, Heredia JB, et al (2013) The Folin-Ciocalteu assay revisited: Improvement of its specificity for total phenolic content determination. Anal Methods 5:5990–5999. https://doi.org/10.1039/c3ay41125g

Sharma S, Majumdar RK, Mehta NK, Nirmal NP (2022) Effects of Pineapple Peel Ethanolic Extract on the Physicochemical and Textural Properties of Surimi Prepared from Silver Carp (Hypophthalmichthys molitrix). Foods 11:. https://doi.org/10.3390/foods11203223

Shen R, Lin D, Liu Z, et al (2021) Fabrication of Bacterial Cellulose Nanofibers/Soy Protein Isolate Colloidal Particles for the Stabilization of High Internal Phase Pickering Emulsions by Anti-solvent Precipitation and Their Application in the Delivery of Curcumin. Front Nutr 8:1–16. https://doi.org/10.3389/fnut.2021.734620

Shi Z, Zhang Y, Phillips GO, Yang G (2014) Utilization of bacterial cellulose in food. Food Hydrocoll 35:539–545. https://doi.org/10.1016/j.foodhyd.2013.07.012

Shraim AM, Ahmed TA, Rahman MM, Hijji YM (2021) Determination of total flavonoid content by aluminum chloride assay: A critical evaluation. Lwt 150:111932. https://doi.org/10.1016/j.lwt.2021.111932

Snyder JF, Steele J, Dong H, et al (2013) Optical Properties of Nanocellulose Dispersions in Water , Dimethylformamide and Poly (Methyl Methacrylate). Army Res Lab

Soeiro VS, Carvalho RS, Martins D, et al (2021) Alginate - amphotericin B nanocomplexes covered by nanocrystals from bacterial cellulose : physico - chemical characterization and in vitro toxicity. Sci Rep 1–8. https://doi.org/10.1038/s41598-021-03264-1

Sopade PA, Gidley MJ (2009) A rapid in-vitro digestibility assay based on glucometry for investigating kinetics of starch digestion. Starch/Staerke 61:245–255. https://doi.org/10.1002/star.200800102

Spinei M, Oroian M (2024) Characterization of Băbească Neagră Grape Pomace and Incorporation into Jelly Candy: Evaluation of Phytochemical, Sensory, and Textural Properties. Foods 13:. https://doi.org/10.3390/foods13010098

Srilakshmi A (2020) Texture Profile Analysis of Food and TPA Measurements: a Review Article. 708–711

Sultana S, Lawag IL, Lim LY, et al (2024) A Critical Exploration of the Total Flavonoid Content Assay for Honey. Methods Protoc 7:1–17. https://doi.org/10.3390/mps7060095

Takei T, Yoshihara R, Danjo S, et al (2020) Hydrophobically-modified gelatin hydrogel as a carrier for charged hydrophilic drugs and hydrophobic drugs. Int J Biol Macromol 149:140–147. https://doi.org/10.1016/j.ijbiomac.2020.01.227

Tangkanakul P (2022) Designing Instant High Fiber Beverage with Nata de Coco. Food 32:270–278

Teixeira-Lemos E, Almeida AR, Vouga B, et al (2021) Development and characterization of healthy gummy jellies containing natural fruits. Open Agric 6:466–478. https://doi.org/10.1515/opag-2021-0029

Vojvodić Cebin A, Bunić M, Mandura Jarić A, et al (2024) Physicochemical and Sensory Stability Evaluation of Gummy Candies Fortified with Mountain Germander Extract and Prebiotics. Polymers (Basel) 16:. https://doi.org/10.3390/polym16020259

Wanyo P, Chamsai T, Toontom N, et al (2024) Differential Effects of In Vitro Simulated Digestion on Antioxidant Activity and Bioaccessibility of Phenolic Compounds in Purple Rice Bran Extracts. Molecules 29:. https://doi.org/10.3390/molecules29132994

Xavier JR, Ramana KV (2022) Development of slow melting dietary fiber-enriched ice

cream formulation using bacterial cellulose and inulin. J Food Process Preserv 46:1–8. https://doi.org/10.1111/jfpp.15394

Ziółkiewicz A, Kasprzak-Drozd K, Wójtowicz A, et al (2023) The Effect of In Vitro Digestion on Polyphenolic Compounds and Antioxidant Properties of Sorghum (Sorghum bicolor (L.) Moench) and Sorghum-Enriched Pasta. Molecules 28:. https://doi.org/10.3390/molecules28041706

CHAPTER 7

CONCLUSION AND RECOMMENDATION

7.1 Conclusion

This thesis presents a comprehensive exploration of optimizing bacterial cellulose (BC) production using kombucha fermentation technology based on Thai tea, followed by structural modification and application in jelly candy as a nutraceutical or functional food model.

7.1.1 Pre-Optimization of Bacterial Cellulose Production: Investigating Key Factors Affecting Yield and Properties

The research successfully optimized BC yield by leveraging different Thai tea substrates, additives, and carbon source combinations. Among the four tea types examined, Thai Red Tea (RTC) and *Assamica* Black Tea (BTC) demonstrated the highest BC production, with yields of 168.00 ± 2.93 g/L and 158.56 ± 3.96 g/L, respectively. Yield was further improved through the use of additives, particularly ethanol (RTC-EtOH), which produced 218.36 ± 12.85 g/L of BC. Among carbon source combinations, sucrose-glucose (RTC-SGlu) resulted in the highest BC yield at 259.54 ± 8.92 g/L, outperforming sucrose-dextrose (RTC-SD), although the difference was not statistically significant.

Subsequently, essential cultivation parameters, including initial pH, harvesting period, tea concentration, and cultivation method, were systematically studied. Optimal BC yield was obtained at an unadjusted initial pH of ~5.20, a tea concentration of 2%, and biweekly harvesting over four weeks in each separated experiment. Static cultivation proved most effective for producing uniform, dense BC pellicles, while shaking conditions enhanced water-holding capacity (WHC).

7.1.2 Optimization of Bacterial Cellulose Production from Thai Red Tea Kombucha Using Central Composite Design in Response Surface Methodology

Further statistical optimization through response surface methodology (RSM) developed a highly efficient formulation (RTC-V1) comprising 7.97% 9w/v) sucrose, 2.03% (w/v) glucose, 1.41% (w/v) tea, and 1.56% (v/v) ethanol, achieving a remarkable wet BC yield of 621.71 ± 24.06 g/L, representing a 238% increase compared to the RTC-SGlu sample. The optimized BC displayed desirable physical and chemical properties, including well-defined nanofiber morphology, high crystallinity, thermal stability, and strong mechanical performance.

7.1.3 Impact of High-Pressure Microfluidization Treatment on The Properties of Bacterial Cellulose Derived from Thai Red Tea Kombucha

To improve BC versatility, high-pressure microfluidization (HPM) was applied to reduce fiber size and tailor material properties. Treatment at 10,000 psi for 10 to 20 cycles effectively reduced fiber diameters from 37 nm to approximately 25 nm and decreased WHC from 96.58 ± 13.91 g/g to about 31 g/g. These modifications were confirmed through SEM, XRD, and TGA analyses, establishing HPM as a practical tool for producing bacterial cellulose nanofibrils (BCNFs) with controlled structural and functional characteristics.

7.1.4 Effects of Bacterial Cellulose Nanofibrils on Jelly Candy Properties and Bioactive Compound Profiles During Simulated Digestion

In the final phase, microfluidic-treated bacterial cellulose nanofibrils (BCNF) were incorporated into jelly candy (JC) to evaluate their effects on texture and bioactive compound bioaccessibility. BCNF did not affect appearance but reduced color a* and b* values as treatment cycles and concentration increased. Texture analysis showed BCNF increased hardness, gumminess, and chewiness while reducing

adhesiveness, cohesiveness, and resilience; the BCH20 formula (5 g BCNF) achieved the best texture balance.

During digestion simulation, JC with vitamin E and BCNF (JC-VEBC) showed minimal or no release of active compounds, indicating limited bioaccessibility, whereas the sample without BCNF (JC-VENBC) exhibited the highest total phenolic content and better antioxidant release. The consistently low flavonoid levels across samples likely reflect low concentrations, suggesting more sensitive analytical methods are needed to confirm their presence. BCNF protected antioxidant activity in the vitamin C formulation (JC-VCBC) better than its non-BCNF counterpart (JC-VCNBC), but no antioxidant release was observed in JC-VEBC, possibly due to protective interactions. BCNF provided limited antioxidant protection in jelly candies containing butterfly pea flower powder (BF) and tomato extract (TOM). Overall, microfluidic BCNF influences texture and modulates bioaccessibility depending on the bioactive ingredient.

7.2 Recommendations

Building on the successful optimization of bacterial cellulose (BC) production from Thai red tea kombucha fermentation and its structural modification through high-pressure microfluidization, several avenues are recommended to advance research and application:

1) Scale-Up of Bacterial Cellulose Production

To meet future industrial needs, it is recommended that the optimized bacterial cellulose (BC) production process developed in this study be scaled up to pilot or industrial levels. The key parameters established—namely fermentation duration, substrate composition, and harvesting intervals—should be further validated under larger-scale conditions to ensure consistent yield, quality, and reproducibility. For effective scale-up, the implementation of real-time monitoring and process control strategies is also strongly advised.

2) Expanding Functional Food Applications and Bioactive Delivery

Future research should explore the interactions between bacterial cellulose (BC) nanofibrils and various bioactive ingredients—such as vitamins, antioxidants, and plant-based extracts—within different food matrices. This includes potential applications in beverages, gummies, dairy-based products, and other functional food systems. Understanding how BC influences the stability, release behavior, and bioaccessibility of these compounds during processing and digestion will be crucial for the development of targeted, health-promoting foods with enhanced nutritional value and consumer appeal.

3) In Vivo Evaluation of Digestibility and Health Benefits

Although in vitro digestion studies offered valuable preliminary insights into the effects of BC nanofibrils (BCNF) on bioaccessibility, in vivo studies are strongly recommended to validate these findings under physiological conditions. Such studies are essential to further evaluate the digestibility, safety, and health impacts of BC-enriched foods. They will also help clarify how BC interacts within the digestive system, its effect on nutrient absorption, and its potential role in modulating gut health. Ultimately, this will support the evidence-based development of BC as a functional ingredient in nutraceutical and health-oriented food products.

4) Product Development and Consumer Acceptance

Further research into the sensory attributes—particularly texture and mouthfeel—shelf-life stability, and consumer acceptance of bacterial cellulose (BC)-containing products is essential to ensure successful market introduction. Understanding consumer preferences, especially among target groups such as children, the elderly, and health-conscious individuals, will guide the development of formulations that meet their expectations. Additionally, expanding BC applications beyond jelly candy into diverse food formats, including functional beverages, dairy alternatives, and bakery products, can significantly broaden its commercial potential in the functional and health food markets.

APPENDICES

APPENDIX A

STANDARD CURVE FOR SUGAR ANALYSIS

Table 1 Standard Curve Data for Sucrose, Fructose, and Glucose in Sugar Analysis for BC Production with Various Teas and Additives.

Sugar (g/L)	Peak Area		
	Sucrose	Glucose	Fructose
0	0	0	0
3	136,661	235,880	192,231
6	262,110	488,085	394,293
9	409,466	713,853	580,040
12	547,536	950,286	771,482
RL Equation	y=45596x - 24208	y = 79285x + 1911.8	y = 64359x + 1454.6
R^2	0.9994	0.9998	0.9998

Remark: Retention times (minutes) of spectra peaks for Sucrose (±14.94), Glucose (±16.14), and Fructose (± 17.89). and Glycerol (±18.70)

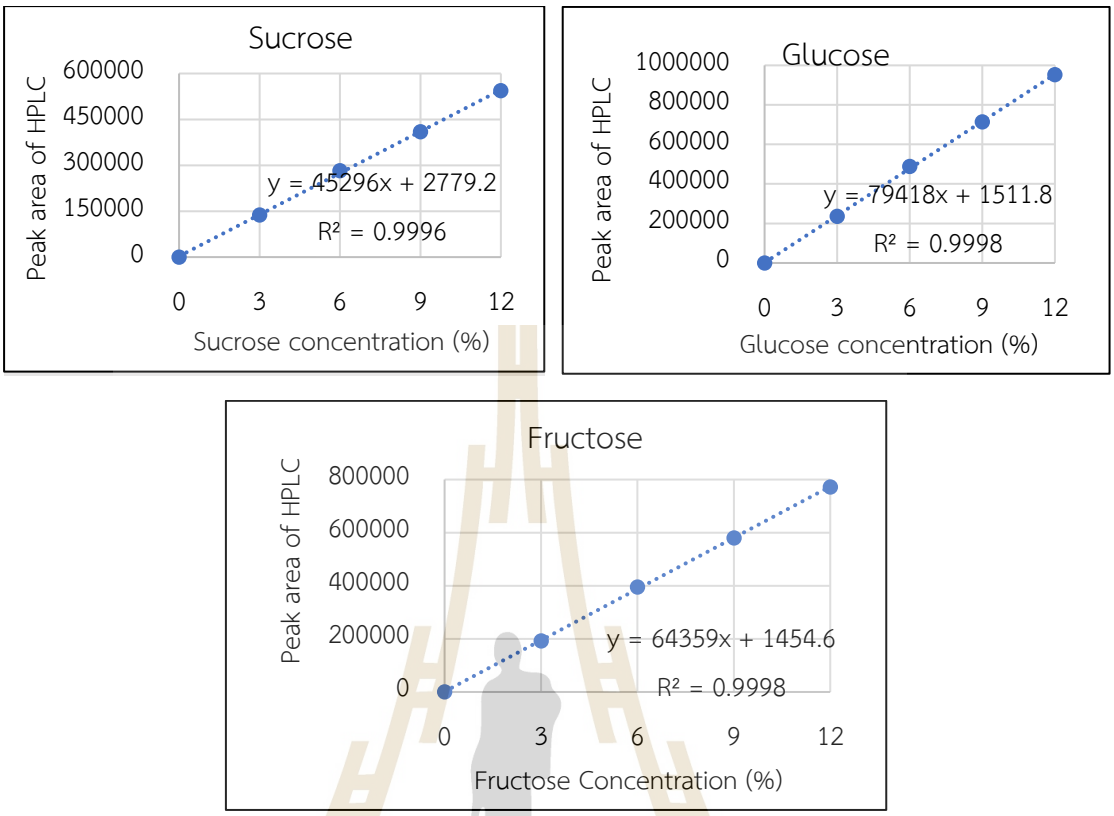

Figure 1. Standard Curve for Sugar Analysis of Kombucha Samples with Various Types of Tea and Additives.

Table 2 Standard Curve Data for Sucrose, Fructose, Glucose, and Glycerol in Sugar Analysis for BC Production with Various Carbon Sources Combinations.

Sugar (g/L)	Peak Area			Glycerol (g/L)	Peak Area
	Sucrose	Glucose	Fructose		
0	0	0	0	0	0
3	136,661	235,880	192,231	2.5	117,356
6	262,110	488,085	394,293	5.0	239,595
9	409,466	713,853	580,040	7.5	352,241
12	547,536	950,286	771,482	10.0	470,883
RL Equation	y=45596x-24208	y = 79285x + 1911.8	y = 64359x + 1454.6	RL Equation	y = 47066x + 684.8
R^2	0.9994	0.9998	0.9998	R2	0.9999

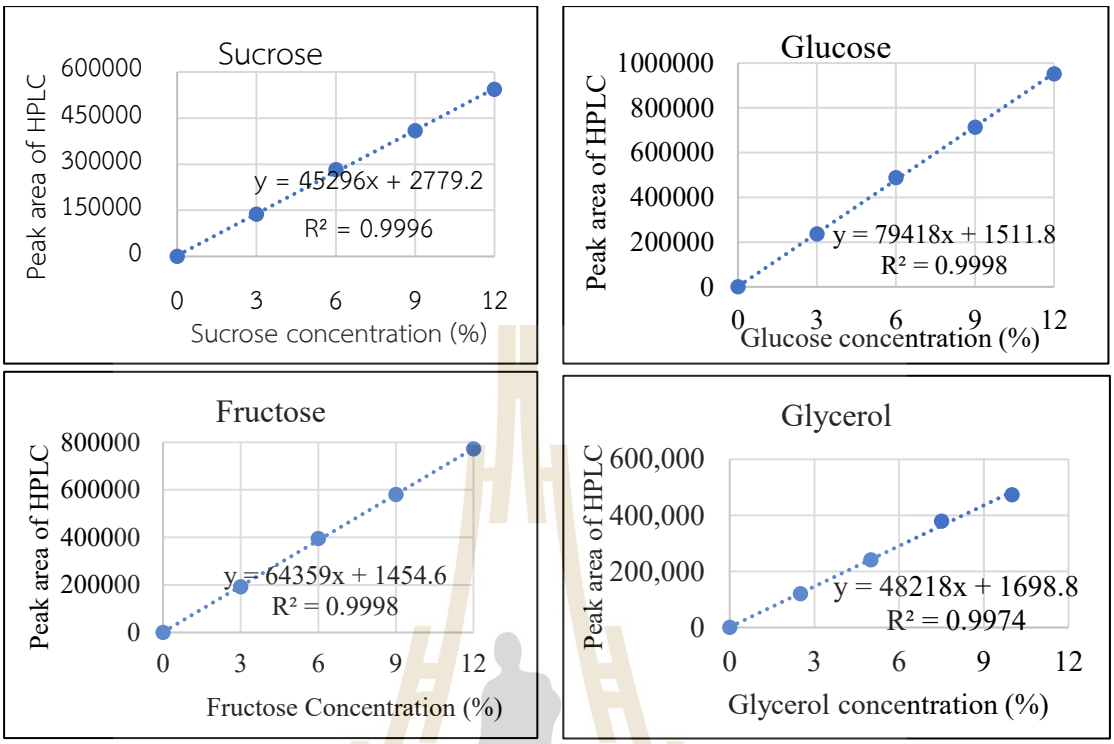

Figure 2 Standard Curve for Sugar Analysis of Kombucha Samples with Various Types of Carbon Sources Combinations.

APPENDIX B

DATA OF THE FIBER SIZE ANALYSIS OF BC FROM SEM IMAGE USING "ImageJ" SOFTWARE

Table 3 Data analysis of the BC particle size distribution from kombucha with different types of tea

No	Diameter size (nm)				
	NDC -Fiber	RTC-C	GTC	BTC-30k	RBTH
1	21.148	18.127	19.866	25.953	22.009
2	21.960	19.654	21.645	27.815	22.009
3	23.212	20.668	23.392	28.230	22.848
4	24.199	23.464	24.492	28.562	24.241
5	24.383	23.742	24.561	28.930	24.369
6	24.866	23.945	25.146	29.874	24.561
7	25.133	24.538	25.255	30.483	24.832
8	25.588	24.803	25.499	31.899	25.315
9	26.318	24.884	25.850	32.050	25.514
10	26.445	25.779	26.907	32.329	25.645
11	27.586	26.424	27.727	32.743	26.488
12	28.067	26.483	27.954	32.842	26.945
13	28.272	26.504	28.774	32.892	26.945
14	28.435	26.586	29.034	33.083	27.721
15	28.435	26.656	29.040	33.139	27.840
16	28.724	26.764	30.617	34.501	27.942
17	28.915	26.779	31.132	34.752	28.085

Table 3 Data analysis of the BC particle size distribution from kombucha with different types of tea (Continued)

No	Diameter size (nm)				
	NDC -Fiber	RTC-C	GTC	BTC-30k	RBTH
18	29.271	26.948	31.192	34.940	28.427
19	30.024	27.022	31.445	35.090	28.746
20	30.842	27.669	31.601	35.426	29.042
21	31.034	27.880	31.843	36.347	29.912
22	31.656	28.166	32.265	36.471	30.197
23	31.908	28.166	32.691	37.115	30.280
24	32.001	28.186	32.832	37.640	30.572
25	32.019	28.706	33.297	37.813	30.632
26	32.279	29.522	33.746	38.100	30.979
27	34.958	29.592	34.059	38.290	31.089
28	35.651	29.923	34.099	38.573	31.742
29	36.094	31.002	34.324	39.759	31.993
30	36.248	31.075	34.602	40.122	32.188
31	36.248	32.718	35.185	40.663	32.540
32	36.656	32.836	35.978	41.035	33.096
33	36.656	32.874	36.016	42.151	33.251
34	36.800	33.973	36.061	42.479	34.047
35	37.109	34.052	36.136	42.699	34.223
36	37.813	34.262	36.262	43.139	35.215
37	37.948	34.393	38.606	43.440	35.489
38	39.013	34.700	38.614	44.202	35.537
39	40.213	34.878	39.460	44.725	35.587
40	40.213	35.855	39.835	45.720	36.299
41	40.982	35.892	40.389	46.446	37.351

Table 3 Data analysis of the BC particle size distribution from kombucha with different types of tea (Continued)

No	Diameter size (nm)				
	NDC -Fiber	RTC-C	GTC	BTC-30k	RBTH
42	48.399	36.095	41.249	47.830	37.367
43	48.766	36.334	42.340	48.130	37.610
44	49.425	36.805	47.401	48.328	37.867
45	50.913	38.562	47.861	51.230	38.330
46	53.643	39.047	51.356	51.470	38.782
47	53.864	41.530	51.598	51.569	41.651
48	55.709	44.263	57.119	54.948	41.855
49	56.134	46.506	57.548	55.187	43.135
50	56.134	47.139	58.844	56.031	44.903
Mean	**35.166**	**30.647**	**34.855**	**39.144**	**31.465**
SD	**9.700**	**6.463**	**9.189**	**7.782**	**5.692**
Min	**21.148**	**18.127**	**19.866**	**25.953**	**22.009**
Max	**56.134**	**47.139**	**58.844**	**56.031**	**44.903**

Table 4 Data analysis of the BC particle size distribution from kombucha with different types of additives

No	Diameter size (nm)						
	NDC-Fiber	RTC-EtOH	RTC-SPI	RTC-YE	RTC-Vit C	RTC-PC	RTC-C
1	21.148	30.658	23.353	25.005	13.738	21.322	19.356
2	21.960	30.918	23.508	25.422	15.520	26.946	19.825
3	23.212	32.039	27.525	26.858	18.050	41.898	20.019
4	24.199	33.709	27.688	26.909	19.352	35.927	21.460

Table 4 Data analysis of the BC particle size distribution from kombucha with different types of additives (Continued)

No	Diameter size (nm)						
	NDC-Fiber	RTC-EtOH	RTC-SPI	RTC-YE	RTC-Vit C	RTC-PC	RTC-C
5	24.383	34.218	27.902	27.073	20.059	37.38	22.108
6	24.866	34.462	28.609	27.574	20.063	31.424	22.608
7	25.133	34.833	29.360	27.640	20.219	41.356	23.862
8	25.588	35.866	30.533	27.662	20.875	34.507	24.307
9	26.318	36.783	30.697	27.711	21.008	27.184	25.022
10	26.445	36.923	31.373	28.096	21.313	30.696	25.423
11	27.586	38.506	32.385	28.469	21.757	27.335	26.638
12	28.067	38.746	32.540	28.676	22.450	18.004	26.693
13	28.272	39.565	33.124	30.286	22.450	28.792	26.895
14	28.435	39.763	33.136	30.716	22.838	51.847	26.912
15	28.435	39.768	33.751	30.786	23.009	45.053	27.177
16	28.724	40.842	33.751	31.123	23.182	36.859	27.919
17	28.915	40.842	33.751	31.137	23.250	29.021	28.312
18	29.271	41.242	33.916	31.265	23.564	38.862	28.328
19	30.024	41.349	34.508	31.351	23.599	54.841	28.554
20	30.842	43.283	37.132	32.361	23.812	39.52	28.740
21	31.034	43.578	37.392	33.088	24.413	30.906	28.775
22	31.656	43.725	37.491	33.180	24.779	40.168	28.815
23	31.908	44.776	37.767	33.381	25.725	45.017	28.970
24	32.001	44.883	38.267	34.209	25.918	43.411	29.347
25	32.019	45.346	38.788	34.457	25.959	40.168	29.447
26	32.279	45.467	39.684	34.590	25.965	34.131	29.661
27	34.958	45.663	40.964	34.878	25.965	34.554	29.736

Table 4 Data analysis of the BC particle size distribution from kombucha with different types of additives (Continued)

No	Diameter size (nm)						
	NDC-Fiber	RTC-EtOH	RTC-SPI	RTC-YE	RTC-Vit C	RTC-PC	RTC-C
28	35.651	46.705	40.964	35.095	25.986	31.424	29.873
29	36.094	47.115	41.594	35.187	25.986	47.731	29.912
30	36.248	47.285	43.970	35.367	26.132	45.854	30.027
31	36.248	47.420	44.165	36.097	26.681	38.341	30.046
32	36.656	47.791	44.195	36.464	26.816	34.751	30.951
33	36.656	48.722	44.595	36.529	27.145	40.876	31.118
34	36.800	48.886	44.991	36.547	27.164	52.215	31.146
35	37.109	49.180	45.393	36.794	27.241	56.299	31.465
36	37.813	49.538	45.905	36.862	27.448	28.842	31.726
37	37.948	50.149	46.028	37.094	27.661	36.107	32.602
38	39.013	50.943	47.934	37.211	27.703	39.101	33.723
39	40.213	51.841	48.765	37.451	27.774	32.357	33.965
40	40.213	52.429	49.032	37.516	27.788	28.06	34.132
41	40.982	54.207	49.065	37.646	27.979	28.06	34.333
42	48.399	54.207	49.328	37.763	27.985	17.964	34.533
43	48.766	54.473	50.042	38.524	28.368	32.335	34.914
44	49.425	56.553	51.063	39.528	31.125	29.627	35.445
45	50.913	60.047	51.816	39.965	31.418	41.898	36.180
46	53.643	60.896	56.807	39.984	33.059	41.003	36.287
47	53.864	61.211	57.849	41.459	34.218	36.107	36.524
48	55.709	66.050	62.746	41.621	35.201	30.591	37.999
49	56.134	67.230	66.053	42.830	36.380	32.534	39.138
50	56.134	68.436	74.896	44.859	38.461	21.928	44.216

Table 4 Data analysis of the BC particle size distribution from kombucha with different types of additives (Continued)

No	Diameter size (nm)						
	NDC-Fiber	RTC-EtOH	RTC-SPI	RTC-YE	RTC-Vit C	RTC-PC	RTC-C
Mean	35.166	45.981	40.922	33.846	25.491	37.737	29.703
SD	9.700	9.380	10.923	4.901	4.915	6.447	5.172
Min	21.148	30.658	23.353	25.005	13.738	24.112	19.356
Max	56.134	68.436	74.896	44.859	38.461	53.342	44.216

Table 5 Data analysis of the BC particle size distribution from red Thai tea kombucha with different types of carbon source combination.

No	Diameter size (nm)					
	NDC -Fiber	RTC-C	RTC-SD	RTC-SF	RTC-Gly	RTC-Glu
1	21.148	19.356	26.756	22.237	22.413	23.317
2	21.960	19.825	27.199	22.801	25.275	23.374
3	23.212	20.019	28.585	24.524	25.431	24.485
4	24.199	21.460	28.794	25.779	26.419	24.919
5	24.383	22.108	29.464	27.746	26.737	24.919
6	24.866	22.608	30.305	28.128	26.868	25.208
7	25.133	23.862	31.944	28.441	27.460	25.389
8	25.588	24.307	32.055	29.835	27.538	26.213
9	26.318	25.022	33.216	30.257	27.560	26.898
10	26.445	25.423	33.333	30.334	27.848	27.494
11	27.586	26.638	33.355	30.875	28.017	27.577
12	28.067	26.693	34.090	31.406	28.081	28.496
13	28.272	26.895	34.359	32.994	29.095	29.589

Table 5 Data analysis of the BC particle size distribution from red Thai tea kombucha with different types of carbon source combination (Continued)

No	Diameter size (nm)					
	NDC -Fiber	RTC-C	RTC-SD	RTC-SF	RTC-Gly	RTC-Glu
14	28.435	26.912	35.240	33.526	29.830	30.072
15	28.435	27.177	35.395	34.682	31.023	30.175
16	28.724	27.919	35.675	34.725	31.868	30.553
17	28.915	28.312	36.285	34.759	31.868	30.715
18	29.271	28.328	36.770	35.113	31.944	30.945
19	30.024	28.554	36.924	35.113	31.944	31.357
20	30.842	28.740	37.268	35.749	32.268	31.887
21	31.034	28.775	37.287	35.913	32.320	32.234
22	31.656	28.815	37.590	37.071	33.827	32.268
23	31.908	28.970	37.881	37.233	34.151	32.338
24	32.001	29.347	38.114	38.190	35.592	32.926
25	32.019	29.447	38.341	38.190	35.659	33.000
26	32.279	29.661	38.392	38.308	36.413	33.323
27	34.958	29.736	38.434	38.776	36.529	33.803
28	35.651	29.873	38.631	38.969	37.620	33.866
29	36.094	29.912	39.930	39.544	37.892	34.489
30	36.248	30.027	41.071	40.035	37.956	35.020
31	36.248	30.046	41.802	40.334	38.225	35.044
32	36.656	30.951	41.802	40.594	38.852	35.714
33	36.656	31.118	41.807	41.618	40.001	35.725
34	36.800	31.146	41.938	41.763	40.293	36.047
35	37.109	31.465	42.333	41.942	40.346	36.498
36	37.813	31.726	42.857	42.193	41.058	37.363
37	37.948	32.602	44.176	43.353	41.247	37.477

Table 5 Data analysis of the BC particle size distribution from red Thai tea kombucha with different types of carbon source combination (Continued)

No	Diameter size (nm)					
	NDC -Fiber	RTC-C	RTC-SD	RTC-SF	RTC-Gly	RTC-Glu
38	39.013	33.723	45.527	43.353	41.888	38.852
39	40.213	33.965	46.360	45.020	41.960	39.698
40	40.213	34.132	46.975	45.220	42.075	39.819
41	40.982	34.333	48.049	47.173	42.744	40.540
42	48.399	34.533	48.082	48.088	42.913	41.190
43	48.766	34.914	48.343	48.555	43.956	41.494
44	49.425	35.445	52.732	48.555	43.984	41.773
45	50.913	36.180	53.093	48.679	44.011	42.075
46	53.643	36.287	54.222	49.657	44.353	43.918
47	53.864	36.524	54.398	53.785	46.324	44.713
48	55.709	37.999	57.143	55.329	47.558	50.862
49	56.134	39.138	61.652	55.600	49.071	53.891
50	56.134	44.216	63.275	55.923	54.868	57.335
Mean	**35.166**	**29.703**	**40.385**	**38.560**	**35.863**	**34.338**
SD	**9.700**	**5.172**	**8.654**	**8.514**	**7.357**	**7.564**
Min	**21.148**	**19.356**	**26.756**	**22.237**	**22.413**	**23.317**
Max	**56.134**	**44.216**	**63.275**	**55.923**	**54.868**	**57.335**

APPENDIX C

DATA ON THE OPTIMIZED SOLUTION FORMULA FOR BC PRODUCTION GENERATED BY SOFTWARE

Table 6. Predicted Optimized Formula Solution for BC Production Generated by Software

No	Sucrose	Tea	Ethanol	Wet yield	Dry yield	WHC	Desirability
1	7.973	1.405	1.595	630.159	5.238	119.265	0.939
2	7.973	1.405	1.589	630.061	5.231	119.423	0.939
3	7.973	1.405	1.581	629.927	5.221	119.643	0.939
4	7.973	1.405	1.573	629.787	5.210	119.864	0.939
5	7.973	1.405	1.566	629.668	5.201	120.046	0.938
6	7.947	1.405	1.595	630.790	5.243	119.289	0.938
7	7.973	1.405	1.557	629.507	5.190	120.29	0.938
8	7.951	1.406	1.595	630.571	5.242	119.275	0.938
9	7.973	1.405	1.543	629.228	5.171	120.686	0.938
10	7.932	1.405	1.590	631.076	5.239	119.436	0.938
11	7.923	1.405	1.595	631.377	5.247	119.312	0.938
12	7.973	1.410	1.595	629.580	5.236	119.214	0.938
13	7.973	1.405	1.519	628.78	5.142	121.289	0.937
14	7.973	1.405	1.505	628.487	5.123	121.66	0.937
15	7.973	1.405	1.474	627.831	5.086	122.427	0.936
16	7.973	1.405	1.449	627.281	5.056	123.016	0.935
17	7.847	1.405	1.595	633.162	5.260	119.378	0.935
18	7.973	1.405	1.444	627.171	5.050	123.129	0.935

Table 6. Predicted Optimized Formula Solution for BC Production Generated by Software (Continued)

No	Sucrose	Tea	Ethanol	Wet yield	Dry yield	WHC	Desirability
19	7.973	1.405	1.436	626.996	5.041	123.304	0.935
20	7.84	1.405	1.589	633.224	5.254	119.539	0.935
21	7.973	1.418	1.595	628.637	5.231	119.131	0.935
22	7.973	1.405	1.415	626.502	5.017	123.774	0.934
23	7.926	1.405	1.461	628.616	5.078	122.787	0.934
24	7.973	1.405	1.406	626.299	5.008	123.961	0.934
25	7.968	1.42	1.595	628.480	5.231	119.109	0.934
26	7.791	1.405	1.595	634.458	5.269	119.425	0.933
27	7.973	1.405	1.349	624.844	4.945	125.153	0.932
28	7.973	1.43	1.594	627.133	5.223	119.004	0.931
29	7.973	1.405	1.278	622.875	4.872	126.466	0.93
30	7.973	1.437	1.595	626.274	5.22	118.918	0.928
31	7.973	1.405	1.212	620.884	4.81	127.523	0.927
32	7.598	1.405	1.595	638.700	5.301	119.571	0.927
33	7.973	1.405	1.158	619.093	4.761	128.294	0.925
34	7.536	1.405	1.595	639.992	5.31	119.612	0.924
35	7.973	1.405	1.133	618.231	4.74	128.613	0.924
36	7.973	1.405	1.11	617.452	4.722	128.877	0.922
37	7.493	1.405	1.594	640.876	5.317	119.645	0.922
38	7.973	1.405	1.104	617.225	4.717	128.949	0.922
39	7.973	1.405	1.068	615.902	4.689	129.335	0.92
40	7.973	1.405	1.061	615.624	4.683	129.409	0.92
41	7.826	1.405	1.16	621.87	4.778	128.511	0.919

Table 6. Predicted Optimized Formula Solution for BC Production Generated by Software (Continued)

No	Sucrose	Tea	Ethanol	Wet yield	Dry yield	WHC	Desirability
42	7.973	1.405	1.02	614.071	4.654	129.777	0.918
43	7.969	1.466	1.589	622.673	5.196	118.736	0.918
44	7.973	1.405	0.971	612.104	4.62	130.147	0.915
45	7.973	1.405	0.936	610.653	4.598	130.359	0.913
46	7.260	1.407	1.595	645.117	5.35	119.754	0.912
47	7.973	1.405	0.881	608.26	4.565	130.609	0.91
48	7.973	1.405	0.855	607.104	4.551	130.69	0.909
49	7.973	1.405	0.812	605.083	4.529	130.775	0.906
50	7.973	1.405	0.787	603.91	4.518	130.795	0.904
51	7.973	1.405	0.777	603.406	4.513	130.796	0.903
52	7.973	1.405	0.638	596.306	4.461	130.465	0.894
53	7.973	1.405	0.580	593.081	4.446	130.125	0.889

Glucose was added to sucrose to achieve a total sugar concentration of 10%. Formulas No. 1, 46, and 53 were selected for laboratory validation

BIOGRAPHY

Mr. Wawan Agustina was born on August 29, 1981, in Brebes District, Central Java, Indonesia. He completed his elementary education at *SD Negeri Pabuaran 2*, continued to *SMP Negeri 02 Salem* for junior high school, and graduated from *SMA Negeri Kota Tegal* for senior high school. In 2005, he earned a Bachelor's degree in Chemistry from Jenderal Soedirman University, Purwokerto. Motivated by a deep interest in life sciences and applied biotechnology, he pursued further studies at the School of Life Sciences and Technology (SITH), Institut Teknologi Bandung (ITB), where he obtained his Master's degree in 2019.

He is currently a researcher at the National Research and Innovation Agency (BRIN) in Indonesia, specializing in bioprocess technology, with a particular focus on fermentation technology and functional food. His research explores the development of sustainable food processing methods and the enhancement of nutritional and functional properties through microbial fermentation and biotechnological approaches.

In parallel with his professional role, Mr. Wawan is pursuing a Doctoral degree at the School of Biotechnology, Institute of Agricultural Technology, Suranaree University of Technology, Thailand. His current research focuses on the production, optimization, and functional application of bacterial cellulose derived from Thai tea kombucha fermentation. He has authored several scientific publications, which are accessible through his Google Scholar profile.